THE MEMBRANE FUSION ACTIVITIES OF NATIVE AND RECONSTITUTED MUMPS AND SENDAI VIRUSES

Thesis by
Christopher Di Simone

In Partial Fulfillment of the Requirements for the
Degree of Doctor of Philosophy

California Institute of Technology
Pasadena, California
1992
(Defended October 17, 1991)

Acknowledgements

A number of people have been helpful in providing knowledge for me to complete this thesis and in collaborating on some of the projects. I am grateful to them all. The mumps project was initiated with advice from Fred Server and Neal Waxham, who also sent me virus with which to start the project. Viral preparation and plaque assays were accomplished in the research labs of John Zaia at the City of Hope Hospital Pediatric Department. John was very supportive and encouraging. Delilah Stephans was also extremely helpful and instructive in helping me learn the techniques for working with virus. Caroline Lowry upheld Delilah's high standards after Delilah departed for medical school. Collaborative experiments were also conducted at City of Hope with Sean Sullivan and Roy Chang, who were working with John Rossi on the delivery of ribozyme to cells. As an undergraduate SURF for two summers, Alex Wein provided an extra hand in carrying out experiments. David Baselt was very helpful at the end of my project in showing me how a real programmer with a real computer could reduce my timeload for kinetic fitting to seconds rather than hours.

At a time when the mumps project was not going well, Tom Amatruda contacted our group on a collaboration on transfection of HL60 cells which provided me with something exciting to work on. Although we did not accomplish our goal, we found out a few interesting things. Tom's expertise in cloning and transfection provided us with an opportunity to test the reconstituted virus as drug delivery vehicles.

John has served as a helpful, supportive, and encouraging advisor. Looking back on my decision to join the JDB group, I now know that it was

the best decision I've made at Caltech. I enjoyed my time at Caltech a great deal and learned a lot about a variety of subjects.

Regardless of how interesting or exciting my research project was, if my work environment had been hell, grad school would have been no fun. The people in our lab for the last five years have been really great in both scientific and social interactions. Both the old guard, Tracy Handel, Steve Novick, Ray Goodrich, John Kramer, Bob Driscoll and Shenda Baker, and the new guard, Mitsuko Fujiwara, Mike Youngquist, Roxanne Male, Kyoung Joon Oh, Steve Clark, and David Baselt, have all been very humorous and supportive (long live the Triumvirate). Wilton Vannier has served as a lab sage with information about everything immunological and has convinced me more than anyone else I've met that one can be personally happy in science.

The people out of my lab have also been very supportive. The people at Caltech have been much more interesting than I anticipated before I came here (yes, I was prejudiced). Tom Brown, Chris Sipes, David Long, Dom McGrath, John Kellamis and Jon Vernick have all been good friends. My parents and sisters have been ever so supportive. Without Paul Hobe and David Draper, my high school and college chemistry mentors, I would never have come to Caltech. The best part of my experience here at Caltech is that I met Deborah here. She has shown me everything that is beautiful about living.

Thanks to you, whoever you are, for reading my thesis.

Abstract

The structure and activities of whole and reconstituted Sendai and mumps viruses were examined using a number of physical and biological techniques: electron microscopy, photon correlation spectroscopy, perturbed angular correlation spectroscopy, gel electrophoresis, hemagglutination assays, plaque assays, fluorescence microscopy and fluorescent assays of membrane fusion. The fluorescent probe octadecyl rhodamine (R18) was found to have a proximal transfer behavior which reduced usage of the probe as a membrane fusion indicator to short time periods. Simple bireactant and mass action kinetic models were sufficent to fit the data provided by the fluorescent assays on viral fusion with cell membranes. The reconstitution of mumps virus was optimized by using the detergent Triton X-100. Reconstituted virus envelopes which were the same size as whole virus and which were active in binding and fusing to cells were produced. The reconstituted Sendai and mumps virus accumulated in the reticuloendothelial system when injected into mice and hamsters, respectively. The kinetics of the membrane fusion activity of mumps with ghost erythrocytes and CV-1 cells was measured and analysed. A general rate of reaction of 3 ($\pm$1) x 10^9 M^{-1} sec^{-1} was found. The membrane fusion activity of reconstituted Sendai with HL60, U937, Cos, H9 and PBL cell lines was also measured and analyzed. The fusion activity was utilized to deliver plasmids for transfection to the interiors of the HL60 and Cos cells. Luciferase expression was found in the Cos cells but not in the HL60 cells. Loading of plasmids into the vesicle interiors was enhanced by a factor of ten by complexing the DNA with the positive proteins polylysine, lysozyme and protamine.

Table of Contents

Chapter 1: Introduction

Conceptual Background

Liposomes were first conceived as a mechanism for drug delivery shortly after the discovery that one could form these self assembling bilayer vesicles from purified lipids.[1] A tremendous amount of research has been done on characterization of the physical properties of liposomes in terms of preparation techniques and lipid composition.[2] A variety of different size vesicles can be prepared with variable degrees of loading of internal contents into the vesicles.

As a potential drug carrier, a liposome should protect a drug from interacting with undesired tissue or other bodily elements (and vice versa), specifically accumulate in a tissue, and deliver its drug product to that tissue.[3]

To deliver a drug product efficiently to a specific tissue, a cancer for example, the liposome must be stable in the blood (assuming an intravenous approach) and must avoid uptake by the cells of the reticuloendothelial system (RES), i.e., the Kupffer cells and hepatocyte cells in the liver and spleen. Most liposomes will accumulate in the RES shortly after introduction in a body.[4] Two mechanisms of drug delivery to a specific tissue can be envisioned, the first, active targeting to a tissue and the second, a passive accumulation in tissue.

Active targeting could occur by placing on the surface of the vesicle a moiety such as an antibody, a lectin, or a lipid type that specifically binds to a specific tissue. Unfortunately the addition of such a molecule often reduces vesicle stability and increases the rate of uptake by the RES.[5] Exploration of active targeting has proceeded much more slowly than passive targeting

mechanisms. Active targeting could allow enhancement of drug dosage in a very specific tissue site if a ligand or receptor could be found for that specific tissue.

Passive targeting utilizes reduced drug toxicity and passive tissue accumulation to allow drug delivery to occur. A stable vesicle which is taken up slowly by the RES is desired. The two cases of successful commercial drug delivery both employ passive drug delivery. Lipids complexed with amphoteracin B have proved to be successful in treating fungal infections due to a reduction in the toxicity allowing an increased dosage of delivered drug to be applied.[6] In the second case, extremely stable small liposomes have been shown to accumulate in cancerous tissue due to poorly developed vesicular walls with large fenestrae, i.e., the liposomes leak into the tissue.[7] Liposomes can be loaded with radioisotopes for diagnostic imaging of the cancer or drugs for tumor chemotherapy.

Regardless of the mechanism of targeting to a cell exterior, delivery of liposome contents to a cell can only occur if a cell takes up the liposomes through endocytosis (and other related mechanisms) or if the liposome is able to fuse with some cellular membrane.

Liposome endocytosis is mediated by the cell. The liposomes will be taken into endosomal and lysosomal compartments where the vesicle is exposed to low pH conditions and vesicle breakdown occurs.[8] Any delivered drug must be stable under these conditions if it is going to have a therapeutic effect. Enhancement of the rate of endocytosis by attaching certain moieties to the vesicle surface may be plausible.

Membrane fusion of a liposome with a cell would allow direct delivery of liposome contents into the cellular interior.[9] Membrane fusion and

vesicle formation are normal components of cellular activity in forming and fusing cellular subcompartments, i.e., endocytotic vesicles, exocytosis of material (release of acetylcholine by nerve cells for example), and transport of glycoproteins from ribosome to cellular surface via the golgi. However, unmodified lipid vesicles are very stable and do not fuse spontaneously.[10] Modification of lipid vesicles surfaces by proteins or polymers may make them more fusogenic.

In many ways a virus is a highly optimized drug delivery system. The virus can enter the body by various pathways, bind to a tissue, and deliver its nucleic acid to the cellular interior. Those viruses which have been characterized for entry behavior generally contain a ligand for a cellular surface moiety and an active mechanism for cell entry. The availability of a cellular receptor for the virus and ability of the virus to enter the cell can determine tissue tropism, i.e., the range of tissues which a virus can infect.[11] A number of viruses (vaccinia virus, retroviruses, baculoviruses) have been altered to serve as delivery devices of genetic material for cellular expression.[12]

Of the 21 major families of animal viruses, 13 families have an exterior "shell" made of lipids and glycoproteins.[13] These lipid coated viruses undergo protein mediated membrane fusion with a host cell, with the cellular membrane or endosomal membrane, in order to deliver their nucleic acids to the cellular interior.[14] These viruses are essentially liposomes with glycoproteins incorporated into their bilayers that are responsible for viral surface activity. A liposome-like drug delivery system might be designed using viruses or viral proteins.

A number of workers have previously worked on the reconstitution of viral glycoproteins into lipid vesicles made of endogenous viral lipid or exogenous lipid. The viruses influenza, vesicular stomatitis virus, Semliki Forest virus, and Sendai have all been reconstituted by dissolving the viral glycoproteins and lipid in detergent, removing the viral interior proteins and nucleic acids, and dialyzing away the detergent to reform hollow vesicles containing the viral proteins.[15] These vesicles have been called virosomes or reconstituted viral envelopes. These reconstituted systems are functional in binding and fusion with target cells and can serve as delivery vehicles to cellular interiors.

In undertaking this project, we wished to explore further the possibility of using reconstituted viruses as drug delivery systems. To add further incentive to our studies we choose a viral system with a neuroinvasive property and which was infective to humans, the paramyxovirus mumps.[16] Drug delivery to the brain is especially difficult due to the existence of a blood brain barrier. The fenestrate junctions between the endothelial cells lining the capillaries in the brain are closed so that all material that enters the brain must be specifically transported into the brain or be so hydrophobic that it can diffuse across the lipid bilayers of the lining cells.[17] The mumps virus is able to invade and propagate throughout the CNS.

Though the potential for achievement of our goal was slim, that being specific drug delivery to the central nervous system, the possibilities for serendipitous discovery are always high in such cases and the project was undertaken. Other related projects were also undertaken as new questions arose and other experiments became possible. A number of these experiments used another paramyxovirus, Sendai.

Thesis Preview

Each of the chapters summarizes some of the experiments to answer hypotheses and questions which arose throughout this project. As each of the individual chapters include introductory material, this section is brief.

Chapter 2-

How reliable are the available assays for membrane fusion? How can we describe the kinetics of fusion between virus and target cells?

A number of different techniques were used to characterize the activities and structures of the viruses and reconstituted viruses throughout my work. Electron microscopy, photon correlation spectroscopy, gel electrophoresis, and protein assays were used to quantitate dimensional aspects of the virus, i.e , viral size, form, and number. Viral activity was monitored by plaque assays, hemagglutination assays, fluorescence microscopy and several quantitative fluorescence assays of membrane fusion. The fluorescence assays used to monitor membrane fusion represent the bulk of the actual experimental time during my thesis and much of the original data collected. Chapter 2 provides a discussion of the fluorescence fusion assays and some of my observations on these assays. A discussion on viral fusion kinetics is also presented in this chapter.

Chapter 3-

Can one reconstitute functionally active mumps? What is the optimal detergent for reconstitution? What happens to reconstituted virus when it is introduced into animal systems?

The techniques mentioned above were used to determine an optimal procedure for reconstituting mumps and Sendai virus so that they were functionally similar to the parent viruses in activity. Morphology was also closely studied, as a product that was capable of carrying drugs or other materials was desired. The hypothesis that mumps envelopes would accumulate in the CNS was tested.

Chapter 4-

What are the fusion activities and kinetics of the mumps virus? What do these activities tell us about the neurotropism of the virus?

This chapter could have preceded the previous one as it describes the fusion activities of whole virus but in the historical context the work occurred later. After studying the reconstituted virus we realized that there was little information on the activities of the whole virus and this information could be useful for comparison to the reconstituted systems and understanding of the infective behavior of the virus.

Chapter 5-

Can reconstituted Sendai virus be used as a delivery vehicle to H9 and PBL cells, model cell lines for HIV infection?

This work was in collaboration with John Zaia and Delilah Stephens at the City of Hope Hospital with a long term goal of *in vitro* drug delivery to HIV infected cells.

Chapter 6-

Can reconstituted Sendai virus be used as a delivery vehicle to HL60 and Cos cells? How can one optimize the loading of nucleic acids into the reconstituted Sendai viral envelopes?

These experiments were done in collaboration with Thomas Amatruda in Melvin Simon's research group in biology. Tom Amatruda was looking for an alternate method for transfecting HL60 cells as other more standard methods had failed. The literature protocols for using reconstituted Sendai viral envelopes as delivery vehicles of DNA were optimized.

Footnotes and References

1 Bangham, A., Standish, M. and Watkins, J. (1965) Diffusion of Univalent ions across the Lamellae of Swollen Phopholipids. *J. Mol. Biol.*, **13**, 238-252.

2 Reviewed by
Szoka, F., and Papahadjopoulos, D. (1980) Comparative Properties and Methods of Preparation of Lipid Vesicles (Liposomes). *Ann. Rev. Biophys. Bioeng.*, **9**, 467-508.

3 For a recent review of liposomes as therapeutic delivery systems see
Roerdink, F., Daemen, T., Bakker-Woudenberg, I., Storm, G., Crommelin, D., and Scherphof, G. (1989) "Therapeutic Utility of Liposomes," in Drug Delivery Systems, Vol. 1, (eds. P. Johnson and G. Lloyd), Ellis Horwood Ltd., 1-30.

4 Hwang, K., and Mauk, M. (1977) Fate of lipid vesicles *in vivo*: A gamma-ray perturbed angular correlation study. *Proc. Natl. Acad. Sci. USA*, **11**, 4991-4995.
Mauk, M., and Gamble, R. (1979) Stability of lipid vesicles in tissues of the mouse: A gamma-ray perturbed angular correlation study. *Proc. Natl. Acad. Sci. USA*, **76**, 765-769.

5 Patel, K., Schuh, J., and Baldeschwieler, J. (1985) Modification of vesicle surfaces with amphiphilic sterols. Effect on permeability and *in vivo* tissue distribution. *Biochimica et Biophysica Acta*, **814**, 256-264.
Wu, P., Wu, H., Tin, G., Schuh, J., Croasmun, W., Baldeschwieler, J., Shen, T., and Ponpipom, M. (1982) Stability of carbohydrate-modified vesicles *in vivo*: Comparative effects of ceramide and cholesterol glycoconjugates. *Proc. Natl. Acad. Sci. USA*, **79**, 5490-5493.

Some recent work on modification of the surface of vesicles with polyethylene glycol derivatives has led to reported increase in circulation time,
Senior, J., Delgado, C., Fisher, D., Tilcock, C., and Gregoriadis, G. (1991) Influence of surface hydrophobicity of liposomes on their interaction with plasma protein and clearance form the circulation: studies with poly(ethylene glycol)-coated vesicles. *Biochimica et Biophysica Acta*, **1062**, 77-82.
Blume, G., and Ceve, G. (1990) Liposomes for the sustained drug release *in vivo*. *Biochimica et Biophysica Acta*, **1029**, 91-97.
Klibanov, A., Maruyama, K., Beckerleg, A., Torchilin, V., and Huang, L. (1991) Activity of amphipathic poly(ethylene glycol) 5000 to prolong the circulation time of liposomes depends on the liposome target size and is unfavorable for immunoliposome binding to target. *Biochimica et Biophysica Acta*, **1062**, 142-148.

6 There is limited literature on this application, perhaps due to its development principally in industry. An article with some references is
Grant, C., Hamilton, K., Hamilton, K., and Barber, K. (1989) Physical biochemistry of a liposomal amphoteracin B mixture used for patient treatment. *Biochimicia et Biophysica Acta*, **984**, 11-20.
Also see USA patent number 5043107, entitled "Preparation of SUV including polyene antifungal antibiotics, issued to Vestar Inc., San Dimas, CA, which gives some information on this application.

7 Proffitt, R., Williams, L., Presant, C., Tin, G., Uliana, J., Gamble, R., and Baldeschwieler, J. (1983) Liposomal Blockade of the Reticulendothelial System: Improved Tumor Imaging with Small Unilamellar Vesicles. *Science*, **220**, 502-505.
Proffitt, R., Williams, L., Presant, C., Tin, G., Uliana, J., Gamble, R., and Baldeschwieler, J. (1983) Tumor-Imaging Potential of Liposomes Loaded with In-111-NTA: Biodistribution in Mice. *J. Nuc. Med.* , **24**, 45-51.

8 Straubinger, R., Hong, K., Friend, D., and Papahadjopoulos, D. (1983) Endocytosis of Liposomes and Intracellular Fate of Encapsulated Molecules: Encounter with a Low pH Compartment after Internalization in Coated Vesicles. *Cell*, **32**, 1069-1079.

9 Membrane fusion has been reviewed by
Blumenthal, R. (1989) Membrane Fusion. *Curr. Top. in Membranes and Transport*, **29**, 203-254.
Wilchut, J., and Hoekstra, D. (1984) Membrane Fusion: from liposomes to biological membranes. *TIBS*, 479-483.
Bentz, J., and Ellens, H. (1988) Membrane Fusion: Kinetics and Mechanisms. *Colloids and Surfaces*, **30**, 65-112.
Nir, S., Bentz, J., Wilchut, J., and Duzgunes, N. (1983) Aggregation and Fusion of Phospholipid Vesicles. *Progress in Surface Sciences*, **13**, 1-124.

10 For review of the forces which prevent bilayers from fusing see
Rand, R., and Parsegian, V. (1989) Hydration forces between phospholipid bilayers. *Biochimica et Biophysica Acta*, **988**, 351-376.

11 Reviewed by
Tyler, K.L. and Fields, B. N. (1990) "Pathogenesis of Viral Infections," from Virology, (eds. B. N. Fields, D. M. Knipe, et al.), Raven Press, 191-239.

12 Briefly reviewed by
Kaufman, R. (1990) Vectors Used for Expression in Mammalian Cells. *Meth. Enzymol.* , **185**, 487-511.

13 Murphy, F., and Kingsbury, D. (1990) "Virus Taxonomy", from Virology, (eds. B. N. Fields, D. M. Knipe, et al.), Raven Press, 9-36.

14 Reviewed by
Hoekstra, D., and Kok, J. (1989) Entry Mechanisms of Enveloped Viruses. Implications for Fusion of Intracellular Membranes. *Bioscience Reports*, **9**, 273-305.
White, J. (1990) Viral and Cellular Membrane Fusion Proteins. *Annu. Rev. Physiol.*, **52**, 675-697.

15 There is no overall review article on viral glycoprotein reconstitution. I have listed several key papers for each virus reconstitution.

Sendai-
Vainstein, A., Hershkovitz, M., Isreal, S., Rabin, S., and Loyter, A. (1984) A New Method for Reconstitution of Highly Fusogenic Sendai Virus Envelopes. *Biochimica et Biophysica Acta*, **773**, 181-188.
Inuoe, J., Nojima, S., and Inoue, K. (1985) The activity of membranes reconstituted from HVJ envelope proteins and lipids to induce hemolysis and fusion between liposomes and erythrocytes. *Biochimica et Biophysica Acta*, **816**, 321-331.

Influenza-

Nussbaum, O., Lapidot, M., and Loyter, A. (1987) Reconstitution of Functional Influenza Virus Envelopes and Fusion with Membranes and Liposomes Lacking Virus Receptors. *J. Virol.*, **61**, 2245-2252.

Sizer, P. , Miller, A., and Watts, A. (1987) Functional Reconstitution of the Integral Membrane Proteins of Influenza Virus into Phospholipid Liposomes. *Biochemistry*, **26**, 5106-5113.

Semliki Forest Virus-

Helenius, A., Sarvas, M., and Simons, K. (1981) Asymmetric and Symmetric Membrane Reconstitution by Detergent Elimination. *Eur. J. Biochem.*, **116**, 27-35.

Vesicular Stomatitis Virus-

Petri, W. and Wagner, R. (1979) Reconstitution into Liposomes of the Glycoprotein of Vesicular Stomatitis Virus by Detergent Dialysis. *J. Biol. Chem.*, **254**, 4313-4316.

Metsikko, K., Meer, G. and Simons, K. (1986) Reconstitution of the fusogenic activity of vesicular stomatitis virus. *EMBO J.*, **5**, 3429-3435.

16 For a good text on viral infection of the CNS see,

Johnson, R. T. (1982) Viral Infections of the Nervous System, Raven Press, 1-288.

A good review on the properties of mumps see

Wolinsky, J. and Waxham, M. (1990) "Mumps Virus", from Virology, (eds. B. N. Fields, D. M. Knipe, et al.), Raven Press, 989-1012.

17 Articles on the Blood Brain Barrier

Bodor, N. (1985) Targeting of Drugs to the Brain. *Meth. Enzymol.*, **112**, 381-396.

VanDeurs, B. (1980) Structural Aspects of Brain Barriers, with Special Reference to the Permeability of the Cerebral Endothelium and Choroidal Epithelium. *International Review of Cytology*, **65**, 117-191.

Bates, I. (1985) Permeability of the blood-brain barrier. *TIPS*, 447-450.

Cutler, R. (1980) Neurochemical Aspects of Blood-Brain-Cerebrospinal Fluid Barriers. from Neurobiology of Cerebrospinal Fluid, Vol 1., 41-51.

Westergaard, E. (1980) Ultrastructural Permeability Properties of Cerebral Microvasculature Under Normal and Experimental Conditions After Application of Tracers. *Advances in Neurology*, **28**, 55-73.

Chapter 2: Use of the fluorescent probes R18 and NBD-PE/Rd-PE to measure virus fusion with cell membranes

Introduction

Membrane fusion can be described as the process where continuity is established between the lipid bilayers of two separate membranes (Figure 1a) (Reviewed by Blumenthal, 1989). After this continuity has been established the contents of the membranes are free to mix. The mechanisms and intermediates in membrane fusion have not yet been well characterized. Membrane fusion is an important process in the internal organization of living cells as it allows compartimentalization to be a reversible process. In animal cells, membrane vesicles are used to transport materials into the cell and to store materials for release into the extracellular environment.

The work in this thesis has focused on the fusion of virus membranes with cellular membranes. This fusion process is catalyzed by viral glycoproteins responsible for adhesion of the virus to the cellular surface and fusion with the cellular membrane (reviewed by Hoekstra and Kok, 1989, White, J., 1990). The fusion process is necessary for introduction of the viral genetic material into the cellular interior (Figure 1b).

The fusion of lipid membranes can be measured using a variety of fluorescent probes. These probes can be grouped into two general classes, membrane mixing probes and contents mixing probes. Both types of probes have been used extensively to observe model fusion events (calcium induced fusion, peptide induced fusion, etc.) between liposomes. The primary contents mixing probe pairs used for examining liposome fusion are

Tb/DPA[1] and ANTS/DPX. These probes are loaded into separate vesicle populations and upon vesicle fusion interact to cause an increase (Tb/DPA) or decrease (ANTS/DPX) in fluorescent intensity. These probes must be loaded during formation of the liposomes; this is also true with the majority of fluorescent membrane mixing lipid probes. Lipid probes also give an increase or decrease in fluorescent intensity upon fusion due to the dilution or mixing of the probes into other bilayers. The membrane probes used in this thesis were R18 and the resonance energy transfer pair NBD-PE / Rd-PE.

R18

For experiments with intact cells or virus, probes that must be "loaded" into the system during formation are not useful. A membrane probe that does allow labeling of intact systems is octadecyl rhodamine B (R18). The probe can be dissolved in a small solution of ethanol and mixed with a suspension of cells or virus and will spontaneously insert into the cellular or viral bilayer. R18 is essentially a rhodamine modified with a long alkyl tail. This hydrophobic tail causes the probe to partition preferentially into the bilayer (Ediger et al., 1984) and reduces the rate of exchange out of the bilayer (Figure 2). The probe was originally synthesized as a resonance energy transfer probe in conjunction with the probe F18 (Keller et al., 1977). The probe was reintroduced as a method to monitor membrane fusion using the probe alone in a self quenching fashion (Hoekstra et al., 1984)

The probe is selfquenching at concentrations up to 9 mole percent of the membrane. The quenching is linear over this range (Figure 3c,d,f). The probe's emission band (max ≈ 590 nm) overlaps with its excitation band (max

≈ 560 nm)(Figure 3e). If resonance energy transfer were the dominant mechanism of quenching then one would expect a nonlinear quenching curve ($1/r^6$ for normal resonance energy transfer). Resonance energy transfer is the dominant mechanism of quenching at very low concentrations (< 1%) while quenching at higher concentrations (1-10%) is due to the formation of R18 aggregates that are highly quenched, i.e., a static quenching mechanism (Johansson and Niemi, 1987, Ediger et al., 1984). Under the conditions of the experiments conducted in this thesis, no signs of R18 photobleaching were observed.

For a R18 experiment with virus, the virus is labeled with R18 and then purified by centrifugation or column chromatography to remove free R18. The labeled virus is suspended in buffer in a cuvette at regulated temperature in the fluorimeter sample chamber. The fluorescence intensity is recorded continually and target membrane is added to the cuvette. A kinetic recording is taken as shown in Figure 4. As the viral particles fuse with the target membrane the fluorescent intensity increases. This is due to the dilution of the R18 probe from the viral membrane into the cellular membrane (Figure 5). The lateral movement rate of the probe in bilayers is very rapid and should not serve as a rate limiting factor in observation of the fusion event (Chen and Blumenthal, 1989, Rubin and Chen, 1990, Morrison et al., 1990).

To determine the fluorescence intensity of the probe in the unquenched or infinitely diluted state the labeled viral sample is treated with the detergent Triton X-100 at a concentration of 1% at the completion of the fusion experiment. This disrupts the membrane vesicles and disperses the R18 probe into detergent micelles. In the literature it is often assumed that

this intensity represents the 100% value of dequenching although we have not been able to find any direct data presentation confirming this assumption. A correction factor might be required as the detergent micelle should present a different dielectric environment than the lipid membrane and the R18 may exist in different aggregation states in the detergent micelles as compared to the lipid membrane. We have tested this assumption by preparing PC liposomes containing different mole percents of R18 and determining their fluorescent intensities. As the percentage of R18 decreased a linear intercept of the abscissa was found, representing fluorescence at infinite dilution (Figure 3a,b). This value agreed very closely (±5%) with the value given when the vesicles were treated with 1% Triton X-100. Other workers have assigned a correction value of 1.54 to the triton intensity when working with cellular membranes. This value was determined by adding known amounts of R18 to the cells and measuring the quenching observed with and without Triton X-100 (Blumenthal et al., 1987). This correction value might be due to the association of R18 with proteins in the membrane.

The experiments in this thesis all involve the study of whole or reconstituted virus fusing with ghost erythrocytes or mammalian cells. The surface area of these target membranes is many times larger than the surface area of the virus. For Sendai virus fusing with an erythrocyte ghost this ratio is 1000:1 (.125 μ^2 surface area for Sendai versus 125 μ^2 for an erythrocyte), for fusion with a green monkey kidney CV-1 cell the ratio is 16,000:1 (with a surface area of 2000 μ^2 for the CV-1 cell). Thus when a virus fuses with a cell, the R18 probe can be considered to dilute nearly infinitely into the target membrane and to be subject to no selfquenching. Thus if one had 10 viruses that were 90% quenched giving a fluorescent signal of 100 units (1000 units in

the unquenched state), when one of the viruses fused (10% fusion) the fluorescent intensity would increase to 190.

The assumption of infinite dilution is not strictly correct in cases where a large number of fusion events occurs with a target cell. We have derived a correction formula to determine the true number of fusion events based on the ratio of surface area of the virus to the target cell and the amount of R18 in the viral bilayer. The formula is:

$$\text{True \# Fusion Events (N)} = \frac{\text{Observed \# Fusion Events (OBS)}}{1-\left(\frac{\text{N x \% Quench of R18 in the Virus (Q)}}{\text{Do+N}}\right)},$$

where Do is the ratio of surface areas of the virus and target cell. R18 quenches ≈ 10 % per mole % it constitutes of the native lipid, i.e., 50% quenching is observed when the R18 is added at 5 mole percent of the membrane lipid (Figure 3c,d,f). This equation can be rearranged to give

$$N = \frac{-Do + OBS \pm \sqrt{(Do - OBS)^2 - 4(1-Q)(-OBS \times Do)}}{2-2Q}.$$

For the amount of R18 used in our usual experiments (3%) in which up to 20 virus fuse with one erythrocyte the correction is trivial (20 events correct to 20.1 events).

Perturbation of the viral interaction process by the R18 has been examined by a number of workers. Some conflicting evidence has been presented. Examination of R18 labeled Sendai showed equivalent binding and hemolysis with or without label (Hoekstra et al., 1985). However, other evidence has shown that the binding of labeled VSV virus to liposomes is

enhanced upon R18 labeling (Puri et al., 1991). Labeled virus appears to work equivalently to unlabeled virus in cell syncytial assays (Anne Walter, personal comm.).

In Sendai and mumps virus the binding and membrane fusion activities are contained in separate glycoproteins. Control experiments can be conducted to confirm that the dequenching of the R18 probe is due to membrane fusion and not due to other transfer processes. Sendai virus is able to fuse with ghost erythrocytes (Hoekstra et al., 1985). Trypsin treatment of Sendai virus causes cleavage of the F protein and should prevent viral fusion. After trypsin treatment a slow dequenching (slower than that observed with untreated virus) occurred in all of our experiments (Figure 4). This observation led us to consider carefully possible artifacts with the R18 assay and conduct a number of control experiments that are outlined below.

Mechanisms of Dequenching

I would propose that there are four mechanisms by which the virus associated R18 could dequench upon addition of target cells to a virus containing solution.

The first mechanism is transfer through solution, i.e., the probe leaves the viral membrane, crosses solution, and inserts into the target membrane. The probe would likely be quenched in an aqueous environment so any free probe would not give any fluorescent intensity. The probe could also leave the viral membrane and form micelles but again these would be quenched. Fluorescent microscopy shows that the R18 probe is actually incorporated into the target cell after incubation with labeled virus indicating that the probe

does end up in the target membrane. Control experiments which inhibit viral binding to the cells totally eliminate dequenching upon the addition of target cells indicating that transfer through solution is not a mechanism for transfer (Figure 4). The binding can be inhibited by treatment with protease K or extracellular viral receptor (fetuin, which contains a large number of terminal sialic acid residues that serve as the viral receptor on cells).

The second possible mechanism of transfer is proximal transfer, transfer of the R18 probe to the target cell when the virus is in close proximity or bound to the cellular surface. This type of activity can measured by using a control experiment where virus binds to the cell but does not fuse. Trypsin, PMSF (Phenyl Methyl Sulphonyl Fluoride), and dithiothreitol are all capable of selectively inactivating the Sendai F protein while leaving the binding protein HN intact. As already mentioned, trypsin treatment does not completely inhibit the R18 dequenching, i.e., a low residual rate is apparent (Figure 4). A number of papers in the literature also use R18 to examine viral fusion and show some residual dequenching after trypsin treatment, although the authors of these papers do not comment on this effect. The residual dequenching observed from the literature is 13±6% (n=9) of the uninhibited fusion values (Figure 6). An examination of my accumulated data shows an average of 15% residual dequenching of the uninhibited dequenching value (Figure 7).

R18 labeled Sendai virus treated with trypsin was prepared and allowed to interact with cells at various ratios of virus to target cell. The observed dequenching was compared to that obtained with untreated virus. The amount of dequenching observed correlated well with the ratio of target cells to virus as would be expected if binding were a precursor to transfer, as a

greater amount of target cells provides a larger number of receptors for viral binding (Figure 8).

The observed slow dequenching after trypsin treatment could be due to non-F dependent fusion, incomplete inactivation of F by the trypsin treatment, or spontaneous proximal transfer.

Trypsinized virus is incapable of causing cell-cell fusion and trypsinized virus has not been observed to fuse by electron microscopy. Reconstituted vesicles containing just the HN protein are unable to fuse with cellular membranes at neutral pH. The HN protein is capable of causing membrane fusion at low pH but at the neutral pH used in these experiments non-F dependent fusion is unlikely.

Gel analysis of trypsin treated virus shows that trypsin will cleave the F protein until it is no longer visible on a silver stained gel. Even if this worker's trypsin treatments were inadequate it is unlikely that all those reported in the literature are also inadequate although there may be some F proteins which are protected from cleavage. Further it has been suggested to me that the R18 may protect the F protein from trypsin treatment. A series of control experiments were run where the trypsin treatment was applied at various times in the preparation procedure. In addition both ultracentrifugation and gel chromatography were compared for purification. In all cases the residual dequenching existed (Figure 9).

Further evidence for spontaneous transfer was found by allowing the virus to interact with target cells for long time periods. After 18 hours of interaction the fluorescent dequenching in trypsin treated samples was the same as untreated samples (Figure 10). The *rate* of dequenching was much faster initially in untreated samples but the *extent* of dequenching was

equivalent. In both cases the number of binding sites should be the same and hence over long time periods equilibrium of the probe in the two bilayers is reached in both treated and untreated samples.

Spontaneous proximal transfer has been shown to occur in the interaction of R18 labeled influenza virions with small unilamellar vesicles (Wunderli-Allenspach and Ott, 1990)

A third mechanism of dequenching is protein mediated transfer. In this mechanism the fluorescent probe transfer is catalyzed by the presence of hydrophobic material such as proteins which would bridge the gap between bilayers (Figure 11). The Sendai F protein contains a highly hydrophobic N terminus which most likely enhances lipid transfer between bilayers as an early intermediate to membrane fusion. Hydrophobic polymers such as PEG have been shown to enhance transfer of lipids in and out of membranes (Wu and Lentz, 1991). The range of effects of hydrophobic molecules (such as the mellitin peptide) should range from enhanced transfer to hemifusion (fusion of the outer bilayers) to full fusion to membrane disruption.

Due to the hydrophobic nature of the R18 molecule it could directly associate with the hydrophobic portions of the F protein. Fluorescent spectra were taken of R18 labeled virus as a control. The fluorescence maxima of the probe is different for association with protein or lipid (Loyter et al., 1988, Chejanovsky et al., 1988). The spectra of R18 labeled virus indicated an emission wavelength consistent with the probe being present in the lipid bilayer , λ=590 nm (Figures 3e,12). Kinetic spectra were taken during trypsin cleavage of labeled virus. If the probe were associated with the F protein then one would expect the fluorescence of the probe to go down as the F protein is cleaved away from the viral surface and exposed to buffer. The fluorescent

intensity actually increased slightly after trypsin cleavage (Data not shown). This result is difficult to interpret, although the cleavage of the F protein should result in altered fluidity in the viral membrane which could alter the aggregation state of the R18 molecule.

The fourth mechanism of dequenching is actual membrane fusion and transfer of the probe into the target membrane by lateral diffusion through the bilayer. The lateral diffusion process is very rapid and should not be a rate controlling factor in these virus-cell fusion experiments.

It is extremely difficult to carry out a control experiment that will distinguish protein enhanced transfer from actual membrane fusion. Correlation of membrane fluorescent probes with other evidence is one method. Membrane fusion does exist as shown by electron microscopy of Sendai virus fusing with target membranes (Knutton, 1977).

A fluorescent contents mixing assay could also provide correlatory quantitative measurement of fusion to which the membrane mixing assays could be compared. Membrane and contents mixing can occur at different rates due to the requirement of opening of a pore between the fused membranes before contents mixing can occur (Figure 1a). A fluorescent contents mixing assay should allow visualization of membrane fusion under a fluorescent microscope as fluorescent molecules are delivered to the interior of a target cell, given that the target cell is large enough for visualization. The best example of this type of experiment in the literature is a measurement of the fusion of membrane labeled (R18) and content labeled (NBD-taurine) ghost erythrocytes fusing with cells expressing the influenza HA fusion protein on their surface (Morris et al., 1988, Sarkar et al., 1989). In this case the kinetic profiles of dequenching were similar for both probes but

the measured extent of fusion differed greatly (20% of the R18 and 80% for the NBD-Taurine).

Reconstituted Sendai viral envelopes (RSVE) can be loaded with material during their formation. Chapter 6 of this thesis discusses experiments where these viral vesicles were used to deliver DNA to cellular interiors. Qualitatively, it is clear that DNA delivery does take place but the quantitation of fusion by DNA delivery is not feasible. During these experiments the RSVE were loaded with carboxy fluorocene, ethidium bromide, DNA complexed with ethidium bromide, or trypan blue , allowed to interact with cells, and examined under a fluorescence microscope. Carboxy fluorocene was visually observed in the interior of the cells but this could not be documented with photography as the bleaching of the dye was more rapid than the time required for photographic exposure. No successful observation of the Ethidium Bromide, Ethidium Bromide/DNA or trypan blue in the interior of the cells was made. The cells exposed to RSVE loaded with ethidium bromide were dead by the next day, most likely due to the introduction of EtBr into their interiors.

Several attempts were also made to develop a quantitative contents mixing assay using RSVE or Sendai in order to compare fusion rates with the R18 membrane mixing probe.

Whole Sendai virus were mixed with EtBr loaded erythrocyte ghosts. If fusion occurs then the EtBr in the ghost interior should be able to intercalate into the viral RNA and an increase in fluorescence should be observed. At the concentrations at which the experiment was conducted no change in signal was found. Control experiments showed that the maximal potential increase in fluorescence was less than the noise in the fluorescent

signal. (The signal was 500±5 fluorescence units, with 5 being the maximal change in fluorescence upon addition of amounts of RNA equivalent to the viral interiors to amounts of EtBr equivalent to the ghost interiors.) An ethidium dimer probe was also loaded into ghosts as its fluorescent enhancement is reported to be 50 times greater than EtBr upon binding to nucleic acid (Markovits et al., 1979). Upon mixing of virus and ghosts, no change in fluorescence signal was found when using this probe.

The use of carboxyfluorocene loaded RSVE to quantitatively measure fusion was also explored, but the RSVE appeared to be leaky in containing CF. CF is also prone to photobleaching during long term light exposure.

RSVE were loaded with Rd-Dextran polymer at a concentration of 1 mM and mixed with ghost erythrocytes. No change in fluorescent intensity was observed during controled lysis of the virus with Triton X-100, showing that the polymer was not selfquenched at this concentrations.

NBD-PE/ Rd-PE

The fluorescent membrane probes NBD-PE and Rd-PE were used in a number of experiments in this thesis (Figure 13). These fluorescent lipids can be incorporated into liposomes during formation or into reconstituted virus during detergent dialysis reconstitution. The emission band of the NBD probe overlaps the excitation band of the Rhodamine-PE, thus allowing a resonance energy transfer to occur (Figure 14). In our experiments the probes are both incorporated into the same membrane at a concentration of 1-2 mole percent of the membrane. We (C. DiSimone and A. Wein) have generated quenching curves for several different ratios of NBD/Rd (Figure 15). Upon

fusion with an unlabeled target membrane, the probes dilute into the target membrane and the energy transfer rate is decreased due to a reduced density of probes (Struck et al., 1981). The change in the intensity of the NBD emission band is the most reliable indicator of the fusion event; upon fusion the intensity increases. The maximal dequenching is determined in the same fashion as with the R18 assay: the vesicles are solubilized in 1% Triton X-100. The NBD probe has been reported to be slightly quenched in the micelle (Struck et al., 1981), but the correction factor for this behavior was not reported in this reference or in subsequent reports. The identical correction formula as given for the R18 assay can be applied in cases where large number of fusion events occur.

Alternately the NBD/Rd probes can be incorporated into separate vesicle populations which fuse together and thus cause a decrease in the intensity of the NBD emission. This method is more prone to artifactual signals as vesicles which are aggregated but not fused can cause quenching of the NBD emission signal (Figure 16) (Duzgünes et al., 1987).

Comparison of NBD/Rd and R18

The fluorescent dequenching kinetic traces given during interaction of RSVE with ghost erythrocytes were measured using either R18 or NBD-PE/Rd-PE (Figure 17). The NBD/Rd probes could be incorporated into the RSVE during formation of the vesicles. The NBD/Rd probes should be less likely to undergo transfer out of the membrane due to the presence of two acyl chains as opposed to one for the R18. Indeed, following trypsin treatment no dequenching of the NBD emission was observed, providing further

evidence that the F protein is necessary for fusion, that trypsin treatment can be 100% effective, and that proximal transfer occurs when using the R18 assay. Curiously, the R18 assay reported less dequenching than the NBD-Rd assay at equal ratios of virus to cells (Figure 18). The R18 molecule may not disaggregate completely upon fusion; this conclusion is supported by the results of Sarkar et al. (Sarkar et al., 1989) in which the R18 reported less fusion than a NBD-taurine contents mixing assay. Alternatively, the R18 molecule might inhibit membrane fusion.

Contents Mixing Assays

The contents mixing probe pair Tb/DPA were used to conduct experiments on the effects of chaotropic agents on Calcium induced fusion of phophatidylserine vesicles (data not shown). Unfortunately, I was unable to see any fluorescence intensity alterations when the Terbium was chelated with DPA. Another worker in our laboratory (R. Goodrich, personal communication) was unable to achieve any success with this probe system to measure membrane fusion.

A recent report presents data showing that the probe DPX of the ANTS/DPX pair used to monitor liposome fusion causes major alterations in the membrane behavior in terms of fluidity and hydrophobicity (Walter et al., 1991). Many of the literature results gathered with this probe may need to reinterpreted in light of this observation.

Kinetic Analysis

With an understanding of the methodology and shortfalls of the fluorescent assays, a kinetic evaluation of the obtained data can be undertaken. The virus target interaction can most simply be described by the scheme

$$V+nG \rightarrow Fused,$$

where V is Virus, nG is a cellular receptor and Fused is the Fused product. In the following fittings ghost erythrocytes (G) with n receptors on their surface act as the fusion target for the virus.

The rate of formation of fused product can be described by the equation,

$$\frac{d(Fused)}{dt} = k\,[Vo - Fused][nGo - Fused].$$

The amount of fused product at time t can be determined by integrating the formula,

$$\int k\,dt = \int \frac{d(Fused)}{(Vo - Fused)(nGo - Fused)}$$

with the limit Fused=0 when t=0 to give,

$$kt = \frac{1}{(Vo - nGo)} \ln\left(\frac{nGo * (Vo - Fused)}{Vo * (nGo - Fused)}\right)$$

which can be rearranged to the form,

$$\text{Fused} = \left(\frac{Vo * e^{k(Vo - nGo)t} - Vo}{\frac{Vo}{nGo} * e^{k(Vo - nGo)t} - 1} \right).$$

This function was put into a macro subroutine in the plotting and fitting program IGOR and used to fit a number of kinetic curves. Fittings for three experiments (Figures 8,17,19) already presented in this chapter are shown (Figures 20,21,22).

The fusion of NBD/Rd labeled RSVE with ghosts is shown in Figure 17 and fits in Figure 20. In this experiment the number of ghost erythrocytes was increased while the amount of RSVE was held constant. As the number of ghosts was increased, the maximum amount of RSVE fused plateaued at a value of 31.6%. Thus only about 31.6% of the RSVE were fusion competent. The number of ghost sites involved in fusion in each experiment can be determined by dividing the concentration of fusion events by the concentration of ghosts. Under non saturating conditions, low ratio of RSVE to ghost, increasing the amount of ghost leads to a linear decrease in the number of fusion sites per ghost. However, as saturation of the surface occurs the number of apparent sites will near the theoretical maximum. In this experiment a maximum of 87 sites of fusion per ghost was determined. These values were used to determine RSVE and ghost concentrations and kinetic fitting were determined. A maximal k of 2.3 $x10^8$ M^{-1} sec^{-1} was determined. As the concentration of ghosts was increased the apparent k linearly decreased.

A more exact description of the viral cell interaction would be

$V+nG \Leftrightarrow VGB \rightarrow Fused,$

where VGB represents unfused bound virus. No exact solvation for the amount of Fused material can be derived, but numerical integration can be used to model this behavior. A simple looped algorithm of the Euler form can be used,

```
From 0 to time t, increment i
        dVGB= (k1*[V]*[nG] -k2[VGB] - k3 [VGB])*i
        dFused= k3*[VGB]*i
        VGB=VGB+dVGB
        Fused=Fused+dFused
        V=Vo-VGB-Fused
        nG=nGo-VGB-Fused
Next t.
```

k1 is the forward rate in the binding interaction, k2 is the reverse rate in the binding interaction, and k3 is the fate of fusion for bound virus.

Programs were initially written in the basic language with both Euler and Runge Kutta methods (Boyce and DiPrima, 1977) for solution of a number of kinetic models (see Chapter 4 on mumps). Ultimately the mass action model proved to be optimal for data fitting of our data on Sendai fusion. In order to increase computation speed, a data modeling program written by David Baselt in the language C was modified to fit mass action kinetic data. The program included a "evolutionary" fitting routine which allow optimization of data fits. This subroutine takes the provided rate guesses and randomly varies them 0 to 10% and then computes the closeness

of fit by the standard deviation from the data. A series of 10 variants are compared to the original data and optimal fits are selected for the next round of evolution.

Optimal data fitting with mass action kintics requires fitting multiple curves with the same sets of rate constants. For a single curve a number of different combinations of rate constants can be found that fit the curve very precisely. Most notably increasing or decreasing the k1 rate can be compensated for by doing the opposite to the k3 value. In figure 23 three fits to two data curves from the NBD/Rd RSVE experiment are shown. While three set of constants can fit the lower data curve, only one set of constants will fit *both* curves.

For the NBD/Rd labeled RSVE a consistent set of rate constants was found to fit all of the data curves. For RSVE fusion activity of 31.7% and 87 RSVE receptors per ghost, the constants obtained were 1 $x10^9$ $M^{-1}sec^{-1}$ for k1, .0223 sec^{-1} for k2, and .0078 sec^{-1} for k3. The data curves have some sigmoidal character which is fit more accurately by the mass action model (Figure 24) rather than the simpler exponential fitting (Figure 21).

Mass action fits were also obtained for the data on Sendai fusing with erythrocyte ghosts as shown in Figures 8 and 19. For viral fusion activity of 15% and 8 receptors per ghosts, *optimal* values of 5.41 $x10^9$ $M^{-1}sec^{-1}$ for k1, 8.7 $x10^{-4}$ sec-1 for k2 and .02 sec-1 for k3 were obtained from the data in Figure 8. Values of 3.87 $x10^9$ $M^{-1}sec^{-1}$, 7.5 $x10^{-4}$ sec^{-1} and .04±.01 sec^{-1} were obtained from the data in Figure 19 , given viral fusion activity of 14±2% and 7 receptors per ghost. This second set of constants also gave a very good fit to the first data set. Given the various errors in data measurement and protein determination, general rate constants of 4.5±1 $x10^9$ $M^{-1}sec^{-1}$, 8±1 $x10^{-4}$ sec^{-1},

and .035 ±.015 sec^{-1} for k1,k2, and k3, respectively, with 7.5 ±1 receptor sites per ghost, adequately fit all the data on fusion of Sendai with erythrocyte ghosts.

The rate constants show a very rapid binding process with a much slower release from the vesicle surface, consistent with other studies of Sendai fusion (Hoekstra and Klappe,1986). The apparent number of receptors for Sendai fusion interaction (n=8) is much lower than that reported in the literature (n=180) (Hoekstra and Klappe, 1986). The method used in the literature to determine the number of receptors was long term incubation of R18 labeled virus with cells. As discussed above this could lead to spontaneous dequenching occurring and artificially high estimation of the number of fusion events.

The apparent number of fusion sites for the reconstituted virus was higher than the number for whole virus. This may be a real effect or due to a poor estimate of the number of particles. The number of whole viral particles was determined from the molecular weight of the virus and the amount of protein per virus: MW= 5-7 $x10^8$ MW, protein content= 70%, gives 1.3 $x10^9$ particles per microgram protein. For reconstituted virus only glycoprotein is recovered. The glycoprotein was estimated to make up 20% of the viral protein and thus the number of particles was estimated as five times higher for a set amount of protein, 6.5 $x10^9$ particles per μg protein. The reconstituted viral particles tend to be actually smaller than whole virus so this would be a *low* estimate of the number of viral particles. The interaction of reconstituted virus with ghost erythrocyte may be less specific or fusion less impeded, perhaps due to the loss of the matrix protein during reconstitution.

This protein lines the inside of the viral envelope and may deter viral membrane instability and fusion.

Conclusions

The probe octadecyl rhodamine was originally chosen to measure viral membrane fusion due to its ability to label whole virus, and due to the presentation of this system in the literature as a simple method to measure membrane fusion. Careful examination of the behaviors of this probe has shown that the probe is susceptible to providing artifactual signal due to proximal transfer between adjacent membranes. With the R18 probe one should be careful of attributing slow dequenching (<1% per minute) as membrane fusion.

The general literature interpretation of the mode of quenching of R18 as resonance energy transfer is incorrect, as shown by the quenching curve of the probe, an aggregation behavior is likely to be responsible for the quenching.

Even when accounting for the slow proximal transfer behavior with control experiments, the fast dequenching seen in viral cell fusion can not be attributed with one hundred percent certainty to be membrane fusion. A protein mediated transfer of probe could account for this behavior. Qualitative observation by electron microscopy or fluorescent microscopy shows that fusion does occur. Attempts to correlate contents mixing with membrane mixing have not been successful. Furthermore, it is clear that the rates of content mixing may not be the same as membrane mixing due to difference in the mechanics of the two behaviours. The preferred literature contents mixing assays are subject to other artifactual behaviors. At this time

there is no "yardstick" assay for membrane fusion to which other assays can be compared. Comparison of the different techniques to one another can produce a variety of "fusion" values (Duzgunes et al., 1987). Comparison of the R18 and NBD/Rd probes actually showed the R18 to *underreport* the fusion reported by NBD/Rd, the opposite of what one would expect if proximal transfer were occuring with the R18. The data from these assays can be used in a semi quantitative fashion to compare various cells and virus and to study inhibition processes. To facilitate reading throughout the rest of this thesis I will in general refer to rapid dequenching as fusion, though the reader should keep the above discussion in mind.

The NBD/Rd membrane fusion assay system has the advantage of using double chained lipid membrane anchors that are less susceptible to transfer processes. This assay system was used to study fusion when allowed (with reconstituted virus) *after* the problems with R18 were recognized.

Kinetic models of the early dequenching rates were constructed and numerical iteration by computer was used to determine optimal rate constants. A rapid and tight binding interaction ($4x10^9$ M^{-1} sec^{-1} forward and $7.5x10^{-4}$ sec^{-1} reverse) was apparent as was a limited number of viral fusion sites per ghost.

[1] Abbreviations: Tb, Terbium; DPA, dipicolinic acid; ANTS, 1-aminonaphthalene-3,6,8-trisulfonic acid; DPX, N,N'-*p*-xylylenebis(pyridinium bromide); NBD-PE, 7-nitro-2,1,3-benzoxadiazol-4-yl phosphatidylethanolamine; Rd-PE, lissamine Rhodamine B sulfonyl phophatidylethanolamine; R18, octadecyl rhodamine B; F18, octadecyl fluorescein isothiocyanate; PC, phosphitidylcholine; DOPC, dioleayl phosphitidylcholine; MLV, multilamellar vesicle; SUV, small unilamellar vesicle.

Literature

Blumenthal, R. (1989) Membrane Fusion. *Curr. Top. in Membranes and Transport*, **29**, 203-254.

Blumenthal, R., Bali-Puri, A., Walter, A., Covell, D., and Eidelman, O. (1987) pH-dependent Fusion of Vesicular Stomatitis Virus with Vero Cells. *J. Bio. Chem..*, **262**, 13614-13619.

Boyce, W., and DiPrima, R. (1977) "Numerical Methods", from Elementary Differential Equations and Boundry Value Problems. John Wiley & Sons, New York, NY. 336-378.

Chejanovsky, N., Henis, Y., and Loyter, A. (1986) Fusion of Fluorescently Labeled Sendai Virus Envelopes with Living Cultured Cells as Monitored by Fluorescent Dequenching. *Exp. Cell. Res.*, **164**, 353-365.

Chejanovsky, N., Nussbaum, O., Loyter, A., and Blumenthal, R. (1988) Fusion of Enveloped Viruses with Biological Membranes: Fluorescence Dequenching Studies. *Subcell. Biochem.*, **13**, 415-456.

Chen, Y., and Blumenthal, R. (1989) On the use of self-quenching fluorophores in the study of membrane fusion kinetics: the effect of slow probe redistribution. *Biophysical Chemistry*, **34**, 283-292.

Citovsky, V., Blumenthal, R. and Loyter, A. (1985) Fusion of Sendai virions with phosphtidylcholine-cholesterol liposomes reflects the viral activity for fusion with biological membranes. *FEBS Letters*, **193**, 135-140.

Citovsky, V, Laster, Y., Schuldiner, S., and Loyter, A. (1987) Osmotic Swelling Allows Fusion of Sendai Virions with Membranes of Desialized Erythrocytes and Chromaffin Granules. *Biochemistry*, **26**, 3856-3864.

Citovsky, V., Rottem, S., Nussbaum, O., Laster, Y., Rott, R., and Loyter, A. (1988) Animal Viruses Are Able to Fuse with Prokaryotic Cells. *J. Biol. Chem.* , **263**, 461-467.

Düzgünes, N., Allen, T., Fedor, J., and Papahadjopoulos, D. (1987) Lipid Mixing during Membrane Aggregation and Fusion: Why Fusion Assays Disagree. *Biochemistry*, **26** , 8435-8442.

Ediger, M., Domingue, R., and Fayer, M. (1984) Picosecond studies of excitation transport in a finate volume: The clustered transport system octadecyl rhodamine B in triton X-100 micelles. *J. Chem. Phys.*, **80**, 1246-1253.

Hoekstra, D., de Boer, T., Klappe, K., and Wilchut, J. (1984) Fluorescence Method for Measuring the Kinetics of Fusion between Biological Membranes. *Biochemistry*, **23**, 5675-5681.

Hoekstra, D., Klappe, K., de Boer, T., and Wilchut, J. (1985) Characterization of the Fusogenic Properties of Sendai Virus: Kinetics of Fusion with Erythrocyte Membranes. *Biochemistry*, **24**, 4739-4745.

Hoekstra, D., and Klappe, K. (1986) Sendai Virus-Erythrocyte Membrane Interaction: Quantitative and Kinetic Analysis of Viral Binding, Dissociation and Fusion. *J. Virology*, **58**, 87-95.

Hoekstra, D., and Kok, J. (1989) Entry Mechanisms of Enveloped Viruses. Implications for Fusion of Intracellular Membranes. *Bioscience Reports*, **9**, 273-305.

Johansson, L., and Niemi, A. (1987) Electronic Energy Transfer in Anisotropic Systems. 1. Octadecylrhodamine B in Vesicles. *J. Phys. Chem.*, **91**, 3020-3023.

Keller, P., Person, S., and Snipes, W. (1977) A Fluorescence Enhancement Assay of Cell Fusion. *J. Cell. Sci.*, **28**, 167-177.

Knutton, S. (1977) Studies of Membrane Fusion. II Fusion of Human Erythrocytes by Sendai Virus. *J. Cell. Sci.*, **28**, 189-210.

Loyter, A., Citovsky, V., and Blumenthal, R. (1988) The Use of Fluorescence Dequenching Measurements to Follow Viral Membrane Fusion Events. *Methods of Biochemical Analysis.*, **33**, 129-164.

Markovits, J., Roques, B., and LePecq, J. (1979) Ethidium Dimer: A New Reagent for the Fluorimetric Determination of Nucleic Acids. *Analytical Biochemistry*, **94**, 259-264.

Morris, S. J., Sarkar, D., White, J., and Blumenthal, R. (1988) Kinetics of pH-dependent Fusion between 3T3 Fibroblasts Expressing Influenza Hemagglutinin and Red Blood Cells. *J. Biol. Chem.* , **264**, 3972-3978.

Morrison, I., Anderson, C., Georgiou, G., and Cherry, R. (1990) Measuring diffusion coefficients of labeled particles on cell surfaces by digital fluorescence microscopy. *Biochemical Society Trans.*, 938.

Nir., S. Klappe, K., and Hoekstra, D. (1986) Kinetics and Extent of Fusion between Sendai Virus and Erythrocyte Ghosts: Application of a Mass Action Kinetic Model. *Biochemistry*, **25**, 2155-2161.

Puri, A., Grimaldi, S., and Blumenthal, R. (1991) Role of Steric and Electrostatic Barriers in Fusion of Vesicular Stomatitis Virus with Cells. *Biophys. J.*, **59**, 133a.

Rubin, R., and Chen, Y. (1990) Diffusion and redistribution of lipid-like molecules between membranes in virus-cell and cell-cell fusion systems. *Biophys. J.* **58**, 1157-1167.

Sarkar, D., Morris, S., Eidelman, O., Zimmerberg, J., and Blumenthal, R. (1989) Initial Stages of Influenza Hemagglutinin-induced Cell Fusion Monitored Simultaneously by two Fluorescent Events: Cytoplasmic Continuity and Lipid Mixing. *J. Cell Biology*, **109**, 113-122.

Steck, T., and Kant, J. (1974) Preparationof Impermeable Ghosts and Inside-out Vesicles from Human Erythrocyte Membranes. *Meth. Enzymol*, **31**, 172-180.

Struck, D., Hoekstra, D., and Pagano, R. (1981) Use of Resonance Energy Transfer To Monitor Membrane Fusion. *Biochemistry*, **20**, 4093-4099.

Walter, A., Banschbach, J., and Siegal, D. (1991) Measuring Vesicle Fusion Rates Using Fluorescence Assays: Some Considerations Revisited. *Biophysical J.*, **59**, 128a.

White, J. (1990) Viral and Cellular Membrane Fusion Proteins. *Annu. Rev. Physiol.*, **52**, 675-697.

Wu, J., and Lentz, B. (1991) Mechanism of Poly(ethylene glycol)-Induced Lipid Transfer between Phosphatidylcholine Large Unilamellar Vesicles: A Fluorescent Probe Study. *Biochemistry*, **30**, 6780-6787.

Wunderli-Allenspach, H., and Ott, S. (1990) Kinetics of Fusion and Lipid Transfer between Virus Receptor Containing Liposomes and Influenza Viruses As Measured with the Octadecylrhodamine B Chloride Assay. *Biochemistry*, **29**, 1990-1997.

Methods

One μg of Sendai virus is equivalent to 1.3×10^9 viral particles while one μg of erythrocyte ghost protein is equivalent to 1.8×10^6 ghost erythrocytes. One mg of Sendai virus protein is associated with 240 nmoles of lipid.

R18 labeling of virus- General Procedure-

A solution of R18 in ethanol was prepared at a concentration of 1 mg/ml. 1 to 2 mg of virus protein was labeled with R18. The R18 was added to the virus while rapidly vortexing the viral solution at a concentration of 3 mole percent lipid or 5-10 μl (R18 mw = 731). The solution was then incubated in the dark for 30 minutes. Removal of unincorporated probe was usually accomplished by centrifugation of the viral particles at 30,000 rpm (≈ 100,000g) in the SW50.1 rotor in the ultracentrifuge for one hour.

Figure 8- 1.8 mg of Sendai viral protein was labeled with 13 μg R18 and purified by centrifugation.

Figure 9- 1.3 ml Sendai sample @ 1.8 mg/ml was divided into five experiments. Sample concentration was maintained throughout these experiments by resuspending centrifuge pellets in volumes of PBS equivalent to precentrigugation volumes. Experiments 2 and 3 contained 200 μl Sendai and were treated with 40 μl of trypsin (10 μg/μl) and then labeled with 2 μg R18. They were then purified by ultracentrifugation (2) or G50 column chromatography (3). Experiments 1,4, and 5 (900 μl) were labeled with 13 μg R18. For experiment 4, 200 μl was removed and treated with 40 μl of trypsin and then purified by ultracentrifuge. For experiment 5, 200 μl were pelleted

by ultracentrifugation, resuspended in 200 µl PBS and then treated with 40 µl trypsin. Experiment 1 was not trypsin treated. All trypsin treatments lasted for one hour at 37°.

Figure 10- 1.8 mg Sendai and .3 mg mumps virus were labeled with 12 µg and 4 µg, respectively, of R18. The sample were purified by centrifugation. 50 µg of labeled virus was then treated with 50 µg trypsin for 2.5 hours at 37° C.

Erythrocyte ghosts-

Erythrocyte ghosts were prepared by standard lysis procedures, 3 washes with PBS and then 7-8 washes with the 5P8 buffer (Steck and Kant, 1974). Ghost could be stored in liquid nitrogen with or without 10% glycerol, this appeared to have little impact on their ability to serve as fusion targets.

Fluorescent fusion measurements- General procedure-

Set amounts of labeled viral solution were added to 2ml of PBS and placed in the fluorimeter sample chamber. The chamber was maintained at a temperature of 37° for most experiments. Emission and excitation slit widths were set at 8 nm. The fluorescent signal is a unitless measurement as it represents the ratio of intensity of light striking a PMT after the emission monochrometer versus the intensity of light striking a standard PMT that receives unfiltered light that has not passed through the sample. The standard PMT (PMT B) was generally set to a reading of 5 on the scale, equivalent to approximately 1.1 kV. The sample PMT (PMT A) was generally set between 1.5 and 2.0 kV, such that a ratio reading of greater than 100 but less than 1000 was obtained. The signal must be kept low enough so that

upon maximal dequenching (Triton X-100 addition) the signal does not exceed 10000. The kinetic data were collected using the provided SLM software package.

The kinetics runs were initiated and run for a short time period (60-100 seconds) without cell addition to confirm a stable baseline. Ghosts or cells were then added to the cuvette, ghosts by means of Hamilton syringe, cells by pipetman (in order to avoid shear stress). Records of 600 to 1000 seconds were generally undertaken, with one point being accumulated per second, but some longer term runs were also recorded. At the conclusion of the experiment a solution of 10% Triton X-100 in buffer was added the cuvette and allowed to incubate for 2 to 5 minutes in order to solubilize virus and cells. A manual reading of the fluorescence was then taken and recorded.

Sendai Reconstitution- General Procedure-

1 to 2 mgs of Sendai protein was collected by ultracentrifugation (30,000rpm, 100,000g for one hour), and was resuspended in 50µl of 10% Triton X-100 per mg of viral protein in buffer. The sample was shaken at RT for 4 hours and then the nucleocapsid material was pelleted by ultracentrifugation. The supernatant was removed and transferred to an eppendorf tube to which 50 mg SN-2 biobeads / µl Triton X-100 was then added. Any additional material to be loaded into the interior or lipid bilayer of the vesicles is added at this point to the solution. After four hours shaking at room temperature, 50 µl of high salt solution A (140mM NaCl, 20mM Hepes) and an additional 50mg of SN-2 biobeads per mg starting protein was added. The sample was shaken overnight. The cloudy reconstituted viral

containing solution was then pelleted by ultracentrifugation and the RSVE pellet resuspended in PBS.

Figure 4- Two mg of virus were used and 100 µl of Triton X-100. 6 µg of R18 was added before the biobead dialysis. The RSVE product was resuspended in 500 µl of PBS at a concentration of .65µg RSVE / µl.

Figure 17- 1.4 mg of Sendai virus was divided into two experiments, each of which was solubilized in 30 µl Triton X-100. One half was labeled with 4 µg of R18, while the other half was labeled with 1 µg of NBD-PE and 2 µg of Rd-PE. Approximately 58 µg of RSVE were recovered from each of the two reconstitutions.

Figure Captions

Figure 1. (a) Two models for intermediates in membrane fusion. (b) Schematic drawing of the morphology of (A) exocytosis and (B) viral fusion. The drawing is an interpretation of images seen in electron microscopy. Four stages going from left to right are shown as follows: (1) the membranes of a secretory granule of virion are separate from the plasma membrane; (2) triggering, movement, and recognition brings the two into close apposition (prefusion state), perhaps forming a pentalaminar complex; (3) fusion results in merging of membranes and contiguity of aqueous compartments; and (4) in the final stage the membrane components and aqueous components are completely mixed. The membranes of the granule and virion are stippled and plasma membrane is cross hatched to indicate separate membrane components (lipids, proteins). After fusion they are intermixed. The granule core material (checkered) is seen extruding into the medium during fusion. Cytoskeletal components are not shown. The nucleocapsid of the virion (drawn as two wavy lines) is seen in the cytoplasm after fusion. The spikes on the virion represent viral spike proteins, and the fuzzy motes on the plasma membrane represents cell surface carbohydrates (glycoproteins, glycolipids).

Taken from Blumenthal, 1989.

Figure 2. Structure of octadecyl rhodamine B (R18). Molecular weight of 731. Figure originally drawn by Steven Novick.

Figure 3. (a) Fluorescence for different mole percentages of R18 in DOPC MLV's. R18 in EtOH was mixed with lipid in chloroform at different concentrations and dried down. The samples were resuspended in PBS and the fluorescence intensities of the samples were measured before and after the addition of 1% Triton X-100. The "Average Triton Value" represents a dilution corrected fluorescent average of all the samples.

(b) Fluorescence for different mole percentages of R18 in EggPC SUV's. Lipid was dried from chloroform with the addition of 2 mole percent R18. Fluorescence was measured on the initial sample. Lower R18 concentrations were obtained by addition of EggPC MLV vesicles which were co-sonicated with the labeled vesicles. At the conclusion of the serial dilution experiments, Triton X-100 was added to the sample and the fluorescence was recorded. This value is recorded at the "0" point of the x axis. A separate control was run after this experiment giving a fluorescent value of 670 before and 1098 after addition of Triton X-100.

(c) Quench curve for data shown in part (a).

(d) Quench curve for data shown in part (b).

(e) Excitation (_ · _) and emission (——) spectra of R18. Curves a are excitation and emission spectra of 2 mol % R18 in DOPC vesicles. Curves b and c show the emission spectra of R18 in ethanol and chloroform, respectively. R18-containing viruses of ghosts gave identical spectra as those obtained in a. From Hoekstra et al., 1984.

(f) Efficiency of self-quenching in R18 in DOPC vesicles (A) and relief of selfquenching upon addition of Triton X-100 to R18-containing Sendai virus (B). (A) SUV were prepared containing various amounts of R18. The percentage of self-quenching was determined by measuring fluorescence

before and after addition of Triton X-100 (1% v/v). (B) R18 was incorporated into Sendai virus membranes (ca. 20 nmol/mg of viral protein). Emission spectra (ex=560nm) were recorded before (___) and after (- - -) addition of Triton X-100 (1% v/v). From Hoekstra et al, 1984.

Figure 4. Fusion of reconstituted Sendai virus envelopes (RSVE) with H9 cells, monitored by the R18 assay. (A) 26μg RSVE interacting with $1x10^6$ H9 cells in PBS. (B,C,D) 13μg RSVE with $5x10^5$ H9 cells. (B) The virus was pretreated with 100 μg (1μg/μl) trypsin for 2 hours at 37° C. (C) The virus was treated with 1 mg Fetuin (10μg/μl). (D) The virus was suspended in two ml's of media with serum.

Figure 5. Schematic representation of R18 diffusion during viral fusion.

Figure 6. Summary of selected literature values for viral fusion inhibition.

Figure 7. Summary of some of my own experimental values for viral fusion inhibition.

Figure 8. Comparison of the extent of dequenching of uninhibited and trypsinized samples at different ratios of Sendai virus to target ghost erythrocyte. In all cases 120 μg of ghost erythrocytes were used as the target cells. 5 μl of virus contained 9 μg of Sendai protein.

Figure 9. Comparison of effects of order of trypsin treatment, R18 labeling, and purification on dequenching.

Figure 10. Comparison of dequenching after overnight incubation of R18 labeled virus with and without trypsin treatment. 10 μg of mumps (a) or Sendai (b) were incubated with various amounts of erythrocyte ghosts for 18 hours.

Figure 11. Schematic representation of F protein hydrophobic terminus serving as a bridge between membrane bilayers.

Figure 12. Spectrum of R18 incorporated into the viral bilayer.

Figure 13. Structures of the fluorescent lipid probe pair NBD-PE and Rd-PE.

Figure 14. (a) Excitation (- - -) and emission (___) spectra in phosphatidylserine vesicles containing 1 mol % fluorescent analogues. (A) Spectra of NBD-PE; (B) Spectra of Rh-Pe.

(b) Efficiency of energy transfer as a function of the number of energy acceptors per phospholipid molecule (surface density). The molar ratio of NBD-PE to total phospholipids (1:99) was kept constant while the amount of Rh-PE was varied to give the indicated surface densities.

From Struck et al.,1981.

Figure 15. Quenching of NBD-PE by Rd-PE at two different ratios of acceptor to donor. Chloroform solutions containing the fluorescent lipid probes and egg phosphatidylcholine (PC) were mixed at set ratios, dried, and resuspended in phosphate buffered saline (PBS) as multilamellar vesicles (MLV's).

Fluorescent reading before and after the addition of Triton X-100 were compared to determine the % Quenching (%Q = 1- (Initial Fluorescence/Triton Fluorescence).

Figure 16. Summary of the behavior of lipid probes and of the corresponding fluorescence in the probe mixing assay (A) and the probe dilution assay (B).

Figure 17. Dequenching profiles of NBD/Rd labeled and R18 labeled RSVE interacting with erythrocyte ghosts. The erythrocyte ghost amounts are shown as the underlined number and represent µl of ghost added where 10 µl of ghosts contains 13 µg of ghost protein.

Figure 18. Comparision of the extent of dequenching observed with R18 versus that observed with NBD/Rd in interaction of RSVE with ghost erythrocytes.

Figure 19. Five kinetic curves obtained from reaction of labeled Sendai virus (from experiment 1 of figure 8 , i.e., native virus) with various amounts of ghost erythrocytes. 5 µl of virus was equivalent to 9.0 µg of viral protein and 40 µl of ghost erythrocytes was equivalent to 96 µg of erythrocyte ghost protein. (a) Two raw data curves and (b) three smoothed data curves are presented to provide the reader with a perspective on the difference between raw and smoothed fluorescence data.

Figure 20. Kinetic fits to data from Figure 17 using the simple bimolecular model.

Figure 21. Kinetic fits to data from Figure 8 using the simple bimolecular model.

Figure 22. Kinetic fits to data from Figure 19 using the simple bimolecular model.

Figure 23. Three mass action fits to a pair of data curves from Figure 17. The constants used to fit these two curve were:

A- k1=.52 $x10^9$, k2= .00223, k3= .002;

B- k1= 1 $x10^9$, k2= .00223, k3= .00078;

C- k1= 5 $x10^9$, k2= .00223, k3= .0002.

Figure 24. Kinetic data from Figure 17 with curve fits provided by the rate constants of the mass action kinetic model.

Figure 1a.

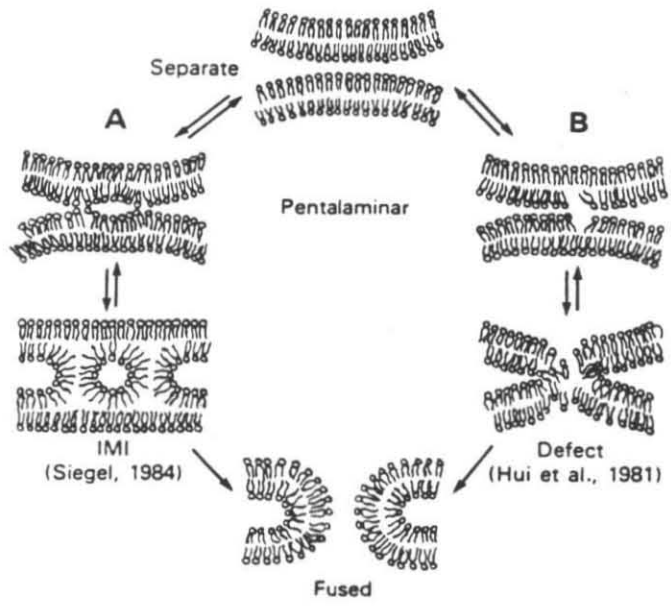

Figure 1b.

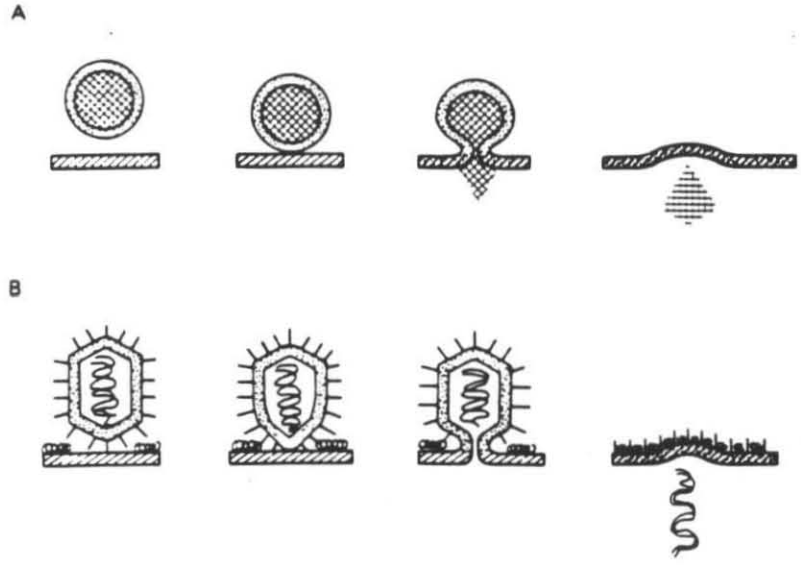

Figure 2.

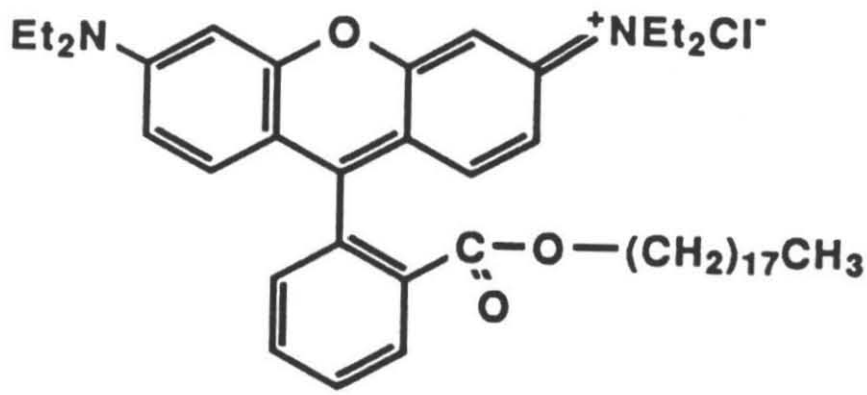

R_{18}

Figure 3a.

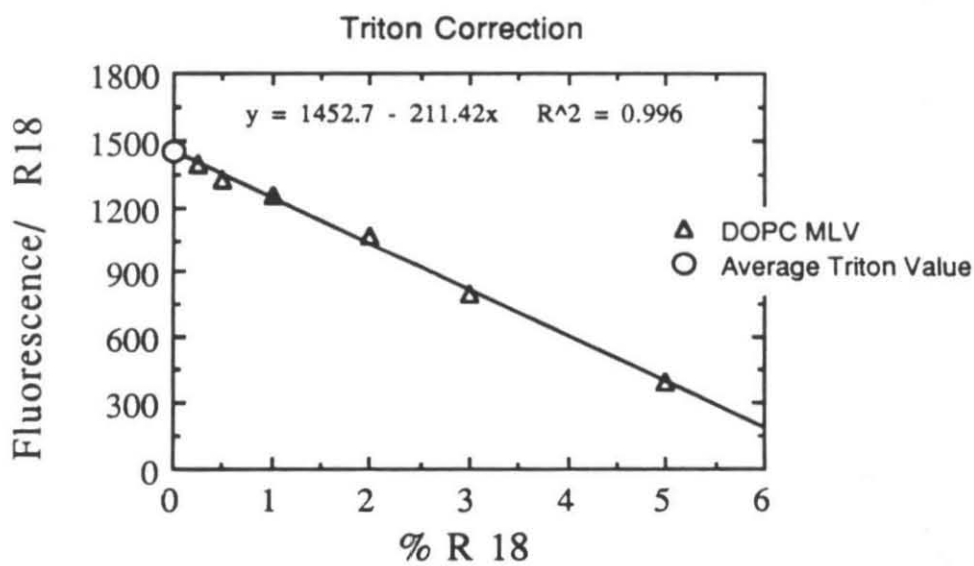

Figure 3b.

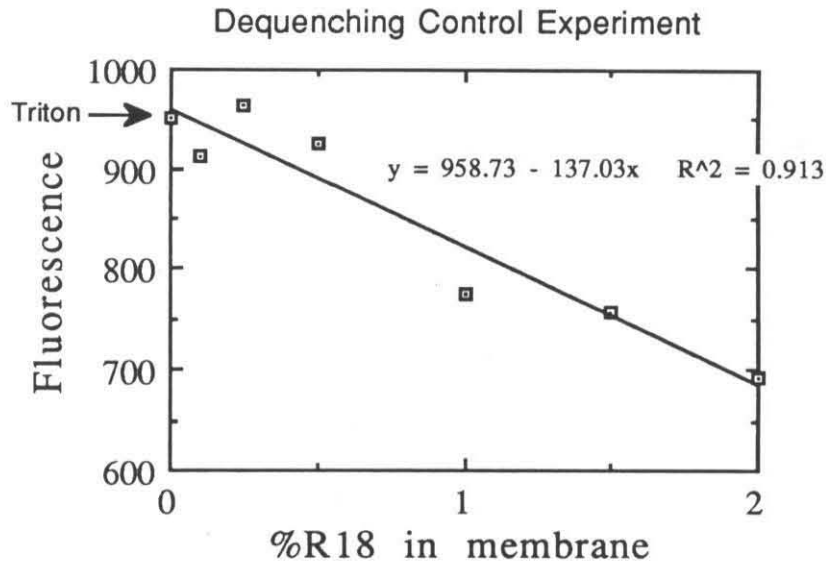

Figure 3c.

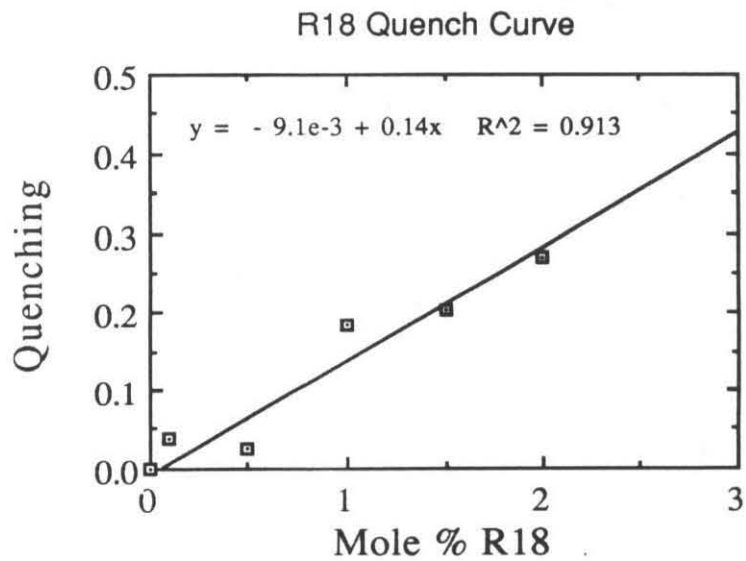

Figure 3d.

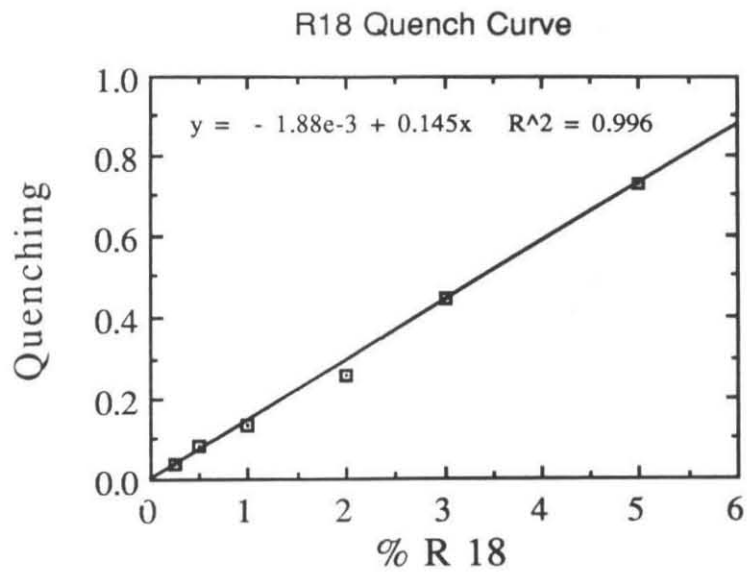

Figure 3e.

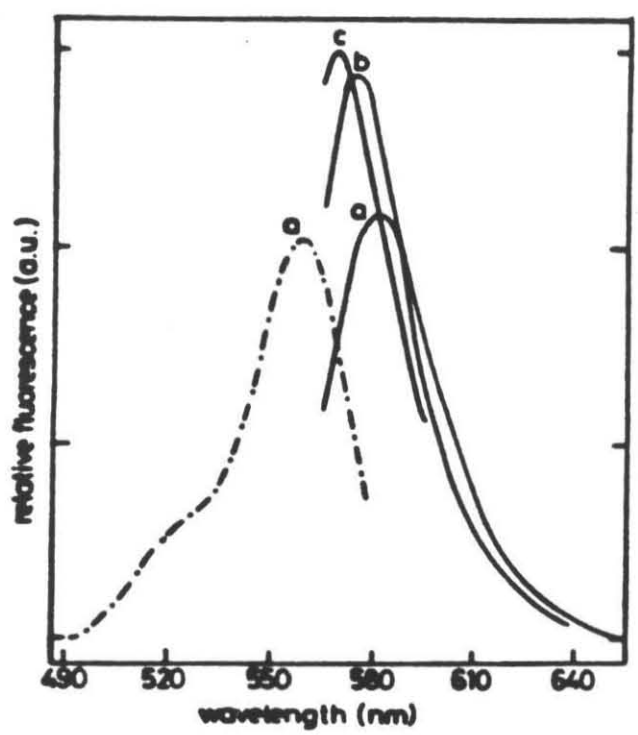

Figure 3f.

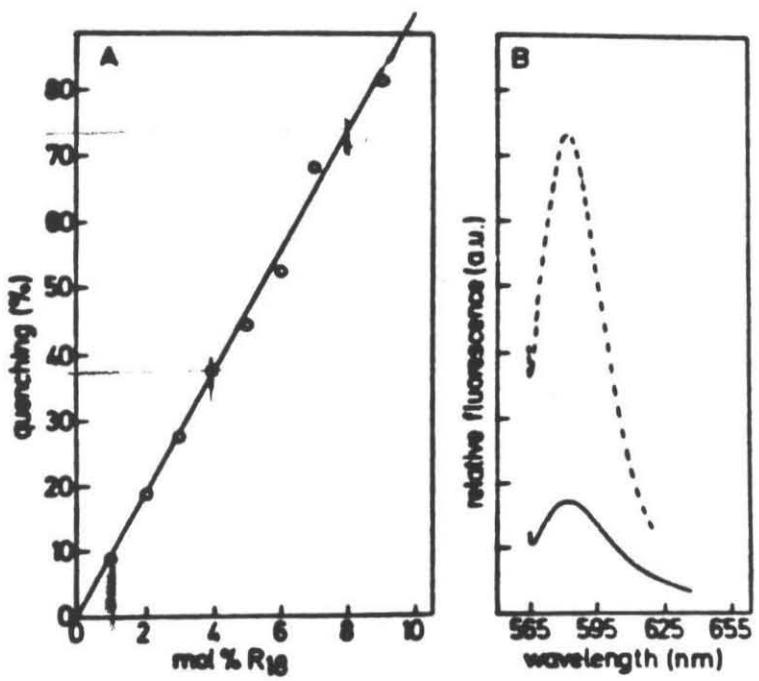
A
quenching (%)
0
10
20
30
40
50
60
70
80
0
2
4
6
8
10
mol % R18
B
relative fluorescence (a.u.)
565
595
625
655
wavelength (nm)

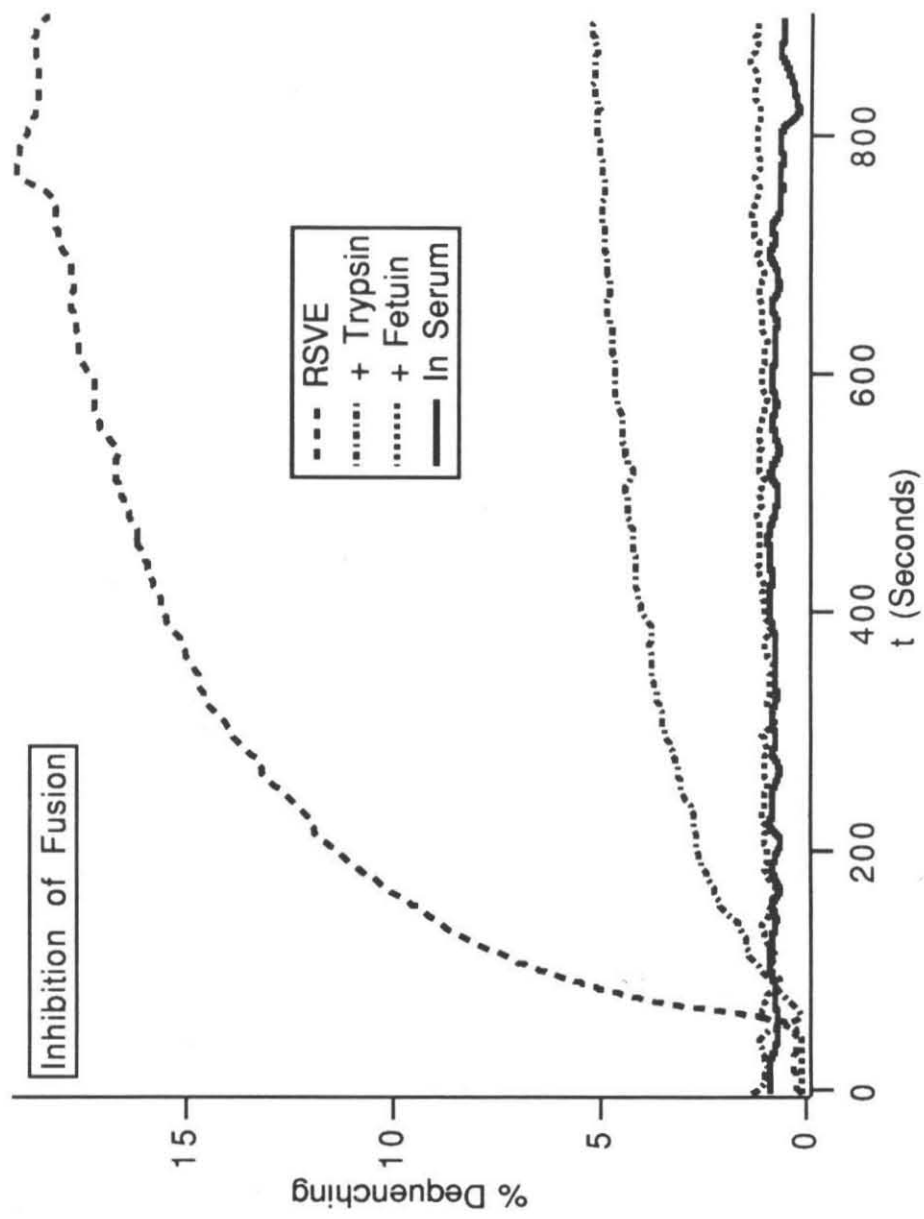
Inhibition of Fusion
RSVE
+ Trypsin
+ Fetuin
In Serum
% Dequenching
0
5
10
15
0
200
400
600
800
t (Seconds)

Figure 4.

Figure 5.

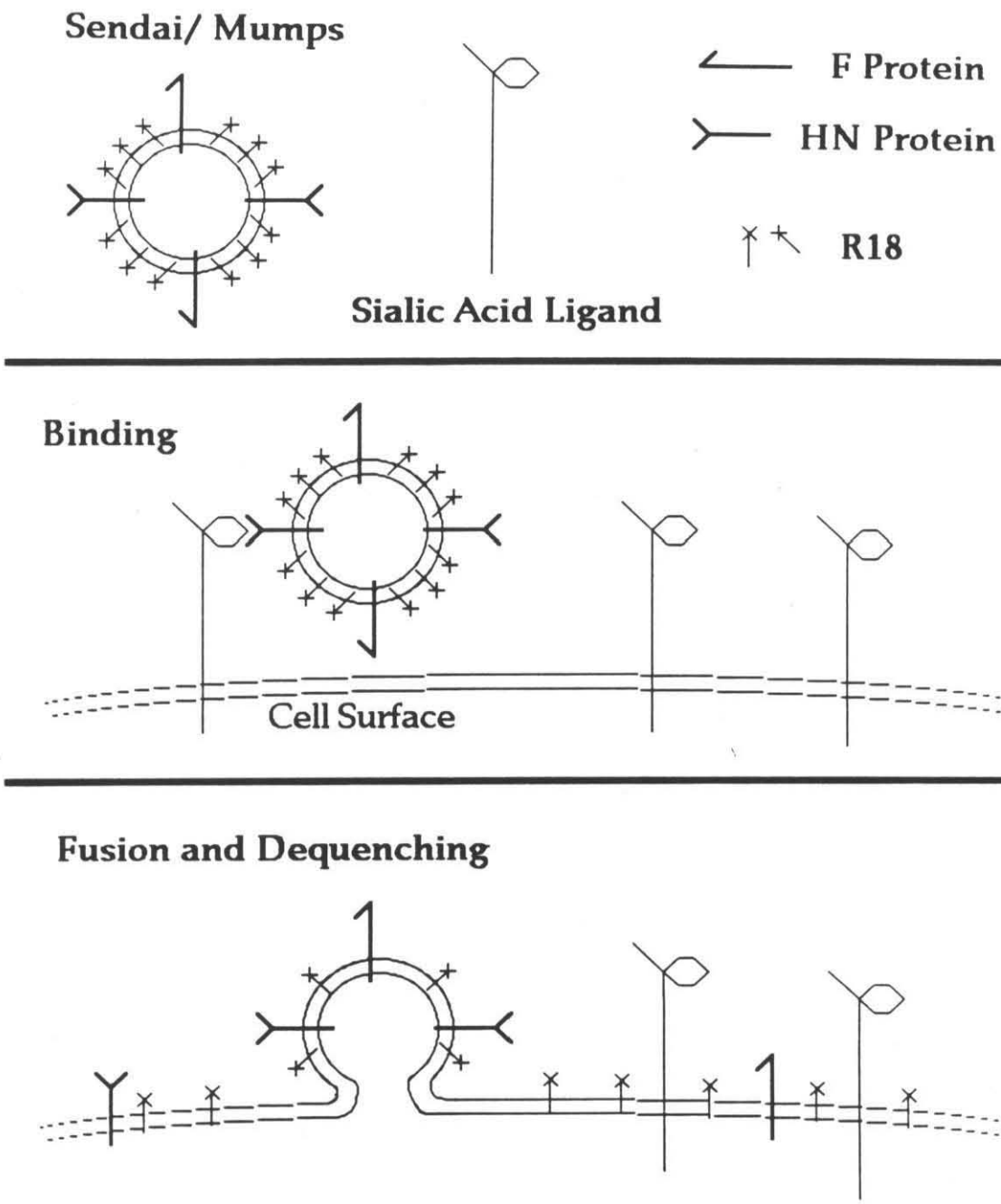
Sendai/ Mumps
F Protein
HN Protein
R18
Sialic Acid Ligand
Binding
Cell Surface
Fusion and Dequenching

Figure 6.

Author	System	Inhibitor	% Uninhibited
Chejanovsky et al.(1986)			
NBD	RSVE/FELC	Trp	20.5
	RSVE/FELC	Trp	16
	"	DTT	6.3
	"	PMSF	15
	"	Neuroaminidase	21
NBD-Cl	Sendai/FELC	DTT	.4
	"	Trp	2.3
	"	Neuro.	8
	"	PMSF	2.1
	RSVE/FELC	DTT	5.5
	"	Trp	11.8
	"	Neuro.	17.4
	"	PMSF	17.4
Chejanovsky et al. (1988)			
R18	Sendai/HELA	DTT	9.6
	"	Trp	15.3
	"	PMSF	15.3
	Sendai/Ghost	DTT	12
	"	HN	12
	"	F	16
	"	HN-F	104
Citovsky et al. (1985)			
NBD	RSVE/Ghost	Trp	5
	RSVE/HTC	Trp	7.6
	RSVE/PC	Trp	14.2
	RSVE/PC+	Trp	13.3
Citovsky et al. 1988)			
R18	Sendai/M. Capri.	DTT	15
	"	PMSF	17
	"	Trp	15

Figure 7.

Date	System	Time	Inhibitor	Fusion	Notes
7/2/87	Mumps/Ghosts	1 hr	None	7.7	R18
	"	"	Trp	0	
	"	"	DTT	0	
	"	8 hr	None	22.7	R18
	"	"	Trp	.7	
	"	"	DTT	9.4	
4/1/89	Mumps/Ghosts	27 min	None	17.7	R18
	"	"	Trp	5.6	
4/11/90	Mumps/Cells	15 min	None	25.0	R18
	"	"	Trp	4.0	
5/24/90	Mumps/Cells	15 min	None	12.0	R18
	"	"	Fet	6.0	
6/16/87	RSVE/Ghost	15 min	None	12.5	R18
	"	"	Trp	8.3	
	"	"	DTT	6.2	
6/24/87	RSVE/POPC	15 min	None	11.2	R18
	"	"	Trp	9.0	
	"	"	DTT	3.0	
6/25/87	Sendai/Ghost	15 min	None	6.3	R18
	"	"	Trp	3.8	
	"	"	DTT	0.5	
6/25/87	Sendai/POPC	15 min	None	12.4	R18
	"	"	Trp	13.1	
	"	"	DTT	7.5	
10/5/87	RSVE/Ghosts	2000 sec	None	7.4	R18
	"	"	Trp	2.8	
	"	"	Pro	1.4	

10/7/87	RSVE/Ghosts	2000 sec	None	24.1	NBD/Rd
	"	"	Pro	1.7	
	RSVE/PBL	600 sec	None	37.1	
	"	"	Fet	4.6	
	"	"	Trp	2.1	
3/14/90	RSVE/Ghost	1000 sec	None	24.0	Rd-PE
	"	"	Fet	11.2	
	"	"	Trp	2.9	
4/2/90	RSVE/PBL	900 sec	None	23.0	Rd-PE
	"	"	Fet	4.0	
	"	"	Trp	15	
	"	"	Serum	0	
4/5/90	RSVE/H9	900 sec	None	20	Rd-PE
	"	"	Trp	4	
	"	"	Hanks	4	
	"	"	Fet	1	
	"	"	Serum	0	

Figure 8.

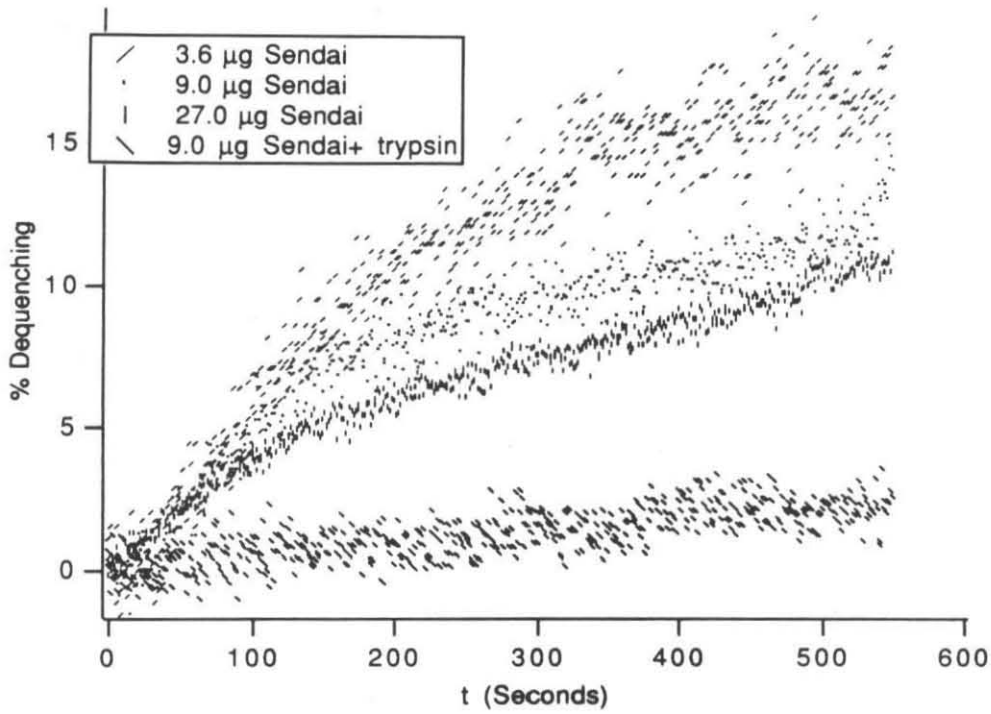

Sendai Amount (µl)	%Fusion (540 sec.)	Trp. Fusion	% Uninhibited
2	16.9	2.8	16.5
5	12.2	2.3±.1	18.8
15	10.6	1.45±.1	13.6

Figure 9.

Trypsin Digestion Controls

Procedures

1. Normal Uninhibited- Label with R18, Purify by Centrifugation

2. Inhibited- Trypsinize, Label with R18, Purify by Centrifugation

3. Inhibited- Trypsinize, Label with R18, Purify with G50 column

4. Inhibited- Label with R18, Trypsinize, Purify by Centrifugation

5. Inhibited- Label with R18, Purify by Centrifugation, Trypsinize

	% Dequenching (t= 940 sec)	
Procedure	9 µg Sendai/96 µg Ghosts	18 µg Sendai/ 192 µg Ghosts
1	14.3	13.8
2	4.0	1.7
3	5.7	5.1
4	3.8	2.8
5	2.4	1.5

Figure 10.

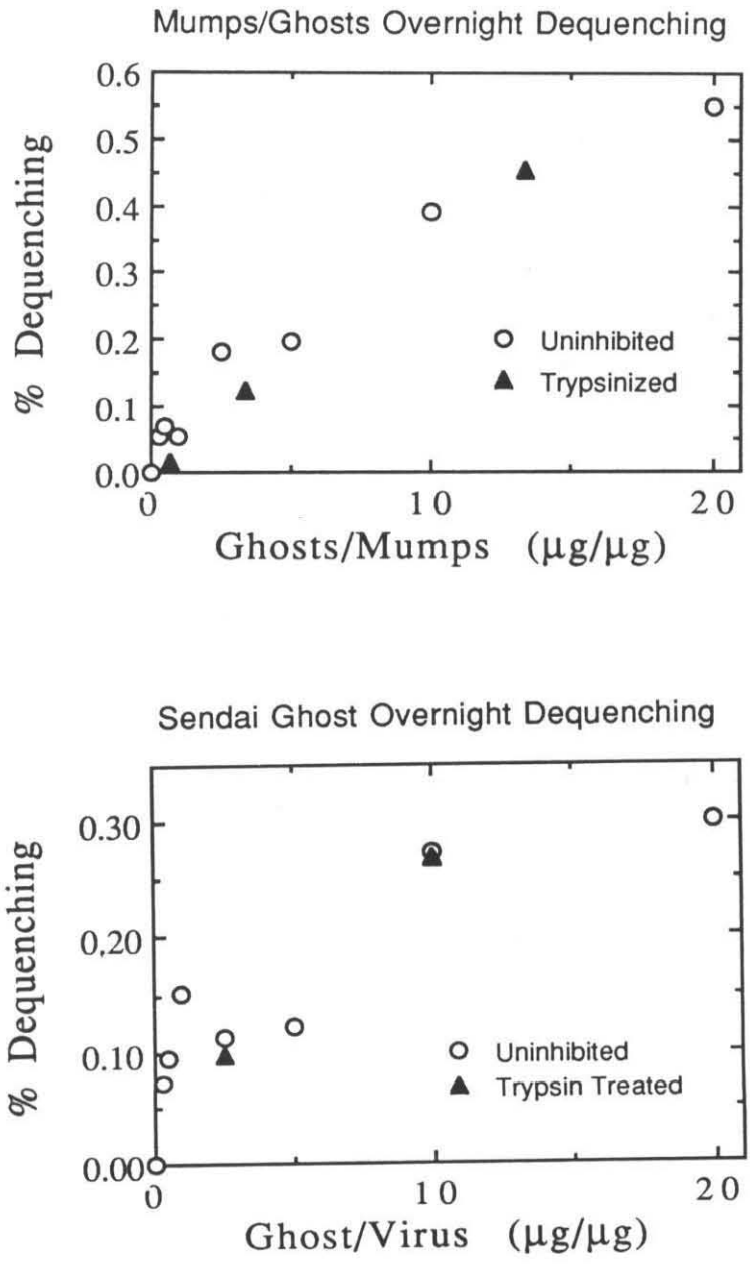
Mumps/Ghosts Overnight Dequenching
% Dequenching
0.6
0.5
0.4
0.3
0.2
0.1
0.0
0
10
20
Ghosts/Mumps (µg/µg)
Uninhibited
Trypsinized
Sendai Ghost Overnight Dequenching
% Dequenching
0.30
0.20
0.10
0.00
0
10
20
Ghost/Virus (µg/µg)
Uninhibited
Trypsin Treated

Figure 11.

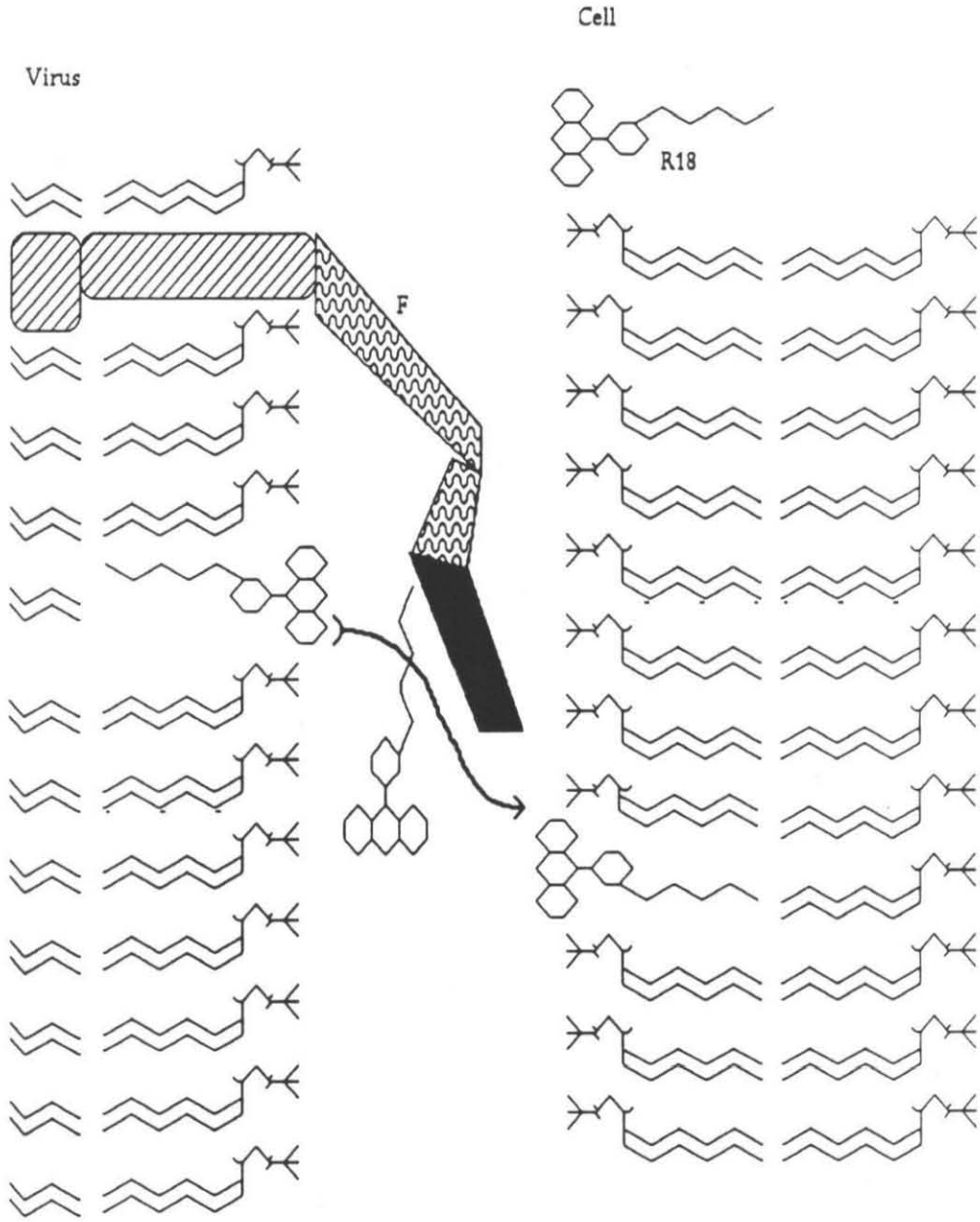

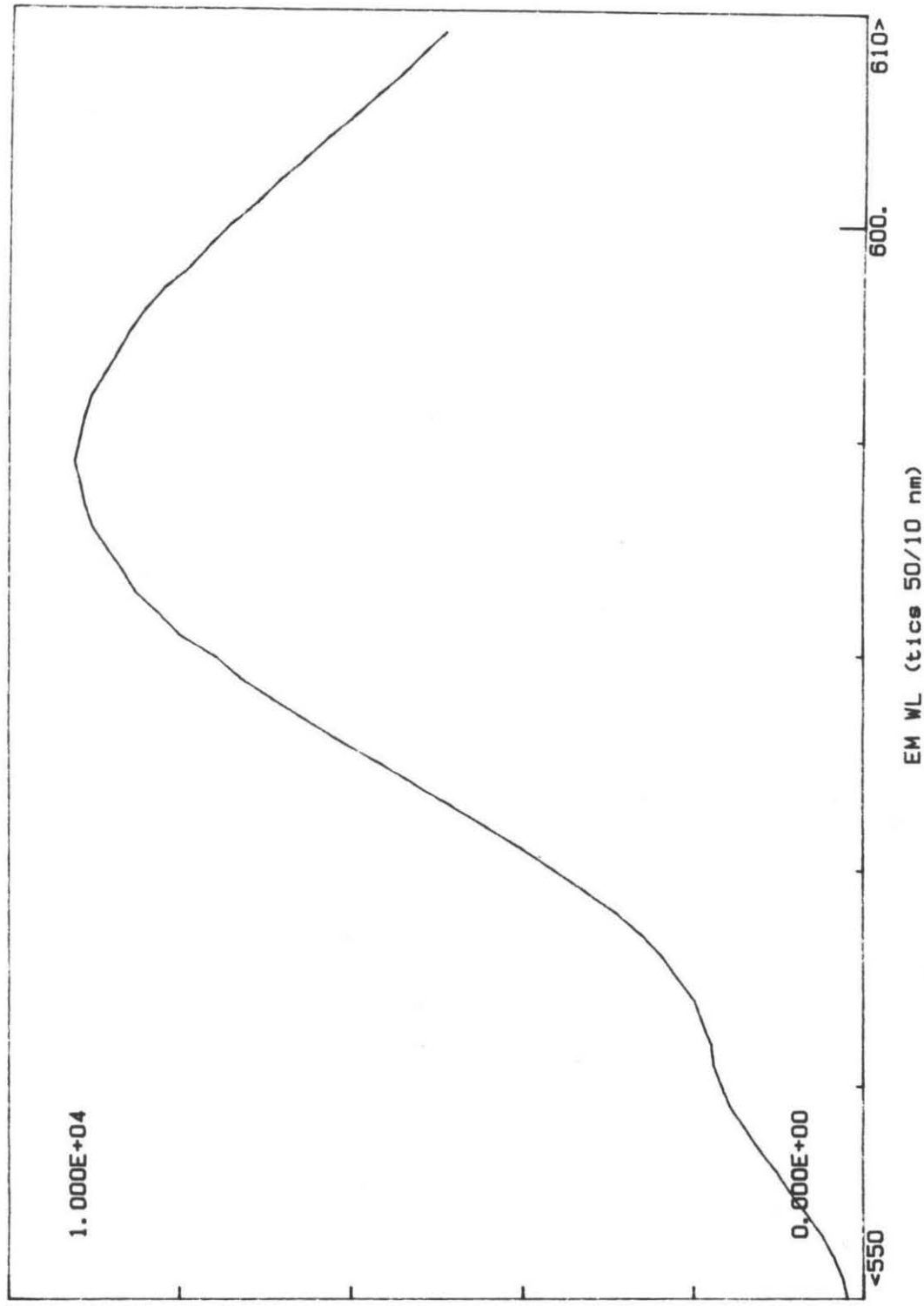

Figure 12.

Figure 13.

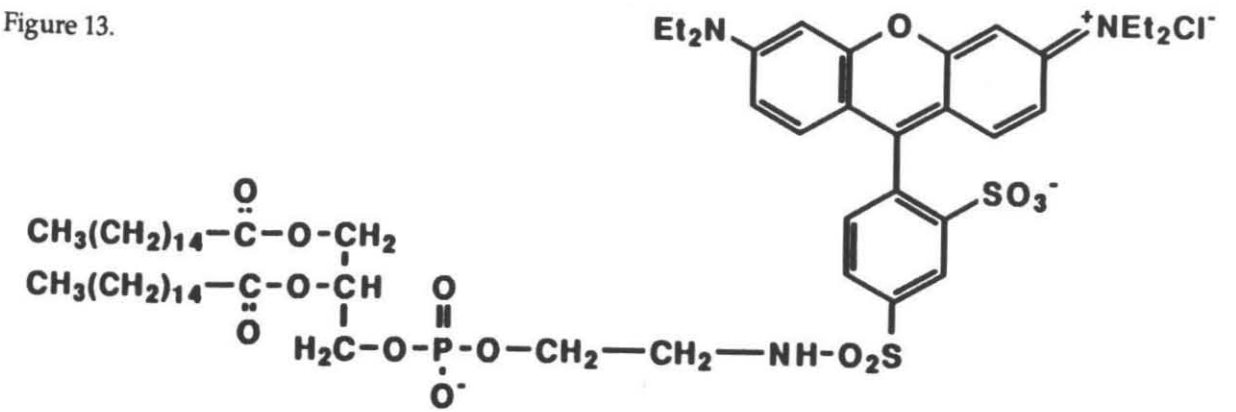

N-Rh-PE

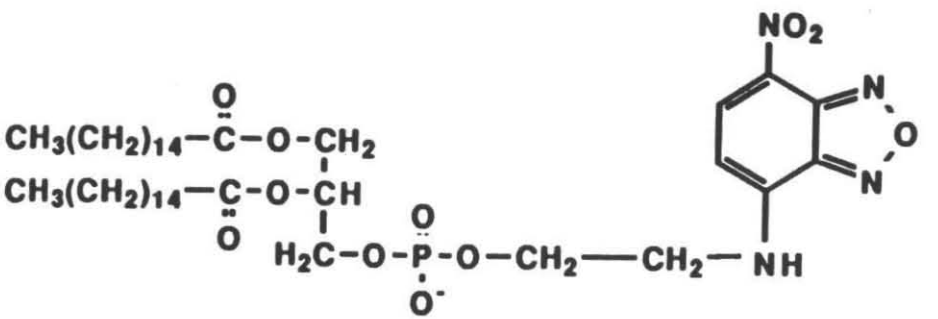

N-NBD-PE

Figure 14a.

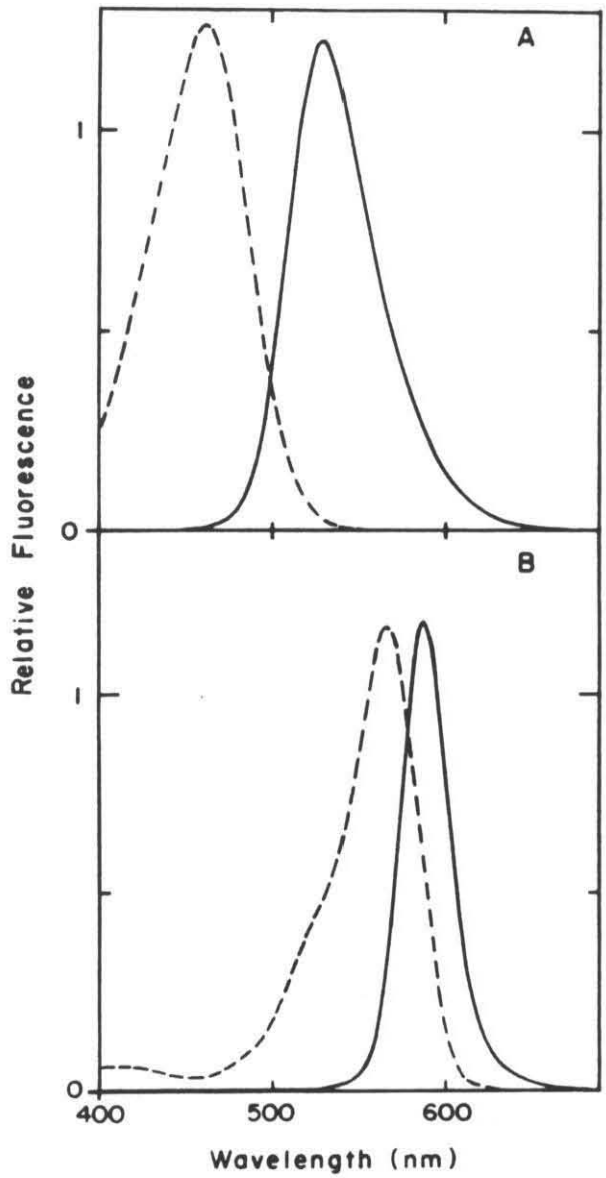

Figure14b.

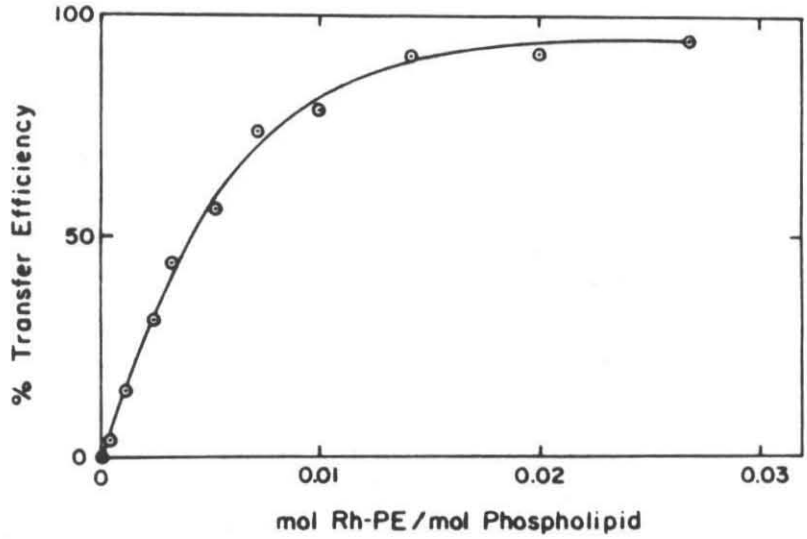

Figure 15.

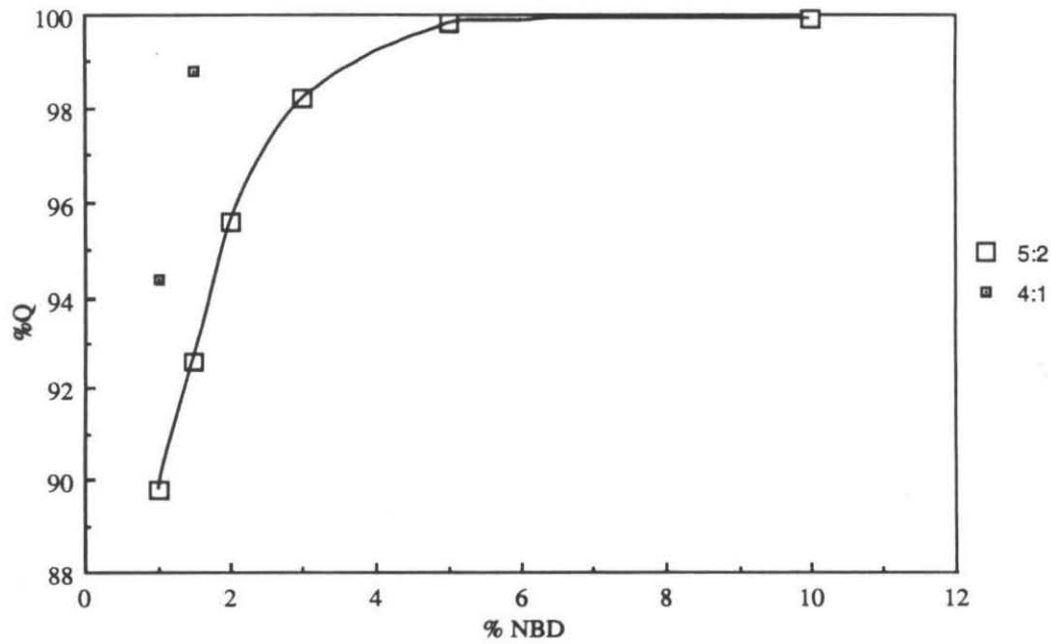

Figure 16.

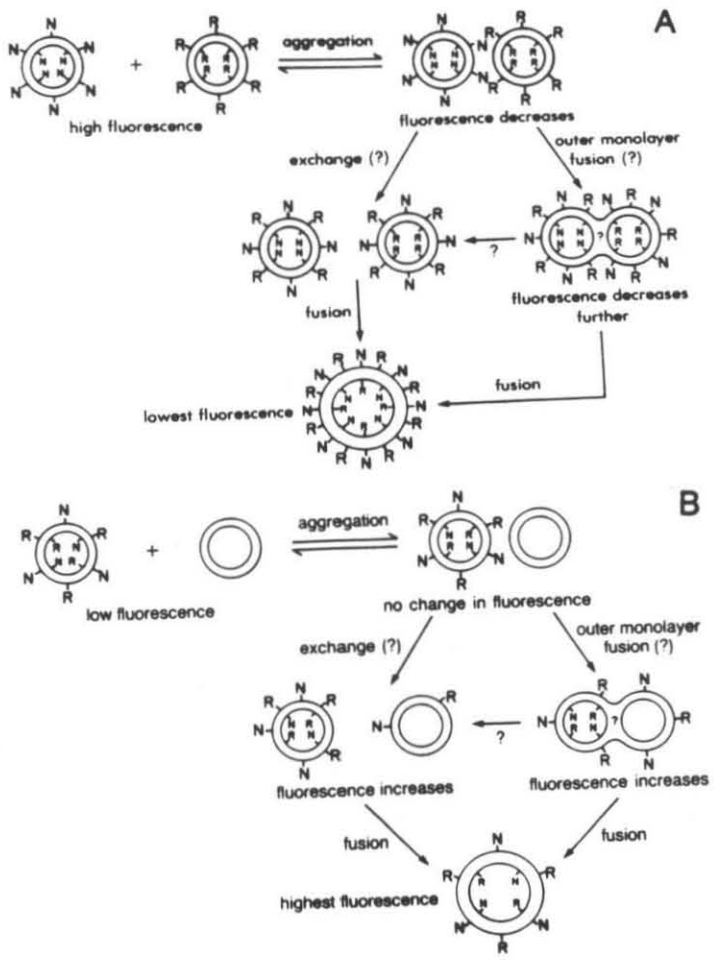
A
aggregation
high fluorescence
fluorescence decreases
exchange (?)
outer monolayer fusion (?)
?
fusion
fluorescence decreases further
fusion
lowest fluorescence
B
aggregation
low fluorescence
no change in fluorescence
exchange (?)
outer monolayer fusion (?)
?
fluorescence increases
fluorescence increases
fusion
fusion
highest fluorescence

Figure 17.

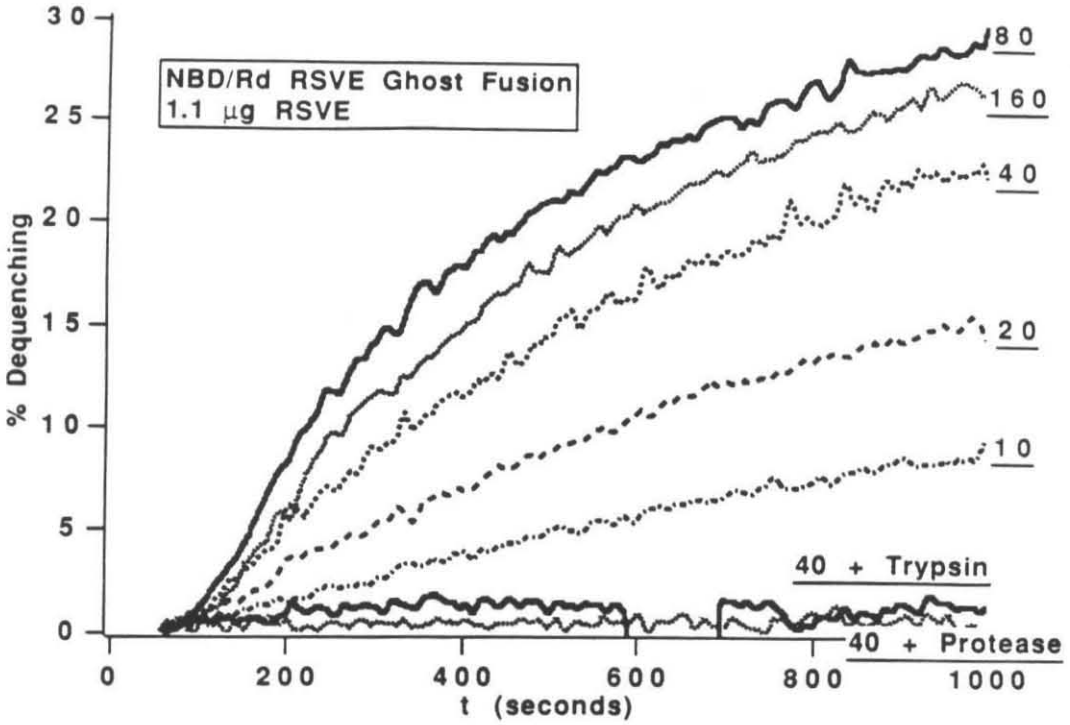
NBD/Rd RSVE Ghost Fusion
1.1 µg RSVE
% Dequenching
t (seconds)
80
160
40
20
10
40 + Trypsin
40 + Protease
0
5
10
15
20
25
30
0
200
400
600
800
1000

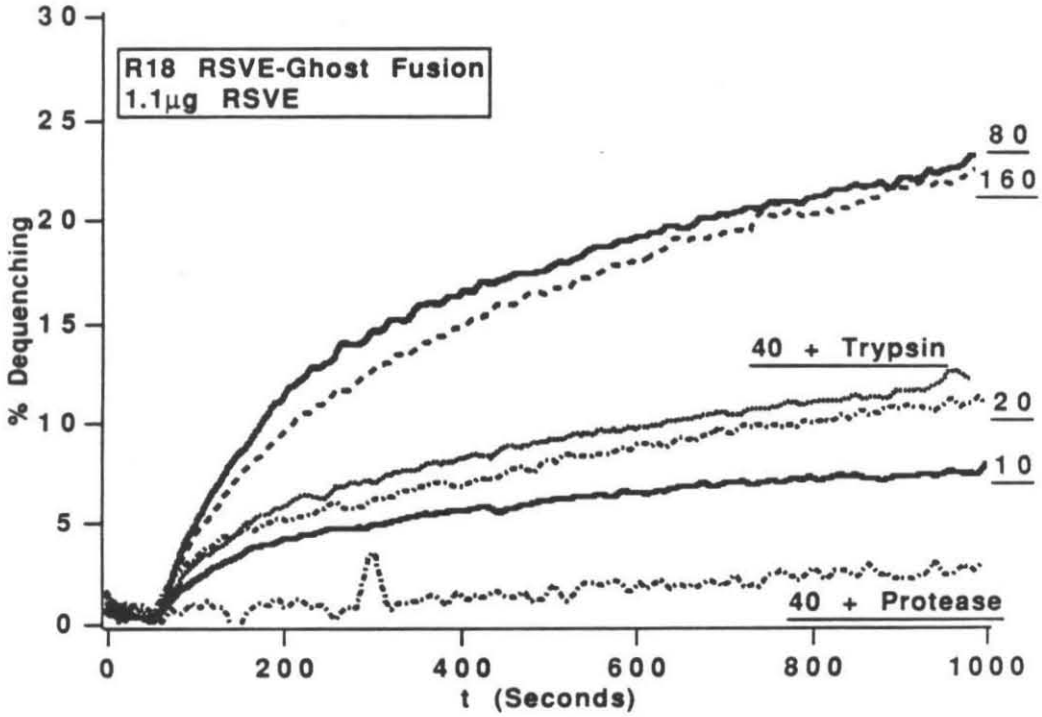
R18 RSVE-Ghost Fusion
1.1µg RSVE
% Dequenching
t (Seconds)
80
160
40 + Trypsin
20
10
40 + Protease
0
5
10
15
20
25
30
0
200
400
600
800
1000

Figure 18.

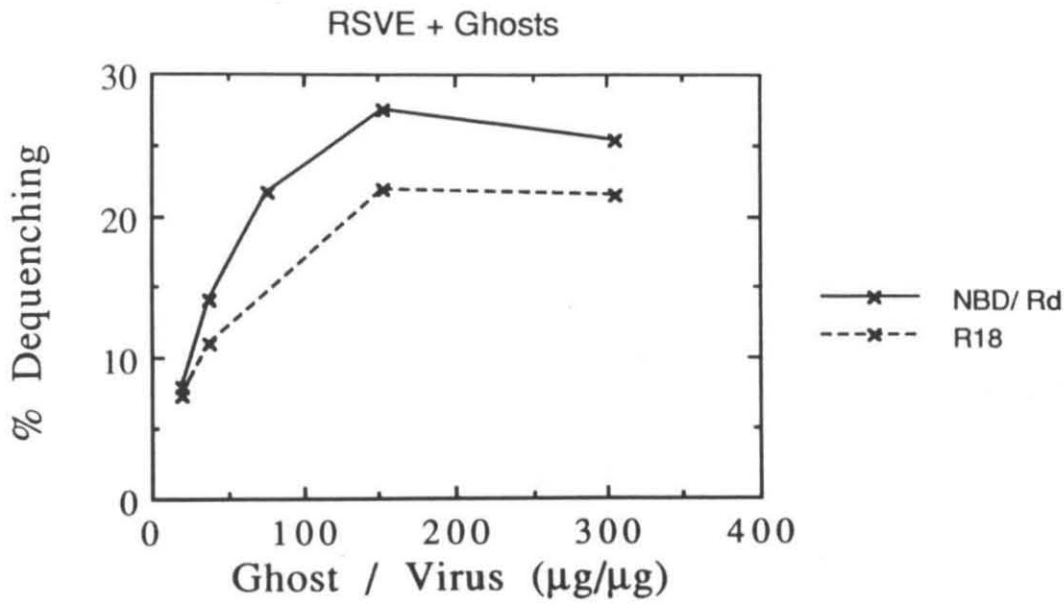
RSVE + Ghosts
% Dequenching
30
20
10
0
0
100
200
300
400
Ghost / Virus (µg/µg)
NBD/ Rd
R18

Figure 19.

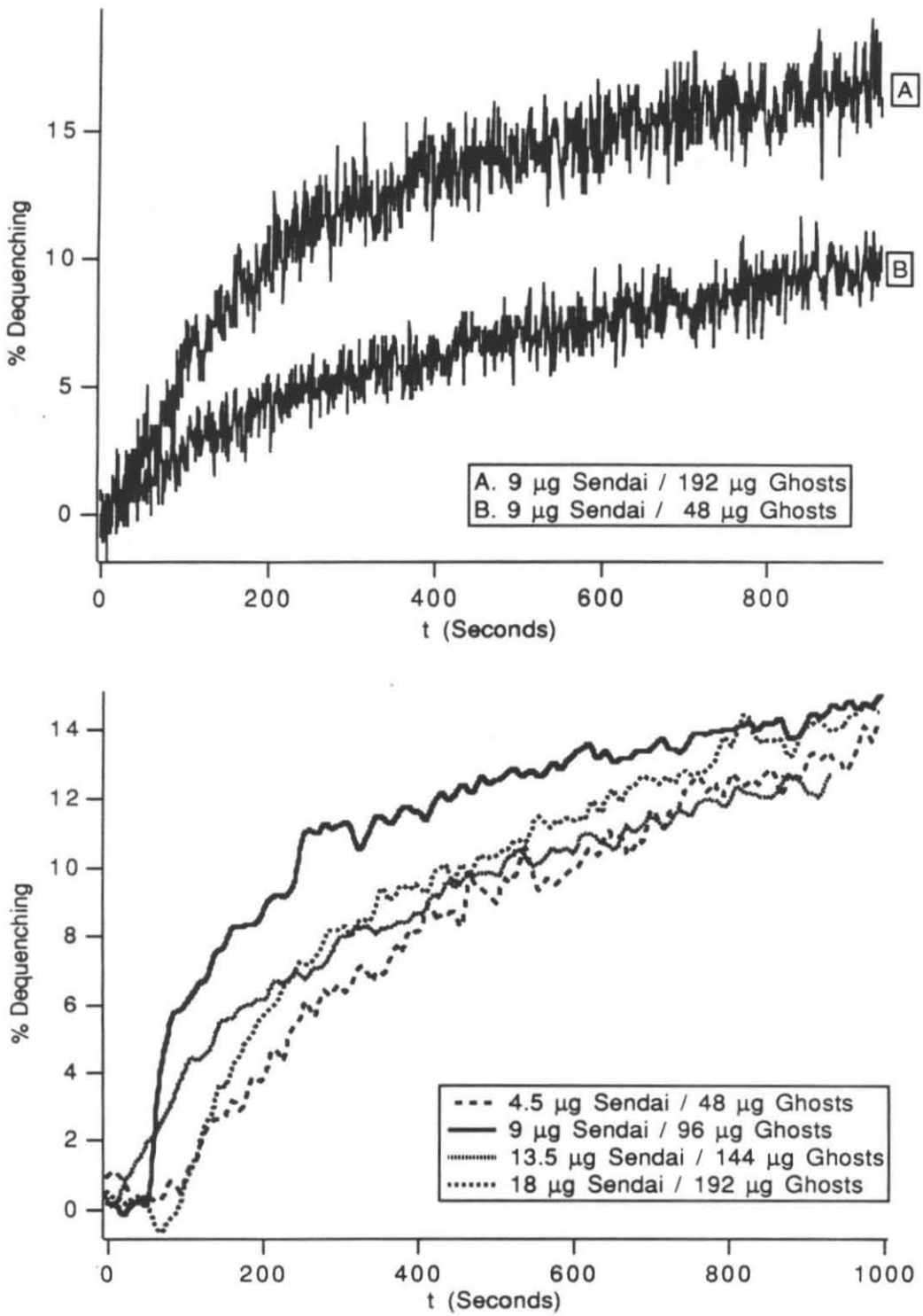
% Dequenching
t (Seconds)
A
B
A. 9 µg Sendai / 192 µg Ghosts
B. 9 µg Sendai / 48 µg Ghosts
4.5 µg Sendai / 48 µg Ghosts
9 µg Sendai / 96 µg Ghosts
13.5 µg Sendai / 144 µg Ghosts
18 µg Sendai / 192 µg Ghosts

Figure 20.

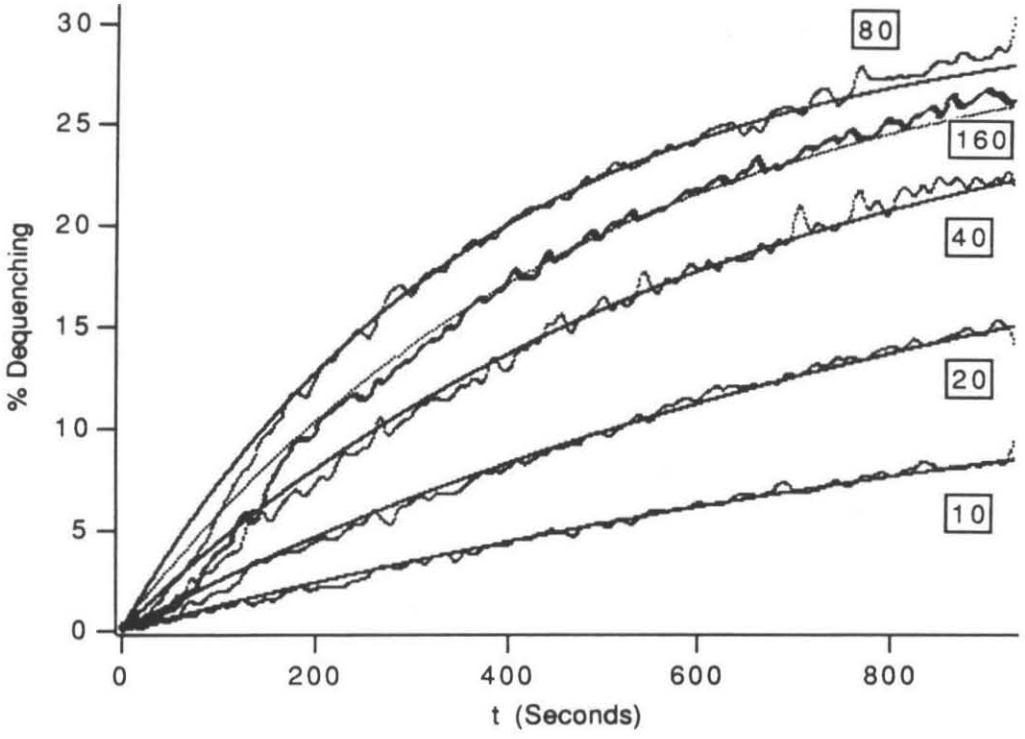

RSVE(µg)	Ghost (µl)	Vo (M)	Go (M)	nGo (M)	k
1.1	10	1.86e-12	2.09e-14	1.81e-12	2.24e+8
1.1	20	1.86e-12	4.17e-14	3.63e-12	2.27e+8
1.1	40	1.86e-12	8.30e-14	7.27e-12	2.08e+8
1.1	80	1.86e-12	1.60e-13	1.45e-11	1.82e+8
1.1	160	1.86e-12	3.30e-13	2.90e-11	6.80e+7

Figure 21.

V (M)	V act (M)	Go (M)	nGo (M)	k
3.85e-12	5.77e-13	1.79e-13	1.44e-12	4.08e+9
9.63e-12	1.44e-12	1.79e-13	1.44e-12	2.72e+9
2.89e-11	4.33e-12	1.79e-13	1.44e-12	4.04e+9

Figure 22.

Sendai (µg)	Ghosts (µg)	V (M) x 1e-12	G (M)	k
9.0	96	1.73	1.45e-13	8.1e+8
18.0	192	3.46	2.90e-13	7.0e+8
9.0	192	1.73	2.90e-13	9.1e+8
4.5	48	8.66	7.25e-14	1.9e+9
9.0	48	1.73	7.25e-14	1.4e+9
13.5	144	2.60	2.18e-13	6.1e+8

Figure 22.

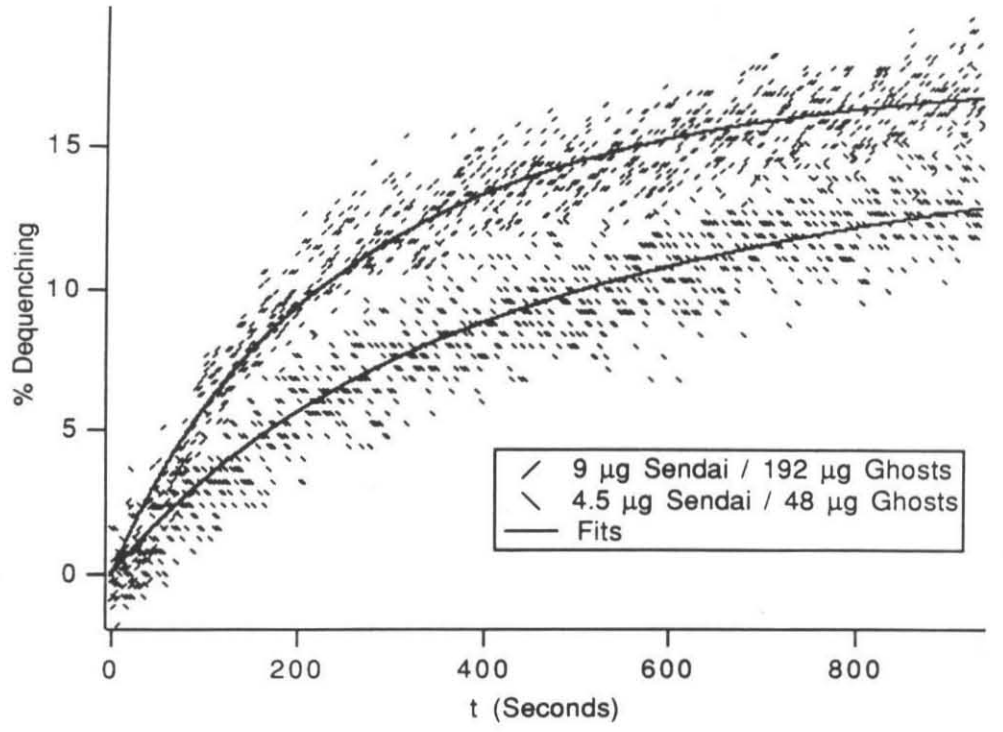
% Dequenching
15
10
5
0
0
200
400
600
800
t (Seconds)
9 µg Sendai / 192 µg Ghosts
4.5 µg Sendai / 48 µg Ghosts
Fits

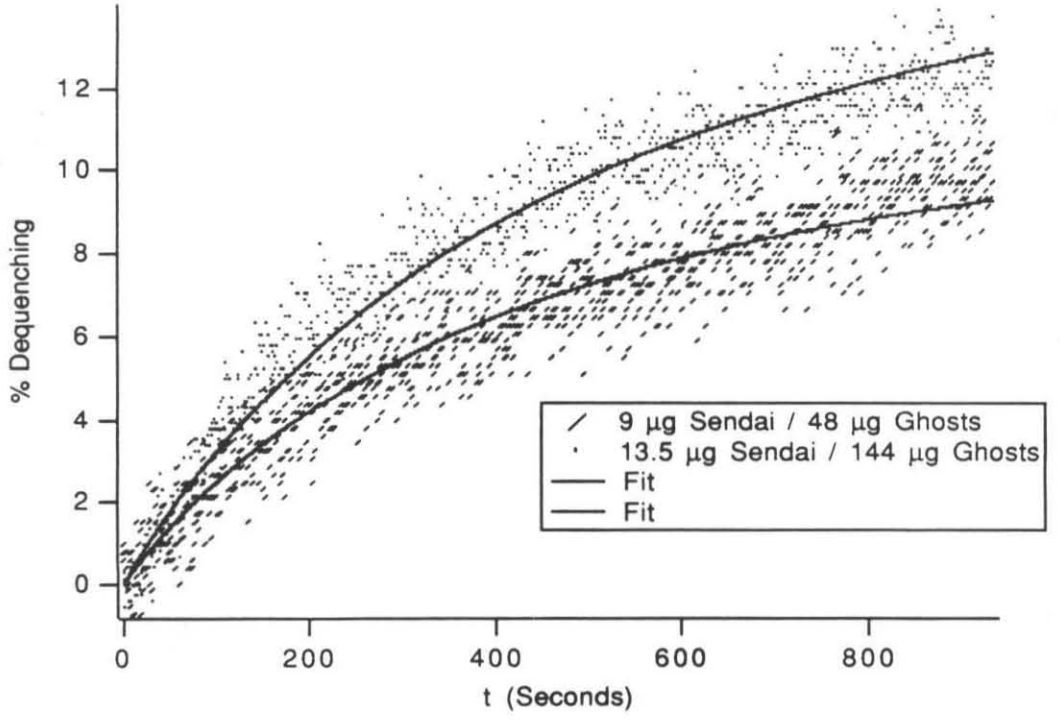
% Dequenching
12
10
8
6
4
2
0
0
200
400
600
800
t (Seconds)
9 µg Sendai / 48 µg Ghosts
13.5 µg Sendai / 144 µg Ghosts
Fit
Fit

Figure 23.

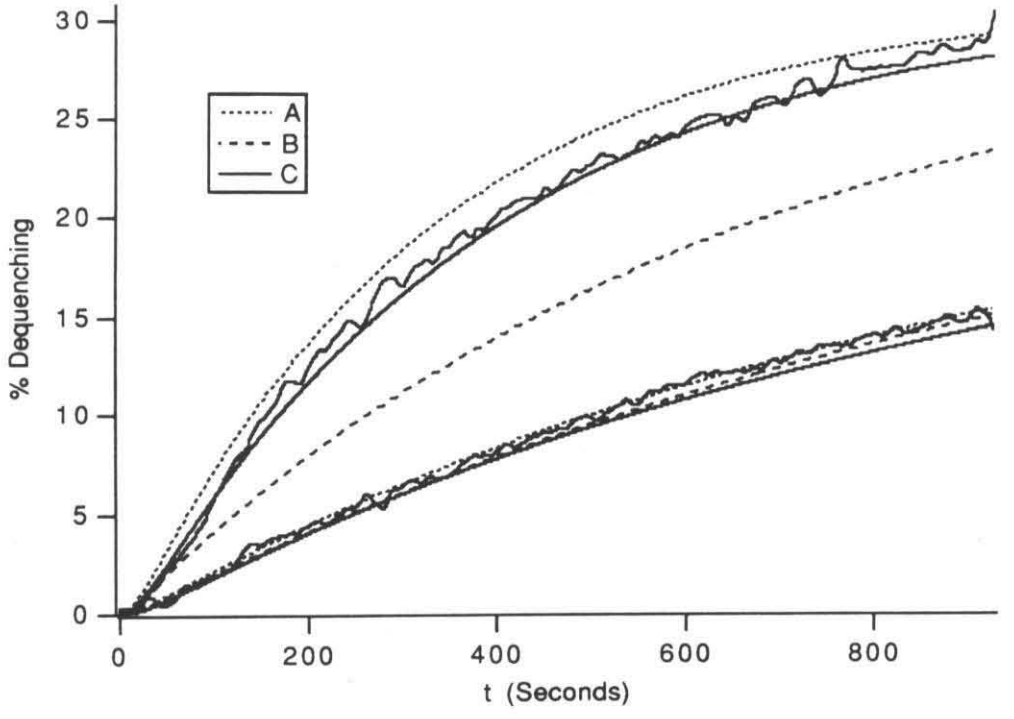

Figure24.

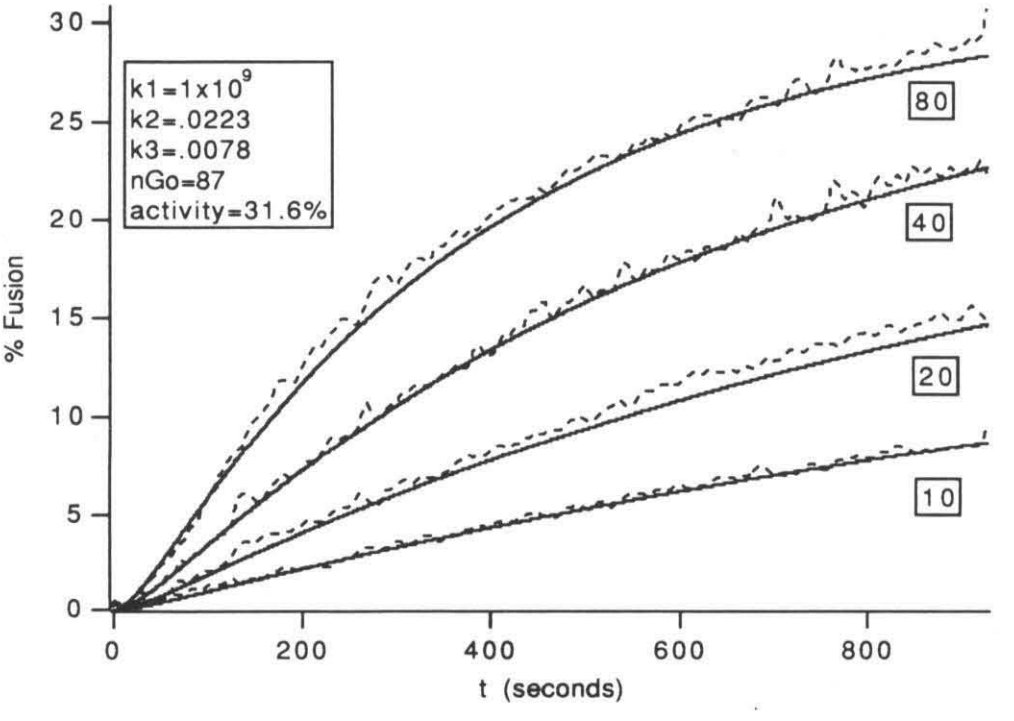

Chapter 3: The Reconstitution of Mumps and Sendai Virus

I. Introduction

For a tissue to be infected with a virus it must be exposed to that virus and it must be capable of supporting a complete virus replication cycle. These two factors determine viral tissue tropism, i.e., selective tissue infection.

Entry pathways (skin, respiratory tract, gastrointestinal tract, etc.) determine initial cellular exposures, while bodily transport systems and viral infection pathways determine later cellular exposures. For example, a virus which is directly injected into the blood (by an insect, a wound, a needle, etc.) will be initially exposed to lymphoid and erythroid cell lines as well as those endothelial cells lining the blood transport system. A virus could then infect the capillary linings and bud prodigy virus into the gut organ tissue.

For a virus to successfully infect a cell, it must transport its replicative material to the cellular interior, all replication proteins must be active in the cell, functional viral proteins and nucleic acid must be produced, and the progeny virus must successfully exit the cell.

Entry phase behavior is moderated by the proteins on the surface of the virus. A binding ligand is necessary on the viral surface for the virus to become associated with a cell. The viral surface proteins can confer direct specificity for certain cells by the recognition of factors on the surface of the cells. A tissue specific drug delivery system could be developed if this targeting behavior could be incorporated into an artificial delivery system.

The paramyxovirus mumps was chosen to test the feasibility of this idea, due to its infective properties and tissue tropism.

Mumps only known natural host is man, where the infection is located in the T cell lymphocytes, the respiratory tract, the kidneys, the pancreas, the salivary glands (the swelling in the parotid salivary gland gives mumps its name) and, most significantly, the central nervous system (CNS) (Wolinsky et al.,1985).[1] Mumps can be detected in the CNS of 50% of infected humans (Wolinsky and Server, 1985). The infection of the CNS in humans is usually benign although meningitis is a common complication and encephalitis occurs rarely, which can result in terminal illness or permanent brain damage. The virus has been adapted to cell lines, chicken eggs and newborn hamsters (Cantell, 1961). In the newborn hamsters certain mumps viral strains will cause terminal encephalitis within 5 days of infection. The mechanism by which mumps enters and infects the CNS is unclear. Infection appears to cross into the brain at the choroid plexus, as shown by infection of these tissues and antibody staining of infected hamster brains.

Drug delivery to the CNS of humans is an unresolved pharmaceutical problem, due to the existence of a blood brain barrier. This barrier is due to tight junctions existing between the endothelial cells lining the brain capillaries. For material to cross into the brain it must be selectively transported across the barrier or be highly hydrophobic and diffuse across the barrier via the lipid bilayers. The possibility of CNS targeting was one incentive for researching the mumps system.

The mumps virus is made up of 6 proteins, a single stranded RNA, and a lipid outer membrane. The six regular proteins are the Large (L),

NucleoCapsid (NC), Polymerase (P), Matrix (M), Fusion (F) and Hemagglutination- Neuraminidase (HN) proteins (Jensik and Silver, 1976). The last two are glycoproteins and based on Sendai parallels are responsible for cell entry behavior (Tsao and Huang, 1986; Hoekstra and Klappe, 1986). The HN protein contains two activities, a Neuraminidase activity by which it can cleave terminal sialic acids from sialated glycosylations and a Hemagglutination activity, which is a binding activity that allows the agglutination of red blood cells. The F protein initiates fusion between host and viral membranes. The fusion protein (F_0) is cleaved upon appearance of the virus on the infected cell surface before viral budding to give a disulfide associated pair of proteins called F_1 (containing the transmembrane sequence and a highly hydrophobic N terminus) and F_2 (containing the signal sequence)(Herrler and Compans, 1983; Merz et al., 1983). Under examination by electron microscopy, these proteins appear on the surface of the virus as spike-like projections with knobbed heads and are often refered to as "spike proteins."

Mumps virus belongs to a group of viruses that enter the interior of a cell by fusion with the exterior cell membrane bilayer in a pH independent manner, as opposed to viruses like influenza which enter the cell interior by fusing with the walls of a lysosomal compartment at low pH (White et al., 1983). Fusion with the cell surface leaves the fusion and binding proteins on the surface of the infected cell. These proteins might then cause the formation of syncytia or giant cells by causing cells to fuse with one another. The other possibility for syncytial formation is the simultaneous fusion of a virus with two cells. The target on the cell surface for the mumps virus is most likely a negatively charged ganglioside, as the HN

protein naturally has a neuraminidase activity for such residues. The neuraminidase activity and binding activity appear to be located in the same site in the HN protein (Klamm, 1980; Server et al., 1982). In the related paramyxovirus Sendai it has been shown that the primary target is the ganglioside GQ1b, with the gangliosides GD1a and GT1b as secondary targets (Markwell et al., 1981). The N terminus of the F protein is highly hydrophobic and may play a direct role in membrane fusion by disrupting or bridging opposed viral and cellular bilayers.

Mumps virus has evolved into a multitude of strains which can be divided into two classes, based upon their behaviors (Wolinsky and Stroop, 1978; McCarthy et al., 1980). The first class causes little syncytia formation or cell-to-cell fusion, has low pathogenicity in animal models, and contains a high ratio of neuroaminidase activity to hemagglutination activity. The second class of mumps strains causes a high rate of syncytia formation, is highly pathogenic and neuroinvasive and has a low ratio of neuroaminidase to hemagglutination activity (Merz and Wolinsky, 1981). The neuroinvasive activity of the virus can be related to the activities of the HN protein (Server et al., 1982; Wolinsky et al., 1985). Further evidence that the neuroinvasive properties are caused by the HN protein rather then the F protein is provided by the fact that the F protein is conserved in sequence across the strains while the HN protein varies in sequence and size, from 75,000 daltons to 80,000 kilodaltons (Server et al., 1985a&b; McCarthy and Johnson, 1980). The other mumps virus proteins also show conservation in size across the strains.

The reconstitution of the lipid and glycoprotein viral envelope has been previously accomplished for several viruses, including the influenza

virus, Semliki Forest virus, vesicular stomatitus virus and Sendai virus. The mumps virus is closely related to Sendai virus, another paramyxovirus, whose glycoproteins have been reconstituted into artificial membranes and tested for activity with ghost erythrocytes (Harmsen et al., 1985). The activity of Sendai virus glycoproteins has been examined in reconstituted "virosomes" or RSVE (Reconstituted Sendai Viral Envelopes)(Harmsen et al., 1985; Vainstein et al., 1984). The glycoproteins or membrane associated proteins are separated from the internal core of the virus and placed into a lipid bilayer made up of natural viral lipids or some synthetic lipids. A reconstituted system is noninfectious and allows one to study the behavior of the surface proteins. The reconstituted vesicles might carry drugs or markers in various *in vitro* (Uchida et al., 1979) or *in vivo* (Vainstein et al., 1983) delivery schemes. See Figure 1 for a schematic representation of a RSVE drug delivery to a target cell.

It was my hope in beginning this project that one might successfully reconstitute the mumps glycoproteins HN and F in a similar fashion to that of Sendai. With such a system one could look at the tissue targeting behavior of the glycoproteins *in vitro* and *in vivo* in order to demonstrate whether tropism is determined by viral surface constraints. Of greatest interest in the *in vivo* animal studies was the possible interaction of the reconstituted vesicles with the central nervous system. The *in vitro* interactions of the vesicles with cells and ghost erythrocytes could also be studied by physical techniques in order to better understand the interaction of the viral proteins with the cell surface, and any conformational properties or changes in the viral protein structure created by interaction with a target cell surface.

II. Initial Reconstitution Studies with Mumps

Introduction

Initial reconstitution attempts were made with the mumps virus based on a method used previously with Sendai. The detergent reconstitution technique using octyl glucoside developed by Harmsen et al. was first examined (Harmsen et al., 1985). Octyl glucoside has a high critical micelle concentration (CMC) giving it the desirable property of easy removal via dialysis. The general protocol of detergent reconstitution calls for the addition of detergent to the virus, dissolving surface glycoproteins and lipids. The interior proteins and nucleic acids are then removed by centrifugation. When the detergent is dialyzed away vesicles can form with the glycoproteins incorporated into their membranes. These vesicles can then be physically characterized and assayed for activity.

Methods

Virus- ^{3}H Leucine labeled Kilham strain of mumps virus was grown in CV-1 cells in roller bottles at the University of Texas Department of Neurology by Neal Waxham and associates (Server et al., 1982). The virus was purified on a discontinuous 25/50 sucrose gradient and then frozen at -80°. All work with live virus was performed at the viral facilities run by Dr. John Zaia at the City of Hope Hospital.

Reconstitution- In a series of experiments a variety of reconstitution methods were attempted, the conditions are summarized in Table 1. Procedures were very similar in form. The virus was washed in a 100,000 g centrifuge spin. The virus pellet was resuspended in buffer and octyl glucoside detergent was added to the solution. The solution was incubated for one hour at room temperature and then nondissolved material was pelleted out at 100,000 g. Dialysis was performed to remove the detergent octyl glucoside. The dialysed solution was centrifuged at 100,000g and the product pellet was resuspended in appropriate buffer.

Five different reconstitutions were performed. Reconstitutions #1 and #2 were based on the method of Harmsen et al. (Harmsen et al., 1985). Reconstitution #3 used CV-1 cells as target membranes for the reconstituted products in the fluorescent fusion assay. Reconstitution #4 involved running a parallel set of experiments using Sendai virus. Half of the reconstitutes used high pH/high salt conditions, based on work by Jensik and Silver showing a higher rate of protein solvation using these conditions (Jensik and Silver,1976). Reconstitution #5 focused on the physical characterization of the products. Reconstitution was done in the presence of 20 mM magnesium as other reconstitution studies have indicated that magnesium facilitates the proper insertion of membrane proteins during reconstitution (Levitzki, 1985).

Lipid and Protein Assays- Modified Lowry (Peterson,1977) and Bartlett (Itoh et al.,1986) assays were used to determine the protein and lipid contents of the samples at various times. Protein concentrations could also be correlated to the amount of Tritium in a sample.

Transmission Electron Microscopy- 10 µl of sample at various concentrations (~300µg protein/ml) was applied to carbon covered glow discharged grids and allowed to dry. 10 µl of stain was then applied. 1% Phosphotungstic acid, 1% Uranyl Acetate, and 2% Ammonium Molybdate were used as stains. The samples were examined at the Caltech Biology EM facility using the Phillips EM201 transmission electron microscope. 35 mm photos were processed in the lab used the Ectamatic film photo development system.

Sucrose gradients- Sucrose gradients were prepared by the method of Luthe (Luthe, 1983). Gradients from 0-25% density were formed with a 50% bottom cushion. Reconstituted vesicles, vesicles treated with trypsin, and vesicles treated with pronase were placed on the surface of the gradient and centrifuged for 5 hours at 150,000 g. The gradient was removed from the centrifuge tube by puncture of the bottom of the tube and fractions were collected. The fractions were monitored for Tritium counts.

Ghost Preparation- O^+ and A^+ human erythrocyte ghosts were prepared by the method of Steck (reviewed by Steck and Kant, 1974).

Cell Line- Attached Green Monkey Kidney endothelial CV-1 cells were obtained from Neal Waxham and from the Caltech cell culture facility (run by Norm Davidson). The cells were grown in Eagle's Minimum Media with 10 % Fetal Calf Serum. Cells were passed every 4-5 days.

Fluorescent Fusion Assays- All fluorescent measurements were made on a SLM 4800 fluorimeter attached to an IBM AT computer using SLM software. Two sets of fluorescent indicators were used in the fluorescent fusion experiments.

NBD-PE and Rd-PE resonance energy transfer probes were incorporated into reconstituted vesicles by addition to the viral solution during detergent solvation (Struck et al., 1981). Probe concentration was based on lipid content of the viral vesicles: NBD-PE and Rd-PE were added at 1.5 mole % and 2 mole % of the lipid content respectively. In a fluorescent fusion assay 5-25 mg of viral protein were placed with 2 ml buffer in a quartz cuvette. An emission prescan was made, exciting at 470 nm and monitoring emission between 500 and 600 nm. Kinetic data were acquired by monitoring emission at 530nm (NBD emission) with the addition of ghost erythrocytes or CV-1 cells to the cuvette. After acquiring kinetic data, a post-fusion scan of emission wavelengths was taken. The solution was then brought to a concentration of 1% Triton X-100 so that maximal NBD fluorescent output could be determined. The NBD emission value with Triton X-100 represents maximal NBD fluorescence.

The R18 self quenching fluorescent probe was added directly in an ethanol solution to the reconstituted vesicles (Hoekstra et al., 1984). Unincorporated R18 was removed by passing the sample over a G50-100 Sephadex 5 ml chromatography column. R18 was added at 2 mole % of the lipid content. In the R18 system the excitation wavelength was 560 nm while the emission at 590 nm was monitored. Kinetic data was acquired previous to and after the addition of ghost erythrocytes or CV-1 cells to the

sample cuvette. Maximal emission was determined by adding Triton X-100 to the solution.

Hemagglutination Assay- Hemagglutination was assayed for by method of Salk (Salk, 1944). Serial dilutions of the virosomes were made and mixed with .5% O+ red blood cells in a conical bottomed titer plate. Readings were made after several hours at room temperature. Hemagglutinated cells settled uniformly across the bottom of the plate while non-agglutinated cells settled into a dark spot at the bottom of the conical well.

Fluorescence Microscope Studies- NBD/Rd labeled vesicles were applied to PBS rinsed CV-1 cell monolayers grown on cover slips. The monolayers were observed under a Nikon fluorescent microscope using NBD and Rd emission and excitement wavelength based filters.

Light Scattering Studies- Measurements were made using a Malvern 4700c photon correlation spectrometer equipped with a 455nm 5 watt Spectrophysics laser attached to an ATT PC with Malvern software. Most measurements were made at 90^{o} with no size bias and maximum modal distribution parameters. Measurements at other angles were made to check for any major amplitude variations. Size bias parameters were inserted after initial data collection to further clarify size distributions.

Results

Fluorescent Fusion Studies- In order to determine whether the fusion protein was still functional after reconstitution, the fluorescent resonance energy transfer probes NBD-PE/Rd-PE were added to several of the reconstituted systems. If fusion were to occur one would expect to see increased emission from the NBD probe as the spacing of the probes in the bilayer will increase and the rhodamine absorption effects will lessen due to the dilution of the virus associated probe into the target membrane (Struck et al., 1981). The distance dependency behavior of resonance energy transfer is $1/r^6$, and therefore small changes in probe density can be detected by this method. RMVE were added to CV-1 cells and human ghost erythrocytes (O+ and B+). In no case was there any evidence of probe dequenching .

The probe R18 was also used as a monitor of fusion by observation of lipid transfer. Transfer of the R18 probe to the target bilayer is indicated by increased fluorescence as the self quenching probe is diluted into the target bilayer (Hoekstra et al., 1984). Transfer of the R18 probe was observed in every reconstituted mumps experiment where it was used, even in cases where trypsin or DTT was added in order to inhibit protein mediated fusion. Table II presents some of the results found with the labeled products of reconstitution #4. There would appear to be a base line transfer of probe through solution without bilayer fusion. With reconstituted Sendai systems a higher rate of dequenching (~12%) was seen that was affected by DTT and trypsin, being brought down to baseline transfer levels (~5%).

Hemagglutination assay and Fluorescence Microscope Studies- The Hemagglutination assay showed a high amount of binding activity in the reconstituted systems, requiring between 2 and 10 ng of glycoprotein to agglutinate 50µl of .5% red blood cells. Fluorescence microscopy showed CV-1 cells with hundreds of glowing points attached to them, even after several buffer rinses, indicating that the virus readily bound to the CV-1 cells.

Electron Microscopy, Sucrose Gradient and Light Scattering- Initial studies with the electron microscope using PTA as a stain showed many >150 nm vesicles. Surface features were poorly contrasted with this stain. Upon usage of 2% Ammonium Molybdate, surface features became clear. Three different populations of reconstituted products became apparent. The first population was composed of large liposomes lacking surface projections and ranging between 250 and 400 nm in size. The second population was composed of small liposomes covered with surface protein projections, between 50 and 90 nm in size. These vesicles were similar to the reconstituted vesicles shown in the reconstitution paper of Harmsen. The third population consisted of filamentous protein aggregates. These elongated structures were covered with viral protein spikes and appear very much like a caterpillar in form. The aggregates ranged from 40-70 nm in length and 15-20 nm in width. Light scattering data also indicated that two size populations existenced, a large 250-400 nm population and a smaller 50-100 nm population.

Sucrose gradients showed three populations of products, a population which floated on the surface of the gradient and two populations in the

gradient which settled to 25% and 20% sucrose concentrations in the gradient, see Figure 2. These two populations disappeared from the middle of the gradient and appeared on the surface of the gradient upon addition of trypsin or pronase to the RMVE, indicating that these populations may have been protein aggregates digested into smaller less dense fragments or proteins cleaved from the surface of vesicles. Protein free vesicles are of low density and will float near the surface of the gradient.

Conclusions

Multiple reconstitution procedures to functionally reconstitute the fusion activity of the mumps virus were tried. While some fusion activity could be seen with Sendai via this octyl glucoside procedure, mumps failed to produce any protein dependent fusion activity. The lack of fusion activity might be due to the products observed by light scattering and electron microscopy, mainly protein aggregates rather then protein covered vesicles.

Some parallels can be drawn between these results and experiments done by Helenius and collaborators with the alphavirus Semliki Forest virus. The Semliki Forest virus has two large glycoproteins (E1 and E2) and one small glycoprotein on its surface (E3). Helenius reports that when the Semliki Forest virus E proteins were solubilized in Triton X-100 the three proteins remained in the form of a complex (Helenius and Soderland, 1973, Helenius et al., 1977) but were dissociated when treated with SDS or deoxycholate (Helenius et al., 1976; Becker et al.,1975). When the E proteins were purified and reconstituted into synthetic membranes using octyl

glucoside as a detergent, Helenius et al. found that E1 formed vesicles with the protein inserted, E2 formed *protein aggregates* and E3 precipitated out of solution (Helenius and Kartenbeck, 1980). They also reported that with parainfluenza, influenza, and Sendai virus, protein aggregates were the predominant octyl glucoside reconstitution product (Helenius et al., 1981).

Hsu, Scheid, and Choppin also experimented with the introduction of isolated Sendai glycoproteins into artificial bilayers (Hsu et al., 1979). They found that at low ratios of lipid to F protein, protein aggregates were formed. At a high ratio of lipid to F protein, vesicles with incorporated protein spikes were formed. Vesicles with incorporated protein were formed at all concentrations attempted with the HN protein. In Harmsen's reconstitution paper using octyl glucoside he reports "Occasionally, thin filamentous structures were seen, entirely surrounded by spikes" (Harmsen et al., 1985).

My results show that the major fate of the viral proteins in octyl glucoside dialysis is protein aggregation. The highly hydrophobic N terminus of the Sendai and mumps F1 protein may cause the F1 to *preferentially* form protein aggregates. This in agreement with all of the above cited literature.

Helenius attributes incorporation of glycoproteins into vesicles to be dependent on a number of factors, one of which is the rate of detergent removal (Helenius et al., 1981). It is useful to have a detergent that is easily removed in dialysis, i.e., a detergent with a high CMC. However, in several viral reconstitutions in the literature and in my work with mumps, the rapid removal of octyl glucoside appears to be non-beneficial as some viral proteins do not preferentially incorporate into the lipid bilayer but rather

form protein aggregates. A detergent with a lower CMC will dialyse away at a slower rate but may give the protein more time to incorporate itself into the lipid bilayer.

In order to avoid the formation of the protein aggregates, alternative detergent systems were tested and compared to the octyl glucoside products (section III). The detergents Triton X-100 and $C_{12}E_8$ were used based upon their lower CMCs and the success of other workers using these detergents for reconstitution. The experiments were done with the model system Sendai, due to the ease and availability of working with Sendai, compared with the difficulties of working with and scarcity of the mumps virus. Careful examination to the actual reconstituted product forms were made.

III. Reconstitution Studies on Sendai Virus Using Octyl Glucoside, Triton X-100, $C_{12}E_8$, and Short Chain Lipids

Introduction

Reconstitution of Sendai using either octyl glucoside or Triton X-100 has been reported in the literature (Harmsen et al., 1985; Vainstein et al., 1984). Harmsen et al. reported successful reconstitution of the virus based upon successful fusion of the vesicles with erythrocyte ghosts. They reported that Triton X-100 reconstituted vesicles were defective in fusion ability. Vainstein et al. have reported a Triton X-100 reconstitution of Sendai and upon the basis of hemolysis activity maintain that Triton X-100 reconstituted vesicles were functional while octyl glucoside vesicles were defective in fusion ability. The use of SN-2 Biobeads to remove the Triton X-100 selectively from solution allows the use of Triton X-100 as an alternative detergent to octyl glucoside (Holloway, 1973). The Harmsen vesicles were reported to be 75nm in diameter while the Vainstein vesicles were 100-300nm in diameter. A larger vesicle may be of more use in drug delivery of aqueous drugs as it has a much larger volume of encapsulation. Both reconstitutions were repeated in order to test the literature statements.

A third detergent, $C_{12}E_8$, has been used to reconstitute vesicular stomatitis virus (VSV)(Metsikko et al., 1986). The effects of this detergent in Sendai reconstitution were also examined. In addition the usage of shortchain lipids was investigated in reconstitution (Gabriel and Roberts, 1984, Gabriel and Roberts, 1986, Roberts and Gabriel, 1987).

The rigorous NBD/Rd fusion assay was used to determine vesicle fusion. It has been documented (Duzgunes, 1987) and shown in our lab that this probe system gives the most consistent results in other systems less complex than viral fusion, such as Ca^{++} induced PS fusion and freeze-thaw induced SUV fusion (Goodrich and Baldeschwieler, 1988).

Methods

Virus- Sendai virus was propagated in 10 day old fertilized chicken eggs. The virus was injected into the allontoic cavity of the eggs and allowed to grow for three days. The allontoic fluid was then harvested and the virus was purified by centrifugation, alternating between spins of 5,000g and 15,000g to pellet debris and virus respectively (Scheid and Choppin, 1976). The virus was stored at -80°.

Reconstitution-In all reconstitution methods the product was stored on ice and used in assays within 48 hours. If the products were frozen and then thawed before any assays were performed, hemagglutination activity was preserved while fusion activity was destroyed.

Octyl glucoside reconstitution was performed by the method of Harmsen et al. (Harmsen et al., 1985). 1 mg of virus was pelleted at 100,000 g for 1 hour and resuspended in 140 mM NaCl, 10 mM Hepes, 50 μM PMSF, and 50 mM octyl glucoside. The solution was incubated for one hour at room temperature (RT) and nondissolved material was removed by 100,000 g centrifugation for 1 hour. The sample was dialyzed against 25 ml buffer for 1 hr at RT. The dialysis was repeated and then the sample was dialyzed

against 50 ml buffer for 2.5 hr at room temperature. Dialysis was completed by 3 six hour dialysis periods against 250 ml of buffer at 4° C temperature. The products were then collected by centrifugation at 100,000 g for 1 hr.

Triton X-100 reconstitution was performed by the method of Vainstein et al. (Vainstein et al., 1984). 1 mg of virus was pelleted and resuspended in 20 µl of 100 mM NaCl, 50 mM Tris-HCL, .1 mM PMSF, and 10% Triton buffer. The solution was shaken for 1 hr at RT. Nondissolved material was removed by centrifugation at 100,000 g for 1 hr. 15 mg of SN-2 Biobeads were added to the solution. The solution was incubated for 4 hours while shaking. An additional 15 mg of Biobeads was then added along with 20 µl of 160 mM NaCl /20 mM Tris-HCl buffer. This solution was shaken for 14 hours at room temperature. The cloudy solution was removed from the beads via a Hamilton syringe and the products were isolated by pelleting at 100,000 g for an hour.

$C_{12}E_8$ reconstitution was based on the above Triton reconstitution and Metsikko's work on reconstitution of VSV with $C_{12}E_8$ (Metsikko et al., 1986). 2 mg of virus was pelleted at 100,000 g for 1hr. The pellet was resuspended in 70 µl of 100 mM NaCl/50 mM Tris/ .5 mM EDTA/ .5 µM PMSF/ 100 mM $C_{12}E_8$. The solution was shaken for 1 hr at RT. The nondissolved material was removed by centrifugation at 100,000g for 1 hr . 20 mg of SN-2 Biobeads were added and the solution was shaken for 2 hours. Shaking was resumed for 14 hours after the addition of 20 mg more biobeads. The product was removed by Hamilton syringe and collected by centrifugation at 100,000 g for a 1hr.

Short chain lipid reconstitution was based on the work of Gabriel and Roberts (Gabriel and Roberts, 1984, Gabriel and Roberts, 1986,Roberts and

Gabriel, 1987). Virus was collected by centrifugation at 100,000 g and resuspended in 450µl of 100 mM NaCl/50 mM Tris/.5 mM EDTA buffer. To this a 50 µl solution of 20mM Diheptanoyl-PC was added. The short chain lipid solution was prepared by vortexing dried short chain lipid with buffer. The ratio of viral lipid to short chain lipid was 1:2 at this point. This solution was shaken for 1 hr at RT and then centrifuged for 40 minutes at 100,000 g. The supernatant was added to a 100µl solution of 50 mM DPPC MLV's. The mixed solution was vortexed for several minutes and then shaken at RT for 4 hours. The DPPC MLV's were prepared from a dried solution of DPPC which was vortexed with buffer for several minutes and bath sonicated for 1 minute. The DPPC solution was exposed to a 46° bath for 20 seconds in order to disperse aggregates of DPPC. The product of the reconstitution was then collected by centrifugation at 100,000 g for 1hr.

Fluorescent Monitoring of Fusion- The resonant energy pairs of probes of NBD-PE and Rd-PE were used to monitor fusion in these systems (Struck et al., 1981). Each of the probes was added at 1.5 mole % of the lipid content of the reconstituted vesicles. The probes were added to the detergent dissolved virus in the octyl glucoside, Triton X-100 and $C_{12}E_8$ reconstitutions and were incorporated into the DPPC MLV's in the shortchain lipid reconstitution. Fluorescent measurements were made on a SLM 4800 using SLM software in an attached IBM AT computer. The reconstituted virus was excited at 470 nm and prescanned for emission between 500 nm and 600 nm. Kinetic data was collected by monitoring at 530nm. A+ human erythrocyte ghosts were used as the target membranes in all cases. Post fusion scans were made with and without the addition of

Triton X-100. The fluorescence at 530 after the addition of .5% Triton was treated as maximal fluorescence for NBD, after correction for Triton quenching.

Fluorescence Microscope studies, Transmission Electron Microscopy, Hemagglutination Assay, Light Scattering Measurements- Performed as in Section II.

Animal Studies-Virus was reconstituted by the Triton X-100 method and loaded with ^{111}In. Reconstitution buffers included 10 mM NTA. Nonencapsulated NTA was removed by centrifuging at 100,000g through NTA free buffer twice. 10 µl ^{111}In was dryed under a heat lamp and resuspended in 10 µl HCl by vigorous vortexing. 100 µl buffer was added to the ^{111}In solution along with 3 µl of ACAC. This loading buffer was then added to the NTA filled virosomes. The solution was incubated at 37^{o} or RT for 1 hr; both temperatures led to satisfactory loading (Beaumier and Hwang., 1982). Nonencapsulated ^{111}In was then removed by centrifuging the sample three times at 100,000g for 40 minutes through 5 ml of Indium free buffer. Serum stability studies were performed on the vesicles by monitoring the <G22> of the ^{111}In by PAC for up to two days (Hwang et al., 1980). Alternately 200 µl samples of 2 mg starting virus were injected into the tail vein of female adult BalbC mice. At two time intervals mice were sacrificed by heart puncture and their organs were counted for distribution. <G22> values were taken for organs with enough counts to monitor using the PAC device.

Results

Light Scattering and EM Data- Sendai virus appeared as polyploidal objects with spike projections on the viral surface. The virus ranged between 330-400nm in size. See Figure 3 for size distributions.

Octyl Glucoside dissolved virus consisted of micelles less than 2.4 nm in diameter and mostly less then 1.4 nm in diameter.

Three products were formed after detergent dialysis. The majority of the volume was made up of large protein-free or "bald" vesicles between 300-400 nm in size. Light scattering showed a second set of particles between 50-130 nm, see Figure 4. EM revealed this to be made up of two populations, protein-covered or "spiked" liposomes and protein aggregates. These aggregate structures were filamentous with spike-like projections, appearing in form like a caterpillar. The aggregates tend to be no longer than 70nm long and 20 nm wide. The protein aggregates make up the majority of the visible products under the electron microscope.

RSVE's prepared by the Triton X-100 method also showed two populations by light scattering. The large population ranged between 250-600nm, with the majority of vesicles between 300 and 400 nm, while the small population ranged from 80-170 nm (see Figure 5). Under examination in the electron microscope both populations consisted of vesicles covered with viral protein spikes. The large population made up 90% of the total mass and 30% of the total number of particles.

RSVE's prepared with $C_{12}E_8$ appeared as fairly uniform viral spike-protein-covered vesicles under EM examination. Light scattering showed a

major population between 300 and 500nm with a shoulder of vesicles tailing down to 160nm (Figure 6).

Protein-free large liposomes 300-500nm in size were observed when the short chain final products were examined. Protein-spiked vesicles were found, however, in the pelleted non short chain lipid dissolved material. These "Jumbosomes" ranged between 600 and 2500 nm, the majority being between 680 and 1200 nm in size, see Figure 7. Viral spikes covered both their external and internal surfaces.

Fusion monitored by Fluorescent quenching release- The products of octyl glucoside, Triton X-100, and $C_{12}E_8$ reconstitution all showed protein dependent fusion with target A+ ghost human erythrocytes. Some kinetic investigation into the $C_{12}E_8$ fusion was made, see Figure 8. This binding curve was created by using various ratios of reconstituted virus to ghost erythrocytes. A saturation of the available fusion sites can be seen with a limit of approximately .5 µg viral protein per µg ghost protein. Fusion activity was destroyed by freezing the reconstituted product at -70° C.

Hemagglutination assay- The Triton X-100 vesicles required a minimum of 4-6 ngs of protein to agglutinate 50 µl of .5% A+ red blood cells.

Fluorescence Microscope Observation- RSVE's produced by octyl glucoside, Triton X-100, or $C_{12}E_8$ could be observed bound to the surface of CV-1 cells. Some glowing auras could be detected around the cells which could be interpreted as probe released by fusion into the cellular membrane.

Animal Injections- The distributions of ^{111}In radiation in mice are shown in Figure 9. The bars shown are calculated by dividing the counts in an organ by the weight of the organ in grams and then dividing by the total counts injected into the animal. The material was fairly stable in the blood and accumulated in the reticuloendothelial organs, i.e., liver and spleen.

Conclusions

While octyl glucoside, Triton X-100 and $C_{12}E_8$ detergent reconstitutions of Sendai all produced products that were functional in binding and fusion activity, the sizes and shapes of the reconstituted products differed greatly. The octyl glucoside procedure gave three populations, protein-free 300nm vesicles, protein-spike-covered 100nm vesicles and 60nm protein aggregates. The Triton X-100 reconstitution procedure gave two populations, a smaller 100 nm protein-spike-covered vesicle population and a larger 300nm protein-spike-covered vesicle population. The $C_{12}E_8$ reconstitution gave one broad set of 250nm protein-spiked vesicles.

Octyl glucoside is considered to be a "strong" detergent, i.e., a detergent that will break up protein subunits and replace lipids tightly associated with a glycoprotien. This property and its high CMC make it a useful detergent for many chemical examinations of glycoproteins, including X-ray crystallography. However, for purposes of functional reconstitution a "weak" detergent such as Triton X-100 may function much better, allowing a glycoprotein to stay associated with local lipids and other protein subunits.

Usage of these detergents was in response to the early results with mumps. In the next section the results of using these detergents with mumps is examined, as the Sendai work indicated that the detergents Triton X-100 and $C_{12}E_8$ might be more useful in reconstitution.

The reconstitution using short chain lipids gave rather different results then those expected in designing the experiment. Proposed was a solvation of the virus lipids and glycoproteins in a short chain lipid detergent micelles. These micelles would normally form spontaneously large unilamellar vesicles upon the addition to a solution containing multilamellar vesicles of DPPC (Gabriel, 1984&1986; Roberts, 1987). By this means, protein might be incorporated into a large unilamellar vesicle. Instead initial solvation was only partial and very large vesicles (> 600nm in diameter) that had lost their viral core material were pelleted by centrifugation. These vesicles showed proteins oriented on both sides of the lipid bilayer.

IV. Reconstitution and Animal Studies with Mumps Virus

Introduction

Having completed a survey of reconstitution with the Sendai virus, repetition of the detergent reconstitution methods using mumps was attempted. Similar reconstitutions were performed and tested for fusion and binding activity and were characterized physically by light scattering and electron microscopy. In addition the tissue distribution of reconstituted mumps injected into infant hamsters was investigated, with emphasis on penetration into the central nervous system.

Materials and Methods

Virus- The Kilham strain of virus was again used as obtained from Neal Waxham at the university of Texas.

Reconstitution- Octyl glucoside, Triton X-100 and $C_{12}E_8$ reconstitutions were prepared in the same manner as described in section III, substituting mumps for Sendai virus. All samples were prepared with NBD-PE and Rd-PE fluorescent probes being added to the detergent solution in amounts equivalent to 1.5 mole % and 2 mole % of the total lipid content, for NBD and Rd respectively.

A Triton X-100 reconstitution with lipid supplement was also performed. 1mg of mumps virus was pelleted at 100,000g for one hour. 40

µl of 10% triton buffer with NTA was then added, the pellet was resuspended and shaken for 1 hour. The undissolved material was removed by centrifugation at 100,000g for one hour. To the detergent solution 40 µl of buffer containing 1.5 mg of DSPC and .5 mg of cholesterol was added. 30 mg of SN-2 Biobeads were then added and the mixture was shaken 4 hours at RT. An additional 30 mg of biobeads were then added along with 40 µl of 160 mM KCl/20 mM Tris buffer. The solution was shaken for 14 hours, the solution removed from the beads by a Hamilton syringe and then again centrifuged at 100,000g for one hour to pellet out the product vesicles.

Fluorescent Fusion Studies- Fluorescent fusion studies were performed in the same manner as described in Section III with the modification that O+ ghost erythrocytes were used as fusion targets.

Fluorescence Microscope Studies, Electron Microscopy, Hemagglutination Assays, and Light Scattering Measurements- All these assays were performed as described in section II.

Animal Studies- Reconstituted vesicles were prepared and loaded with ^{111}In as discussed in Section III. Newborn Syrian hamsters between 4 and 6 days of age were injected intraperitoneally with 200 µl of vesicles containing the reconstituted product from 1 milligram of starting mumps viral protein. Animals were sacrificed by heart puncture and their organs removed and counted with a gamma counter with windows for ^{111}In. A summary of the recovered radioactivity is given in figures 13 and 14, based upon % of total

recovered/g tissue, corrected for the blood within each organ (Hwang et al., 1980).

Results

Product Recovery- ^{3}H protein counts showed that 8.5% of the initial viral protein was reconstituted in the Triton X-100 procedure. 18% of the protein was recovered using the $C_{12}E_8$ method and 9% recovered using the octyl glucoside method. A maximal recovery of surface glycoproteins should be about 20%.

Fluorescent Fusion Assays- NBD-PE and Rd-PE labeled vesicles were monitored for fusion after the addition of O- ghost erythrocytes. No fusion activity was seen with any of the reconstituted products.

Hemagglutination Assay-All reconstituted vesicles showed hemagglutination ability. The minimum required protein amounts to agglutinate 50 µl of .5% O+ erythrocytes are shown in Table III.

Fluorescence Microscopy-Binding to CV-1 cells was observed under the fluorescent microscope. All reconstituted vesicles showed strong binding tendencies, as observed as glowing points attached to the surface of the cells.

Light Scattering Data- Triton X-100 reconstituted vesicles showed a wide distribution of vesicle sizes between 200nm and 700nm in size, the majority of vesicles being between 250 and 400 nm in size (Figure 10).

C12E8 reconstituted vesicles also showed a wide distribution of sizes between 200 and 700 nm in size with the majority of vesicles being 250nm to 400 nm in size. Larger sized vesicles were less frequent in the C12E8 reconstitution products as compared to the Triton X-100 reconstitution product.(Figure 11).

Octyl glucoside reconstituted vesicles showed two populations by light scattering. The smaller population was between 90 and 200 nm in size while the larger population was between 250 and 500nm in size. See Figure 12.

The Triton X-100 reconstituted vesicles supplemented with lipid were between 460 and 1200nm in size with a fairly even distribution of numbers across this range.

Animal Studies- As the binding protein of the reconstituted virus appeared to be functional in hemagglutination and fluorescence microscope studies, some preliminary animal experiments were performed. As mentioned in the introduction, the binding or HN protein structure correlates with the ability of the virus to be neuroinvasive. The literature animal system of baby syrian hamsters was used (Kilham and Overman, 1953, Kilham and Murphy, 1952). The animals were injected intraperitoneally, the only available avenue, besides intracerebrally, in animals of their size. The first experiments showed ^{111}In counts in the brain after correction for blood associated counts, due possibly to some blood

brain barrier penetration, see Figure 13. Also observed was a large association of radioactivity with the backbone and spine. The experiments were repeated with a second batch of animals where mumps virus and control DSPC/Cholesterol liposomes were also injected, see Figure 14. It became apparent that much of the blood brain penetration was due to some amount of leakiness in the brains of these animals as some control liposomes also penetrated into the brain. The association of the reconstituted vesicles with the spine and ribs is strong in these animals. The RMVE containing native viral membrane appear to have a higher blood stability than the DSPC/Chol supplemented or plain DSPC/Chol vesicles.

Conclusions

In no case was there evidence that the fusion protein of the mumps virus was reconstituted functionally. Several possible reasons for this inactivity were tested. Early experiments involved reconstituted virus that had been stored at -70°. We have found with Sendai virus that freezing and thawing the reconstituted virus results in loss of fusion activity. In the case of mumps experiments no activity was seen with refrozen virosomes or nonrefrozen virosomes. Multiple reconstitution methods were undertaken in the hope that under certain detergent or buffer conditions activity could be preserved, yet no conditions proved successful in preserving fusion activity. One possibility reason for this failure in reconstitution was that the whole virus did not contain membrane fusion activity. The starting material was prepared in another lab and was not tested for activity before

conducting these experiments. To test the fusion ability of native mumps, one can label whole virus with R18 and look for fusion via fluorescent assay, but, as previously noted this assay tends to give spontaneous non-protein-dependent transfer. This experiment was attempted twice, the first time showing some protein mediated R18 transfer, while the second time no activity was observed (see Chapter 4 Appendix, 1.). When the virus is grown, the Kilham strain of mumps causes a great deal of syncytia and cell disruption. For this reason the virus is purified on a sucrose gradient. This gradient can cause the virus to lose 99% of its infectivity. This loss might be due to a irreversable conformational change in the fusion protein, making reconstitution functionally a difficult task.

Two other possibilities existed for the lack of fusion activity. While attachment is seen to the surface of the target ghost erythrocytes and CV-1 cells, some other target site for the fusion protein might have been missing. There was also the possibility that the virus had a much slower fusion activity than Sendai and that fusion occured at a rate undetectable by the fluorescent methods (<2% fusion per hour). The fusion activity of the native virus had not yet been determined.

The structure and size of the reconstituted products are described in the results section. Reconstitution by Triton X-100 or $C_{12}E_8$ has an advantage over octyl glucoside reconstitution in that the formation of protein aggregates is avoided. Both Triton and $C_{12}E_8$ reconstitution gave a single population of vesicles with mumps, $C_{12}E_8$ vesicles being slightly more homogeneous in distribution. Comparison of mumps reconstituted products with Sendai reconstituted products show that the octyl glucoside and $C_{12}E_8$ reconstitution products are very similar with both viruses. The

Triton X-100 reconstitution, however, gave a much more homogeneous population of vesicles with mumps. Further experiments used vesicles prepared by Triton X-100 and $C_{12}E_8$ methods rather than the octyl glucoside method.

Studies with the preferred literature animal system in terms of targeting to the central nervous system were inconclusive. In any event there was no dramatic targeting to the brain by the mumps envelopes. Future experiments should seek an infectable candidate with a known rigid blood brain barrier. Full grown mice contract a slow infection of the virus and might be used (Overman et al., 1953, Kristensson et al., 1984)

V. Reconstitution with "Caltech/City of Hope" Mumps

Introduction

In order to exam the activities of whole mumps virus and determine if alternative starting material could lead to successful reconstitution, Kilham strain mumps virus was prepared. The whole virus was examined for activity (see Chapter 4) as was Triton X-100 reconstituted virus.

Methods

Mumps Growth and Purification- CV-1 cells were grown in MEM media with 10% FCS in 150 cm^2 bottles until confluent and then transferred to 800 cm^2 roller bottles. The cells required 4-6 days to become confluent in these larger bottles. The medium was then removed and the cells washed with Hanks solution. Seed solution of mumps virus (2 to 5 ml) was then added to the roller bottle along with Hanks buffer to bring the total volume up to 10 ml per bottle. The bottles were then incubated for 2 hours at 37° while rotating. The inoculum was aspirated and new media was added, containing 20 mM Hepes as buffer. Alternatively the bottles were gassed with 5% CO_2 for 60 seconds. After 3 to 4 days large scale destruction of the cell monolayer was apparent and the medium was removed. The media could be frozen at this point for use as "seed" virus in future viral preparations. Cell debris was removed by pelleting at 1500 rpm for 10 minutes in a lab top centrifuge using 50 ml conical tubes. The supernatant

was transferred to high density tubes and centrifuged in a SS-34 rotor for 40 minutes at 15,000 rpm (≈ 25,000g). The pellet was resuspended in PBS and used for later experiments or stored by freezing in liquid nitrogen after the addition of 10% glycerol. This preparation was run on a small scale to prepare "seed virus" and on a larger scale to prepare experimental virus.

Plaque and Cell Death Assays- Plaque and cell death assays were run on the seed and experimental virus in order to determine viral infectivity. Serial dilutions of the virus in 1 ml Hanks buffer were added to six well plates (10 cm^2/well) containing confluent CV-1 cells (media removed) and incubated at 37°C for 2 hours. The inoculum was then removed. The cells were then covered with media in the cell death assay. For the plaque assay agar/media or methylcellulose/media were used to cover the cells. To prepare the agar overlay, agar was dissolved in boiling water and mixed with 2X media. Upon cooling to 35°C, serum was added to the mixture and the overlay was placed on the cells. The methylcellulose overlay consisted of a 1:1 mixture of 2X media and 2% methylcellulose.

Preparation of RMVE-

Short term fusion experiment- Five roller bottles were used to produce virus that was purified and resuspended in 14 ml PBS. Two reconstitutions were conducted on 4 ml samples of this preparation. The virus was pelleted at 100,000g for 1 hour in the SW50.1 rotor. The mumps pellet was then resuspended in 100 µl of Triton X-100 (in 100 mM NaCl, 50 mM Hepes) or 140 µl of C12E8. The mixture was shaken at room temperature for 2 hours and then centrifuged at 100,000g for 40 minutes to remove undissolved

material. The fluorescent probes NBD-PE and Rd-PE were added to the clear supernatants in the amounts of 6 μg NBD-PE and 8 μg Rd-PE to the Triton X-100 mixture and 12 μg NBD-PE and 16 μg Rd-PE were added to the C12E8 mixture. 100 mgs of SN-2 biobeads were then added to the mixture, the solution was vortexed, and then shaken for 4 hours. An additional 100 mg of SN-2 Biobead were then added along with 100 μl of solution A (160 mM NaCl, 20mM Hepes). After shaking at room temperature for an additional 15 hours the cloudy RMVE were removed from the beads with a Hamilton syringe, the beads were washed, and the product was pelleted by ultracentrifugation (100,000g for 40 minutes). Lowry protein measurements gave yields of 125 μg RMVE from the Triton X-100 reconstitution and 95 μg from the C12E8 reconstitution.

Long term fusion experiment- From a seven bottle mumps preparation 2 ml (≈460 μg mumps protein) PBS suspended product were used in the reconstitution. The same general procedure as described above was used with: 100 μl Triton X-100 used to dissolve the virus, 1 μg NBD and 1.2 μg Rd-PE being used to label the virus, 50 mg biobeads used in initial dialysis, 50 mg biobeads and 50 μl solution A used after the 4 hour incubation. The preparation yielded 50 μg of RMVE.

Serum Stability Experiment- RMVE were prepared from the mumps preparation described above in the short term fusion experiment. 1.8 ml of virus solution (≈ .2 mg) was pelleted and reconstituted as described above with: 50 μl Triton X-100 used to solvate the virus, 50 mg biobeads used in initial dialysis, 50 mg biobeads and 50 μl solution A used after the 4 hour incubation. All solutions contained 10 mM NTA, a chelate for the ^{111}In loading. After pelleting the final product the sample was resuspended in

100 µl PBS without NTA. The ^{111}In was prepared by drying 10 µl of $^{111}InCl$ (≈ .1mCi) and then serially adding 10 µl 3 mM HCl, 100 µl PBS, and 3 µl ACAC, with vortexing between each addition. The RMVE were then mixed with this solution and incubated at RT for 1.5 hours. A large volume of PBS was added (4 ml) and the RMVE were pelleted by ultracentrifugation. The wash was repeated. The RMVE were found to contain ≈45% of the added ^{111}In, as measured by radiation output (geiger counter).

Whole virus 125 I Labeling Experiment- One tube out of eleven from a 10 roller bottle preparation was labeled with ^{125}I and then reconstituted. The method of reconstitution was as detailed above with the following parameters: 100 µl Triton X-100 used to solvate the virus, 70 mg biobeads used in initial dialysis, 70 mg biobeads and 100 µl solution A used after a 3 hour incubation.

Reconstituted Sendai labeling experiment- One tube out of eleven from a 10 roller bottle prep was reconstituted and then labeled with ^{125}I. The method of reconstitution was as detailed above with the following parameters: 50 µl Triton X-100 used to solvate the virus, 50 mg biobeads used in initial dialysis, 50 mg biobeads and 50 µl solution A used after a 6 hour incubation.

Labeling with ^{125}I- Disposable glass test tubes were coated (10 µg for a small tube, 30 µg for a large tube) with Iodogen reagent and dryed. Mumps virus or RMVE were placed inside the coated test tube and 5 µl $Na^{125}I$ was added. The reaction was allowed to procede on ice for one hour. The sample was removed from the tube, the tube washed and the virus or RMVE was then pelleted by ultracentrifugation. The pellet was washed with PBS.

Perturbed Angular Correlation Spectroscopy Serum Stability Studies(PAC)- PAC was conducted on ^{111}In loaded RMVE to measure <G22> values in the absence and presence of serum. The PAC was calibrated to give a <G22> reading of .671 for a mixture of ^{111}In and NTA and a reading of .198 for a mixture of ^{111}In and serum.

Fluorescent Fusion Assay, Protein Assay, Ghost Preparation- Conducted as described in section II.

Results

Comments on virus growth and purification-

Initial attempts at virus growth ran into a number of problems, primarily caused by repeated contamination of cell culture. Fungal contamination was present in a number of the seed cultures used to grow virus. Cells were grown to high densities and tended to be very susceptible to contamination when the media became very acidic. After inoculation with virus, the roller bottle cultures are sealed to the external atmosphere and must be buffered by adding external CO_2 to the bottle or by adding HEPES buffer to the media. I found the first method to be very susceptible to error in providing proper pH balance for the cells.

Purification without the use of sucrose gradients was easily achieved. The sucrose gradients were originally used to remove fragmented cellular material from the growth supernatant. Gel elecrophoresis examination of

the protein products showed that little material other than virus and BSA is purified by differential centrifugation.

The one persistent contaminant during purification is bovine serum albumin (BSA) which is a major component of the fetal calf serum (FCS) used as a supplement to the cell growth mixture. This protein is only 66 kD MW and should be separated from the virus by ultracentrifugation but most likely sticks to the centrifuge tube and perhaps to the virus. Quantification of virus amount is aggravated by the presence of this contaminant. Presence of BSA during purification procedures is difficult to detect as it has a very similar apparent molecular weight to the mumps NC protein, the most abundant protein in the virus. Multiple ultracentifuge purification cycles were conducted to remove the BSA and determine the amount of virus present. One additional cycle of ultracentrifugation appears to remove the majority of the BSA. Under standard growth conditions, approximately 250 μg ± 50 μg were prepared per 800 cm^2 roller bottle.

Fluorescent fusion assays-

Short term- Kinetic measurements were made of the fusion of virus with erythrocyte ghosts using the NBD/Rd probe pair system. Fluorescent dequenching was apparent providing evidence for successful reconstitution with Triton X-100 (Figure 15).

Long term- Overnight incubation of RMVE with ghost erythrocytes was conducted. As the amount of target membrane was increased fusion increased and then leveled at ≈28% (Figure 16). Thus only a limited number of reconstituted envelopes contained fusogenic activity. Approximately 350 viral receptors were available per cell.

Serum Stability- PAC spectroscopy was used to observe the stability of RMVE. As vesicles are destabilized and disrupted by serum their NTA chelated ^{111}In becomes exposed to serum and tightly bound by serum proteins. This produces a comparatively low <G22> (.2) to that of the loosely bound ^{111}In/NTA complex (.67). The loaded RMVE gave a <G22> value of (.53±.03). This lower value may be due to interaction of the ^{111}In with the viral proteins. In serum, 30% of the vesicles degraded over 60 minutes (Figure 17). The rest of the vesicles were less susceptible to degradation, with 15% degraded over the next 8 hours.

^{125}I labeling- For purposes of binding studies with human brain epithelial capillary tissue, RMVE was labeled with ^{125}I. Two methods of labeling were attempted, labeling before and after reconstitution. For the recovered product of 20 μg RMVE, labeling before reconstitution gave a specific activity of 44,500 cpm/μg while labeling after reconstitution gave a much higher specific activity, $5.5x10^6$ cpm/ μg. In the experiment where reconstitution occurred after labeling, much of the ^{125}I label may have been lost to residual BSA, as no ultracentrifugation purification was conducted on the sample until after labeling. The experiments for which these samples were prepared for were not conducted due to a lack of enthusiasm by potential collaborators (N.J. Abbott, Kings College London; William Pardridge, UCLA).

Conclusions

The mumps virus can be successfully purified without the use of sucrose gradients. Use of this virus allowed successful reconstitution of fusion active RMVE. RMVE vesicle stability in serum was reasonable with 30% of the vesicles being lost in one hour and the rest appearing to be stable for many hours.

VI. Conclusions

This initial work on mumps reconstitution by detergent dialysis methods concentrated on the recovery of the virus glycoproteins in a form in which the protein's interactions with target membranes could be surveyed. The products given by octyl glucoside detergent dialysis reconstitution were undesirable as any behavior exhibited by the reconstituted virus may be attributed to any of the three different reconstituted products, including protein aggregates. Triton X-100 and $C_{12}E_8$ reconstitute products are better defined in size and character and exhibit all the glycoprotein properties of the native mumps and Sendai virus.

The reason for the lack of mumps fusion activity in the early reconstitutions is unclear. The sucrose gradient run during the initial purification of this virus may have been responsible for destruction of the fusion activity as this gradient will cause loss of infectivity. Alternatively, storage at -196° C in the presence of a cryopreservative may have preserved viral activity better than storage at -80° C. Reconstitutions which involved mumps virus grown in cell culture at the City of Hope Hospital gave fusion functional reconstitutes.

Animal studies with reconstituted Sendai and mumps virus showed that these vesicles acted in principle very similarly to liposomes in circulation behavior. Uptake of the "virosomes" occurred primarily in the reticuloendothelial system, i.e., liver and spleen. The uptake of the mumps by the brain of the hamsters was near background blood levels and too near

the "noise" level of the assay to draw any conclusive positive results. As an experimental system it was unclear whether these animals had a complete blood brain barrier. In general the vesicles had reasonable stability in serum and good circulation time in the blood.

VII. Future Potentials

Given that the mumps and Sendai HN protein activities are preserved in all reconstitutions and the Sendai F protein activity is generally preserved, a combination of mumps and Sendai viral proteins in a reconstituted system could have unique properties. The binding protein of mumps could provide the tissue specific behavior while the Sendai fusion protein allows for entry of the virosome contents into the target cell. Isolation of the individual glycoproteins from both Sendai and mumps is feasible via sucrose gradients or immunoaffinity columns (Hsu, 1979). Reconstitution with other more specific binding moieties should also be feasible. Such a combination of viral targeting and fusion proteins could represent the first generation of tissue tropic drug delivery liposomes.

[1]Abbreviations Used-CNS- Central Nervous System, F-Fusion Protein, F_1 & F_2 -Fusion protein cleavage products, HN- Hemagglutination-Neuroaminidase Protein, RSVE-Reconstituted Sendai Viral Envelope, RMVE- Reconstituted Mumps Viral Envelope, CMC-Critical Micelle Concentration, NBD-PE - N-(7-nitro-2,1,3,-benzoxadiazol-4-yl)-phosphatidylethanolamine, Rd-PE - N-(lissamine Rhodamine B sulfonyl)-phosphatidylethanolamine, R18- Octadecyl Rhodamine B chloride, DTT- Dithiothreitol, PS- Phosphatidylserine, PC- Phosphatidylcholine, Octyl Glucoside- 1-O-n-octyl-Beta-D-glucopyranoside, PMSF- Phenylmethylsulfonyl Fluoride, DPPC-Dipalmitoyl phosphatidylcholine, DOPC- Dioleoyl Phosphatidylcholine, EM- Electron Microscopy, SUV- Small Unilamellar Vesicle, LUV- Large Unilamellar Vesicle, MLV- MultiLamellar Vesicles, ACAC- 2,4-Pentanedione, POPC- 1-Palmitoyl-2-Oleoyl Phosphatidylcholine, MEM- Minimal Essential Media, FCS- Fetal Calf Serum.

References

Beaumier, P., and Hwang, K. (1982) An Efficient Method for Loading Indium-111 into Liposomes Using Acetylacetone. *The Journal of Nuclear Medicine*, **23**, 810-815.

Becker, R., Helenius, A., and Simons, K. (1975) Solubilization of the Semliki-Forest Virus Membrane with Sodium Dodecyl Sulfate. *Biochemistry*, **14**, 1835-1841.

Cantell, K. (1961) Mumps Virus. *Advances in Virus Research*, **8**, 123-164.

Cabasso, V., and Cox, H. (1955) Hemagglutination behavior for mumps virus strains of different origin. *Proc. Soc. Exptl. Biol. Med.*, **88**, 370.

Duzgunes, N., Allen, T., Fedor, J., and Papahadjopoulos, D. (1987) Lipid Mixing during Membrane Aggregation and Fusion: Why Fusion Assays Disagree. *Biochemistry*, **26**, 8435-8442.

Gabriel, N., and Roberts, M. (1984) Spontaneous Formation of Stable Unilamellar Vesicles. *Biochemistry*, **23**, 4011-4015.

Gabriel, N., and Roberts, M. (1986) Interaction of Short Chain Lecithins with Long-Chain Phospholipids: Characterization of Vesicles that Form Spontaneously. *Biochemistry*, **25**, 2812-2821.

Goodrich, R., and Baldeschwieler, J. (1988) The Cryopreservative Action of Synthetic Glycolipids. *Biophysical J.*, **53**, 121a.

Harmsen, M., Wilchut, J., Hukstaert, C., and Hoekstra, D. (1985) Reconstitution and Fusogenic properties of Sendai virus envelopes. *Eur. J. Biochem.* , **149**, 591-599.

Helenius, A., and Soderlund, H. (1973) Stepwise Association of the Semliki Forest Virus Membrane with Triton X-100. *Biochimica et Biophysica Acta*, **307**, 287-300.

Helenius, A., Fries, E., Garoff, H., and Simons, K. (1976) Solubilization of the Semliki Forest Virus Membrane with Sodium Deoxycholate. *Biochimica et Biophysica Acta*, **436**, 319-334.

Helenius, A., and Bonsdorff, C. (1976) Semliki Forest Virus Membrane Proteins. Preparation and Characterization of Spike Complexes Soluble in Detergent-Free Medium. *Biochimica et Biophysica Acta*, **436**, 895-899.

Helenius, A., Fries, E., and Kartenbeck, J. (1977) Reconstitution of Semliki Forest Virus Membrane. *The Journal of Cell Biology*, **75**, 866-880.

Helenius, A., and Kartenbeck, J. (1980) The Effects of Octylglucoside on the Semliki Forest Virus Membrane. *Eur. J. Biochem*, **106**, 613-618.

Helenius, A., Sarvas, M., and Simons, K. (1981) Asymmetric and Symmetric Membrane Reconstitution by Detergent Elimination. *Eur. J. Biochem.* , **116**, 27-35.

Herrler, G., and Compans, R. (1983) Transport of Posttranslational Modification and Intracellular Mumps Virus Glycoproteins. *Journal of Virology*, 1983, **47**, 354-362.

Hoekstra, D., de Boer, T., Klappe, K., and Wilchut, J. (1984) Fluorescent Method for Measuring the Kinetics of Fusion between Biological Membranes. *Biochemistry*, **23**, 5675-5681.

Hoekstra, D., and Klappe, K. (1986) Sendai Virus-Erythrocyte Membrane Interaction: Quantitative and Kinetic Analysis of Viral Binding, Dissociation, and Fusion. *J. Virology*, 1986, **58**, 87-95.

Holloway, P. (1973) A Simple Procedure for Removal of Triton X-100 from Protein Samples. *Analytical Biochemistry*, **53**, 304-308.

Horigome, T., and Sugano, H. (1983) A Rapid Method for Removal of Detergents from Protein Solution. *Analytical Biochemistry*. **130**, 393-396.

Hsu, M., Schied, A., and Choppin, P. (1979) Reconstitution of Membranes with Individual Paramyxovirus Glycoprteins and Phospholipid in Cholate Solution. *Virology*, **95**, 476-491.

Hwang, K., Luk, K., and Beaumier, P. (1980) Hepatic uptake and degradation of unilamellar spingomyelin/cholesterol liposomes: A kinetic study. *Proc. Natl. Acad. Sci. USA*, **77**, 4030-4034.

Itoh, Y., Itoh, T., and Kaneko, H. (1986) Modified Bartlett Assay for Microscale Lipid Phosphorus Analysis. *Analytical Biochemistry*, **154**, 200-204.

Jensik, S., and Silver, S. (1976) Polypeptides of Mumps Virus. *Journal of Virology*, **17**, 363-373.

Kilham, L., and Murphy, H. (1952) Propagation of Mumps Virus in Suckling Mice and in Mouse Embryo Tissue Cultures. *Proc. Exptl. Biol. Med.*, **80**, 495-498.

Kilham, L., and Overman, J. (1953) Natural Pathogenicity of Mumps Virus for Suckling Hamsters on Intracerebral Inoculation. *J. Immunol.*, **70**, 147-151.

Klamm, H. (1980) Some Properties of Mumps Virus Neuraminidase. *Acta Virol.*, **24**, 127-131.

Kristensson, K., Orvell, C., Malm, G., and Norrby, E. (1984) Mumps Virus Infection of the Developing Mouse Brain- Appearance of Structural Virus Proteins Demonstated with Monoclonal Antibodies. *Journal of Neuropathology and Experimental Neurology*, **43**, 131-140.

Levitzki, A. (1985) Reconstitution of membrane receptor systems. *Biochimica et Biophysica Acta*, **822**, 127-153.

Luthe, D. (1983) A Simple Technique for the Preparation and Storage of Sucrose Gradients. *Analytical Biochemistry*, **83**, 230-232.

Markwell, M., Svennerholm, L., and Paulson, J. (1981) Specific gangliosides function as host cell receptors for Sendai virus. *Proc. Natl. Acad. Sci.*, **78**, 5406-5410.

McCarthy, M., and Johnson, R. (1980) A Comparison of the Structural Polypeptides of Five Strains of Mumps Virus. *J. Gen. Virol*, **46**, 15-27.

McCarthy, M., Jubelt, B., Fay, D., and Johnson, R. (1980) Comparitive Studies of Five Strains of Mumps Virus In Vitro and in Neonatal Hamsters: Evaluation of Growth, Cytopathogenicity, and Neurovirulence. *Journal of Medical Virology*, **5**, 1-15.

Merz, D., Server, A., Waxham, M., and Wolinsky, J. (1983) Biosynthesis of Mumps Virus F Glycoprotein: Non-fusing Strains Efficiently Cleave the F Glycoprotein Precursor. *J. Gen. Virol.*, **64**, 1457-1467.

Merz, D., and Wolinsky, J. (1981) Biochemical Features of Mumps Virus Neuraminidases and Their Relationship with Pathogenicity. *Virology*, **114**, 218-227.

Metsikko, K., van Meer, G., and Simons, K. (1986) Reconstitution of the fusogenic activity of vesicular stomatitus virus. *The EMBO Journal*, **5**, 3429-3445.

Novick, S., and Hoekstra, D. (1988) Membrane Penetration of VIral Proteins During Fusion of Sendai Virus with Liposomes Shown by Hydrophobic Photoaffinity Labeling. *Biophysical J.*, **53**, 322a.

Overman, J. (1955) Antibody Response of Suckling Mice to Mumps Virus. *J. Immuno.*, **73**, 244-248.

Peterson, G. (1977) A Simplification of the Protein Assay Method of Lowry et al. Which is More Generally Applicable. *Analytical Biochemistry*, **83**, 346-356.

Roberts, M., and Gabriel N. (1987) Short Chain Lecithin Long-Chain Phospholipid Unilamellar Vesicles- In vitro and In vivo stability studies. *Colloids and Surfaces*, **30**, 113-132.

Salk, J. (1944) A Simplified Procedure for Titrating Hemagglutinationg Capacity of Influenza-Virus and the Corresponding Antibody. *J . Immunol.*, 1944, **49**, 87.

Scheid, A., and Choppin, P. (1976) Protease activation mutants of Sendai viruses: Activation of cell fusion, hemolysis and infectivity by proteolytic cleavage of an inactive precursor protein of Sendai virus. *Virology*, **69**, 265-277.

Server, A., Merz, D., Waxham, M., and Wolinsky, J. (1982) Differentiation of Mumps Virus Strains with Monoclonal Antibody to the HN Glycoprotein. *Infection and Immunity*, **35**, 179-186.

Server, A., Smith, J., Waxham, M., Wolinsky, J., and Goodman, H. (1985a) Comparision of the F1 NH2-Terminal Region of a Fusing and a Non-Fusing Strain of Mumps Virus. *Virus Res.*, **1S**, 72.

Server, A., Smith, J., Waxham, M., Wolinsky, J., and Goodman, H. (1985b) Purification and Amino-Terminal Protein Sequence Analysis of the Mumps Virus Fusion Protein. *Virology*, **144**, 373-383.

Simons, K., Helenius, A., and Garoff, H. (1973) Solubilization of the Membrane Proteins from Semliki Forest Virus with Triton X-100. *J. Mol. Biol.*, **80**, 119-133.

Steck, T. and Kant, J. (1974) Preparation of Impermeable Ghosts and Inside-out Vesicles from Human Erythrocyte Membranes. *Methods in Enzymology*, **31**, 172-180.

Struck, D., Hoekstra, D., and Pagano, R. (1981) Use of Resonance Energy Transfer to Monitor Membrane Fusion. *Biochemistry*, **20**, 4093-4099.

Tsao, Y., and Huang, L. (1986) Kinetic Studies of Sendai Virus Target Membrane Interactions: Independent Analysis of Binding and Fusion. *Biochemistry*, **25**, 3971-3976.

Uchida, T., Miyake, Y., Yamaizumi, M., Mekada, E., and Okada, Y. (1979) Improved Methods Using HVJ (Sendai Virus) for Introducing Substances into cells. *Biochemical and Biophysical Research Communications*, **87**, 371-379.

Vainstein, A., Razin, A., Graessmann, A., and Loyter, A. (1983) Fusogenic Reconstituted Sendai Virus Envelopes as a Vehicle for Introducing DNA into Viable Mammalian Cells. *Methods in Enzymology*, **101**, 492-512.

Vainstein, A., Hershkovitz, M., Isreal, S., Rabin, S., and Loyter, A.(1984) A New Method for Reconstitution of Highly Fusogenic Sendai Virus Envelopes. *Biochemica and Biophysica Acta*, **773**, 184-188.

Wagner, R., and Petri, W. (1979) Reconstitution into Liposomes of the Glycoprotein of Vesicular Stomatitis Virus by Detergent Dialysis. *The Journal of Biological Chemistry*, **254**, 4313-4316.

Waxham, N., Server, A., Goodman, H., and Wolinsky., J. (1987) Cloning and Sequencing of the Mumps Virus Fusion Protein Gene. *Virology*, **159**, 381-388.

White, J., Kielain, M., and Helenius, A. (1983) Membrane fusion proteins of enveloped animal viruses. *Q. Rev. Biophys.*, **16**, 151-195.

White. J. (1990) Viral and Cellular Membrane Fusion Proteins. *Annu. Rev. Physiol.* , **52**, 675-697.

Wolinsky, J., and Server, A. (1985) "Mumps Virus." In Virology, ed. B. Fields, Raven Press, New York, 1255-1284.

Wolinsky, J., and Stroop, W. (1978) Virulence and Persistance of Three Prototype Strains of Mumps Virus in Newborn Hamsters. *Archives of Virology*, **57**, 355-359.

Wolinsky, J., Waxham, M., and Server, A. (1985) Protective Effects of Glycoprotein-Specific Monoclonal Antibodies on the Course of Experimental Mumps Virus Meningoencephalitis. *Journal of Virology*, **53**, 727-734.

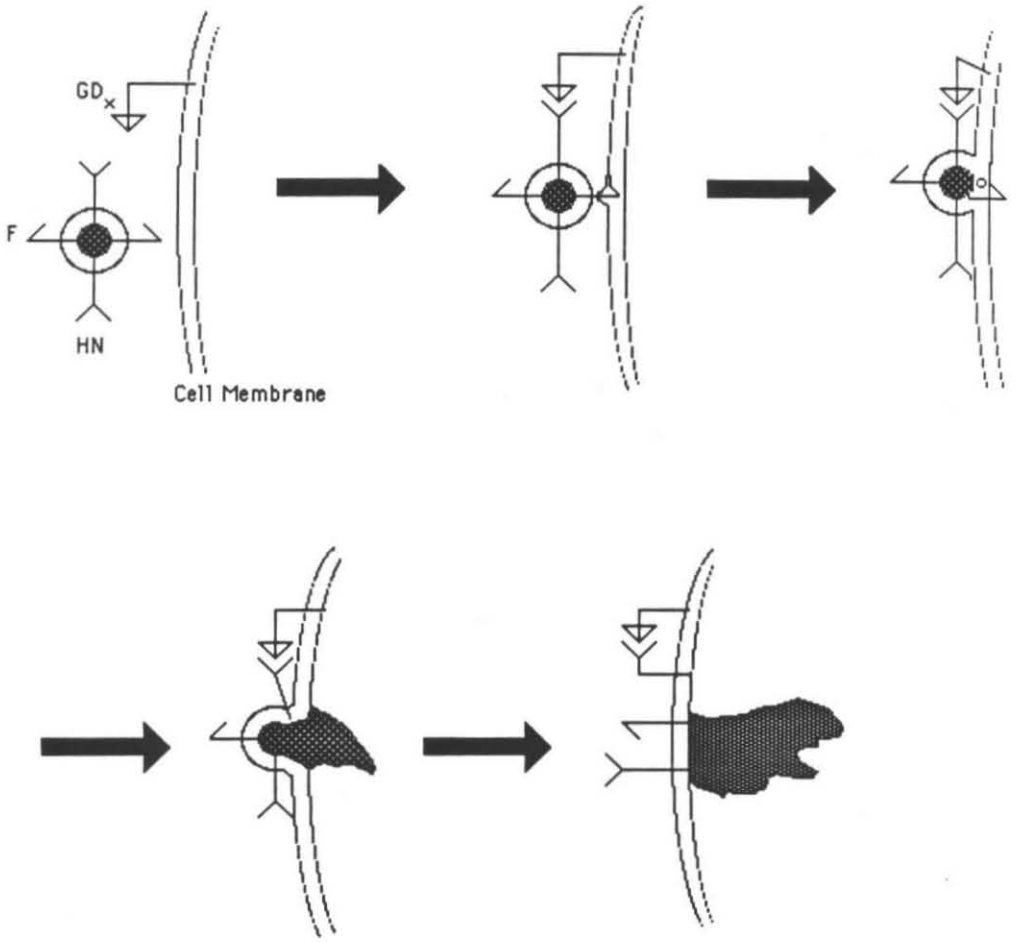

Figure 1. Schematic representation of Reconstituted Sendai Viral Envelope (RSVE) delivering encapsulated drug to the interior of a cell with viral binding sites on its surface.

Table I

Reconstitution Number	1	2	3	4	5
Wash Buffer	140mM NaCl 10mM Hepes pH 7.4 10:1	140mm NaCl 10mM Hepes pH7.4 10:1	140mM NaCl 10mM Hepes pH 7.4 10.1	None	None
Viral Conc.	.66 mg/ml	1.32 mg/ml	.66 mg/ml	1.32 mg/ml	A. 1mg/ml B. 2 mg/ml
Main Buffer	140mM NaCl 10mM Hepes pH 7.4	140mM NaCl 10mM Hepes pH 7.4	140mM NaCl 10mM Hepes pH 7.4	10mM tris 100mM NaCl See notes below	A&B.10mM Hepes 140mM NaCl B. +20mM MgCl
Detergent Conc	50mM, 100mM	50mM	50mM	50mM	50mM
Dialysis Protocal	25ml 1hr RT 25ml 1hr RT 50ml 2.5hr RT 250ml 6hr 4 C 250ml 6hr 4 C 250ml 6hr 4 C	30ml 1hr RT 30ml 1hr RT 50ml 2.5hr RT 125ml 11hr RT 250ml 6hr 4C 250ml 6hr 4C	25ml 1hr RT 25ml 1hr RT 50ml 2.5hr RT 250ml 12hr 4C 250ml 6hr 4C	50ml 6 hr 4C 50ml 2.5hr 4C 250ml 10hr 4C 250ml 11hr 4C	30ml 1hr RT 30ml 1hr RT 50ml 2.5hr RT 250ml11hr RT 250ml 6hr RT
F activity	R18 with B+ ghosts- (+) but No trypsin or DTT controls	R18 increase Trypsin+= Trypsin- NBD/Rd (-)	R18 with (-) O+ ghosts CV-1 cells, no protein specific fusion	R18 (-) O+ ghosts NBD/Rd Ghosts, Cells No Fusion	NBD/Rd (-) O+ ghosts No fusion observed
HN activity		(+)	(+) 19.5 ng min.	(+) for RMVE- 12.5 ng min (-) for RMVE+	(+)
Notes				RMVE- used buffer pH 7.4 RMVE+ used buffer pH 10.0 20mM Sodium Bicarbonate + 2M KCl	

Legend: (-) Protein activity deficient; (+) Protein activity present; RMVE- Reconstituted envelopes prepared in normal buffer (100mM) and pH conditions (7.4); RMVE+ Reconstituted vesicles prepared in high salt (2M) and high pH conditions (10.0).

Table II

Reconstitution #4 R18 Fusion Results
Transfer after 1000 Seconds

	Normal	+Trypsin	+DTT
21µg RMVE(+) 37.3 µg O+ ghosts	4.5-5.4%	4.7-6.8%	
5µg RMVE(-) 37.3µg O+ Ghosts	3.2-4.3%	3.5%	5.0%
25µg RSVE(-) 37.3µg O+ Ghosts	13.2%	8.6%	6.6%
5µg RSVE(-) 37.3µg O+ Ghosts	12.7%		3.8%
5µg RSVE(+) 37.3 µg O+ Ghosts	8.4%		
25µg RSVE(+) 37.3µg O+ Ghosts	2.1-5.3%	1.5%	2.1%
25µg RSVE(+) 90µg POPC SUV's	10.1%	9.9%	2.8%

Legend- RMVE - Reconstituted Mumps Viral Envelopes; (-) -Normal Salt and pH (150mM and 7.4)
(+) High Salt and high pH (2M and 10.0) ; RSVE - Reconstituted Sendai

Figure 2.

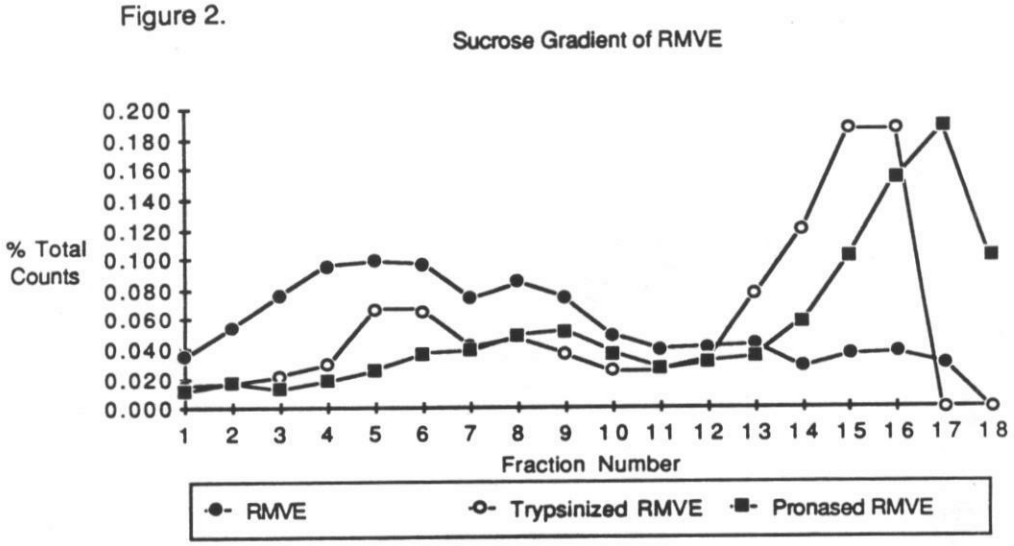

Figure 3.

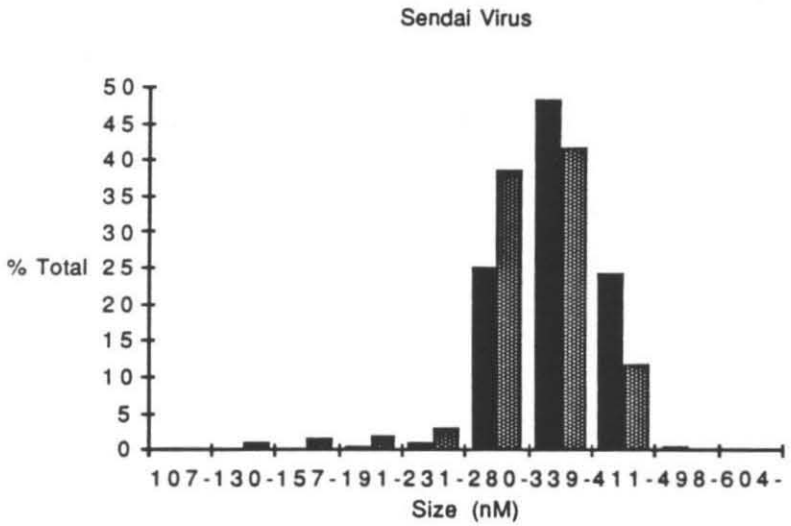

Figure 4.

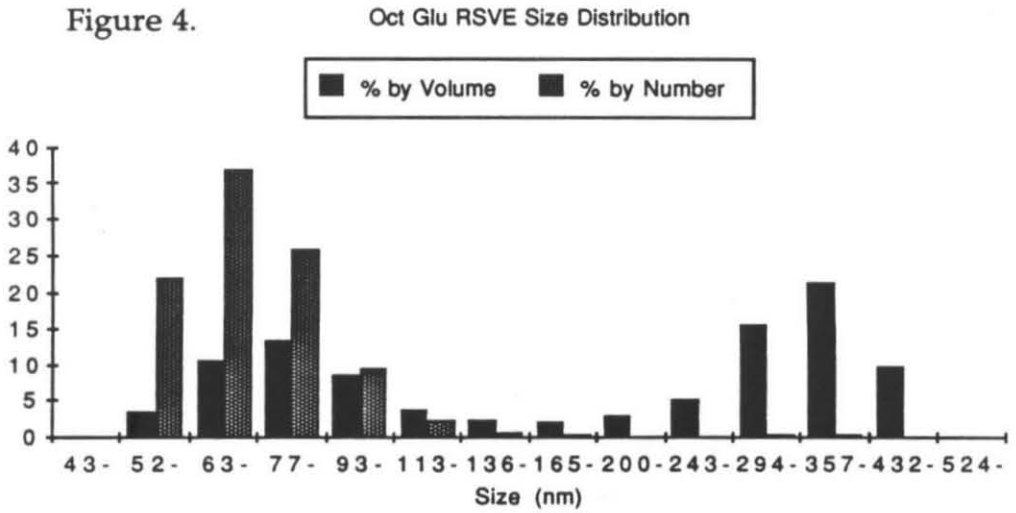

Figure 5.

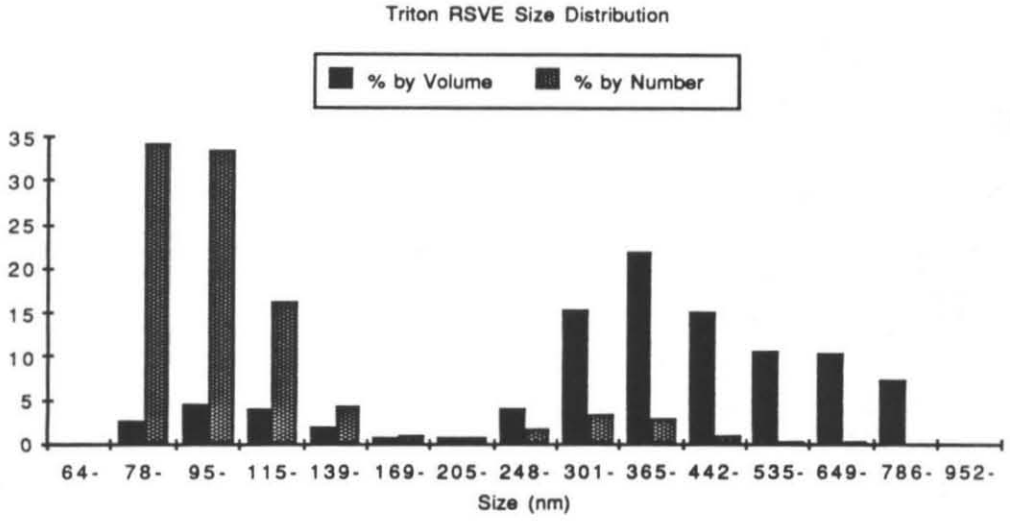

Figure 6.

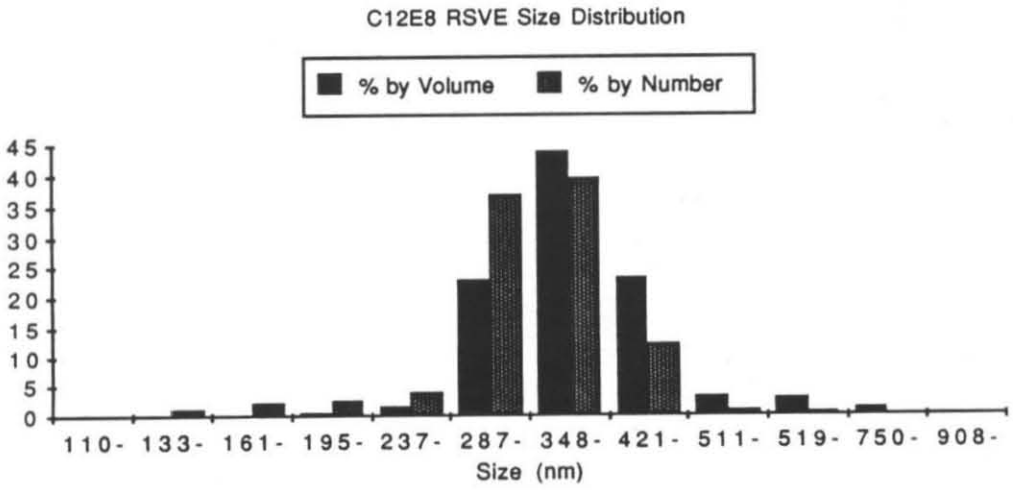

Figure 7.

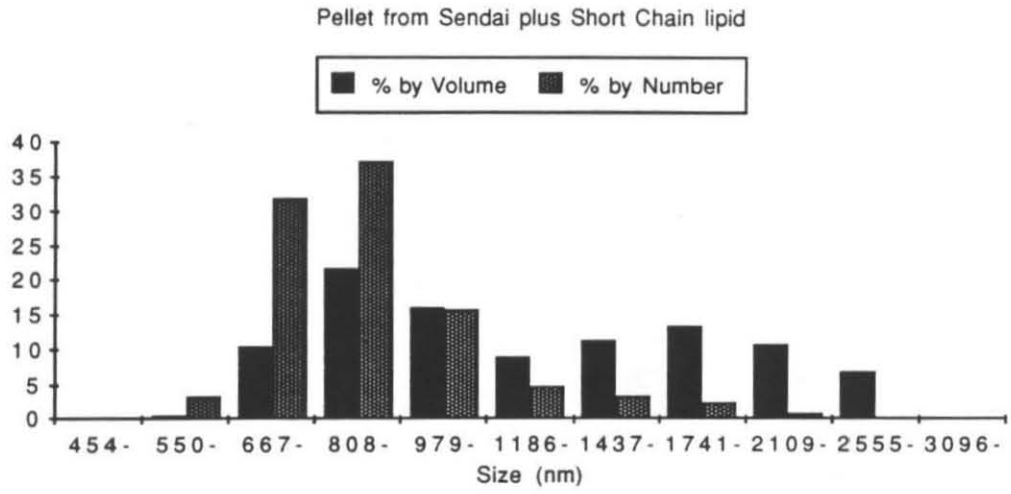

Figure 8.

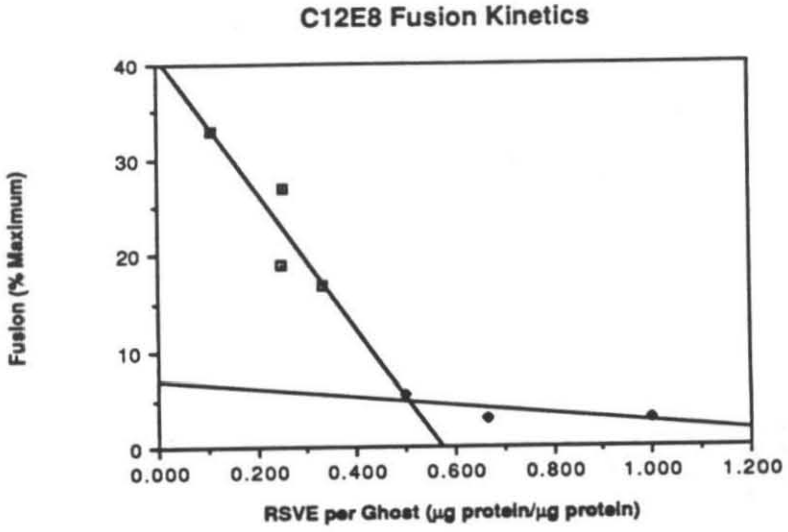

Figure 9.

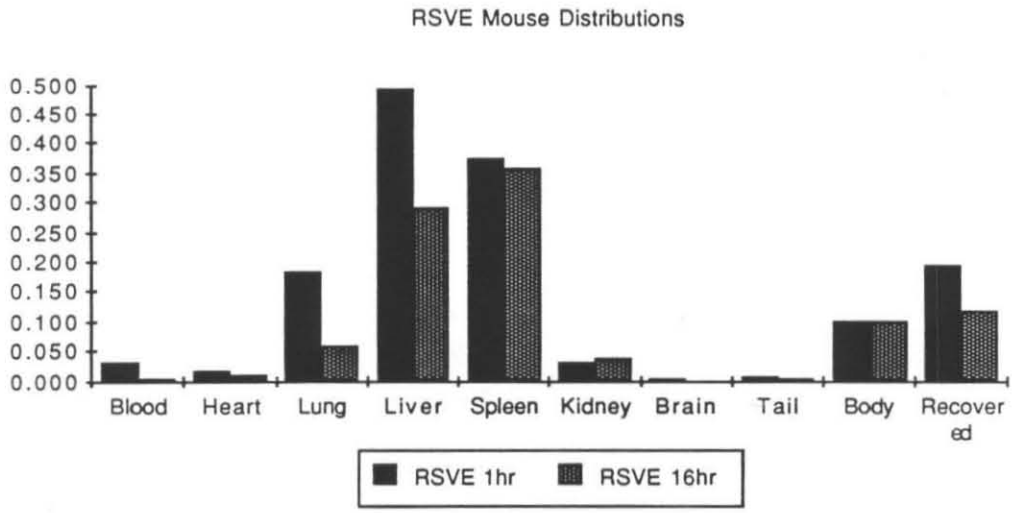

Figure 10.

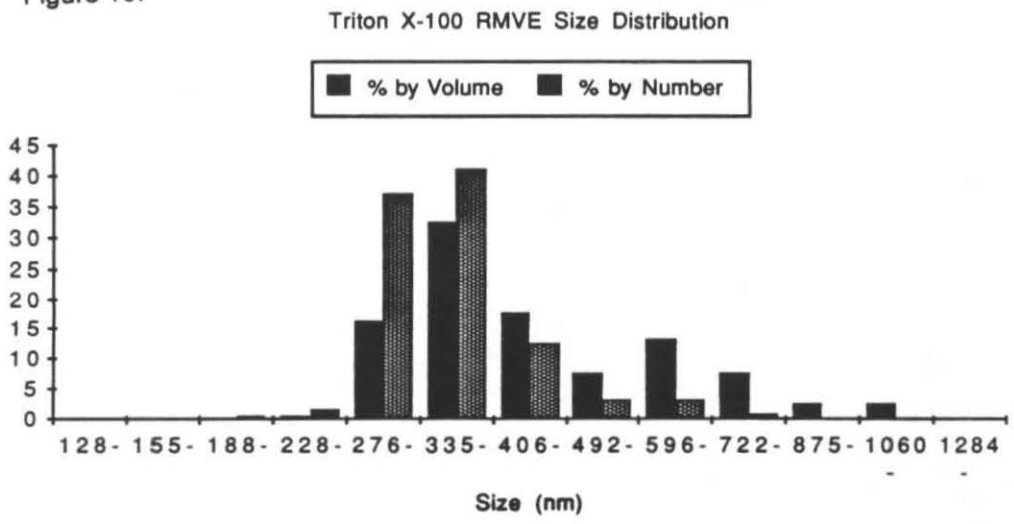

Figure 11.

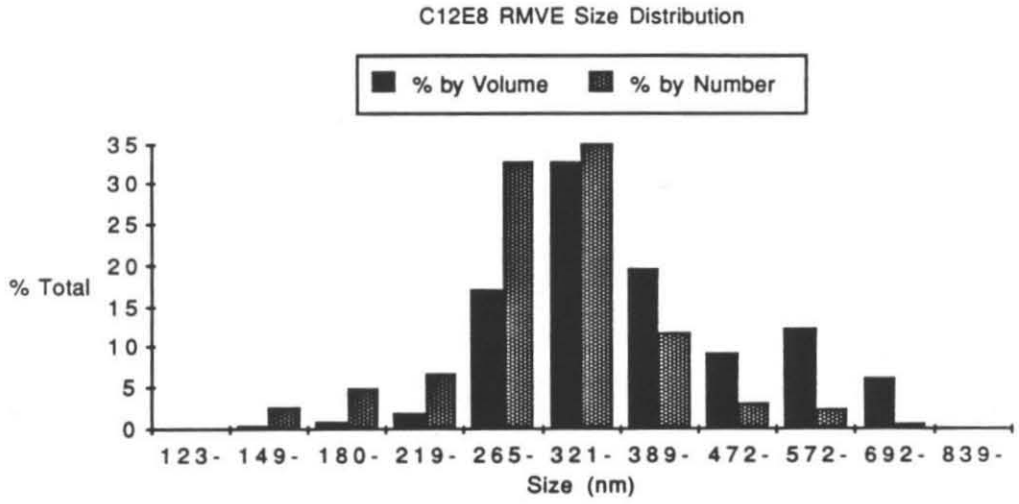

Figure 12.

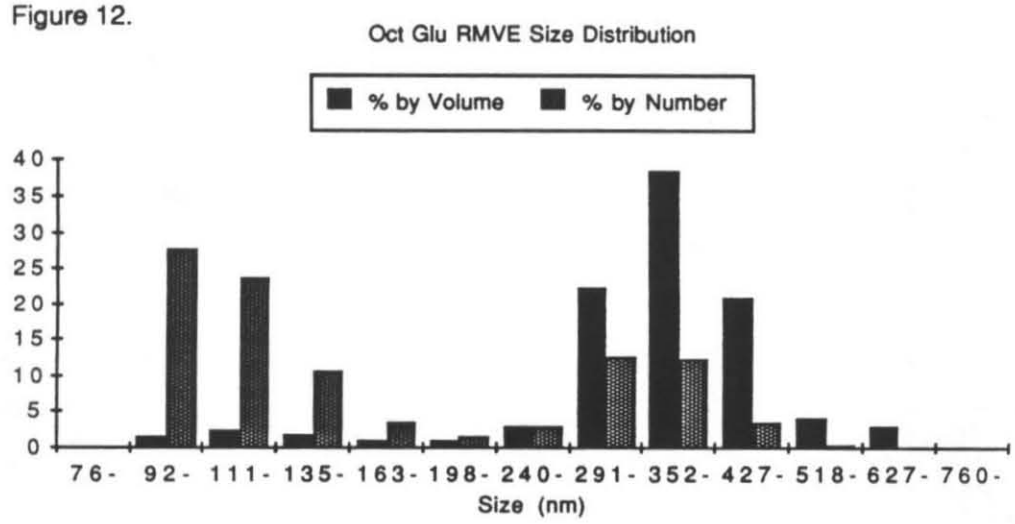

Table III

HA assay	Minimum Protein
Triton X-100 +NBD/Rd	4 ng
C12E8	7 ng
Triton X-100 + Supplement	2 ng
Octyl Glucoside	4 ng
Triton X-100 -NBD/Rd	4 ng

Figure 13.

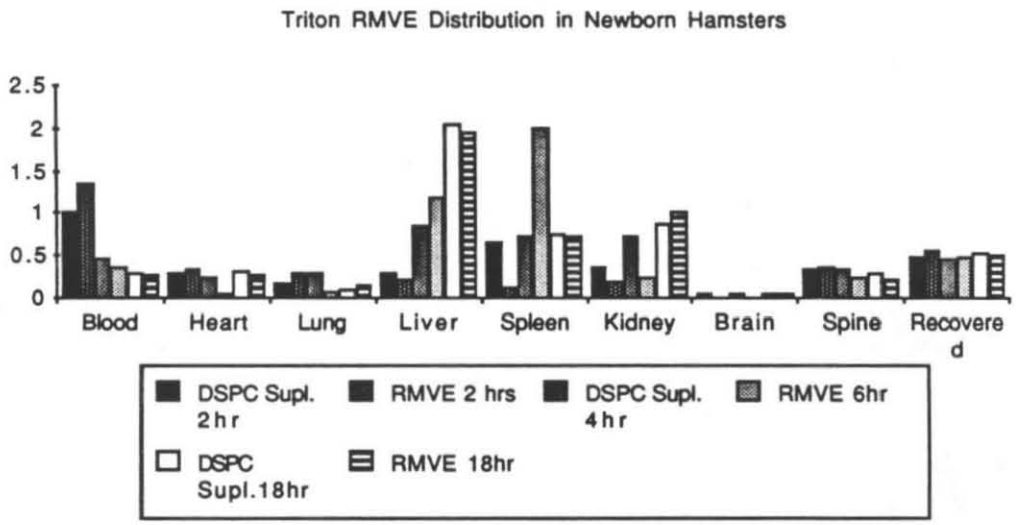

Figure 14

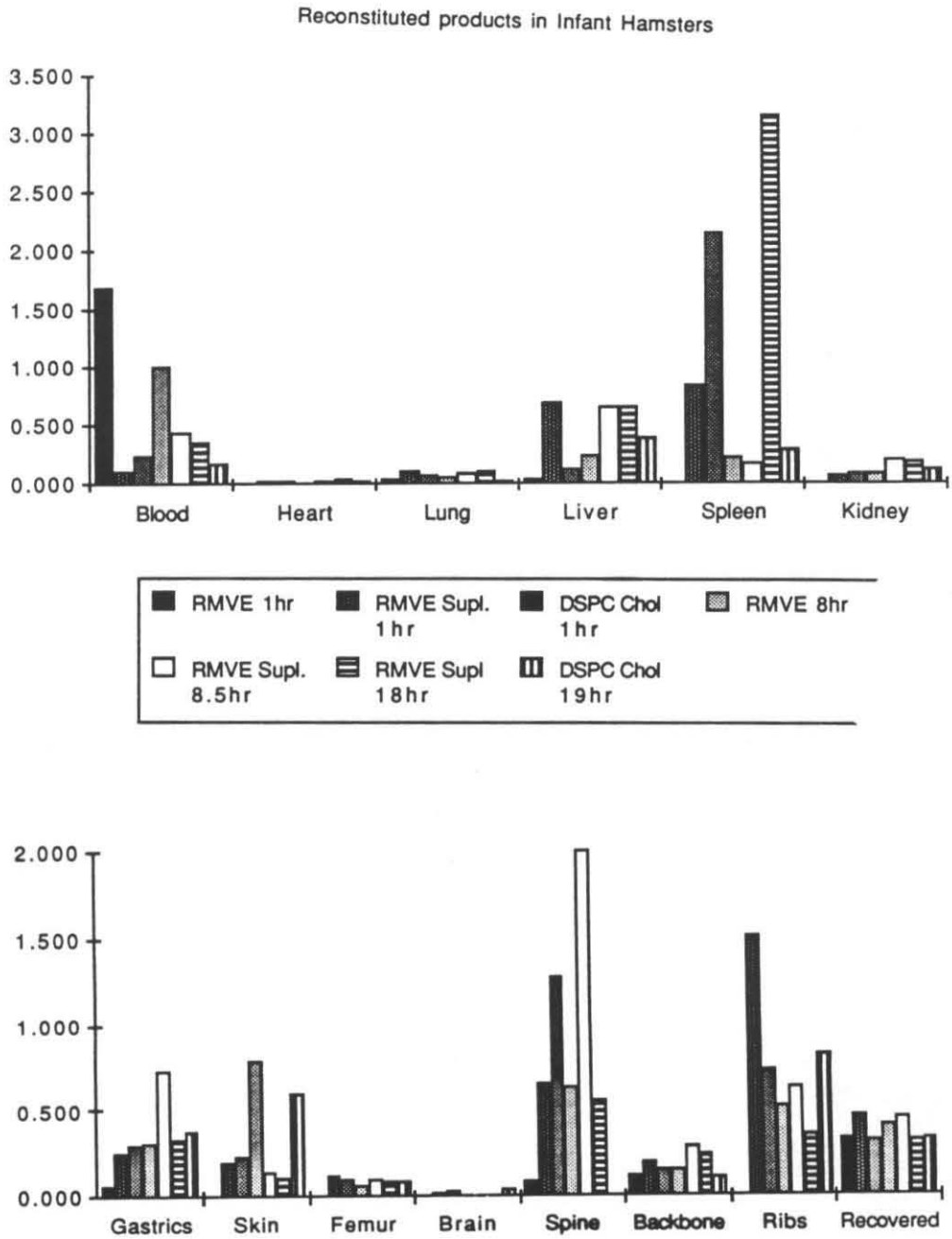
Reconstituted products in Infant Hamsters
3.500
3.000
2.500
2.000
1.500
1.000
0.500
0.000
Blood
Heart
Lung
Liver
Spleen
Kidney
RMVE 1hr
RMVE Supl. 1hr
DSPC Chol 1hr
RMVE 8hr
RMVE Supl. 8.5hr
RMVE Supl 18hr
DSPC Chol 19hr
2.000
1.500
1.000
0.500
0.000
Gastrics
Skin
Femur
Brain
Spine
Backbone
Ribs
Recovered

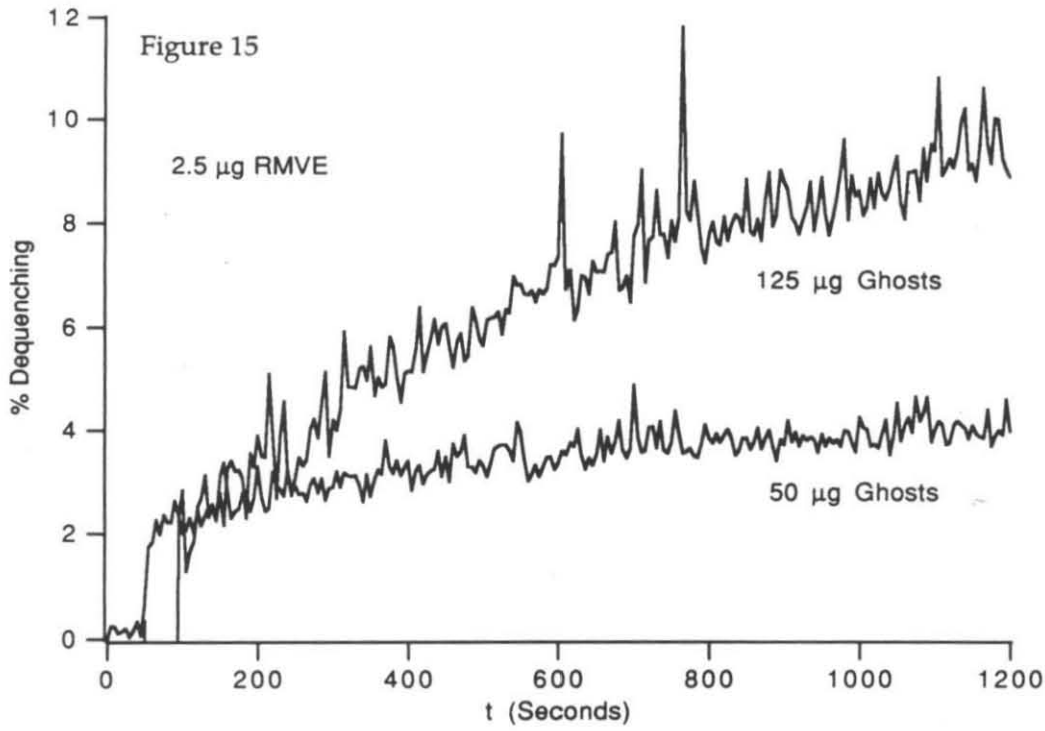
Figure 15
2.5 µg RMVE
125 µg Ghosts
50 µg Ghosts
% Dequenching
t (Seconds)
0
2
4
6
8
10
12
0
200
400
600
800
1000
1200

Figure 16.

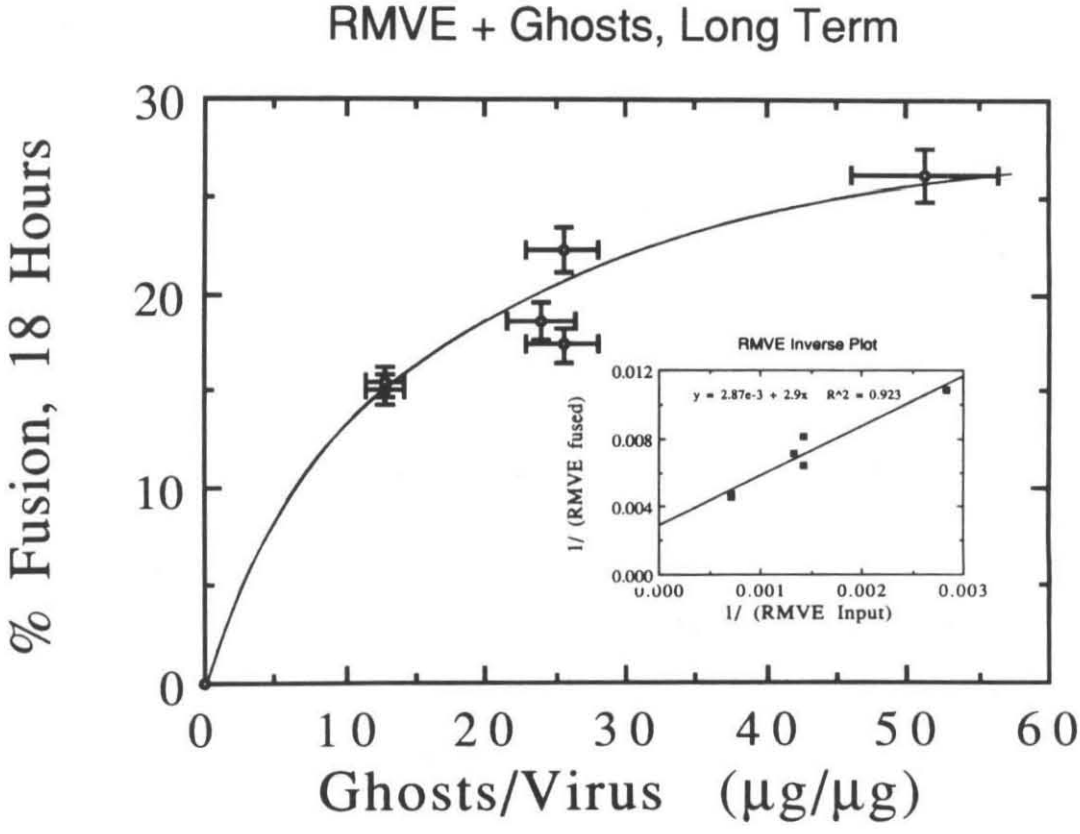

Figure 17

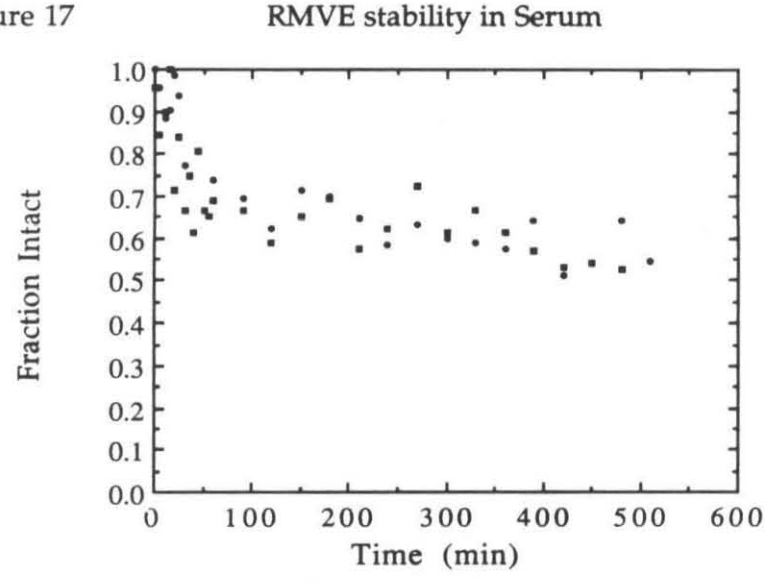

Chapter 4 : Membrane Fusion of Mumps Virus with Ghost Erythrocytes and CV-1 Cells

ABSTRACT

The octadecyl rhodamine (R18) fluorescent dequenching assay was used to examine membrane fusion between mumps virus and cells. Rapid fluorescent dequenching, indicative of fusion, was observed with both ghost erythrocytes and CV-1 cells. After fifteen minutes a saturation limit of 18 virus per erythrocyte ghost and 6400 virus per CV-1 cell was observed. Fetuin was found to inhibit viral fusion, indicating a role for sialic acid in viral binding to the cells. Two dequenching processes were observed of which the faster process is thought to be membrane fusion and the second process thought to be probe proximal transfer. The most rapid dequenching occurred at a rate of 3 ($\pm$1) x 10^9 M^{-1} sec^{-1}, demonstrating that the interaction of mumps virus with the target membrane is a rapid process.

INTRODUCTION

Mumps virus is a paramyxovirus of the genus *paramyxovirus* whose only natural host is man. The virus is tropic for a number of visceral organs and the central nervous system (for a review, see Wolinsky and Server, 1985). Mumps is structurally related to other paramxyoviruses, including Sendai, in terms of protein structure, protein size, and viral size. Paramyxoviruses bind to the target cell by using a Hemagglutination/ Neuraminidase (HN) protein and fuse their membrane with the cell

membrane at neutral pH by means of the Fusion (F) protein (for reviews, see White *et al.*, 1983; White,1990). This allows the genetic material to enter the cellular interior.

A wide variance in neurotropism and neuroinvasiveness has been observed in the various strains of isolated virus (Wolinsky and Stroop, 1978), which can be correlated with differences in function and structure of the HN protein of the virus (Merz and Wolinsky, 1981). A long term goal of these experiments is the explanation of the mechanism of neuroinvasion and neurovirulence. Since neurovirulence appears to be related to the viral entry mechanism, we have begun examining this process. For our experiments, we used Kilham strain mumps, the most neurotropic and neuroinvasive strain known (Kilham and Overman, 1953). In this paper we examined the fusion of mumps virus with ghost erythrocytes and CV-1 cells.

Sendai virus has served as a model system for studying paramyxovirus fusion (Knutton, 1977; Ohnishi, 1988; Loyter *et al.*, 1988a) The fusion activity of Sendai with erythrocyte ghosts has been examined quantitatively (Hoekstra and Klappe, 1986). These experiments with Sendai virus led us to examine the interactions of mumps with ghost erythrocytes.

A fluorescent assay using a self-quenching probe can be used to monitor membrane fusion events as discussed in Chapter two. The probe octadecyl rhodamine (R18) inserts spontaneously into a membrane and exhibits linear fluorescent quenching from 0 to 10% molar concentration (Hoekstra *et al.*, 1984). The advantages of using this system to study membrane fusion have been discussed elsewhere (Loyter *et al.*, 1988b). Upon fusion of the fluorescently labeled virus with a target membrane, the

probe rapidly redistributes into the target membrane and will dequench, resulting in an increase in fluorescent intensity. This provides a direct measurement of the fusion of the viral membrane with the cell membrane. Short term fusion of the virus with target cells was monitored using this probe.

MATERIALS AND METHODS

Cells and Erythrocyte Ghosts

CV-1 cells (ATCC#CCL70) were grown in Minimal Essential Media (MEM) with 10% fetal calf serum (FCS). Sealed, right side out erythrocyte ghosts of A+ human blood were prepared by standard methods (Steck and Kant, 1974).

Mumps Virus

Kilham strain mumps virus was grown in 800 cm roller bottles of cultured CV-1 cells with 50 ml MEM with 10% fetal calf serum. When the cells reached confluence, they were washed with Hank's balanced salt solution and inoculated with 0.1 to 1 plaque forming units/cell or with 1/25th of a previous preparation for 2 hours. The cells were then grown in MEM with 10% FCS with 20mM Hepes or in OptiMEM with 20 mM Hepes. Syncytia and cell death were highly evident by the third day. Virus was harvested on the fourth day by removing the media and pelleting out cell debris at 1500g for 10 minutes. The virus was pelleted by centrifugation at 25,000g. The virus was resuspended in PBS with 10% glycerol and frozen in a liquid nitrogen freezer. BSA was the only major contaminant in the purification procedure and was removed by ultracentrifugation washes (100,000g, 40 minutes) of the virus before experiments. Seed stocks of virus and procedures were provided by Neal Waxham at the University of Texas Medical Center. Virus was grown in the viral facilities of Dr. John Zaia at the City of Hope Hospital.

Size of Virus

A Malvern 4700c photon correlation spectrometer was used to measure the virus size. The system is equipped with a 488 nm tuned 3 watt Spectra-Physics 2020 laser attached to an IBM compatible PC with Malvern software. Most measurements were made at 90° to the beam with no size bias and maximal modal distribution parameters. Measurements at other angles were made to check for any major amplitude variations. In some instances size bias parameters were inserted after initial data collection to further clarify size distributions.

Virus and Ghost numbers

For purposes of conversion of microgram protein quantities of mumps and erythrocyte ghosts to numbers of particles in the results section and figures, it was assumed that 1 μg of ghost protein equaled 1.8×10^6 ghosts (Chi and Wu, 1990) and 1 μg of mumps virus protein equaled 1.3×10^9 viral particles. The molecular weight of the mumps virus is between 5 and 7×10^8 with 70% of the weight being protein (Kingsbury *et al.*, 1978). This is equivalent to $1.22\text{-}1.72 \times 10^9$ viral particles per μg protein .

For surface area calculations, the mumps virus was treated as having an average surface area of .282 μ^2 (radius of 150 nm) and an erythrocyte ghost was treated as having an average surface area of 125 μ^2 (Chi and Wu, 1990; Westermann *et al.*, 1961).

Fluorescent labeling

The fluorescent probe R18 has been used by a number of other workers to examine viral fusion (Loyter *et al.*, 1988b). The R18 probe will spontaneously insert into a membrane and will rapidly equilibrate throughout a membrane when fusion does occur (Rubin and Chen, 1990). Due to the overlap of the emission and excitation fluorescence bands the probe self-quenches, the excited electronic state decaying by trivial mechanisms. In dilute concentrations (<10% of the lipid content), the fluorescent quenching is linearly proportional to the concentration of the probe in the membrane. The surface area of the viral particles is much smaller than the surface area of the ghost erythrocytes or cells. Upon fusion of virus with ghost, the probe in the viral lipid bilayer dilutes into the target membrane and dequenches.

A fresh solution of 1 mM R18 was prepared and an amount equal to 2-6 mole percent of the viral membrane lipid (276 nanomoles lipid/mg viral protein) was added to a 1 ml solution of 250 μg virus, while vortexing. A smaller mole percentage (3%) was found to be most useful for the fluorescent assays as this amount is still highly quenched (50%) and emits more fluorescence, which is useful in increasing the signal to noise ratio. The solution was allowed to sit in the dark for half an hour and then the unincorporated R18 was removed by running the sample over a G75 Sephadex column or by pelleting the virus by ultracentrifugation (100,000g in a SW50.1 rotor).

Fusion Measurements

Fluorescent measurements were made in a SLM4800 fluorimeter by monitoring the emission at 590 nm with a excitation wavelength of 560 nm and a Schott OG550 type filter in the emission path. For kinetic experiments, virus was preincubated at 37°C in the cuvette with 2 ml of phosphate buffered saline (PBS). The sample was stirred in the sample chamber by a magnetic stirrer. Fluorescence data was collected digitally and stored on disk by an IBM AT computer using SLM4800 software. Data collection was initiated and after a baseline had been established, ghosts or cells were added to the virus using a Hamilton syringe for the ghosts or a pipette for the cells. The fluorescence of control aliquots of virus was measured with and without 1% Triton, to determine fluorescent quenching, and baseline scatter was determined with a solution of ghosts or cells. Graphic presentation of the kinetics data in this paper was smoothed with the Igor data processing program (WaveMetrics).

For overnight experiments the components were mixed in a 2ml solution of PBS and incubated in the dark at 37°C. Control aliquots were used to determine the initial fluorescence of the virus and the dequenching obtained upon addition of 1% Triton.

For kinetic experiments with CV-1 cells, the cells were cleaved from the surface of the culture flask by using a solution of 2mM EDTA in PBS. An equal volume of medium was added to the suspension and the cells were pelleted. The cells were then resuspended in a small volume of PBS, from which aliquots were added to the fluorimeter cuvette during a kinetic experiment.

To show that the mumps dequenching was F protein mediated, samples were treated with trypsin. Trypsin cleaves the F protein but not the HN protein. Virus (100 μg protein) was incubated with 100 μg of trypsin for one hour at 37°C in 100 μl volume. The reaction was stopped by the addition of soybean trypsin inhibitor. This virus was subsequently used in the kinetic fusion assay.

Some CV-1 cells were treated with cytochalasin B to disrupt the cellular cytoskeleton and inhibit endocytosis. Cytochalasin B (50 μg) was added to each well of a six well plate ($1x10^6$ cells). The cells were incubated for 40 minutes at 37°C. They were then washed with PBS and fresh media was added. After 30 minutes at 37°C the media was removed, and PBS and labeled virus were then added. After 3 hours the cells were cleaved from the plates with 2 mM EDTA and the fluorescence of cells and supernatant was measured.

Calculation of Fusion

Fusion of the virus was calculated using the formula:

$$\%Fusion=(Fluor._{final} - Fluor._{initial})/(Fluor._{maximum} - Fluor._{initial}).$$

For kinetics experiments $Fluor._{final}$ and $Fluor._{initial}$ represent values taken from the data plots. The $Fluor._{maximum}$ value was determined by taking a solution of labeled virus and adding Triton X-100 to 1% v/v, allowing the R18 to totally dequench.

For overnight experiments $Fluor._{final}$ was measured with the fluorimeter, and $Fluor._{initial}$ was determined from control experiments using set amounts of labeled virus without ghosts. The ratio of fluorescence

with and without Triton (correcting for dilution) in the control experiment was used to determine $Fluor._{maximum}$:

$$Fluor._{maximum} = \frac{Fluor._{initial}}{(Control\ Fluorescence/Control\ Fluorescence+Triton)} .$$

Protein determination, Gel Electrophoresis, Transmission Electron Microscopy

Protein contents of the virus and ghosts were determined by using the Peterson assay (Peterson, 1977) with omission of the TCA precipitation step. Fraction V BSA (Reheis Chemical Company) was used as a protein standard. The BCA protein determination kit (Sigma) was also used.

Acrylamide gel electrophoresis was used to confirm the presence of virus and to check virus purity. Ten percent separating gels were run with six percent stacking gels. Biorad protein standards were used. Gels were silver stained using the Biorad Silver Stain Kit.

Virus samples (10 µl) at various concentrations (about 250 µg protein/ml) were applied to carbon-covered glow-discharged grids and allowed to dry. 10 µl of stain was then applied and allowed to sit for various time periods. 1% Phosphotungstic acid, 1% Uranyl Acetate, and 2% Ammonium Molybdate were used as stains. The samples were examined using a Phillips EM201 TEM.

Kinetics Modeling

Computer programs were written in the BASIC and C language to do numerical integration to solve the multiple differential equations involved in the following viral interaction schemes:

A)The mass action kinetic model

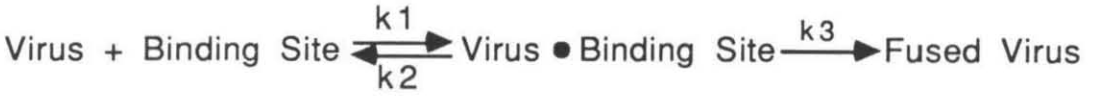

B) The exchange mechanism

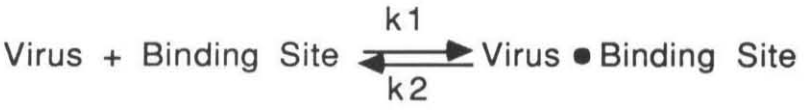

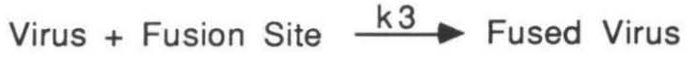

C) The two fusion site mechanism

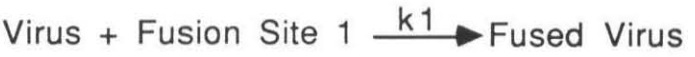

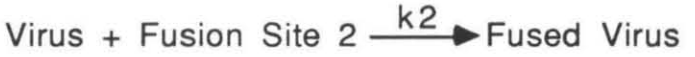

D) The receptor recycling mechanism

To reduce errors in the solutions, the Runge-Kutta method was employed to do the calculations (Boyce and Di Prima, 1977). Fluorimeter data were loaded directly into the program. A fitting parameter measuring the absolute differences between the data and a fit was minimized by using an "evolutionary" fitting subroutine to optimize fitting. After initial rate guesses were inserted into the program the minimization subroutine would make ten random guesses at new kinetic values by varying the old values by 0-10%. The best fit of these guesses was displayed and the fitting cycle was allowed to cycle with the new values until little improvement in fit was apparent.

RESULTS

Purification and Size of Virus

After initial purification, about 250 μg of Mumps virus and 550 μg of BSA were obtained from each roller bottle. This corresponds to about 3250 virus produced per cell, a 25-fold increase over the 130 virus/cell inoculation. An additional ultracentrifugation resulted in removal of the BSA. As an alternative approach in reducing BSA contamination, cells were grown in serum free OptiMEM during the viral infection. A more productive infection was achieved with syncytial destruction of the monolayer by the third day. The yield of virus was also higher, ≈ 500 μg viral protein per roller bottle.

Figure 1 shows the size distribution from a typical batch of Kilham mumps virus obtained by light scattering measurements. The diameter of the virus, 310 nm ± 100nm, is somewhat larger than previously reported (Cantell, 1961). The virus is known to be pleomorphic from EM studies. Electron microscopy showed that the virus was intact and contained the spike glycoprotein structures.

Gel electrophoresis showed the presence of the Nucleocapsid, Fusion, Polymerase, and Matrix proteins. Three larger protein bands were also evident which may represent the Large protein or multimers of the HN protein.

Short Term Fusion of Virus with Ghosts

The kinetic dequenching of virus interacting with ghost erythrocytes was observed directly for short time periods. Figure 3 shows a number of

kinetic curves from mumps-erythrocyte ghost fusion experiments. As the ratio of ghost erythrocyte to virus increased, the percent of virus fusing increased due to the increased availability of viral receptor sites. Under conditions where a large number of ghosts were available the fusion kinetics appeared to be biphasic, with a rapid burst of initial dequenching and a slow secondary dequenching.

The ratio of virus to ghost determined the amount of virus dequenched after 14 minutes, see Figure 4a. The maximum number of possible fusion events can be calculated by using a reciprocal Scatchard-like plot of the fusion data, Figure 4b. After 14 minutes, a maximum of about .025 mg of virus protein per 1 mg of ghost protein was able to fuse. This is equivalent to about 18 viral particles per ghost.

In control experiments the viral fusion can be strongly inhibited by trypsin pretreatment. This is evident from both a kinetic profile, Figure 3 and from the final fusion values, Figure 4a. Trypsin selectively cleaves the F protein, thus allowing binding but no fusion. As discussed in Chapter two, the inhibition is not complete and a residual proximal transfer of R18 occurs.

pH and Temperature Data

Over the temperature range studied, mumps virus interaction with ghost erythrocytes was maximal at 37°C, see Figure 2a. No pH dependence was seen in the interaction of the virus with ghosts, see Figure 2b. The pH profile was nearly identical to that observed with Sendai virus (Ohnishi, 1988). This is consistent with viral entry through the cell membrane as well as the endocytotic compartments.

Saturation of Fusion sites

In order to determine the maximum number of virus that might bind with an erythrocyte ghost, various ratios of fluorescently labeled virus and ghosts were mixed and the fluorescent dequenching after 18 hours was observed. An 18 hour kinetic profile of mumps with ghost erythrocytes showed that dequenching was complete at this time and equilibrium had been reached (data not shown). Figure 5a shows the amount of virus dequenched over an 18 hour time period as related to the amount of virus added per erythrocyte ghost. Due to the proximal transfer of the probe, this dequenching represents virus that have fused with the ghost surface and particles which are bound to the ghost surface. As virus which have fused over a long time course are indistinguishable from those which are bound, the generic term "interacted" is used to describe this assembly of events. Also shown is data from Hoekstra and Klappe (Hoekstra and Klappe, 1986) on Sendai virus fusion with erythrocyte ghosts. The binding activity of the viruses appears to be similar at set ratios of viruses and ghosts; however, less of the total mumps preparation appeared to be active. Up to 75% of the mumps virus was able to interact with the ghosts.

A reciprocal plot was used to calculate the saturation of the binding sites on the ghost surface, see Figure 5b. The Sendai data is from Hoekstra and Klappe. Using a fit of the reciprocal plot, approximately 570 μg of mumps protein can interact with 1 μg of ghost protein; this is equivalent to about 410 mumps virus per ghost. The reciprocal plot is highly linear until more than 200 viral particles interact per ghost. The curve then turns downward as it approaches the y axis indicating that a greater number of

virus can interact when the system is highly saturated. Under such conditions, a large number of fusion events with the ghosts could change the ghost's surface composition and its ability to fuse.

The mumps saturation is compared to the data of Hoekstra and Klappe on Sendai fusion. Mumps virus can undergo a greater number of interaction events per erythrocyte ghost than the Sendai virus: 410 events versus 240 events.

Virus Fusion with CV-1 cells

While ghost erythrocytes serve as interesting model membranes, we also wished to observe the interactions of the virus with cultured cells. CV-1 cells were used as they represent the growth cell line for the Kilham strain of virus. Long term saturation experiments were not performed as cell viability would become questionable before completion of the experiment. Short term kinetics curves of mumps fusion with CV-1 cells were recorded, Figure 6. A biphasic behavior is observed in the interaction of virus with the cells. The reciprocal plot, Figure 7, shows the saturation of fusion as the number of viruses per ghost are increased. Under the conditions of the experiments about 6400 virus were able to fuse per cell after 900 seconds and 14,840 virus after one hour.

To determine if sialic acid plays a role in the viral fusion process, fetuin was added to the solution to serve as a binding site competitor. A large inhibition of fusion was observed, indicating sialic acid as having a role in the viral entry process.

In a control experiment, cells in 6 well plates treated with cytochalasin B were compared to untreated cells in terms of fusion

susceptibility. Cytochalasin B caused some disruption or rounding of the cellular skeletal structure, as observed under a light microscope, and should partially inhibit endocytosis. No difference in fusion was seen between the fusion with treated and untreated cells (see appendix, experiment 4.).

Kinetic Modeling

Four different kinetic models were used to fit the data on mumps erythrocyte interactions.

A binding site competition model was tested that gave curves of proper character but was most dependent on the ratio of binding to fusion sites in determining extent of fusion.

The two site model used a set of available fast fusion sites and a second, more numerous, set of slow fusion sites. The number of fast and slow fusion sites was estimated from the previous kinetic and equilibrium experiments and then adjusted during calculations to give the best possible data fit. For optimal fitting of the fusion of mumps with erythrocyte ghosts, the number of fast fusion sites was 6 (±2) per ghost and the number of slow sites was 400 (±50). The observed fast rate, k_1, for fusion with erythrocyte ghosts was 3 (±1) x 10^9 M^{-1} sec^{-1}. This rate was slowed with high ratios of virus to ghost, due to the negative cooperation mentioned above in the short term virus ghost fusion section. The slow rate, k_2, was about 8 (±1) x 10^5 M^{-1} sec^{-1}.

An alternative model to fit the data used a small number of receptors per cell which were "recycled" for usage. The number of receptors was 6 (±2) per ghost erythrocyte. The fusion rate, k_1, was 3 (±1) x 10^9 M^{-1} sec^{-1}, as observed with the two site model. The rate of receptor recycling was 4 (±1) x

10^{-4} sec^{-1}. This model is likely faulty on two accounts. The slow rate was uninhibited by trypsin and was likely due to proximal probe transfer rather than receptor recycling. Secondly, there is no evidence for receptor recycling in ghost erythrocytes although receptors used in viral fusion could become available at the completion of the event.

The mass action model did not effectively fit the data as it was impossible to achieve steep initial rates in conjunction with a second slower rate. When the second slow rate was removed by subtracting it out, the optimal fit given by the model is one where $k_1 = 3\ (\pm 1) \times 10^9 M^{-1} sec^{-1}$, $k_2 = 0$ sec^{-1}, and $k_3 = 1$ sec^{-1} with 27 percent viral activity and 25 receptors per ghost. These constants indicate that fusion occurs much more rapidly than binding, i.e., that binding is the rate limiting step. The reaction form is essentially $V + BS \rightarrow (V \bullet BS \rightarrow)$ Fused. The dequenching curves appear to be of simple exponential form, reduction of the k3 to a value below one gives the curves a sigmoidal character. Acquisition of binding data would support the hypothesis that binding was rate limiting but binding rates proved to be very difficult to acquire (experiments not shown).

DISCUSSION

No previous quantitative studies on the fusion ability of mumps virus have been conducted. We have quantitatively examined the fusion of mumps virus with ghost erythrocytes and CV-1 cells. The virus was treated as a neutral pH fusing agent with an optimal activity at 37°C. The virus was found to fuse with the model membrane ghost erythrocytes, similar to the behavior of Sendai virus.

The fusion of mumps virus is a rapid process, under non-saturating conditions 20+% of the virus can fuse in 3 minutes. Although a pH dependent fusing virus such as influenza fuses more rapidly than mumps (White,1990), it must first undergo endocytosis which requires a number of minutes. Evolution has chosen a quick viral entry which should allow avoidance of the multiple clearance pathways.

The amount of mumps virus which can fuse with an erythrocyte ghost differs greatly from the amount which can fuse with the CV-1 membrane surface. After 15 minutes a saturation limit of about 20 virus can fuse with each ghost and 6000 virus with each CV-1 cell. Considering the surface area of the erythrocyte ghost to be about 125 μm^2 and CV-1 cell surface area to be 2000 μm^2 (10^5 cells/ cm^2), fusion saturation is about one virus per 7 μm^2 of erythrocyte membrane surface and 0.32 μm^2 of CV-1 membrane surface. For the CV-1 cells this is about the area displaced by placing a virus on the surface of the cell. For the longer overnight experiment, an erythrocyte can also undergo a large number of interaction events, one every 0.3 μm^2. The sites for viral interaction are abundant on the cellular surface in both systems, indicating a common molecule as the

receptor site. A difference in lipid composition between the two cell type bilayers may determine this apparent difference in fusion propensity.

Although the cell receptor for mumps has not been identified, it is likely that the sialic acids on gangliosides or a common sialoglycoprotein would function as a binding site. The HN protein of Sendai has been shown to use gangliosides as a cellular receptor (Markwell *et al.*, 1981). The identified activities of the mumps HN are hemagglutination, the binding of red blood cells, and neuraminidase activity, the cleavage of sialic acid from fetuin; the efficiency of these activities vary from strain to strain and can be directly correlated to neuroinvasiveness. Both these activities appear to reside in the same domain of the protein structure (Merz and Wolinsky, 1981). Gangliosides are common to most cells, allowing the virus to enter a number of cell types. The larger number of virus interaction events with the cell surface is also indicative of a common cell surface moeity. Highly sialated fetuin was shown to inhibit viral cell fusion in these experiments.

The kinetic profiles of virus interacting with ghost erythrocytes or CV-1 cells are very similar. The dequenching of mumps appears to be biphasic. The initial fast dequenching most likely represents F protein induced membrane fusion. The second slower dequenching is uninhibited by trypsin and likely represents a proximal transfer of the R18 probe. As discussed in Chapter two, although the dequenching of R18 is usually attributed to fusion of the membrane bilayers, it is difficult to prove that fusion is actually occurring without a contents mixing assay. Proteases which cleave both HN and F (Protease K) totally inhibit dequenching (data not shown), while some slow dequenching still occurs after trypsin treatment, which only cleaves the F protein. If spontaneous R18 transfer

does occur, it requires binding of the virus to the surface of the cell. A fusion protein mediated non-fusion transfer of the R18 probe is nearly impossible to rule out, but control experiments have been conducted in this lab (Chapter 2, DiSimone and Baldeschwieler, 1991) that show that with reconstituted Sendai viral envelopes the kinetics of fusion are nearly identical when measured with the R18 assay or a NBD/Rhodamine phosphatidyl ethanolamine resonance energy transfer assay (Struck *et al.*, 1981). The probes in the NBD/Rhodamine system are much less likely to transfer spontaneously to another membrane. In a different viral fusion system, Sarkar *et al.* observed similar kinetics for the contents mixing of NBD-taurine and membrane mixing of R18 when fusing erythrocyte ghosts with influenza HA-expressing fibroblasts (Sarkar *et al.*, 1989).

Comparison of the long term interactions with ghosts by Sendai or mumps shows that the viruses are similar in activity but not identical. For short term fusion of Sendai with ghosts, a reciprocal plot analysis of data from Citovsky *et al.* (Citovsky et al, 1985) shows a saturation of about 16 Sendai virus per ghost over 30 minutes, similar to the 18 mumps viral fusion events seen in our experiments. Though there is some conservation of the F protein across the paramxyoviruses, the binding protein HN varies in size and function even within the various mumps strains.

It is unclear why a virus would develop which will fuse with a erythrocyte, as this would seem to be a dead end in viral replication. To the virus the erythrocyte must appear so similar to the target cellular surface that the virus binds and fuses with the surface. The virus appears to be rapid but fairly unspecific in its cellular interactions. Mumps can probably fuse with most cells types, including erythrocytes.

The mechanism by which the mumps virus is neuroinvasive and neurotropic is still unclear. In mice, penetration of the infection into the neurons is determined by replication (Kristensson *et al.*, 1984; Löve *et al.*, 1987). In hamsters, neurotropic and nonneurotropic strains are both able to penetrate as far as the ependymal cells by crossing into the cerebrospinal fluid at the choroid plexus (Wolinsky *et al.*, 1974). Given that the virus fuses with a diverse array of cells, virus-cell fusion would not play a key role in neurotropism but would only allow a widespread dissemination of the virus. Infection of the neurons may be more closely linked to cell-cell fusion and viral budding, other viral activities partially controlled by the glycoproteins. Propagation of virus into the neurons by virus-cell fusion may be difficult due to restricted diffusion of the virus into the neuronal interstitial spaces, while cell-cell fusion would allow infection of nearest neighbors and continued penetration of the neuronal matter. It is also possible that in the neuroinvasive mumps strains the HN or F glycoprotein recognizes a second, more specific receptor on hamster and human neurons.

REFERENCES

BOYCE, W.E. and DI PRIMA, R.C. (1977). Numerical Methods. *In* "Elementary Differential Equations and Boundary Value Problems", pp.336-378. John Wiley & Sons, New York, New York.

CANTELL, K. (1961). Mumps Virus. *Adv. Virus Res.* **8**, 123-164.

CHI, L-M., and WU, W-G. (1990) Effective bilayer expansion and erythrocyte shape change induced by monopalmitoyl phosphatidylcholine. *Biophys. J.* **57**, 1225-1232.

CITOVSKY, V., BLUMENTHAL, R., and LOYTER, A. (1985) Fusion of Sendai virions with phosphatidylcholine-cholesterol liposomes reflects the viral activity required for fusion with biological membranes. *FEBS.* **193**, 135-140.

DI SIMONE, C. and BALDESCHWIELER, J. D. (1991) Membrane Fusion vs. Transfer in Viral Fusion monitored by the Fluorescent Probe Octadecyl Rhodamine (R18). *Biophys. J.* **59**, in press.

HOEKSTRA, D., DE BOER, T., KLAPPE, K., and WILSCHUT, J. (1984). Fluorescence Method for Measuring the Kinetics of Fusion between Biological Membranes. *Biochemistry* **23**, 5675-5681.

HOEKSTRA, D., and KLAPPE, K. (1986). Sendai Virus-Erythrocyte Membrane Interaction: Quantitative and Kinetic Analysis of Viral Binding, Dissociation, and Fusion. *J. Virol.* **58**, 87-95.

KILHAM, L., and OVERMAN, J. R. (1953). Natural pathogenicity of mumps virus for suckling hamsters on intracerebral inoculation. *J. Immunol.* **70**, 147-151.

KINGSBURY, D.W., BRATT, M. A., CHOPPIN, P. W., HANSON, R. P., HOSAKA, Y., TER MEULEN, V., NORRBY, E., PLOWRIGHT, W., ROTT, R., and WUNNER, W. H. (1978). Paramyxoviridae. *Intervirology* **10**, 137-152.

KNUTTON, S. (1977) Fusion of Human Erythrocytes by Sendai Virus. *J. Cell Sci.* **28**, 189-210.

KRISTENSSON, K., ÖRVELL, C., MALM, G. and NORRBY, E. (1984) Mumps virus infection of the developing mouse brain-appearance of structural viral proteins demonstated with monoclonal antibodies. *J. Neuropathol. Exp. Neurl.* **43**, 131-140.

LÖVE, A., ANDERSSON, T., NORRBY, E. and KRISTENSSON, K. (1987) Mumps virus infection of dissociated rodent spinal ganglia *in vitro*. Expression and disappearance of viral structural proteins in neurons. *J. Gen. Virol.* **68**, 1755-1759.

LOYTER, A., CITOVSKY, V., and BLUMENTHAL, R., (1988b). The Use of Fluorescence Dequenching Measurements to Follow Viral Membrane Fusion Events. *Methods Biochem. Anal.* **33**, pp. 129-164.

LOYTER, A., NUSSBAUM, O. and CITOVSKY, V. (1988a). Active Function of Membrane Receptors in Fusion of Enveloped viruses with Cell Plasma Membranes. In "Molecular Mechanisms of Membrane Fusion" (S. Ohki et al., eds.), p. 413-426. Plenum Press, New York, New York.

MARKWELL., M. A. K., SVENNERHOLM, L., and PAULSON, J. C. (1981). Specific gangliosides function as host cell receptors for Sendai virus. *Proc. Natl. Acad. Sci. USA* **78**, 5406-5410.

MERZ, D. C. and WOLINSKY, J. S., (1981) Biochemical Features of Mumps Virus Neuraminidases and Their Relationship with Pathogenicity. *Virology* **114**, 218-227.

NIR, S., KLAPPE, K., and HOEKSTRA, D., (1986). Kinetics and Extent of Fusion between Sendai Virus and Erythrocyte Ghosts: Application of a Mass Action Kinetic Model. *Biochemistry* **25**, 2155-2161.

OHNISHI, S. (1988) Fusion of Viral Envelopes with Cellular Membranes. *Curr. Top. Membr. Transp.* **32**, 257-295.

PETERSON, G. L. (1977) A Simplification of the Protein Assay Method of Lowry *et al.* Which is More Generally Applicable. *Anal. Biochem.* **83**, 346-356.

RUBIN, R. J., and CHEN, Y-D., (1990). Theoretical-studies of diffusion of lipid-like molecules between membranes in virus-cell and cell-cell fusion systems. *Biophys. J.* **57**, 494.

SARKAR, D. P., MORRIS, S. J., EIDELMAN, O., ZIMMERBERG, J., and BLUMENTHAL, R. (1989) Initial Stages of Influenza Hemagglutinin-induced Cell Fusion Monitored Simultaneously by Fluorescent Events: Cytoplasmic Continuity and Lipid Mixing. *J. Cell Biol.* **109**, 113-122.

STECK, T.L., and KANT, J. A., (1974) Preparation of Impermeable Ghosts and Inside-out Vesicles from Human Erythrocyte Membranes. *Methods Enzymol.* **XXXI** , 172-180.

STRUCK, D.K. HOEKSTRA, D., and PAGANO, R. E. (1981) Use of Resonance Energy Transfer to Monitor Membrane Fusion. *Biochemistry* **20**, 4093-4099.

WESTERMANN, M.P., PIERCE, L.E., and JENSON, W.N. (1961) . A Direct Method for the Quantitative Measurement of Red Cell Dimensions. *J. Lab. Clin. Med.* **57**, 819.

WHITE, J. M., KIELIAN, M., and HELENIUS, A. (1983). Membrane fusion proteins of enveloped animal viruses. *Q. Rev. Biophys.* **16**, 151-195.

WHITE, J. M. (1990) Viral and Cellular Membrane Fusion Proteins. *Annu. Rev. Physiol.* **52**, 675-697.

WOLINSKY, J. S., BARINGER, J.R., MARGOLIS, G., and KILHAM, L. (1974) Ultrastructure of Mumps Virus Replication in Newborn Hamster Central Nervous System. *Lab. Invest.* **31**, 403-412.

WOLINSKY, J. S., and SERVER, A. C. (1985) Mumps virus. *In* "Virology" (B. N. Fields et al., eds.), pp. 1255-1284. Raven Press, New York, New York.

WOLINSKY, J. S., and STROOP, W. G. (1978) Virulence and Persistence of Three Prototype Strains of Mumps Virus in Newborn Hamsters. *Arch. Virol.* **57**, 355-359.

ACKNOWLEDGEMENTS

We would like to thank Neal Waxham for providing seed virus and advice on viral growth, Delilah Stevens for much assistance in viral growth and John Zaia for providing equipment and lab space in which to grow the virus. We would also like to thank R. Male, M. Youngquist and R. Driscoll for helpful commentary. Funding was provided by ARO grant #DAAL-03-87-K-0044, Monsanto Company, and the Caltech Consortium in Chemistry and Chemical Engineering; Founding Members: E.I. du Pont de Nemours and Company, Inc., Eastman Kodak Company, Minnesota Mining and Manufacturing Company, Shell Oil Company Foundation.

Figure Captions

Figure 1. Size distribution of mumps particles as measured by light scattering.

Figure 2. (a). Temperature dependence of mumps dequenching with erythrocyte ghosts. Erythrocyte ghosts (66 μg) were added to 2.5 μg of R18 labeled mumps in PBS at 37°C. Kinetic measurements were made as described in methods. Initial rate was measured both by hand and by taking the first derivative of the spectra. Both methods gave the same rate within 2%. **(b).** Effect of pH on the fusion of mumps. R18 labeled mumps virus (5 μg) was incubated with 65 μg of erythrocyte ghosts in PBS adjusted to the various pH's for 30 minutes as 37°C. The fraction fused was determined as described in methods.

Figure 3. Kinetic profiles of mumps virus dequenching interaction with erythrocyte ghosts. Erythrocyte ghosts (260 μg) were added to various amounts of R18 labeled virus and the kinetics of dequenching were measured. One hundred percent virus dequenching was calculated as described in methods.

Figure 4. (a). Extent of dequenching of mumps with ghost erythrocytes after 14 minutes. Erythrocyte ghosts were mixed with R18 labeled virus in PBS at various ratios. Kinetic profiles were obtained as in figure 3. Final

extent of dequenching as calculated in the methods is plotted against the ratio of ghosts to virus. **(b).** A reciprocal plot was used to calculate the maximum number of deequenching events after 14 minutes.

Figure 5. (a). Long term dequenching interaction of mumps with erythrocyte ghosts. R18 labeled mumps virus (16-23 μg) was added to varied amounts of erythrocyte ghosts. Dequenching was measured after an 18 hour incubation at 37°C. Sendai data is from Hoekstra and Klappe, 1986. **(b).** A reciprocal plot of the data shown in Figure 3a used to calculate the saturation of dequenching events.

Figure 6. Kinetic profiles of dequenching interactions of mumps with CV-1 cells. CV-1 cells (6.5×10^6) were added to various amounts of R18 labeled mumps virus in PBS. Kinetics were observed as described in methods.

Figure 7. Saturation of dequenching sites on CV-1 cells. A reciprocal plot of the amount of virus added to 6.5×10^6 CV-1 cells versus the amount of virus dequenched. The data points were calculated from individual kinetic experiments.

Figure 1.

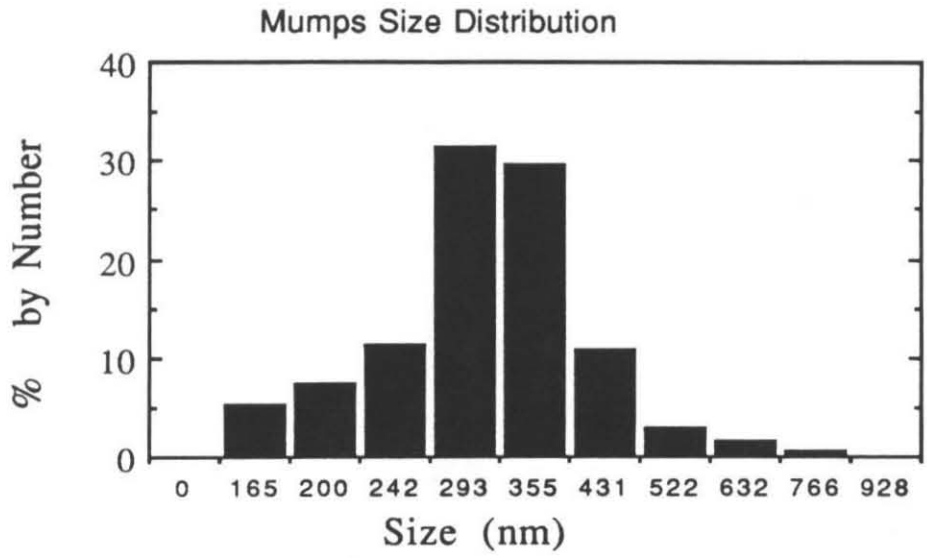
Mumps Size Distribution
40
30
20
10
0
% by Number
0
165
200
242
293
355
431
522
632
766
928
Size (nm)

Figure 2(a).

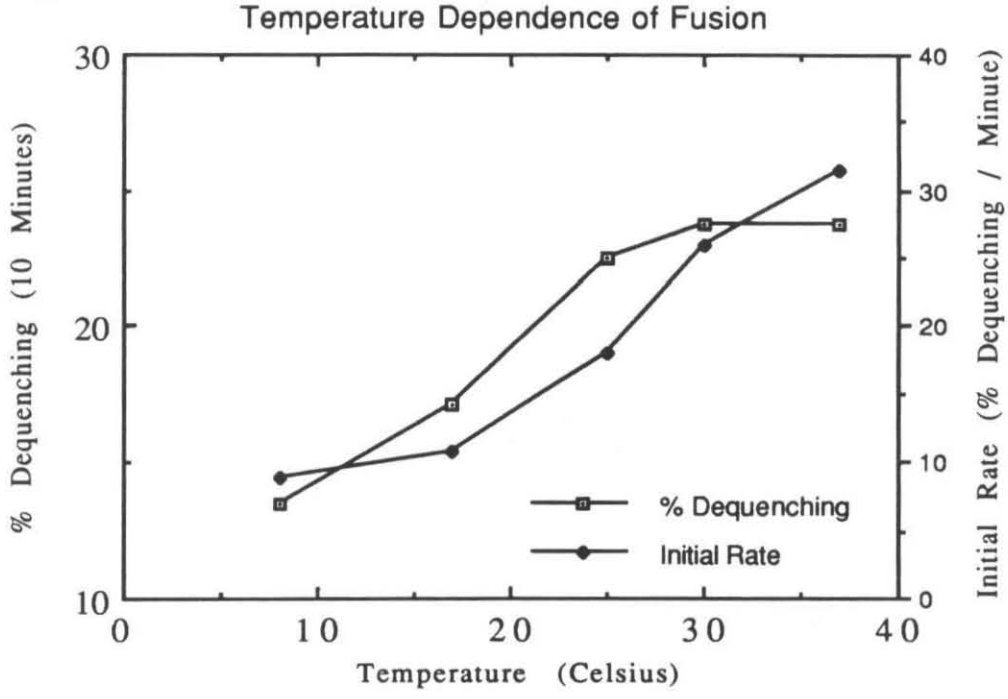

Figure 2(b).

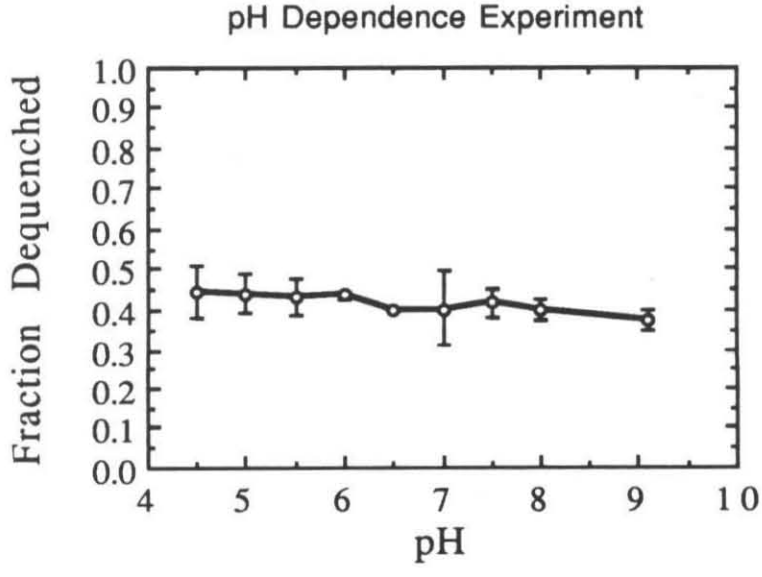

Figure 3.

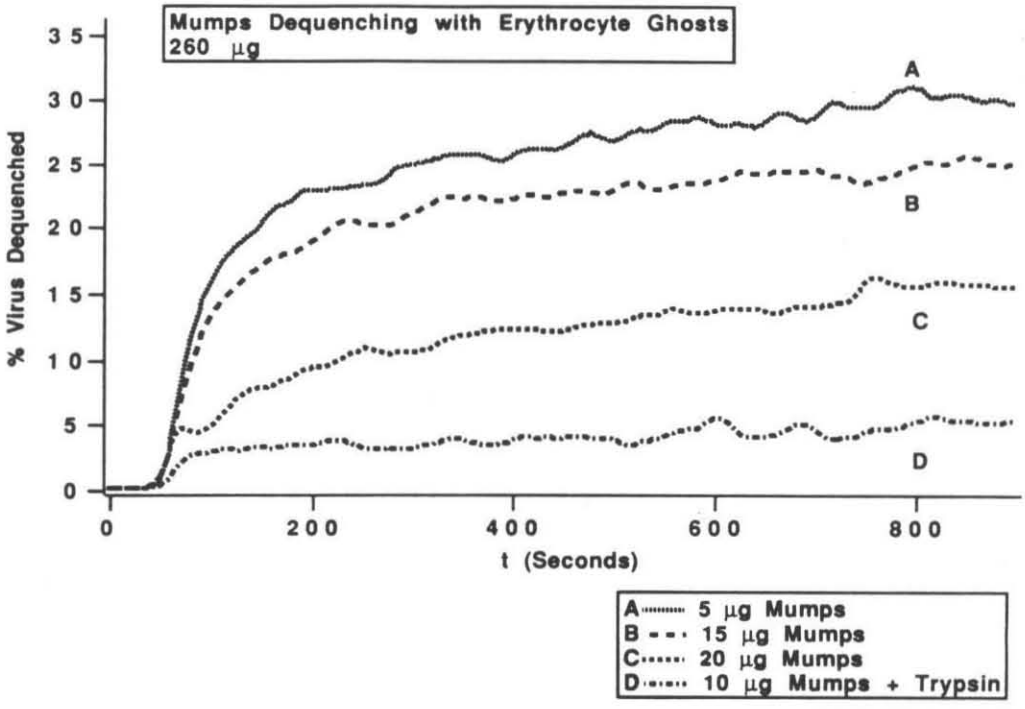
Mumps Dequenching with Erythrocyte Ghosts
260 µg
% Virus Dequenched
35
30
25
20
15
10
5
0
0
200
400
600
800
t (Seconds)
A
B
C
D
A 5 µg Mumps
B 15 µg Mumps
C 20 µg Mumps
D 10 µg Mumps + Trypsin

Figure 4(a).

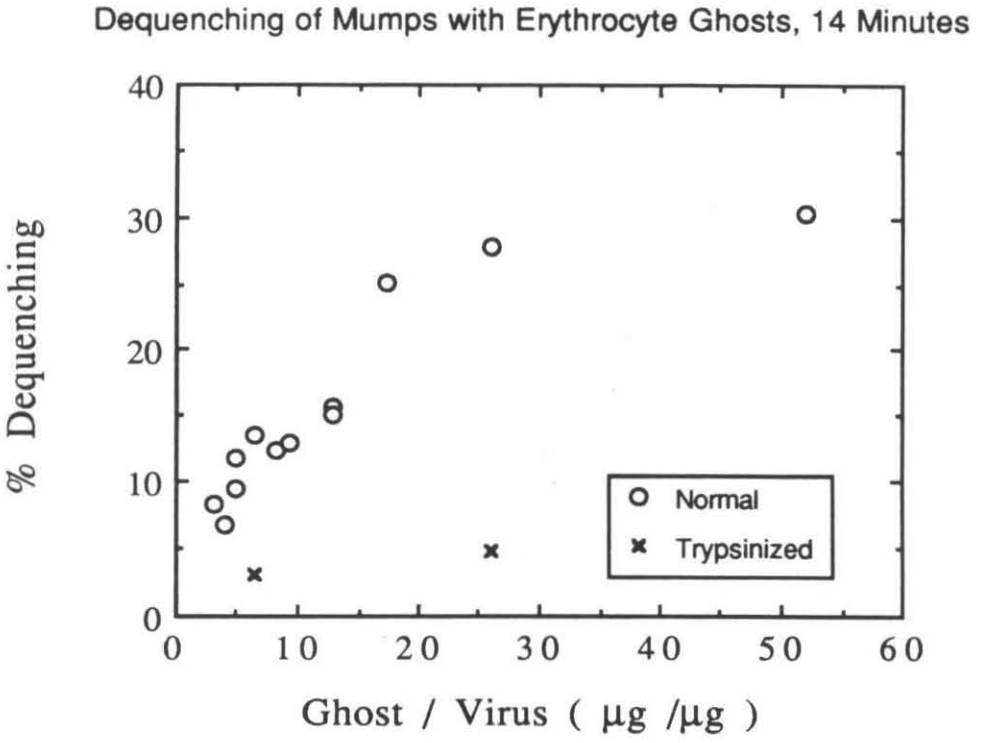

Figure 4(b).

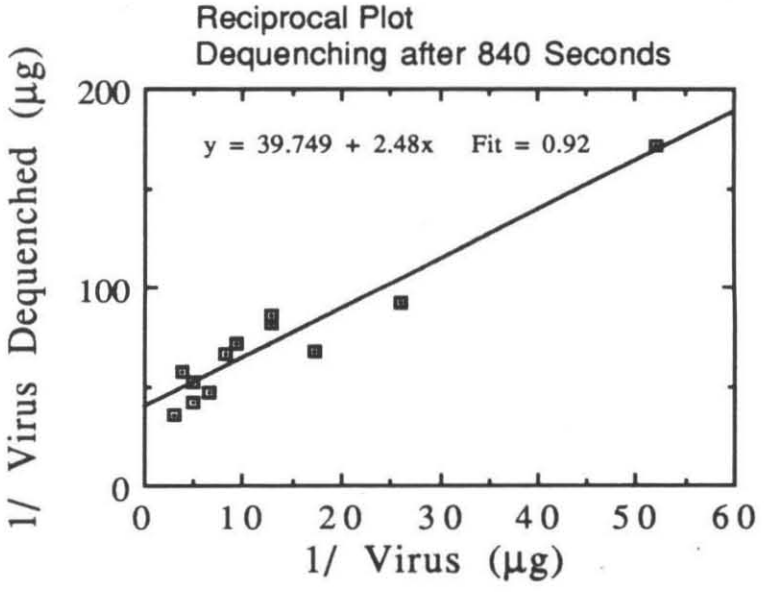

Figure 5(a).

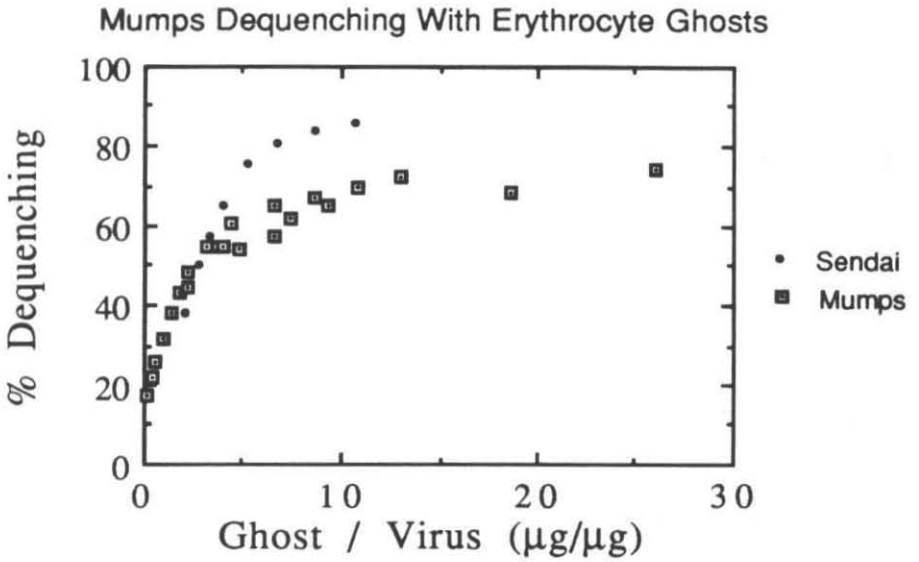

Figure 5(b).

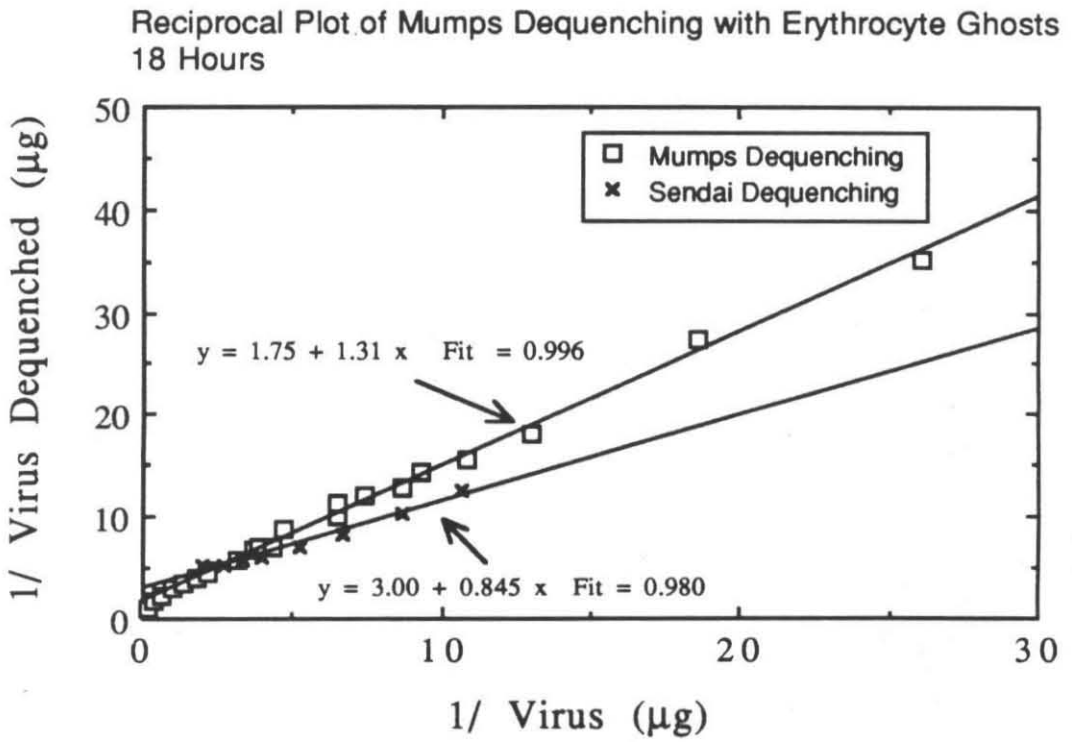

Figure 6.

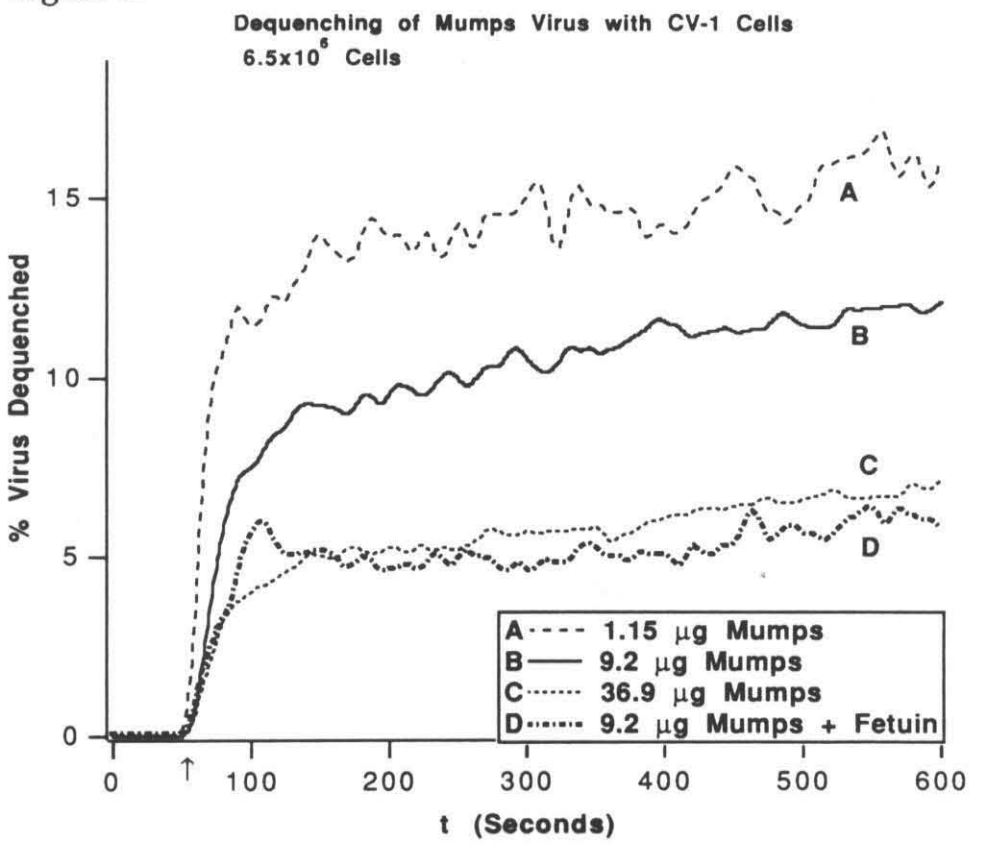

Figure 7.

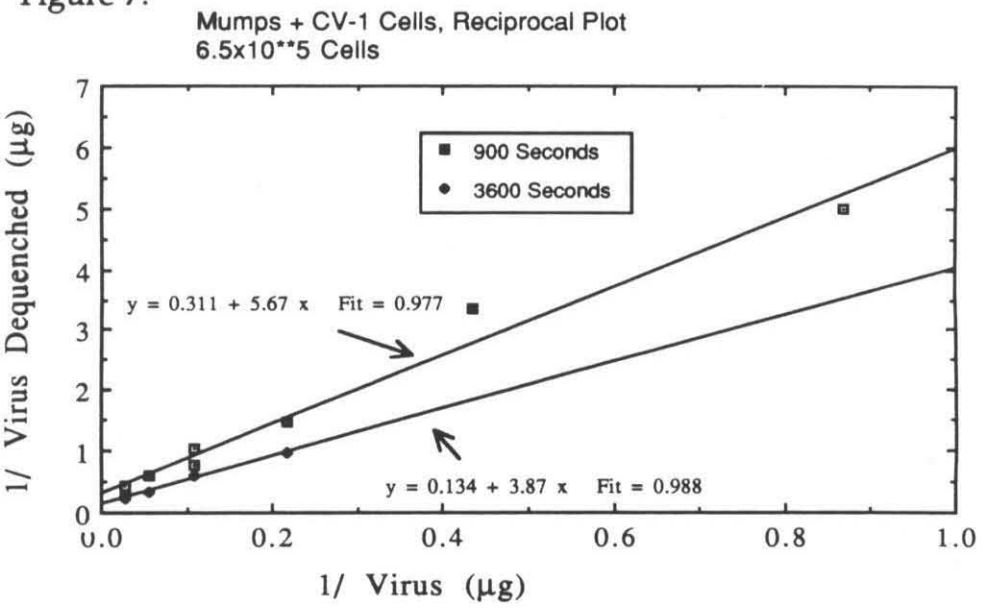

Appendix to Chapter 4- Additional Mumps Fusion Experiments

Introduction- A number of kinetic experiments monitoring mumps virus fusion were conducted which are not detailed in Chapter 4. The details of these experiments and kinetic traces are given below.

1. Two fusion experiments were run with the mumps grown by Neal Waxham at the University of Texas (see Chapter 3). In both of these experiments whole virus was labeled with the R18 probe and allowed to incubate with erythrocyte ghosts. The fusion was measured for separate samples at set time points.

Kilham mumps virus (264 μg, 400 μl) was labeled with 2.41 nmoles R18 (7 μl EtOH). The virus was purified by column and assayed for protein content. 100 μl (≈29 μg) aliquots of mumps virus was mixed with 15 μl O+ ghosts (56 μg) and allowed to incubate. Two of these virus aliquots had been pretreated with DTT or trypsin in order to inhibit fusion. Initial and triton fluorescent values were determined from control aliquots of virus. The following dequenching amounts were observed:

t	Untreated	Trypsin	DTT
0	0	0	0
1hr20min	7.7	0	0
2hr20min	12.1	0	4.3
8hr40min	22.7	.7	9.4
24hr	32.0	.6	22.4

A second experiment was run with a different mumps preparation sent from Texas. 726 μg of virus were labelled with 6 μg of R18, purified by

column chromatography and then mixed in various ratios with ghost erythrocytes. No change in sample fluorescence was apparent after an overnight incubation.

2. One ml out of 3.3 ml mumps preparation (841 μg/ml protein, mumps + BSA) from one roller bottle was labeled with 5 nmoles R18 and purified by column chromatography. The labelled virus fraction contained 278 μg of purified virus per ml with a volume of 450 μl. Kinetic fluorescent fusion experiments were conducted with various amounts of erythrocyte ghosts (6.8 mg/ml) (Figure 1). The extents of dequenching from this experiment were used in Figure 4a in Chapter 4.

3. One ml out of 10 ml mumps preparation (795 μg/ml protein, mumps + BSA) from four roller bottles was labeled with 5 nmoles R18 and purified by column chromatography. The labeled virus fraction contained 230 μg of purified virus. Kinetic fluorescent fusion experiments were conducted with various amounts of erythrocyte ghosts (5.75 mg/ml) (Figure 2). For the trypsinization experiment, 23 μg of mumps virus was treated with 20 μg of trypsin for one hour at 37° C and then the digestion was halted by the addition of 10 μg of trypsin inhibitor. The extents of dequenching from this data were used in Figure 4a in Chapter 4.

4. One ml out of 10 ml mumps preparation (795μg/ml protein, mumps + BSA) from four roller bottles was labeled with 5 nmoles R18 and purified by column chromatography. The labeled virus fraction contained 237 μg of purified virus. Six well plates containing $\approx 9.6 \times 10^5$ CV-1 cells per well were

used in this experiment. Some of the plates were treated with cytochalasin B prior to viral addition. 5 mg of cytochalasin B was added to 200 µl of DMSO to form a stock solution from which 2 µl were added to each plate well. The cells were incubated for 40 minutes and then the media were removed and the cells washed with PBS. The cells were allowed to incubate in PBS for 30 minutes, washed again and covered with PBS. Various amounts of labeled virus were then added. The virus were allowed to react with the cells for three hours at which time the cells were cleaved from the plate by the addition of 1 mM EDTA. The cells were then removed and fluorescence measurements made on the samples. Control aliquots of virus with and without Triton X-100 were used to determine fluorescent quenching, initial, and maximal fluorescence values. The observed dequenching (Figure 3) was corrected for baseline scatter of light due to the introduction of cells into the fluorescent light path.

5. A single kinetic experiment was run on virus labeled mumps virus from the prep described in 4. above. One ml (209 µg) of virus was labeled with 5 nmoles of R18 and purified by pelleting twice by ultracentrifugation. 9.6×10^5 CV-1 cells were mixed with 25 µl of labeled virus in 2 ml PBS. After 1100 seconds 13.2% dequenching was observed, with correction for baseline light scatter. Separation of bound and unbound material was accomplished by centrifugation and showed that 20.0% of the fluorescent probe was found associated with the cells. Emission and excitation spectra were taken before and after the fusion experiment and showed no apparent shifts in wavelength maxima.

6. 1.4 ml out of 16 ml mumps virus preparation (750μg/ml protein, mumps + BSA) from ten roller bottles was labeled with 1.3 μg R18 and purified by ultracentrifugation. The labeled virus fraction contained 250 μg of purified virus. Kinetic measurements were made of the labeled virus interacting with ghost erythrocytes (Figure 4).

7. One ml out of eleven ml from a ten roller bottle mumps preparation was labeled with 1 μg of R18 and purified by ultracentrifugation. Various amounts of the labeled virus (500 μg/ml) were mixed with 1.63×10^6 CV-1 cells and fusion kinetics were recorded (see Figure 5).

8. One ml out of eleven ml from a ten roller bottle mumps preparation was labeled with 2 μg of R18 and purified with ultracentrifugation. Various amounts of labeled virus were mixed with 1.41×10^6 CV-1 cells and the kinetics recorded. Over the range of virus concentration tested (5 μg to 25 μg) observed dequenching values were 17±2%.

Figure 1.

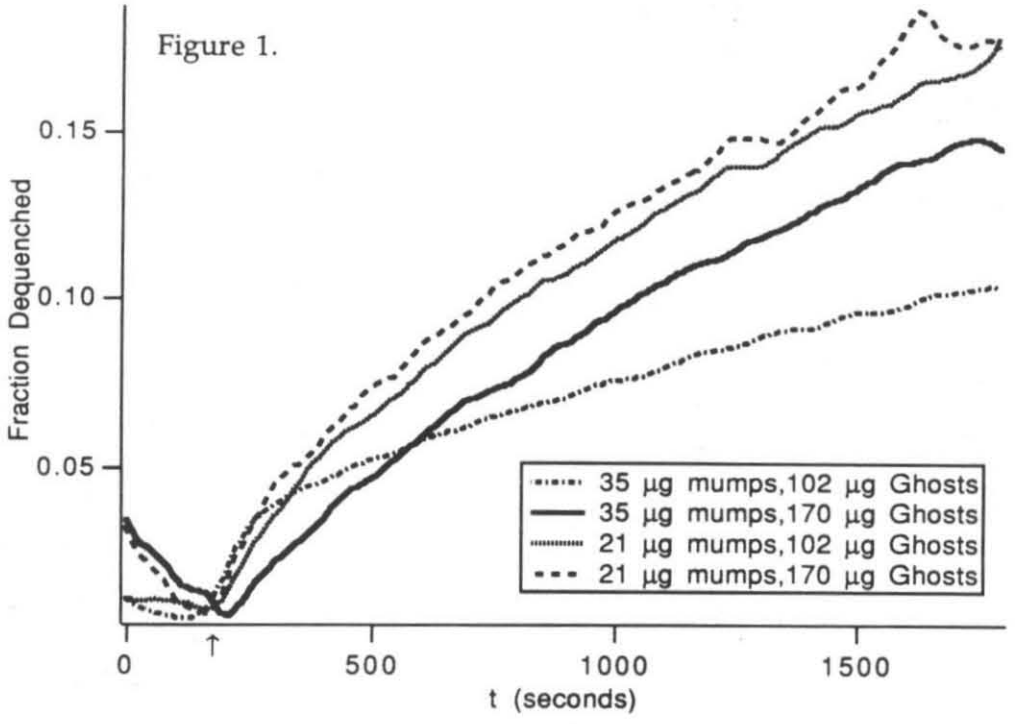

Figure 2.

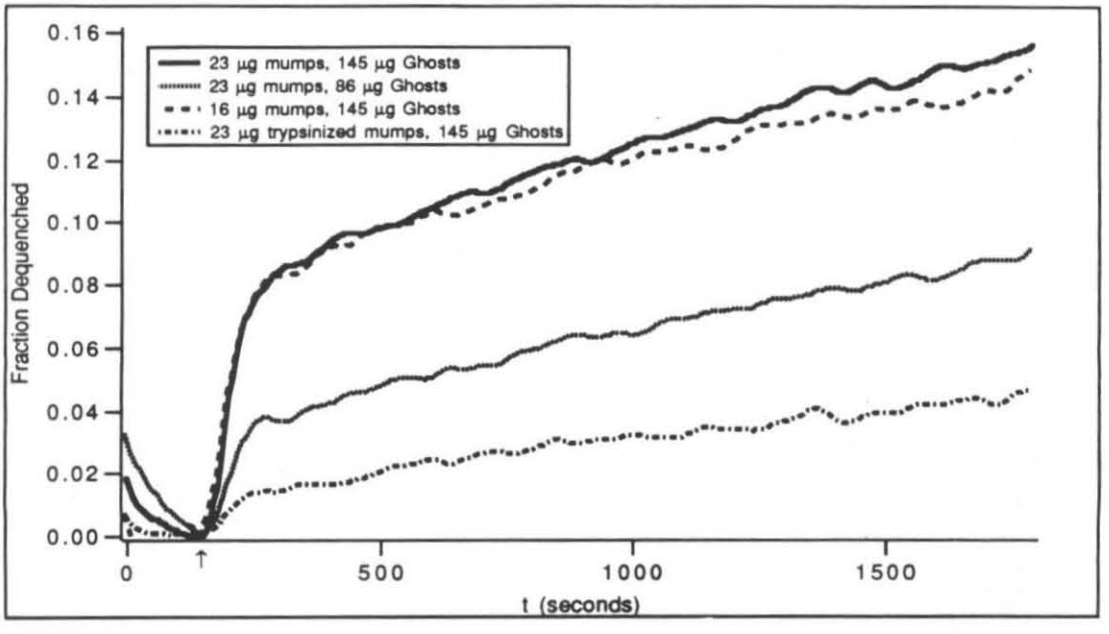

Figure 3.

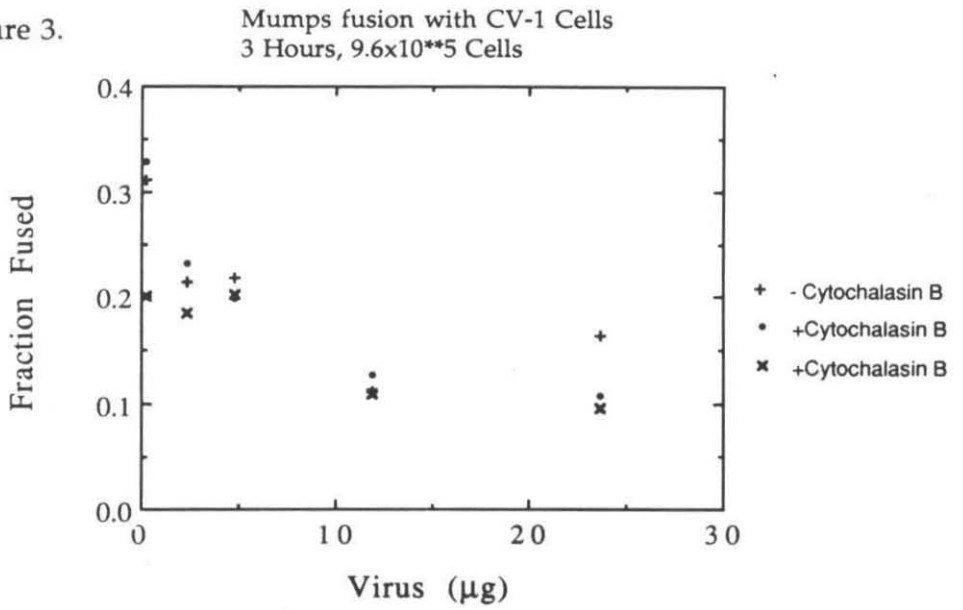

Figure 4(a).

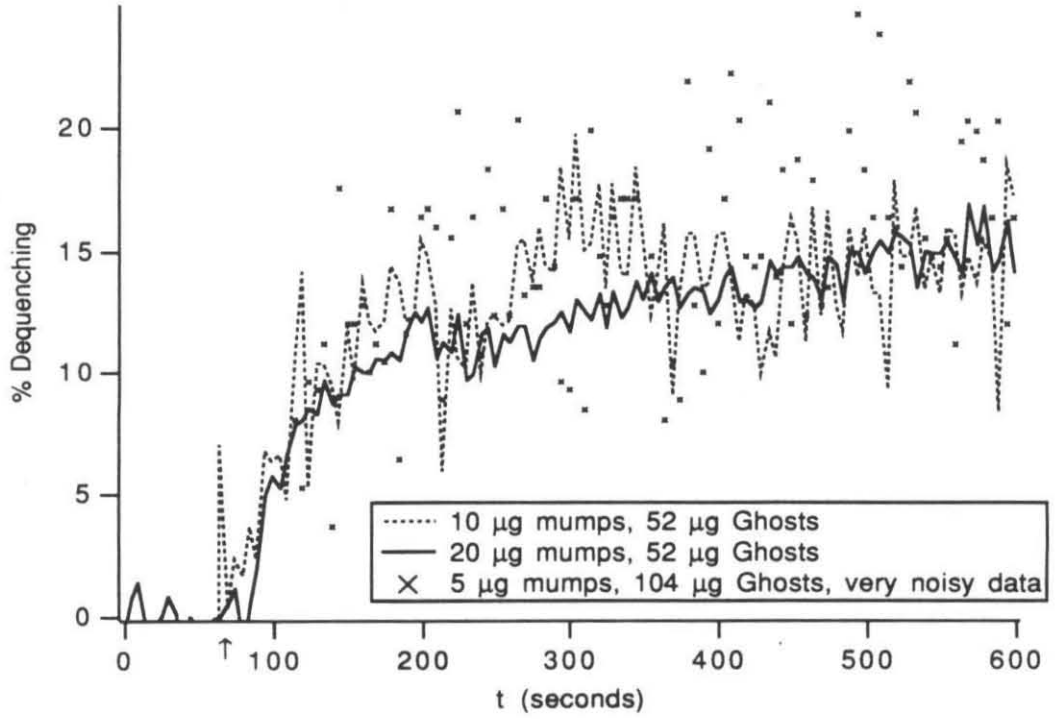

Figure 4(b).

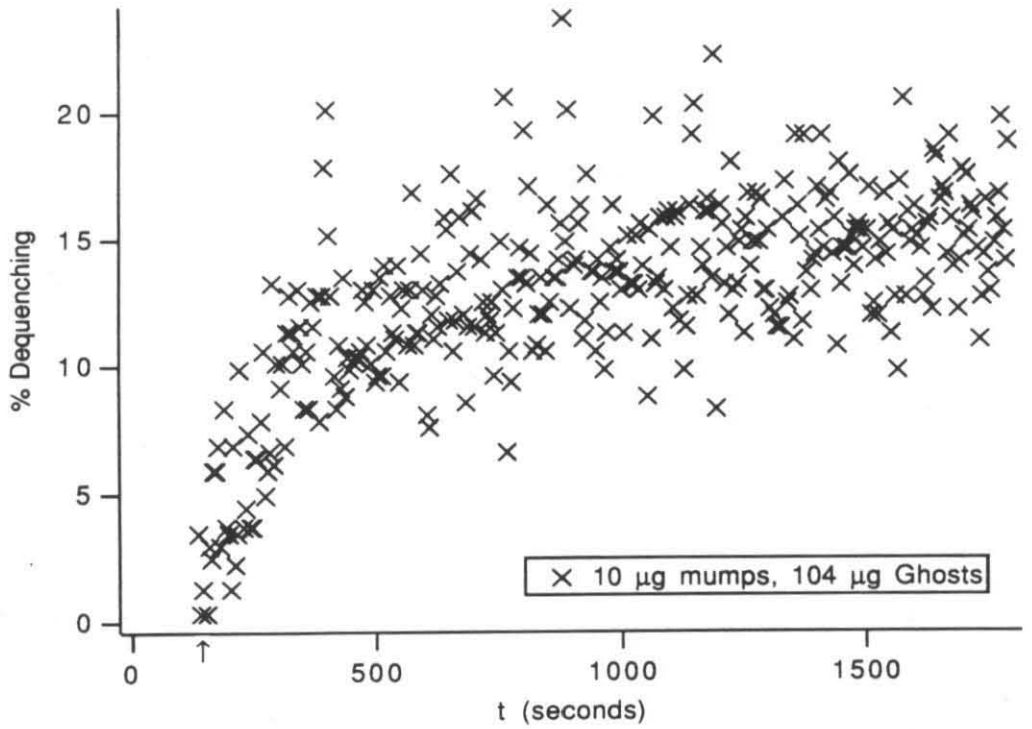

Figure 5.

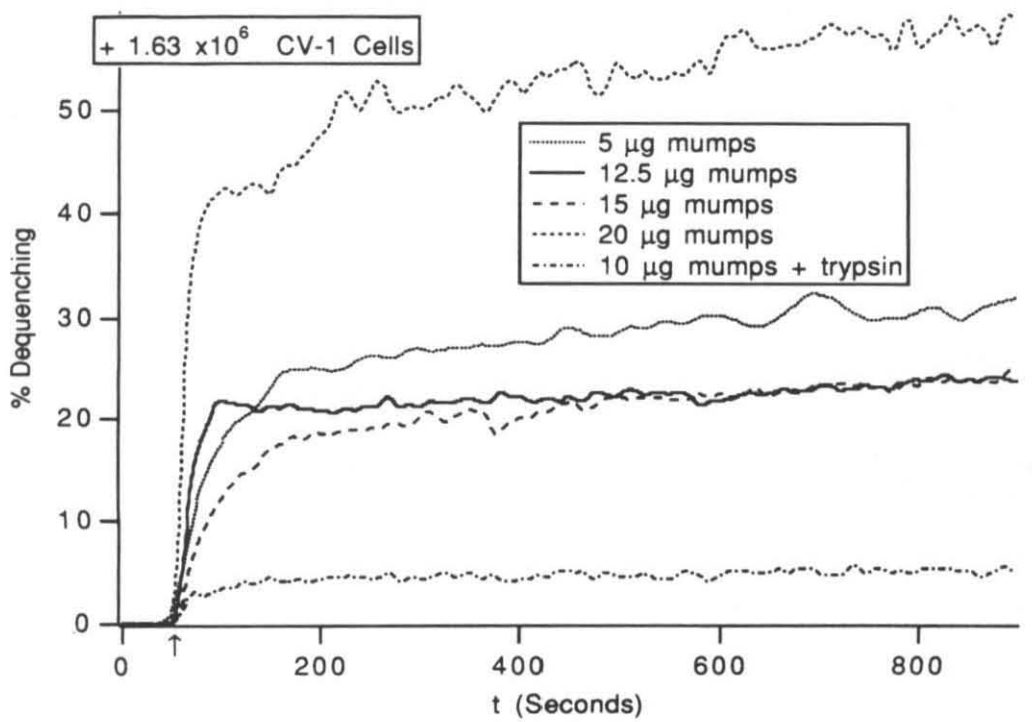

Chapter 5: Fusion of Sendai Virus and Reconstituted Sendai Virus with H9 and Peripheral Blood Lymphocytes.

Christopher Di Simone[1], Delilah A. Stephens[2], John A. Zaia[2], and John D. Baldeschwieler[1]*

[1]Department of Chemistry and Chemical Engineering
California Institute of Technology
Pasadena, CA 91125
[2]Division of Pediatrics
City of Hope National Medical Center
Duarte, CA 91010

Abstract

We have examined the membrane fusion of Sendai virus and reconstituted Sendai virus (RSVE) with H9 cells and peripheral blood lymphocytes (PBL). By using two fluorescent assays we were able to determine the rate and extent of fusion. The fusion of virus and RSVE with the cells was inhibited by fetuin, indicating sialic acid residues as the binding site on the cellular surface. The fusion was also inhibited by trypsin cleavage of the fusion (F) protein, indicating that the fusion was F protein mediated. The number of fusion events with each cell was high, we estimated a saturation limit of 12,000 RSVE were able to fuse with each PBL. Up to 40% of the RSVE were able to fuse with the PBL in 15 minutes. The RSVE may serve as a drug delivery system to these cells.

---

* Corresponding Author

Introduction

Sendai virus is a pneumotropic murine paramyxovirus of the genus *Paramyxovirus*. The viral lipid coat contains two glycoproteins, the fusion protein (F)[1] and the hemagglutination/neuraminidase protein (HN) which are responsible for entry of the viral interior into the cellular cytoplasm (for reviews of viral fusion, see 11, 21, 19, 34). The virus can bind via the HN protein to gangliosides, as shown with ganglioside labeled lipid vesicles (9), with terminal sialic acid residues serving as a receptor for viral binding to cells (18). The fusion of the virus membrane with the cell is mediated by the F protein and is pH independent, indicating that fusion can occur with the cell membrane without the endocytosis required for pH dependent viruses such as influenza. The F protein contains a highly hydrophobic region at its N terminus which has been directly implicated in the fusion process (20).

Detergent reconstitution of the virus envelope produces particles similar in size and activity to the native virus but lacking any interior components (31). In fact, the vesicles can be loaded with drugs, receptors, or nucleic acids and these contents delivered to cellular targets by the same mechanism by which the virus delivers its own genome (2, 8, 14, 17, 32, 33). Some work has been done on using reconstituted Sendai viral envelopes (RSVE) as a system for transfection with a limited number of cells lines (3, 16, 30).

We wished to examine the interactions of Sendai and RSVE with H9 and Peripheral Blood Lymphocytes (PBL) as these cell systems serve as models and hosts of HIV infection (23). RSVE's might serve as a drug

delivery system for various AIDS therapeutics, including phosphorylated AZT, antisense DNA (35) , and HIV cleaving Ribozymes (26).

Two fluorescent assays using self-quenching probes were used to monitor membrane fusion events. The probe octadecyl rhodamine B (R18) inserts spontaneously into a membrane and can be used to monitor the fusion of whole virus membranes with target cell membranes The advantages of using this system to study membrane fusion have been discussed elsewhere (5, 15). In addition, reconstituted virus was labeled with a fluorescently labeled phospholipid analog, Lissamine Rhodamine B Sulfonyl Phosphatidylethanolamine (Rd-PE), which can be incorporated into the RSVE during the reconstitution process. This labeling procedure represents a novel use of rhodamine's self-quenching fluorescent behavior.

Materials and Methods

Virus Preparation-

Strain Z Sendai virus (200µl at 2µg/ml) was inoculated into the allantoic compartment of 10 day old chicken eggs. After three days the eggs were cooled to near 0°C and the allantoic fluid was removed and cell debris pelleted by centrifugation at 5000 g for 30 minutes. The virus was pelleted at 15,000 g for 40 minutes and resuspended in PBS (1mg/ml, each egg yielding ≈.3 mg). The virus was then filtered through 1.2 and .8 µm filters to remove aggregates and bacteria. The purified virus was checked for HA activity (25) and flash frozen in liquid nitrogen. Ten percent glycerol was added to the virus before freezing as a cryopreservative (1).

H9 Cells and PBL Cells -

H9 cells were maintained in RPMI 1640 supplemented with 10% fetal bovine serum (RPMI 10).

Lymphocytes were prepared by the general method of Böyum (4). Buffy coat from human blood was diluted three fold with phosphate buffered saline and then placed on top of a cushion of Ficoll-paque (Pharmacia). After centrifugation for 30 minutes at 400g the cells at the serum/Ficoll-paque interface were removed and washed twice with Puck's salt solution. The cells were resuspended at a concentration of about $2x10^6$ per ml in RPMI medium with 20% fetal bovine serum. Phytohemagglutinin P (Pharmacia) was added at a concentration of 0.8 µg/ml. Cells were expanded for three days prior to being used in experiments.

Determination of Virus Size-

A Malvern 4700c photon correlation spectrometer was used to measure the virus size. The system is equipped with a 488 nm tuned 3 watt Spectra-Physics 2020 laser attached to an IBM compatible PC with Malvern software. Most measurements were made at 90° to the beam with no size bias and maximal modal distribution parameters. Measurements at other angles were made to check for any major amplitude variations. In some instances size bias parameters were inserted after initial data collection to further clarify size distributions.

Virus Reconstitution-

Reconstituted virus envelopes were prepared by the general method of Vainstein *et al.* (29) with a few variations in protocol. One milligram of virus was pelleted by ultracentrifugation (100,000 g) for one hour and then resuspended in 50 µl of a 10% Triton X-100 solution (100 mM NaCl, 50 mM Hepes, 2 mM EDTA, pH 7.4). Pierce Surfact-Amps^{TM} X-100 purified detergent was used. The solution was then shaken for two hours at 20° C. The nucleocapsid was removed by 40 minutes of ultracentrifugation (100,000g) and the supernatant removed to an 1.5 ml eppendorf microfuge tube. Fluorescent probes were added to the detergent supernatant. SM-2 Biobeads were then added at 1 mg biobeads/µl detergent solution. After four hours of shaking, 50 µl of buffer A (160 mM NaCl/20 mM Hepes, pH 7.4) and an additional 50 µg of Biobeads were added to the solution. After shaking for 12 hours at room temperature the RSVE were removed from the beads with a Hamilton syringe and the beads washed three times with

buffer A. The RSVE were pelleted by ultracentrifugation (100,000g, 40 minutes) and resuspended in PBS (500 µl).

One milligram of biobeads should absorb one µl of the given detergent solution in 4 hours (13). As the beads absorb some viral lipid as well as detergent, one should use the least amount of detergent possible to solubilize the virus (13). In later experiments the amount of Triton X-100 solution used was reduced to 30 µl.

Fluorescent labeling-

The fluorescent probe R18 has been used by a number of other workers to examine viral fusion (15). The R18 probe will spontaneously insert into a viral membrane and will rapidly equilibrate into a target membrane when fusion does occur (24). The probe self-quenches by resonant energy transfer and subsequent trivial decay mechanisms due to the overlap of the emission and excitation fluorescence bands. In dilute concentrations (<10% of the lipid content), the fluorescent quenching is linearly proportional to the concentration of the probe in the membrane. The surface area of the viral particles is much smaller than the surface area of the cells. Upon fusion of virus with the cells, the probe in the viral lipid bilayer dilutes into the target membrane and dequenches.

A fresh solution of 1 mM R18 (Molecular Probes) was prepared and an amount equal to 2-6 mole percent of the viral membrane lipid (276 nanomoles lipid/mg viral protein) was added to a 1 ml solution of 1 mg protein Sendai virus, while vortexing. A smaller mole percentage (3%) was found to be most useful for the fluorescent assays as this amount is still highly quenched (50%) and emits more fluorescence, which is useful in

increasing the signal-to-noise ratio. The solution was allowed to sit in the dark for half an hour and then the unincorporated R18 was removed by either running the sample over a G75 Sephadex column or by pelleting the virus with ultracentrifugation (100,000 g in a SW50.1 rotor).

Reconstituted virus were labeled by using the fluorescent labeled lipid Rhodamine-phosphotidyl ethanolamine (Rd-PE). Previous workers have measured fluorescent resonance energy transfer between NBD-PE and Rd-PE in order to monitor fusion (27). We have found that fusion can be monitored by just using the self-quenching properties of the Rd-PE, similar to the R18 experiment described above.

Rhodamine PE (Avanti Polar Lipids) was dried from chloroform and resuspended in the Triton X-100 reconstitution solution. The probe was then added to the reconstitution as described above so that the total amount of lipid added equaled 5 mole percent of the total lipid.

Fusion Measurements-

Fluorescent measurements were made in a SLM4800 fluorimeter by monitoring the emission at 590nm with an excitation wavelength of 560nm and a Schott OG550 or OG570 type filter in the emission path. For kinetic experiments, Sendai virus or RSVE were preincubated at 37°C in the cuvette with 2 ml of PBS. The sample was stirred in the sample chamber by a magnetic stirrer. Fluorescence data were collected digitally and stored on disk by an IBM AT computer using SLM4800 software. Data collection was initiated and after a baseline had been established, cells were added to the virus using a pipette. The fluorescence of control aliquots of virus was measured with and without 1% Triton, to determine quenching, and

baseline scatter was determined with a suspension of cells. The kinetic data was smoothed with the Igor data processing program (WaveMetrics).

The H9 or PBL cells ($1x10^5$ to $1x\ 10^6$) were pelleted from media and resuspended in a small volume of PBS (100µl), and then added to the fluorimeter cuvette during a kinetic experiment.

To show that the Sendai virus or RSVE fusion was F protein mediated, samples were treated with trypsin. Trypsin cleaves the F protein but not the HN protein. Virus (100 µg protein) was incubated with 100 µg of trypsin for one hour at 37°C in 100 µl volume. The reaction was stopped by the addition of soybean trypsin inhibitor. This virus was subsequently used in the kinetic fusion assay.

For binding competition experiments fetuin was preincubated with the labeled virus for 30 minutes at 37°C. The entire solution was then added to the PBS cuvette and cells were added as described above.

Calculation of Fusion-

Fusion of the virus was calculated using the formula:

$$\%\text{Fusion} = \frac{\text{Fluor.}_{(final)} - \text{Fluor.}_{(initial)}}{\text{Fluor.}_{(maximum)} - \text{Fluor.}_{(initial)}} \times 100.$$

For kinetics experiments $\text{Fluor.}_{(final)}$ and $\text{Fluor.}_{(initial)}$ represent values taken from the fluorescent data plots. The $\text{Fluor.}_{(maximum)}$ value was determined by adding Triton X-100 at 1% v/v to a solution of labeled virus, allowing the R18 to totally dequench.

A control experiment showed that the fluorescence of R18 labeled virus + 1% Triton X-100 approximately equaled the fluorescence of an

infinite dilution of the probe, without a correction factor for the fluorescent environment. Phosphatidyl choline (PC) vesicles were labeled with R18 and measured for fluorescence. In a mock fusion experiment, additional unlabeled PC vesicles were then added and co-sonicated. As dilution of the probe increased, the fluorescence linearly approached an infinite dilution value. This infinite dilution value was equivalent to the fluorescent value given after the addition of 1% Triton X-100 to the original labeled PC vesicles.

Conversion of virus protein to number of particles-

To relate quantities of Sendai viral protein to the number of viral particles it was assumed that 1 μg of Sendai virus equaled 1.3×10^9 viral particles. This is based on the data given by Hoekstra and Klappe (10) and the MW measurement and size of the Sendai virus (12). To determine the number of RSVE particles it was assumed that 30 % of the viral protein was glycoprotein. Assuming that the virus and RSVE are similar in size, 1 μg of RSVE protein would be equal to 3.9×10^9 RSVE particles.

Protein determination, Gel Electrophoresis, Transmission Electron Microscopy-

Protein content of the virus was determined by using the Peterson assay (22) with omission of the TCA precipitation step. Fraction V BSA (Reheis Chemical Company) was used as a protein standard. The BCA protein determination kit (Sigma) was also used.

Polyacrylamide gel electrophoresis was used to confirm the presence of virus proteins and to check viral purity. Ten percent separating gels were

run with six percent stacking gels. Biorad protein standards were used. Gels were silver stained using the Biorad Silver Stain Kit.

Virus samples (10 µl) at varying concentrations (about 250 µg protein/ml) were applied to carbon-covered glow-discharged grids and allowed to dry. 10 µl of stain was then applied and allowed to sit for various time periods. 1% Phosphotungstic acid, 1% Uranyl Acetate, and 2% Ammonium Molybdate were used as stains. The samples were examined using a Phillips EM201 TEM.

Fluorescent Microscopy-

A Nikon inverted fluorescent microscope was used to examine the cells after addition of fluorescently labeled virus and RSVE. Virus and RSVE were fluorescently labeled as described above. Virus and cells were incubated at 37° for 30 minutes and then pelleted and washed with PBS to wash away unbound and unfused material. The samples were then placed on slides and examined by microscopy.

Results

Virus Characterization-

The size distribution of Sendai virus and RSVE was determined by photon correlation spectroscopy light scattering measurements (Figure 1). The viral particles had an average diameter of 300 nm. Reconstituted virus envelopes contained two populations of particles, one with a diameter around 90 nm and the other with a diameter around 300 nm.

Electron microscopic examination showed that the Sendai virus and the RSVE were intact vesicles and contained the spike glycoproteins HN and F. Gel electrophoresis showed the presence of the Large, HN, Polymerase, Nuclear Protein, F, and Matrix proteins in the whole virus and only the HN and F glycoproteins in the RSVE.

Fusion of Sendai with H9 cells-

The fusion of the whole virus with H9 cells was tested in a preliminary experiment. Whole virus was labeled with the R18 fluorescent probe as described in the methods. Dequenching kinetics were monitored continuously for one hour using a number of different ratios of virus to cells (Figure 2). As virus numbers were increased a reduction in the percentage of virus dequenching was observed as the receptor sites on the cell surface were saturated with virus. Under the least saturating conditions, 4 % of the viral particles were able to interact with the H9 cells in 14 minutes. Under highly saturating conditions up to 2500 viral particles (1.9 μg viral protein/ 1x 10^6 cells) were observed to interact with each cell after 14 minutes. A reciprocal plot analysis (0.98 r squared fit) of the fusion

values showed a saturation maximum of about 2600 fusion events per cell (2 μg viral protein per $1x10^6$ cells).

Fusion of RSVE with H9 Cells-

The kinetic interaction of RSVE with H9 cells was then examined. RSVE were labeled with the self quenching Rd-PE probe rather than R18 since the Rd-PE probe should be less likely to transfer spontaneously to a target membrane (see discussion). Again, as the amount of viral protein was increased the percentage of particles fusing went down while the absolute number of fusing particles increased, see Figure 3a. Up to 40% of the RSVE were observed to fuse, with up to 6 μg of viral protein observed fusing per 10^6 cells.

Trypsin has been shown to cleave selectively the F protein of Sendai virus (28). Fusion was inhibited 75 % by trypsin treatment of the virus indicating a large role for the F protein in the fusion process, see Figure 3b.

Fetuin is a highly glycosylated protein which should compete with the cellular binding sites for the virus due to the multitude of sialic acid residues on the fetuin protein surface. When fetuin was added to the RSVE before addition of the virus to cells, fusion was inhibited by 93 %. In addition, no fusion was observed (97% inhibition) when the fusion assay was conducted in medium with serum rather than in PBS. Fetal calf serum contains fetuin which should have inhibited fusion.

Fusion of RSVE with PBL-

Experiments were also conducted to determine if RSVE virus could fuse with Peripheral Blood Lymphocytes. Over a time span of 14 minutes up to 40 % of the reconstituted virus could fuse with the PBL, see Figure 4a. A reciprocal plot Scatchard type analysis of the extents of fusion showed a saturation of about 2.9 μg viral protein per 10^6 cells in 14 minutes, Figure 5. As preparations of PBL may vary in content, the experiments were repeated with a second preparation of PBL. Similar behavior was observed with a saturation of about 2.7 μg viral protein per $1x10^6$ cells.

Fusion was highly inhibited (95%) by trypsinization of the virus, see Figure 4b. Fetuin or serum also strongly inhibited fusion (80-85% and 99%, respectively).

Fluorescence Microscopy-

Peripheral blood lymphocytes were examined under the fluorescent scope to qualitatively examine the virus binding to the cellular surfaces. The PBL were covered with fluorescent points indicating a multitude of virus binding to the cells (data not shown). The virus appeared to be surface associated and not located in endocytotic or lysosomal compartments.

Addition of fetuin to the media previous to viral addition resulted in almost complete inhibition of viral binding. No virus were observed associated with cells except in one case where the cell was apparently replicating.

Preliminary Delivery Experiments-

In collaboration with Sean Sullivan (Vestar), Roy Chang and John Rossi (City of Hope Hospital), RSVE were tested for the ability to encapsulate intact ribozyme. In a preliminary experiment, RSVE were incubated with ribozyme and then the ribozyme was examined by column chromatography to confirm the intactness of the ribozyme. No degradation of the RNA was caused by the RSVE. ^{32}P labeled ribozyme (140 mer) was then encapsulated into RSVE (30 μg ribozyme in 2 mg of Sendai protein) and the encapsulated product examined by gel electrophoresis. 50 % of the radiolabel was found associated with the vesicles. The material appeared intact by gel electrophoresis. The loaded RSVE were able to bind to the target H9 cells.

An experiment was designed to determine if ribozyme was being delivered to the cellular interiors by the RSVE. Trypsin treated RSVE are able to bind to the H9 cellular surface but are not fusogenic, because trypsin cleaves the F protein but not the HN protein. After incubation of trypsin treated and untreated vesicles with H9 cells we had hoped to remove unfused vesicles from the cellular surface by treatment with protease K. Unbound virus was easily separated from the H9 cells by centrifuging through a layer of silicon oil. Unfortunately the treatment with protease K made no difference in the amount of material associated with the H9 cell; either the protease K was ineffective in removing the virus from the surface or all the RSVE, trypsin treated or not, were taken up by the cells.

An attempt was made to transfect the H9 cells with the pXGH5 plasmid which contains the human growth hormone under the mouse metallothionein-1 promotor. The Allegro™ assay from Nichols Institue was used to determine if any transient expression was detectable. Little expression above background was found. The H9 cells are refractive to

other mechanisms of transfection. The DNA may be delivered to the cellular interior but not expressed (see Chapter 6 for a further discussion of this phenomenon).

Discussion

After determining that Sendai virus was able to fuse with H9 cells, we found that reconstituted virus was able to fuse with both H9 and PBL cells. The majority of fusion occurred over a time span of thirty minutes and presented a simple single exponential kinetic profile, indicating that only one type of fusion event was occurring. Fusion of the virus with the cells was saturable, with a maximum number of binding receptors or fusion sites available. The process could be blocked by competing for the binding site sialic acids with fetuin or by preventing fusion by cleaving the F protein with trypsin. A large number of fusion events were observed with each cell; for the PBL approximately 2 μg of viral protein were observed to fuse with 1 x 10^6 cells, equal to about 2600 whole virus per cell or 7,800 reconstituted virus per cell. The receptor for the Sendai virus, sialic acid, is common to many cells and fairly numerous in the cell membrane, providing a large number of binding sites for the virus to interact with the cells. It is likely that most mammalian cell lines are susceptible to fusion with the Sendai virus.

We have used a new fluorescence assay to monitor membrane fusion in this paper. For examining the fusion of reconstituted systems or liposomes the self quenching probe Rd-PE can be incorporated into the membrane. Previous workers have used the resonance energy transfer pair NBD-PE/Rd-PE to monitor fusion (27). The Rd-PE probe system produces more fluorescent signal than the NBD/Rd system (data not shown) and is not subject to some of the artifacts seen in the NBD/Rd system (7). The Rd-PE probe has an advantage over the R18 probe as Rd-PE has two

hydrocarbon tails rather than R18's one and thus is less likely to spontaneously transfer out of the membrane. R18 is still the preferred system for labeling whole virus due to its ability to insert into the intact virus envelope.

Reconstituted virus may provide a method for drug delivery to cells. The ability of the reconstituted virus to maintain contents is critical to delivery and is undergoing current examination. AZT loading may require phosphorylation to prevent the drug from crossing the viral membrane. Literature procedures used to load nucleic acids into these reconstituted vesicles have produced very low rates of loading in our hands. The vesicles may be more valuable for the delivery of membrane components and pro drugs; the delivery of Epstein Barr receptors to receptor-negative cells has previously been demonstrated (32).

1-Abbreviations used- Rd-PE, LissamineRhodamine B Sulfonyl Diacyl Phosphatidylethanolamine; R18, Octadecyl Rhodamine B; PBL, Peripheral Blood Lymphocyte; RSVE, Reconstituted Sendai Viral Envelope

Acknowledgments

We would like to thank C. Lowry for her assistance in preparation of this paper and for providing H9 cells for control experiments. Funding for this work was provided by ARO grant #DAAL-03-87-K-0044, and by the Caltech Consortium in Chemistry and Chemical Engineering; Founding Members: E.I. du Pont de Nemours and Company, Inc., Eastman Kodak Company, Minnesota Mining and Manufacturing Company, Shell Oil Company Foundation.

References

1. **Apostolov, K., and Damjanovic, V.** 1973. Effect of distilled water, hypertonic saline, freezing and freeze-drying on the haemagglutinin and haemolytic properties of Sendai virus. Microbios. **8**:257-266.

2. **Ardizzoni, S., Michaels, A., and Arendash. G.** 1988. Labeling of Neural Cells by Gold-Filled Sendai Virus Envelopes Before Intracerebral Transplantation. Science. **239**:635-637.

3. **Barzlett, R.** 1989. Cotransfection of Nucleic Acid Segments by Sendai Virus Envelopes. Biotechnol. Appl. Biochem. **11**:133-135.

4. **Böyum, A.** 1968. Isolation of Mononuclear Cells and Granulocytes from Human Blood. Scand. J. Clin. Lab. Invest. **21(sup. 97)**:77-89.

5. **Chejanovsky, N., Nussbaum, O., Loyter, A., and Blumenthal, R.** 1988. Fusion of Enveloped Viruses with Biological Membranes. Subcell. Biochem. **13**:415-456.

6. **Citovsky, V., Blumenthal, R., and Loyter, A.** 1985. Fusion of Sendai virions with phosphatidylcholine-cholesterol liposomes reflects the viral activity required for fusion with biological membranes. FEBS Lett. **193**:135-140.

7. **Duzgunes, N., Allen, T., Fedor, J., and Papahadjopoulos, D.** 1987. Lipid Mixing during Membrane Aggregation and Fusion: Why Fusion Assays Disagree. Biochemistry. **26**:8435-8442.

8. **Gitman, A. G., Graessmann, A., and Loyter, A.** 1985. Targeting of loaded Sendai virus envelopes by covalently attached insulin molecules to virus receptor-depleted cells: Fusion-mediated microinjection of ricin A and simian virus 40 DNA. Proc. Natl. Aca. Sci. USA. **82**:7309-7313.

9. **Haywood, A. M.** 1974. Characteristics of Sendai Virus Receptors in a Model Membrane. J. Mol. Biol. **83**:427-436.

10. **Hoekstra, D., and Klappe, K.** 1986. Sendai Virus-Erythrocyte Membrane Interaction: Quantitative and Kinetic Analysis of Viral Binding, Dissociation, and Fusion. J. Virol. **58**:87-95.

11. **Hoekstra, D., and Kok, J. W.** 1989. Entry Mechanisms of Enveloped Viruses. Implications for Fusion of Intracellular Membranes. Biosci. Rep. **9**:273-305.

12. **Kingsbury, D. W., Bratt, M. A., Choppin, P. W., Hanson, R. P., Hosaka, Y., Ter Meulen, V., Norrby, E., Plowright, W., Rott, R., and Wunner, W. H.** 1978. Paramyxoviridae. Intervirology. **10**:137-152.

13. **Lévy, D., Bluzet, A., Seigneuret, M., and Rigaud, J-L.** 1990. A systematic study of liposome and proteoliposome reconstitution involving Bio-Bead-Mediated Triton X-100 removal. Biochim. Biophys. Acta. **1025**:179-190.

14. **Loyter, A., Chejanovsky, N., and Citovsky, V.** 1989. Implantation of Isolated Carriers and Receptors into Living Cells by Sendai Virus Envelope-Mediated Fusion. Methods Enzymol. **171**:829-851.

15. **Loyter, A., Citovsky, V., and Blumenthal, R.** 1988. The Use of Fluorescence Dequenching Measurements to Follow Viral Membrane Fusion Events. Methods Biochem. Anal. **33**:129-164.

16. **Loyter, A., Vainstein, A., Graessmann, M., and Graessmann, A.** 1983. Fusion-Mediated Injection of SV40-DNA. Exp. Cell Res. **143**:415-425.

17. **Loyter, A., and Volsky, D. J.** 1982. Reconstituted Sendai virus envelopes as carriers for the introduction of biological material into animal cells, p. 215-266. *In* Poste, G. and Nicolson, G. L. (eds.), Membrane Reconstitution. Elsevier Biomedical Press.

18. **Markwell, M. A. K., Svennerholm, L., and Paulson, J. C.** 1981. Specific gangliosides function as host cell receptors for Sendai virus. Proc. Natl. Acad. Sci. USA. **78:** 5406-5410.

19. **Marsh, M., and Helenius, A.** 1989. Virus Entry into Animal Cells. Adv. in Virus Res. **36**:107-151.

20. **Novick, S. L. and Hoekstra, D.** 1988. Membrane Penetration of Sendai virus glycoproteins during the early stages of fusion with liposomes as determined by hydrophobic photoaffinity labeling. Proc. Natl. Acad. Sci. USA. **85**:7433-7437.

21. **Ohnishi, S.** 1988. Fusion of Viral Envelopes with Cellular Membranes. Curr. Top. in Membr. Transp. **32**:257-295.

22. **Peterson, G. L.** 1977. A Simplification of the Protein Assay Method of Lowry *et al.* Which is More Generally Applicable. Anal. Biochem. **83**:346-356.

23. **Popovic, M., Sarngadharan, M., Read, M., and Gallo, R. C.** 1984. Detection, isolation, and continuous production of cytopathic retroviruses (HTLV-III) from patients with AIDS and pre AIDS. Science. **224**:497-500.

24. **Rubin, R. J., and Chen, Y-D.** 1990. Theoretical-studies of diffusion of lipid-like molecules between membranes in virus-cell and cell-cell fusion systems. Biophys. J. **57**:494a.

25. **Salk, J.** 1944. A Simplified Procedure for Titrating Hemagglutinating Capacity of Influenza-Virus and the Corresponding Antibody. J. Immunol. **49**:87-98.

26. **Sarver, N., Cantin, E., Chang, P., Zaia, J., Ladne, P., Stephens, D., and Rossi, J.** 1990. Ribozymes as Potential Anti-HIV-1 Therapeutic Agents. Science. **247**:1222-1225.

27. **Struck, D., Hoekstra, and Pagano, R.** 1981. Use of Resonance Energy Transfer To Monitor Membrane Fusion. Biochemistry. **20**:4093-4099.

28. **Tsao, Y. and Huang, L.** 1985. Sendai Virus Induced Leakage of Liposomes Containing Gangliosides. Biochemistry. **24**:1092-1098.

29. **Vainstein, A., Hershkovitz, M., Isreal, S., Rabin, S., and Loyter, A.** 1984. A New Method for Reconstitution of Highly Fusogenic Sendai Virus Envelopes. Biochim. Biophys. Acta. **773**:181-188.

30. **Vainstein, A., Razin, A., Graessmann, A., and Loyter, A.** 1983. Fusogenic Reconstituted Sendai Virus Envelopes as a Vehicle for Introducing DNA into Viable Mammalian Cells. Methods Enzymol.**101:**492-512.

31. **Volsky, D. J. and Loyter, A.** 1978. An Efficient Method for Reassembly of Fusogenic Sendai Virus Envelopes After Solubilation of Intact Virions with Triton X-100. FEBS Lett. **92:**190-194.

32. **Volsky, D. J., Shapiro, I. M., and Klein, G.** 1980. Transfer of Epstein-Barr Virus Receptors to receptor-negative cells permits virus penetration and antigen expression. Proc. Natl. Acad. Sci. USA. **77:**5453-5457.

33. **Volsky, D., Sinangil, F., Gross, T., Shapiro, I., Dambaugh, T., King, W., and Kieff, E.** 1983. Functional Mapping of the Epstein-Barr (EBV) Genome using Sendai Virus Envelope-Mediated Gene Transfer, p. 425-434. *In* D. Golde and P.A. Marks (eds.), Normal and Neoplastic Hematopoiesis. Alan R. Liss, Inc.

34. **White, J.** 1990. Viral and Cellular Membrane Fusion Proteins. Annu. Rev. Physiol. **52:**675-697.

35. **Zaia, J., Rossi, J., Murakawa, J., Spallone, P., Stephens, D., Kaplan, B., Eritja, R., Wallace, R., and Cantin, E.** 1988. Inhibition of Human Immunodeficiency Virus by Using an Oligonucleoside Methylphosphonate Targeted to the *tat*-3 Gene. J. Virol. **62:**3914-3917.

Figure Captions

Figure 1. Light scattering size analysis of Sendai virus and RSVE.

Figure 2. Fusion of Sendai virus with H9 cells. Cells were added to R18 labeled Sendai virus as described in Methods. Viral amounts are described in terms of micrograms of viral protein. H9 cells were injected after 100 seconds.

Figure 3a. Fusion of RSVE with H9 cells. H9 cells were added to Rd-PE labeled RSVEs after 60 seconds. Two milliliters of H9 cells contained 6.4 x 10^5 cells. **3b.** Inhibition of fusion. In each experiment 6.4 x 10^5 H9 cells were used.

Figure 4a. Fusion of RSVE with PBL cells. Various amounts of viral protein were mixed with 4.8 x 10^6 PBL cells. **4b.** Inhibition of RSVE fusion with PBL cells. Again, 4.8 x 10^6 PBL cells were used.

Figure 5. Reciprocal Plot of RSVE fusion with PBL's.

Figure 1.

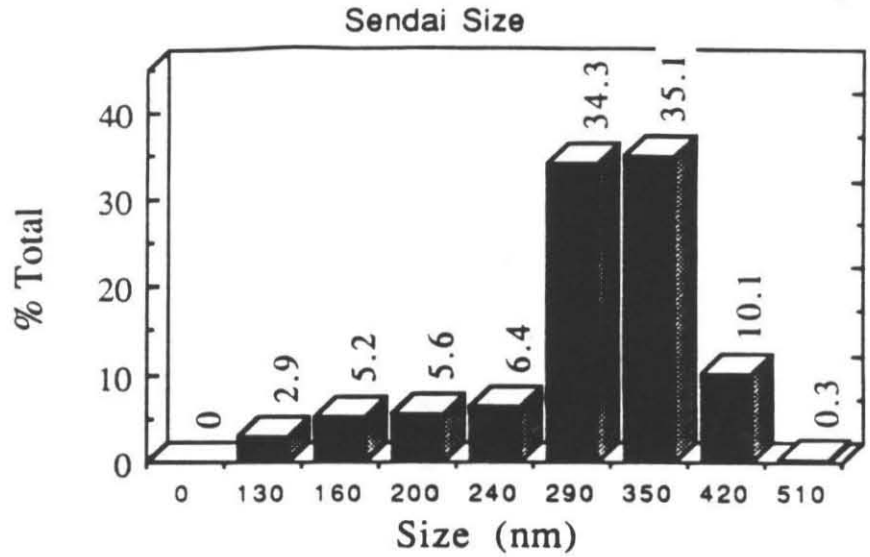
Sendai Size
% Total
40
30
20
10
0
0
2.9
5.2
5.6
6.4
34.3
35.1
10.1
0.3
0
130
160
200
240
290
350
420
510
Size (nm)

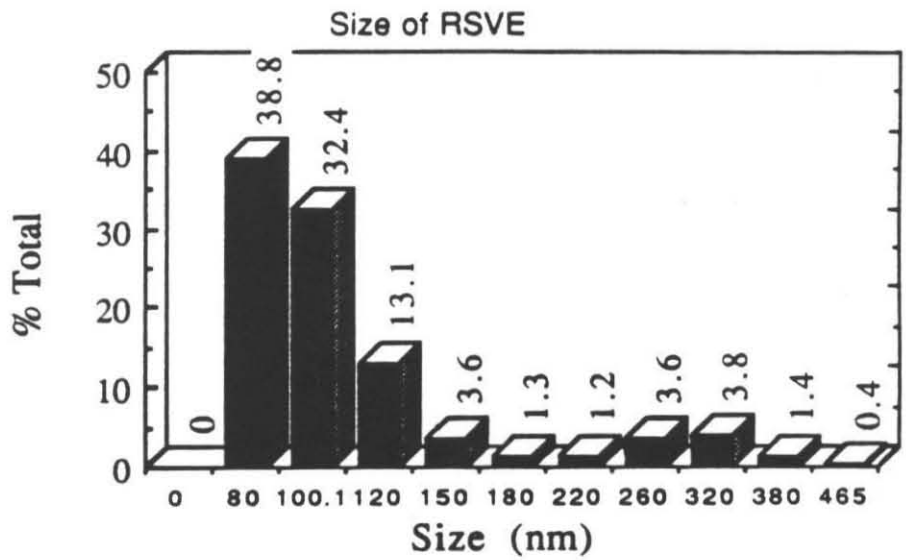
Size of RSVE
% Total
50
40
30
20
10
0
0
38.8
32.4
13.1
3.6
1.3
1.2
3.6
3.8
1.4
0.4
0
80
100.1
120
150
180
220
260
320
380
465
Size (nm)

Figure 2.

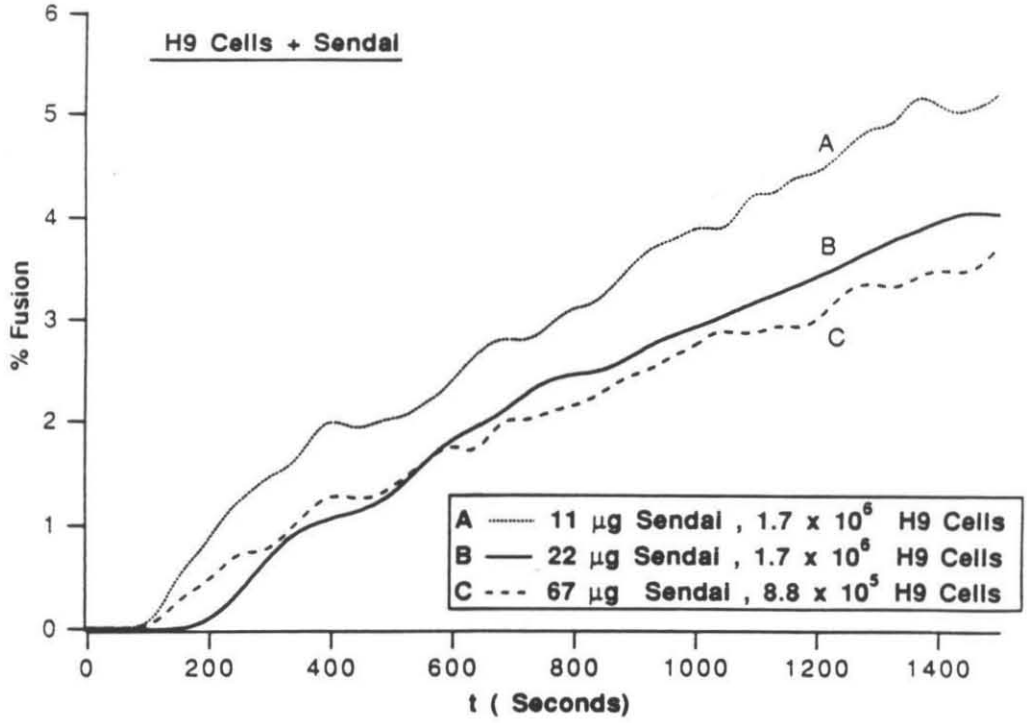
H9 Cells + Sendai
% Fusion
t (Seconds)
A
B
C
A ····· 11 µg Sendai , 1.7 x 10⁶ H9 Cells
B —— 22 µg Sendai , 1.7 x 10⁶ H9 Cells
C - - - 67 µg Sendai , 8.8 x 10⁵ H9 Cells
0
1
2
3
4
5
6
0
200
400
600
800
1000
1200
1400

Figure 3(a).

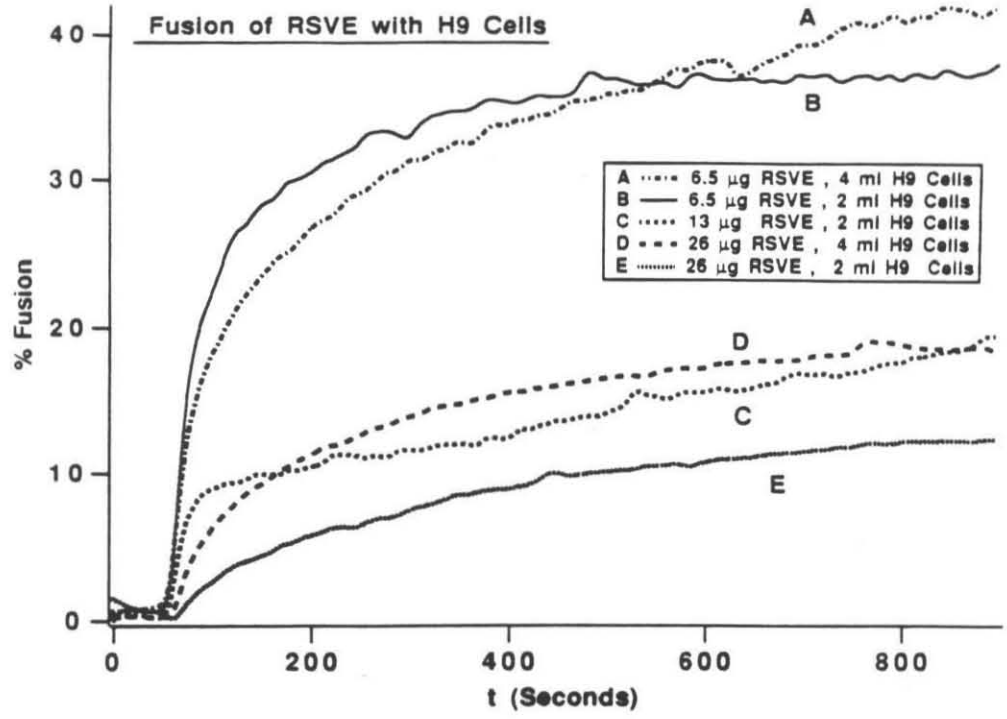

Figure 3(b).

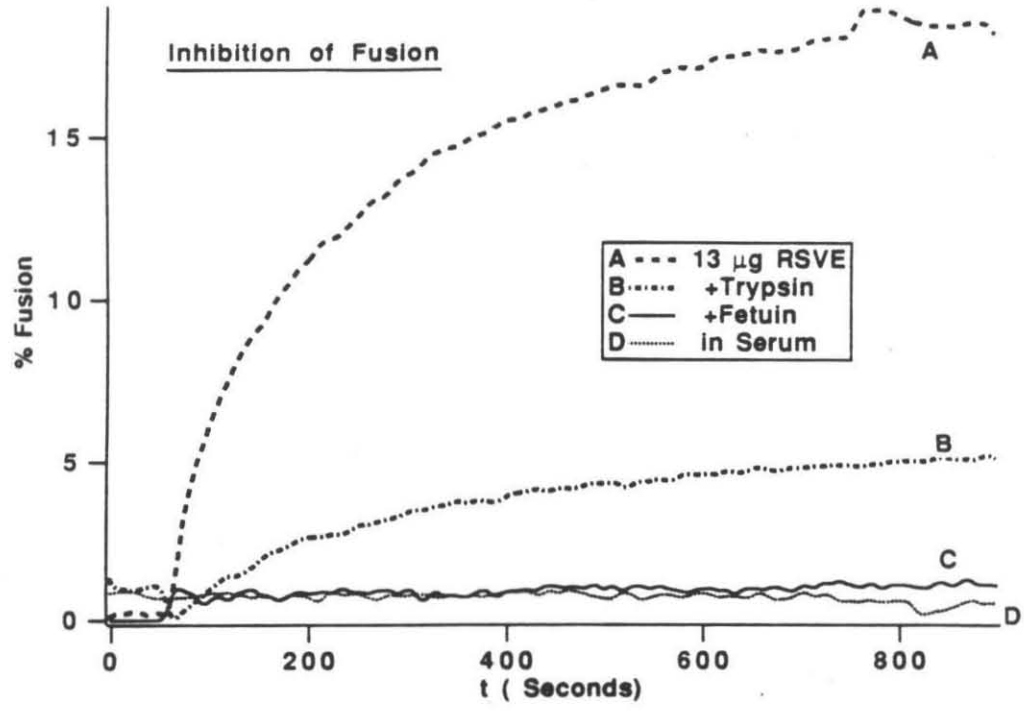

Figure 4(a).

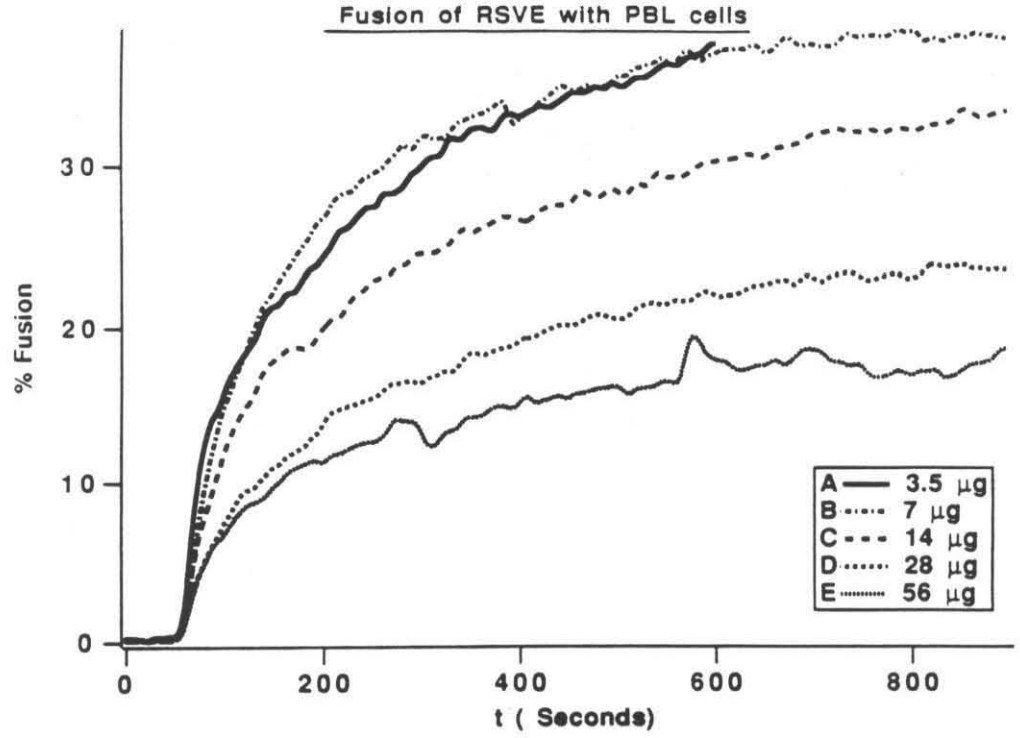

Figure 4(b)

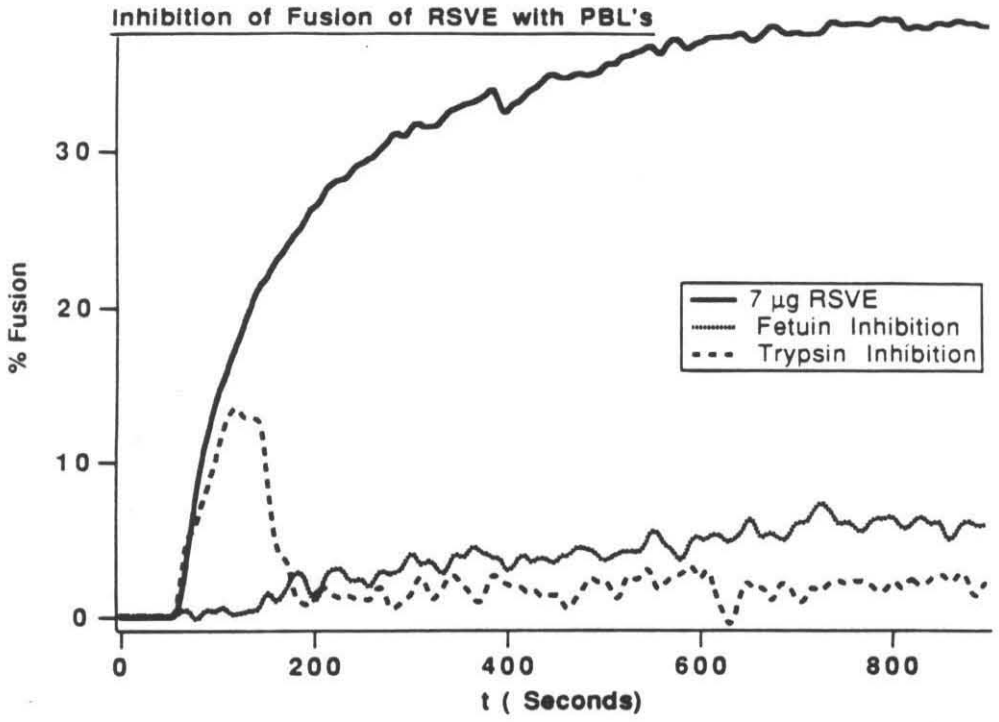

Figure 5

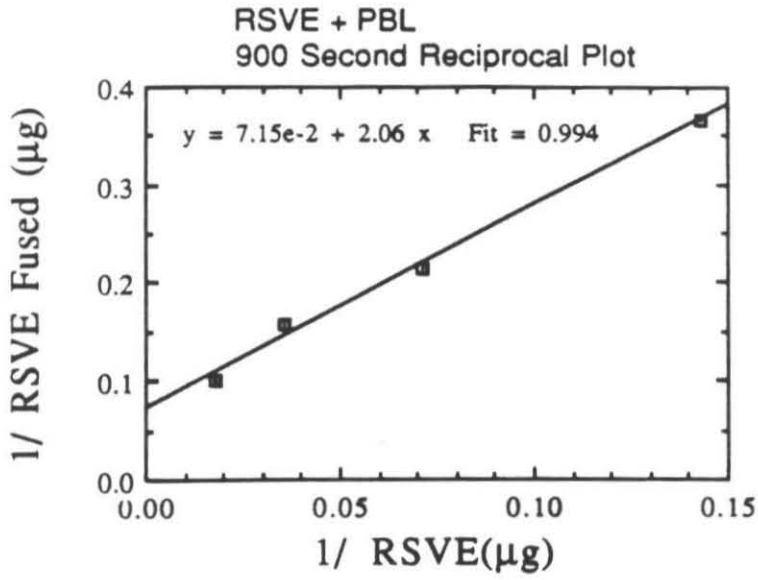
RSVE + PBL
900 Second Reciprocal Plot
y = 7.15e-2 + 2.06 x Fit = 0.994
1/ RSVE Fused (µg)
1/ RSVE(µg)
0.0
0.1
0.2
0.3
0.4
0.00
0.05
0.10
0.15

Chapter 6: Enhanced Loading of Nucleic Acids in Reconstituted Sendai Viral Envelopes

Christopher Di Simone[1], John D. Baldeschwieler[1], Melvin A. Simon[2] and Thomas A. Amatruda[2]

[1]Department of Chemistry and Chemical Engineering, California Institute of Technology, Pasadena, CA 91125

[2]Department of Biology, California Institute of Technology, Pasadena, CA 91125

ABSTRACT

DNA plasmids (≈5000 base pairs) were loaded into Triton X-100 reconstituted Sendai prepared by the general method of Vainstein et al. (Vainstein et al., 1984). Examination by gel electrophoresis of DNAase treated vesicles revealed that the vesicles encapsulated <1% of the input DNA. Protamine, polylysine and lysozyme were used to enhance encapsulation. All three proteins enhanced loading to between 4 and 10 % DNA encapsulated. Accurate values for DNA encapsulation with protamine were difficult to determine as the protamine afforded the DNA some DNAase protection. Transfection experiments using luciferase expression as a marker gave positive results for Cos cells and negative results for HL60 cells.

INTRODUCTION

The paramyxovirus Sendai contains two glycoproteins, HN, which is responsible for viral binding to host cell receptors (sialic acid), and F, which is responsible for fusion of the viral membrane with the cellular membrane. These proteins can be reconstituted into vesicles by solubilizing the viral lipids and glycoproteins in detergent, removing the interior proteins and viral nucleic acid by ultracentrifugation, and dialyzing away the detergent. These reconstituted Sendai viral envelopes (RSVE) maintain the functions of the native viral glycoproteins and thus can be used to deliver material to the interior of a cell. A variety of substances have been encapsulated and delivered using these vesicles (Loyter et al., 1983, Loyter and Volsky, 1982, Vainstein et al., 1983).

We are investigating the use of RSVE in transfecting certain cell lines which are difficult to transfect by normal mechanisms (calcium phosphate, electroporation, lipofection, DNA loaded liposomes). We would like to efficiently load DNA into these viral vesicles and deliver DNA to cellular interiors. In preparing loaded vesicles we found that the loading was highly inefficient. Work by Jay and Gilbert on DNA loading into phospholipid vesicles (Jay and Gilbert, 1987) suggested that positively charged proteins might serve to enhance DNA loading into the reconstituted viral envelopes.

MATERIALS AND METHODS

Materials

Sendai virus was grown in 10 day old embryonic eggs and prepared by differential centrifugation. The virus was further purified by filtration through 1.2 μm and .8 μm filters. Plasmids were prepared by standard methods. The proteins used in the coencapsulation experiment were protamine sulfate (Salmon type II), polylysine hydrochloride (MW 17,300), and lysozyme (egg white).

Reconstitution

A modification of the Triton X-110 reconstitution method of Vainstein et al. (Vainstein et al., 1984) was used in preparation of the vesicles. One mg of viral protein was pelleted at 100,000g for one hour in a SW50.1 rotor. The virus was dissolved in 30 to 50 μl of 10% Triton X-100/100 mM NaCl/50 mM Hepes/2 mM EDTA pH 7.4 buffer. The sample was shaken for 4 hours at room temperature and then the non-dissolved nucleocapsid material was pelleted out with the ultracentrifuge, again at 100,000g.

External DNA, proteins, and fluorescent markers were added to the detergent solubilized lipid and proteins after removal of the nucleocapsid. In general, 5-10 μg of DNA were used with 1 mg of Sendai viral protein. Exact starting DNA ratios are given in the figures and results. Coencapsulated protein was vortexed with the DNA before addition. A ten to one gram/gram ratio of protein to DNA was generally used (50-100 μg protein). Other ratios were also tested. The resonance energy transfer probes NBD-PE and Rd-PE were added at 1.5 mole % of the total lipid.

After addition of materials to be encapsulated, SM-2 Biobeads (30-50 mg) were added to absorb the detergent and the solution was shaken at room temperature for 4 hours. Thirty to fifty milligrams of additional SM-2 biobeads and 30 to 50 µl of 160 mM NaCl/10 mM Hepes solution were then added. The sample was shaken at room temperature for 12-14 hours. The solution was removed from the beads with a Hamilton syringe and the beads were washed three times with the high salt buffer. The RSVE were pelleted by ultracentrifugation and resuspended in PBS.

Fluorescent Fusion Assay

The RSVE were labeled with the resonance energy transfer probes NBD/Rd, described previously (see Chapter 2; Struck et al., 1981), and fluorescent fusion assays were conducted to determine if the reconstituted vesicles retained the fusogenic activity of native viral particles and to determine if the RSVE were able to fuse with target cell lines. In brief, labeled virus were mixed with target cells in a 37° cuvette in a SLM 4800 fluorimeter. The emission of the NBD at 530 nm was monitored continuously while exciting at 470 nm. An increase in NBD fluorescence occurs upon viral fusion due to the diffusion of the fluorescent probes into the membrane of the target cell which reduces energy transfer from the NBD to the Rd. The % of the virus which have dequenched can be determined continually upon mixing of virus and target lipids.

DNAase digestion

Non encapsulated DNA was removed by DNAase digestion. Samples were adjusted to 5 mM $MgCl_2$ and DNAase was added to 20 µg/ml.

Samples were incubated at 37°for one hour. Digestion was stopped by addition of EDTA to 10 mM.

Gel Electrophoresis

To prepare the encapsulated DNA for electrophoresis, both DNAase treated vesicles and untreated vesicles were disrupted with .5% SDS. The samples were treated with .1 μg of Protease K for 6 to 20 hours at 37° to digest viral and added proteins. To remove digested protein, samples were phenol extracted twice, chloroform extracted once, and ether extracted. The DNA was precipitated overnight at -70° with 10% volume sodium acetate and 200% volume ethanol. After pelleting the DNA and drying in a spin vacuum centrifuge, the DNA was resuspended in TBE with bromophenol blue dye.

Standard 1% agarose slab gels were run on the samples with ethidium bromide staining. Photographs were taken and band intensities measured by a LKB scanning densitometer. The peak areas in the densitometry scans were measured by hand.

Light Scattering Size Measurements

A Malvern 4700c photon correlation spectrometer was used to measure the virus size. The system is equipped with a 488 nm tuned 3 watt Spectra-Physics 2020 laser attached to an IBM compatible PC with Malvern software. Most measurements were made at 90° to the beam with no size bias and maximal modal distribution parameters. Measurements at other angles were made to check for any major amplitude variations. In some instances

size bias parameters were inserted after initial data collection to further clarify size distributions.

Cell Extract Preparation and Luciferase Assays

The cells to be transfected were incubated with loaded RSVE for 30 minutes at 37°C in PBS. The cells were then grown for several days. Cell extracts were prepared by thrice washing the cells with PBS (no Ca or Mg), adding 1 ml of extraction buffer (0.1 M KPO_4, 1 mM DTT, pH 7.8) to each 10 cm^2 region of cells and then scraping the cells from the surface into an eppendorf tube. Cells were pelleted at 4° C for 2 minute in an eppendorf centrifuge. Suspension cells were simply pelleted. The cell pellet was resuspended in .1 ml of extraction buffer, vortexed, and freeze-thawed three times from 37° C into liquid nitrogen and back again. The extracts were centrifuged for 5 minutes in a eppendorf centrifuge (4° C) and the supernatant was used for a luciferase assay.

Balb c mice were injected with loaded RSVE intravenously in the tail vein or intraperitoneally. The animals were sacrificed and the tissues frozen in liquid nitrogen. For luciferase experiments with animal tissue the tissue was ground in a dounce homogenizer in the presence of .5 ml extraction buffer and the cell debris was pelleted from the cytoplasm extract by centrifugation.

For a measurement of luciferase activity 10-25 µl of cell extract were mixed with 330 µl of glycylglycine buffer (25 mM glycylglycine pH 7.8, 15 mM $MgSO_4$) and 20 µl of 100 mM ATP. The sample was placed in the luminometer and 100 µl of 1 mM luciferin were injected at the start of a

measurement. In general, 30 second integrations of the photon output were recorded.

RESULTS

Encapsulation of naked DNA is low

In our initial experiments, ^{32}P labeled plasmid DNA was used as reporter of encapsulation. Plasmid loaded RSVE were prepared and treated with DNAase to remove non encapsulated plasmid DNA. A large number of radioactive counts were found associated with the RSVE (see Figure 1). Unfortunately, when these samples were run on agarose gels very little DNA was observed (<1% of the starting material). It is likely that the artificially high counts were given by digested DNA tightly bound to the surface of the RSVE.

This experiment was repeated using various ratios of DNA plasmid to Sendai protein but in all cases the observed encapsulation was less than 1%. An example of one of these experiments is shown in Figure 2. This experiment was performed multiple times as a control for later experiments and did not ever show any encapsulation above 1% plasmid DNA

Polylysine and Lysozyme enhance loading

When DNA was encapsulated along with polylysine or lysozyme a substantial increase in loading was observed. The agarose gels shown in Figures 3a and 3b were quantitatively analyzed for the intensity of bands using densitometry. Reference lanes of set amounts of the plasmid encapsulated were run to establish a calibration curve and the intensities of the samples were compared to this curve. About 3% of the DNA/lysozyme

mixture and 8% of the DNA/polylysine mixture were encapsulated as compared to less than one percent in the naked DNA sample. To determine if the proteins or the vesicles afforded any protection to DNA not in the interior of the RSVE, control digestion experiments were run with preformed RSVE and DNA/protein complexs. These experiments show that virtually no protection was afforded to the whole plasmid, <1% of the starting material was found in the supercoiled, nicked and linear bands. Some protection was afforded to the smaller fragments as evidenced by a long smear in the gel. Naked DNA was completely digested. As a further control DNA was digested in the presence of empty RSVE, in order to determine if RSVE could afford any protection to the DNA. The presence of empty RSVE's made no difference on the DNAase digestion.

Various degrees of efficiency were seen in the encapsulation of the DNA/protein complexes. In general 4 to 10 % of the DNA was found to be encapsulated when complexed with positively charged proteins.

Protamine Loading effects are difficult to quantitate

The positively charged protein protamine was our initial choice as a coencapsulation agent as it might not only serve as a packaging protein for the DNA but also as a transport mechanism to the interior of cells (Weinhaus et al., 1987). Unfortunately protamine was found to afford some protection to whole plasmid, making it very difficult to quantitate the amount of plasmid encapsulated. In control digestion studies with protamine-DNA complexes, linear and nicked circle bands were observed. No supercoiled plasmid was observed in the control digestion. Supercoiled

plasmid was observed in the RSVE encapsulated DNA gel lanes indicating that enhancement of DNA encapsulation was occurring. In Figure 4 approximately 3% of the initial DNA was found inside the vesicles in supercoiled form.

Properties of the Reconstituted vesicles

A summary of the size distribution of the reconstituted vesicles is given in Figure 5. The reconstitution procedure normally produces a bimodal distribution of particles with one set of particles with a mean diameter of about 100 nm and the second set having a diameter of about 300 nm. The addition of DNA/protein complexes to the reconstitution had little effect on the reformation of vesicles, although the number of vesicles in the larger population increased. Some of this size increase may have been due to aggregation of the viral particles. Electron microscopy observation showed that the RSVE were normal in character, covered by the spikelike F and HN proteins.

The activities of the F and HN protein were tested by a fluorescent fusion assay and a hemagglutination assay. Fusion was observed with ghost erythrocytes even when vesicles were loaded with DNA and protamine (Figure 6). Fusion activity did not appear to be affected by the presence of added DNA. Hemagglutination also appeared to be unaffected.

Observation on RSVE interactions with cells

In order to determine if the RSVE were able to deliver their contents to the cells in question a number of different materials were loaded into the vesicles and surveyed for delivery to target cells by fluorescent microscopy.

RSVE labeled with NBD-PE and Rd-PE lipid probes were observed to be bound to HL60 cells with both punctilate and diffuse fluorescence on the cell surface. Some signs of receptor "capping" were observed, with bound virus preferentially accumulated at one end of the cells. Cells treated with trypsin were still able to bind RSVE.

RSVE loaded with ethidium bromide were added to cells and observed under a fluorescent microscope. No direct observation of EtBr was possible; this may have been partially due to a high background fluorescence and improper excitation of the EtBr. However, the cells were all dead within 24 hours, providing some evidence for delivery of the EtBr to the cell interiors.

RSVE loaded with carboxyfluorescein aqueous probe were added to cells and a diffuse fluorescence was observed in the interior of the HL60 cells, although this fluorescence was photobleached more rapidly than it could be recorded by photography. RSVE loaded with trypan blue and a EtBr/DNA complex were added to cells but no observation of these contents markers was made in the cell interiors.

Transfection experiments with the reconstituted vesicles

With some evidence that the RSVE were able to interact with the HL60 cells, transfection experiments were conducted in order to determine the efficiency of the RSVE as carriers of DNA into the cells. Plasmids with the luciferase gene under various promotors were loaded into RSVE vesicles and the vesicles were allowed to interact with HL60, U937 and Cos cells. The luciferase gene product can be detected by mixing cellular extracts with luciferin and ATP, the resulting reaction producing light photons (em ≈ 560 nm)(DeWet et al., 1987),

luciferase + luciferin + ATP $\longleftrightarrow$ luciferase•luciferyl-AMP +PP_i

luciferase•luciferyl-AMP + O_2 $\rightarrow$ luciferase + oxyluciferin + AMP + CO_2 + hv.

Previous attempts to transfect HL60 cells with calcium phosphate, electroporation, and DOTMA (lipofection) have been unsuccessful (T. Amatruda, personal communication).

Four promotors were used, an early promotor from the SV40 virus (SV40 or SV2), a Rous sarcoma virus promotor (RSV), and two early promotors from cytomegalovirus (CMV and CDM).

Under no circumstances was transfection of the HL60 or U937 cells observed with the loaded RSVE (see Figures 7a-e). In one experiment (Figure 7b) a southern blot analysis was performed on nuclear extracts prepared from the HL60 and Cos cells in order to look for the presence of plasmid in the cellular nucleus (gel not shown). A small amount of plasmid material was present in all of the nuclear extracts from the Cos cells

with the uncomplexed DNA appearing to be the least degraded. Large amounts of DNA, much of it degraded, appeared in the HL60 cell nuclei for the RSVE where the DNA was complexed with polylysine or protamine. No DNA was apparent in the nuclei of the HL60 cells where naked DNA was delivered to the cell. It should be noted that the procedures for preparation of nuclear extracts are not very clean and material stuck to the surface of the nucleus or the cell could contaminate the preparation.

The Cos cells were consistently transfected. In general DNA complexed with protamine gave higher transfection then naked DNA (Figures 7c and 7d). Some inconsistency was observed in the transfection efficiencies from experiment to experiment, and in one anomalous result a large amount of expression was seen with the naked DNA loaded into the RSVE (Figure 7b). When compared to electroporation for efficiency of transfection, the RSVE were one to two orders of magnitude less efficient then the transfection with electroporation (Figure 7c,e). In terms of promotor efficiency in expression in the COS cells, the following order of activity was observed: CDM > SV40 > CMV, RSV.

DISCUSSION AND CONCLUSIONS

Theoretical encapsulation

A range of reconstituted vesicle sizes from 150 to 400 nm in diameter was observed. For a reconstituted vesicle having a diameter of 200 nm, 4/3 $\pi \times 10^{-21}$ m^3 of volume is encapsulated (3.37 times this value for a 300 nm diameter). The volume used in a typical reconstitution is 1×10^{-7} m^3 with 1.3×10^{12} reconstituted particles being formed. Thus approximately 5.4 % of the volume is encapsulated by the particles (18% for 300 nm particles). For a small neutral particle this is the amount of material we would expect to encapsulate.

A number of methods can be used to estimate the size of the plasmids used in these experiments. For a 5000 bp plasmid(n=5000) a maximum radius of 850 nm for a rigid rod conformation (.34 nm (L) per base pair) can be calculated. As a rigid circle this radius is reduced to 283 nm. If the DNA is treated as a neutral totally flexible random coil the radius can be determined using the formulas,

$$Rg = \frac{(\sqrt{n} \times L)}{\sqrt{6}}$$

or

$$Rg = \frac{(\sqrt{n} \times L)}{\sqrt{3}},$$

which give radiuses of 9.85 and 13.88 nm, respectively.

A more realistic analysis of DNA plasmid size uses the persistence length, a measure of flexibility for large macromolecules. This parameter, b, is about 70 nm for normal B form DNA. For a linear length of DNA,

$$\sqrt{\langle h^2 \rangle} = \sqrt{L \times b}$$

$$Rg = \frac{\sqrt{\langle h^2 \rangle}}{\sqrt{6}},$$

which gives a radius of 140 nm. The radius of a relaxed circular plasmid can be estimated to be this amount divided by the $\sqrt{2}$ to give a radius of 100 nm. To compare the radius of a piece of relaxed circle DNA versus a piece supercoiled DNA the centrifugation diffusion constants (S) of the respective forms can be compared where

$$Rg \propto \frac{1}{S_{cent}}.$$

For SV40 DNA the relaxed circle has a S value of 16.5 versus 21 for supercoiled (Bauer and Vinograd, 1968). Thus the supercoiled plasmid should have a radius 1.27 times smaller than the nicked circle, giving a value of 80 nm for a 5000 bp plasmid.

This calculation indicates that the plasmid DNA is comparable in radius to the radius of the reconstituted virus envelope (DNA radius of 140 nm, 100nm, and 80 nm for linear, nicked circle, and supercoiled respectively versus reconstituted virus envelope radius of 75-200 nm).

The native virus encloses a number of proteins and a 15,000 nucleotide single stranded RNA.

Effects of charge repulsion, condensation

The addition of basic proteins during reconstitution was effective in enhancing encapsulation. The proteins may have served to reduce electrostatic repulsion of the DNA from the Sendai lipids and proteins, in general the presence of phosphatidyl serine in natural bilayers gives them a net negative charge at neutral pH. In addition, the basic proteins may have reduced internal DNA repulsion and resulted in a condensation of the plasmid DNA into a more compact package. Packaging of chromosomal DNA is accomplished by the presence of positively charged histone proteins.

Literature reports on encapsulation

A number of other workers have loaded nucleic acids into RSVE. In general no quantitation of the amount of encapsulated material was undertaken. In several cases radiolabeled DNA was used as an indicator of encapsulated material, leading to a false reportation of the efficiency of encapsulation. In two cases, gel electrophoresis evidence was published within a paper that contradicted data on encapsulation determined by radiolabeled DNA given within the same paper.

In the first paper (Vainstein et al., 1983), rates of encapsulation of 6.5% (pBR322), 5.5% (pBR322) and 2% (pMB9) for ratios of DNA to protein (μg/mg) of 4, 10 and 10, respectively, were determined using ^{3}H DNA as a tracer. Gel electrophoresis of the recovered product from DNA digestion of 150 μg of pTKx1 DNA loaded into 10 μg of Sendai is shown next to a control

lane containing 3 μg pTKx1 DNA. A loading efficiency of 5% should be equivalent to 3 μg of encapsulated DNA being loaded onto the gel (the same as the control lane). However, virtually no DNA was visible in the lane to which the reconstituted encapsulated product was added, as compared to the control lane.

A similar observation was made in the second paper (Loyter et al., 1983). Encapsulation rates up to 10% are reported at ratios of 10 μg SV40-DNA to 1 mg Sendai protein. For ratios of 40 μg of SV40-DNA to 1 mg Sendai protein rates of encapsulation of 2-4% are reported by ^{3}H radiolabeled DNA digested with DNAase. The encapsulated product was run on gel electrophoresis next to a control lane containing 1 μg of SV-40 DNA and appears much fainter in intensity. For the materials started with, 120 μg DNA with 3 mg Sendai, one would expect a much brighter band of 2.4-4.8 μg of encapsulated DNA to appear on the gel given the 2-4% encapsulation rate.

These literature data support my observations that radiolabeled DNA can overreport the amount of material trapped by RSVE.

HL60 Cells and Transfection

The HL60 cell line is derived from a promyelocytic leukemia and proliferates continually in suspension tissue culture (unlike other isolated myeloid leukemia cells). The HL60 cell is essentially a myeloid cell which is arrested in its differentiation to mature cell type and transformed into a cancerous cell. Of significant experimental interest is the ability of these cells to differentiate into mature cell types upon the addition of external

stimulating factors (Collins, 1987). These cells can differentiate into granulocytes (neutrophils), monocytes, macrophage-like cells and eosinophils. See Table 1 for a listing of the factors that induce this differentiation. Thus, these cells serve as a model system for hematopoietic differentiation and gene regulation as well as a model for leukemia cells. As transformed cells, they also provide information on the mechanisms by which oncogenes control cellular division.

Insertion of exogenous genes could provide a number of insights into cellular control of gene expression and differentiation. The expression levels of "neutral" genes with various promotors and enhancers before, during and after differentiation would provide information on the interaction of cellular transcriptional factors with these *cis* acting elements. The effects of increasing or decreasing proteins integral to the differentiation process could also be investigated (Concannon et al., 1985). In our experiments transfection was desired in order to study the effects on the differentiation process of having mutated G proteins in the phospholipase phosphoinositol signalling pathway (Morgan, 1989).

Although there are many interesting possibilities for transfected HL60 cells, there are virtually no references to gene transfer into these cells in the literature. Our experiments and previous experiments (T. Amatruda) have shown that these cells are particularly refractory to transfection by calcium phosphate, electroporation, lipofection, or reconstituted Sendai viral envelope DNA delivery. There was one literature report of calcium phophate transfection in 1985 but it gave a low yield (2×10^{-5}) and has not been reproducible (Concannon et al., 1985). There is also one meeting

abstract on electroporation of these cells, but the abstract does not give any information on the success rate of transfection (Ikeda et al., 1988)

There is one significant report of retroviral gene transfer in the literature by the discoverer of HL60 cells, Steve Collins, in which he reported that expression in HL60 cells of the retrovirus N2 was low compared to other hematopoietic cell lines (30-40% in K562 cells versus <5% in KG-1 and HL-60 cells)(Collins, 1988a). Southern blots analysis showed virtually no viral DNA was present in the HL60 cells in unintegrated form (24 hours post infection) or integrated form (5 days post infection). In contrast the KG-1 cells contained unintegrated but no integrated DNA, while the K562 contained unintegrated and integrated DNA. Collins suggests three mechanisms for this: 1) the presence of relatively few retrovirus receptors on the HL60 cell surface, 2) inhibition of reverse transcriptase, or 3) enhanced degradation of unintegrated DNA. In an accompanying paper Collins showed that those HL60 cells which were transfected showed enhanced transcription of retroviral mRNA when the cells were stimulated to differentiate (Collins,1988b). No further investigations have been made into the mechanism of resistance (S. Collins, personal communication).

In our experiments there appear to be receptors for viral interaction with the cells and DNA is delivered directly to the cells, eliminating the requirement for any reverse transcriptase activity. A cellular DNAase activity could be responsible for the expression resistance or the promotor sequences used in our plasmids may not be active in these cells. It is interesting to note that in the southern blot experiment done on cell nuclei

after RSVE transfection, protected DNA (protamine associated) was found in the cellular nucleus but no unprotected DNA was observed.

Conclusions

Under normal Triton X-100 reconstitution conditions the encapsulation of DNA is very low, <1%. Radiolabeled DNA does not give valid encapsulation values when compared to direct gel analysis.

Polylysine and lysozyme greatly increase the amount of encapsulated material to between 3 and 10%. This amount of encapsulated material is approximately equivalent to the amount one would expect to find for the encapsulation of a small, neutral molecule. The enhancement in encapsulation may be due to a charge neutralization of the DNA and a condensation of the mean size of the DNA. The protein/DNA complex may also serve as a site of formation for the reconstituted virus, similar to the process of viral budding from the cell.

Protamine may also enhance encapsulation but quantitization was difficult. Protamine partially protected the DNA from digestion. Protamine does not appear to protect supercoiled plasmid from nicking and supercoiled material was observed in the RSVE/DNA/Protamine samples.

Transfection was feasible using the reconstituted virus with luciferase protein being expressed in Cos cells. The efficiency of transfection was no better than already available techniques. No expression was observed in HL60 cells. Experimental evidence supports a hypothesis that material can be delivered to the cells but is not expressed due to an unknown resistance mechanism.

REFERENCES

Bauer, W., and Vinograd, J. (1968) The Interaction of Closed Circular DNA with Intercalative Dyes. *J. Mol. Biol.*, **33**, 141-171.

Concannon, P., Teraoka, S., Nelson, R., and Salser, W. (1985) "HL-60 cells regulate the expression of Transfected genes during in vitro cellular differentiation." from Leukemia: Recent Advances in Biology, UCLA Symposia on Molecular and Cellular Biology, New Series, volume 28, 73-89.

Collins, S. (1987) The HL-60 Promyelocytic Leukemia Cell Line: Proliferation, Differentiation and Cellular Oncogene Expression. *Blood*, **70**, 1233-1244.

Collins, S. (1988a) Different Mechanisms Account for the Relative Resistance of KG-1 and HL-60 Cell Lines to Retrovirus Infection. *J. Virol.*, **62**, 4346-4348.

Collins, S. (1988b) Retinoic Acid-Induced Differentiation of Retrovirus-Infected HL-60 Cells Is Associated with Enhanced Transcription from the Viral Long Terminal Repeat. *J. Virol.*, **62**, 4346-4352.

DeWet, J., Wood, K., DeLuca, M., Helinski, D., and Subramani, S. (1987) Firefly Luciferase Gene: Structure and Expression in Mammalian Cells. *Molecular and Cellular Biology*, **7**, 725-737.

Gad, A., Bental, M., Elyashiv, G., and Weinburg, H. (1985) *Biochemistry*, **24**, 6277-6282.

Gunter, K., Gunter, T., Jarkowski, A. and Rosier, R. (1982) A Method of Resuspending Small Vesicles Separated from Suspension by Protamine Aggregation and Centrifugation. *Analytical Biochemistry*, **120**, 113-124.

Ikeda, K., Sasaki, K., Nagai, M., and Irino, S. (1988) Introduction of pSV2-Neo Gene into HL60 Cells by Electroporation. *Exp. Hematol.*, **16**, 507.

Jay, D., and Gilbert, W. (1987) Basic protein enhances the incorporation of DNA into lipid vesicles: Model for the formation of primordial cells. *Proc. Natl. Acad. Sci. USA*, **84**, 1978-1980.

Loyter, A., Vainstein, A., Graessmann, M., and Graesmann, A. (1983) Fusion-Mediated Injection of SV40-DNA. *Experimental Cell Research*, **143**, 415-425.

Loyter, A., and Volsky, D. (1982) Reconstituted Sendai virus envelopes as carriers for the introduction of biological material into animal cells. *from* Membrane Reconstitution, eds. Poste, G. & Nicolson, G., Elsevier Biomedical Press, 215-266.

Morgan, N. (1989) "Guanine-nucleoside binding proteins as signal transducers" from Cell Signalling, The Guilford Press, 35-54.

Struck, D., Hoekstra, D., and Pagano, R. (1981) Use of Resonance Energy Transfer To Monitor Membrane Fusion. *Biochemistry*, **20**, 4093-4099.

Vainstein, A., Hershkovitz, M., Isreal, S., Rabin, S., and Loyter, A. (1984) A New Method for Reconstitution of Highly Fusogenic Sendai Virus Envelopes. *Biochimica et Biophysica Acta*, **773**, 181-188.

Vainstein, A., Razin, A., Graessmann, A., and Loyter, A. (1983) Fusogenic Reconstituted Sendai Virus Envelopes as a Vehicle for Introducing DNA into Viable Mammalian Cells. *Methods in Enzymology*, **101**, 492-512.

Wienhaus, U., Hosokawa, K., Hoveler, A., Siegmann, B., and Doerfler, W. (1987) A Novel Method for Transfection and Expression of Reconstituted DNA-Protein Complexes in Eukaryotic Cells. *DNA*, **6**, 81-89.

FIGURES

Note- For those who are not familiar with agarose gel electrophoresis, this technique is used to separate large pieces of nucleic acids. In terms of mobility in the gel media of equal length pieces of DNA, supercoiled DNA travels most rapidly, due to its compact structure, while linear DNA travels second in speed and nicked circle travels the slowest, as the linear material is more able to "snake" through the gel matrix than the nicked circular material. A control "ladder" of digested material can be run to determine fragment length for linear pieces, our control ladder consisted of lambda DNA cut by HindIII restriction endonuclease giving fragments of 23 kb, 9.4 kb, 6.6 kb, 4.4 kb, 2.3 kb, 2 kb, .6 kb, and .1 kb.

Figure 1- Radiolabeled DNA is a poor reporter of encapsulation

^{32}P labeled DNA was used as a reporter of encapsulation. RSVE were prepared and treated with DNAase as in methods. No coencapsulation proteins were used in these experiments.

Exp. 1, 2, 3: 1.2 mg Sendai virus protein, ^{32}P DNA (1.45×10^6 cpm)

Exp 1: 1 μg sheared salmon sperm DNA

Exp 2: 10 μg sheared salmon sperm DNA

Exp 3: 40 μg sheared salmon sperm DNA

Exp. 4: 3 mg Sendai, 40 μg RSVL plasmid DNA (≈5000 basepairs)

Recovery of ^{32}P DNA

	BioBeads	Wash	DNAase	Wash	RSVE	Total
exp 1	439722	51450	12000	5850	609200 **(54%)**	1118000 (77%)
exp 2	733028	11500	24760	8010	348720 **(31%)**	1125000 (77%)
exp 3	664425	33600	75780	14130	607200 **(44%)**	1392000 (96%)

These numbers seemed quite high (17.6 μg in exp. 3). An agarose gel was run (Figure 1a) on the samples to visually confirm these numbers.

Lane 1- 30 ng SV_2Lux DNA

Lane 2- 500 ng SV_2Lux DNA

Lane 3- 4% RSVE

Lane 4- 10% RSVE

Lane 5- Other Samples (DRV's)

Lane 6- Other Sample (DRV's)

Lane 7&8- Empty

Unfortunately, very little of the DNA was encapsulated. The DNAased material most likely can bind to the RSVE, giving artificially high encapsulation numbers with the radiolabeled DNA.

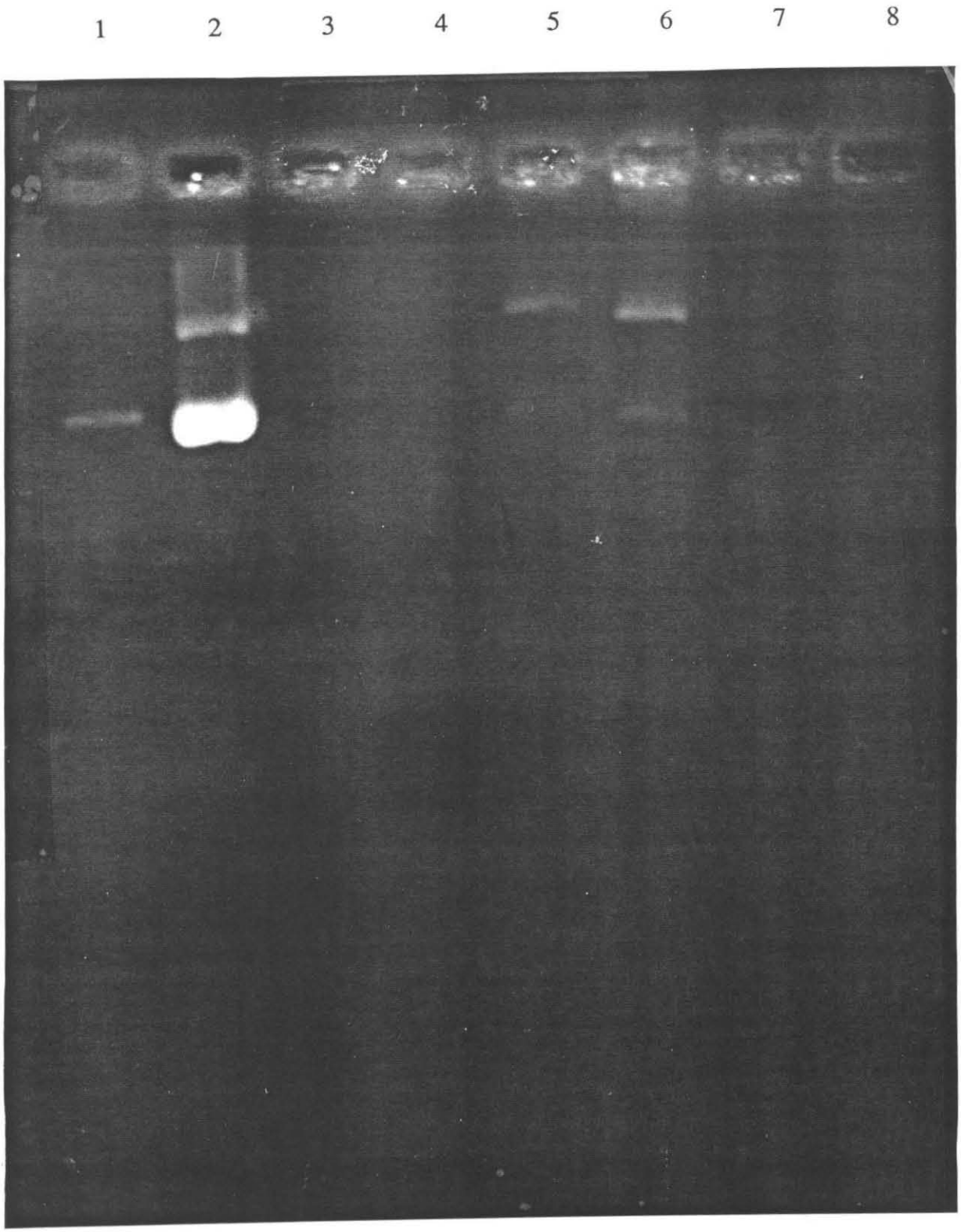
1
2
3
4
5
6
7
8

Figure 2- Normal Encapsulation of DNA is very low

Multiple experiments confirmed that little DNA was loaded into the vesicles using the general procedure. The data from such an experiment is shown below.

1.2 mg of Sendai starting protein was reconstituted with 10 μg, 30 μg, and 50 μg plasmid DNA (4 kilobases). 80% of the RSVE samples were treated with DNAase.

Lanes 1-6: other Samples

Lane 7: 100 ng Plasmid

Lane 8: 250 ng Plasmid

Lane 9: 1 μg Plasmid

Lane 10: 5 μg Plasmid

Lane 11: 20% 10 μg DNA/RSVE

Lane 12: 20% 30 μg DNA/RSVE

Lane 13: 20% 50 μg DNA/RSVE

Lane 14: 64% 10 μg DNA/RSVE +DNAase

Lane 15: 64% 30 μg DNA/RSVE +DNAase ≈250 ng (≈1%)

Lane 16: 64% 50 μg DNA/RSVE +DNAase ≈350 ng (≈1%)

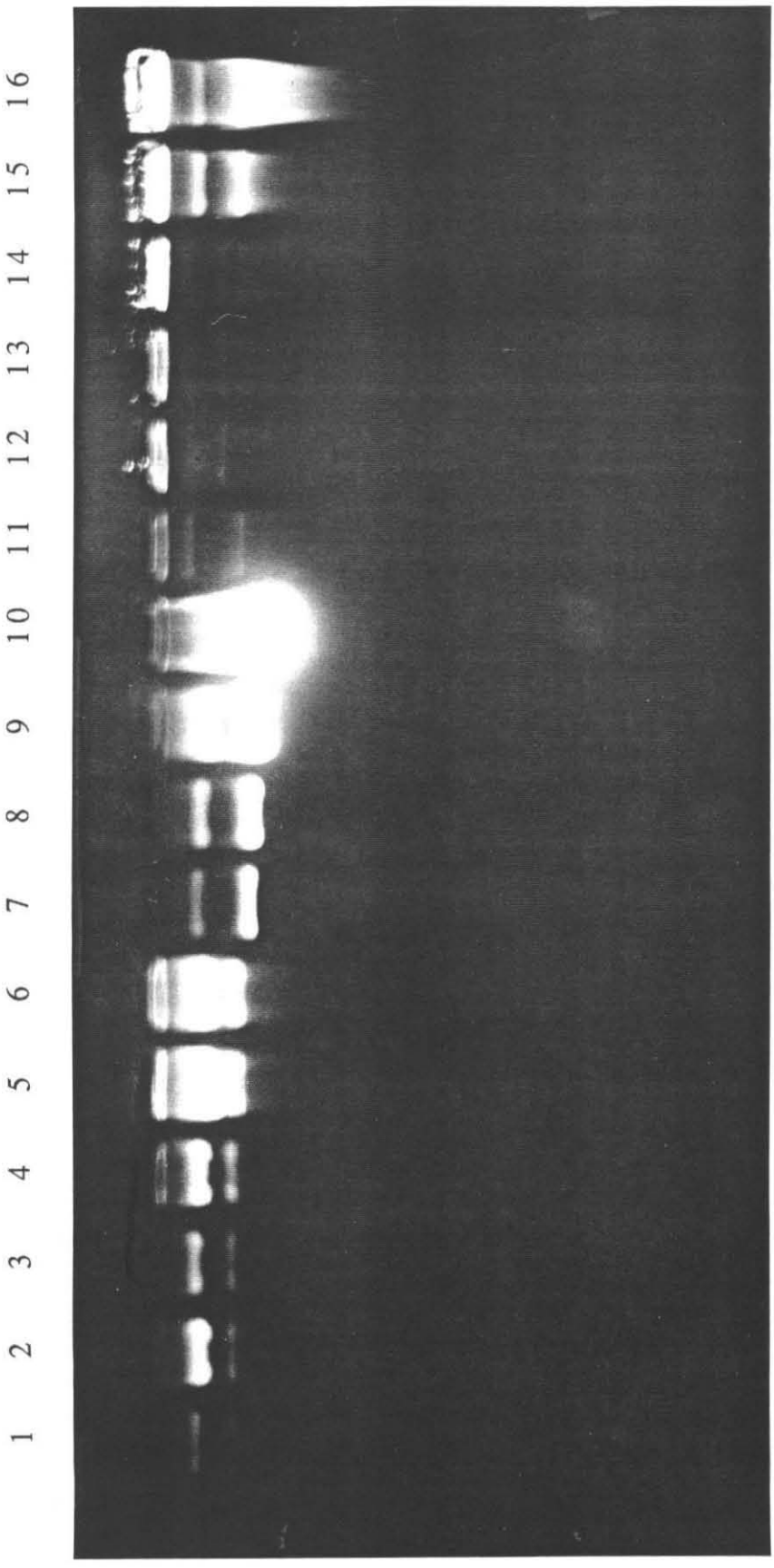
1 2 3 4 5 6 7 8 9 10 11 12 13 14 15 16

Figure 3- Polylysine and lysozyme enhance loading

a) 3.6 μg of HE6 DNA (about 5000 bp) and .75 mg Sendai Protein were used in the reconstitution experiments.

Reconstituted vesicles were prepared and DNAased as in methods. The encapsulation experiments used plain DNA, DNA plus 32 μg lysozyme, and DNA plus 20 μg polylysine.

Three experiments were conducted as controls of DNAase activity and lack of protein protection from such activity. DNAase digestion control experiments were conducted with .8 μg DNA and 250 μg of preformed RSVE in the presence of 20 μg lysozyme, 5 μg polylysine, or nothing.

Densitometry

Lane 1: 400 ng HE 6 Plasmid	
Lane 2: 40 ng HE6 Plasmid	
Lane 3: Lysozyme/DNA RSVE + DNAase	100 ng **(3.1%)**
Lane 4: Polylysine/DNA RSVE + DNAase	260 ng **(8.1%)**
Lane 5: Plain/DNA RSVE + DNAase	<10 ng
Lane 6: DNA/Lysozyme+DNAase	≈10 ng (1.2%)
Lane 7: DNA/Polylysine+DNAase	≈10 ng (1.2%)
Lane 8: DNA + DNAase	<10 ng
Lane 9: 100 ng HE6	
Lane 10: 10 ng HE6	
Lane 11: 200 ng HE6	
Lane 12: HindIII Lambda Ladder	

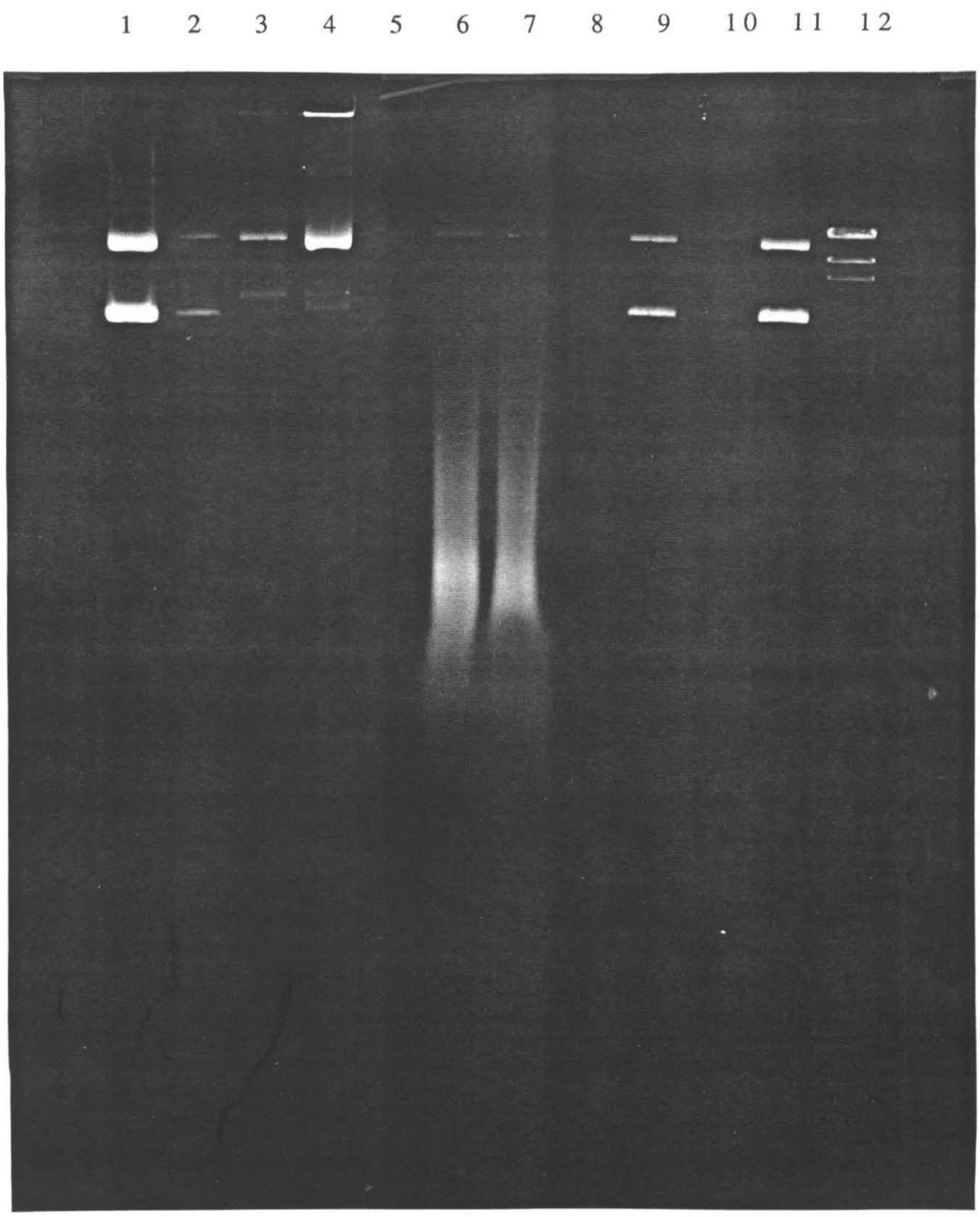
1 2 3 4 5 6 7 8 9 10 11 12

b) 5 μg of HE6 DNA (about 500 bp) and .78 mg Sendai Protein were used in the reconstitution experiments.

Reconstituted vesicles were prepared and DNAased as in methods. The encapsulation experiments used plain DNA, DNA plus 50 μg lysozyme, and DNA plus 20 μg polylysine.

Three experiments were conducted as controls of DNAase activity and lack of protein protection from such activity. DNAase control experiments were run with 2 μg DNA and 250 μg of preformed RSVE in the presence of 20 μg lysozyme, 8 μg polylysine, or nothing.

Densitometry

Lane 1: 400 ng HE 6 Plasmid	
Lane 2: 80 ng HE6 Plasmid	
Lane 3: 20% Lysozyme/DNA RSVE	
Lane 4: 20% Polylysine/DNA RSVE	
Lane 5: 20% Plain/DNA RSVE	
Lane 6: Hind III Ladder	
Lane 7: 80% DNA/Polylysine RSVE +DNAase	150 ng **(3.75%)**
Lane 8: 80% DNA RSVE+ DNAase	<10 ng (<.1%)
Lane 9: 80% DNA Lysozyme+ DNAase	260 ng **(6.5%)**
Lane 10: Polylysine/DNA + DNAase	<10 ng (<.5%)
Lane 11: Lysozyme/DNA + DNAase	<10 ng (<.5%)
Lane 12: DNA + DNAase	≈0
Lane 13: 40 ng HE6	
Lane 14: 10 ng HE6	
Lane 15: 800 ng HE6	

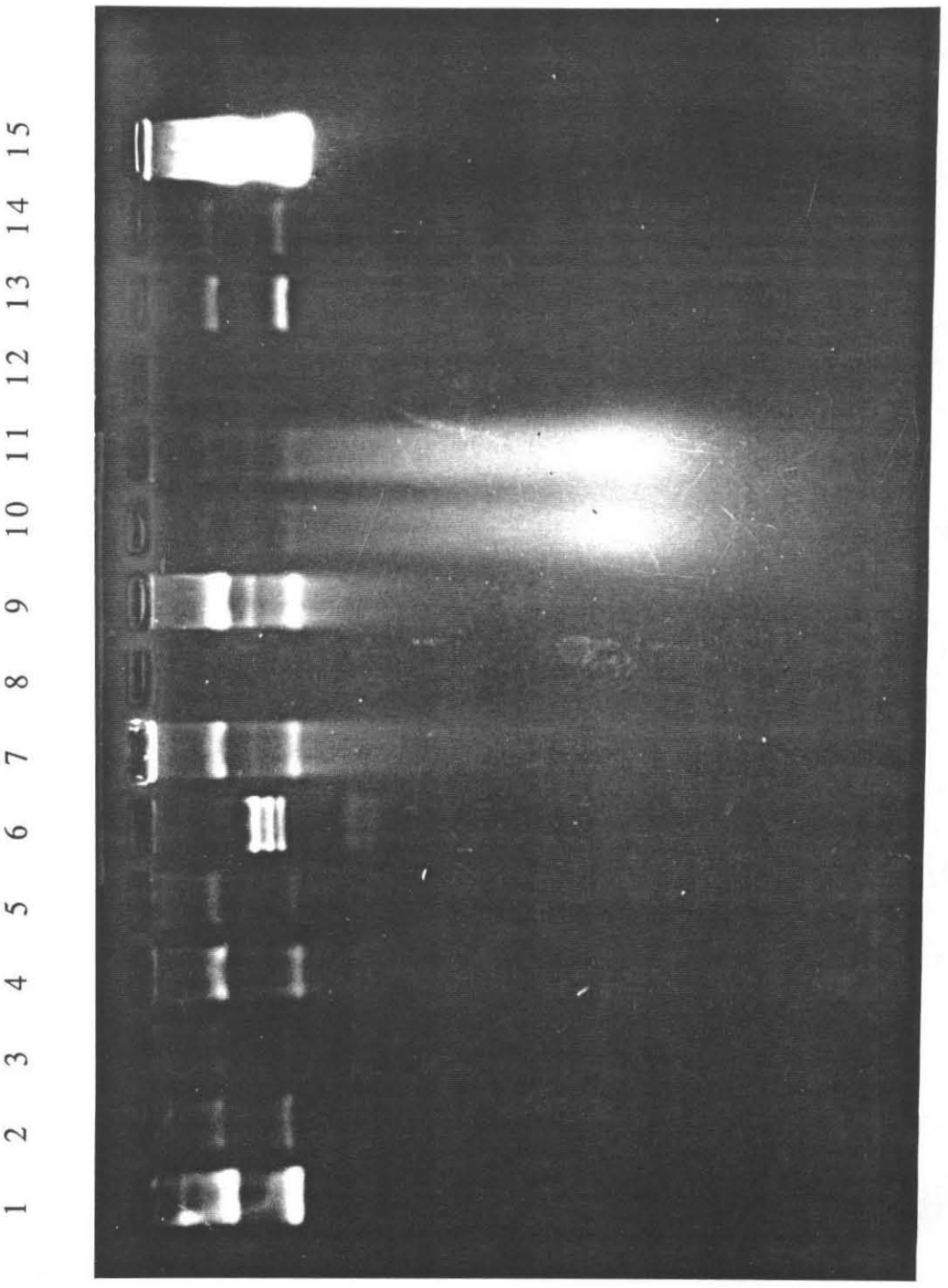
1 2 3 4 5 6 7 8 9 10 11 12 13 14 15

Figure 4- Protamine loading effects difficult to determine

Protamine was the first protein used in this study, mainly due to its ability to enhance transport of DNA into the nucleus. Protamine may enhance DNA loading but the loading is difficult to assay as protamine protects the DNA from digestion.

10 μg of Plasmid DNA (≈5000 basepairs) was loaded into vesicles formed from .77 mg Sendai virus starting protein. 100 μg of protamine or lysozyme were used. For control lanes, 4 μg of DNA and 40 μg of protamine or lysozyme were digested with DNAase.

Gel Lanes	Protected DNA
Lane 1: 80 ng HE6 Plasmid	
Lane 2: 100 ng HE6 Plasmid	
Lane 3: 200 ng HE6 Plasmid	
Lane 4: 50% Protamine/DNA RSVE + DNAase	SuCoil 163 ng **(3.2%)**
	Total 711 ng **(14%)**
Lane 5: 50% Protamine/DNA + DNAase	SuCoil **0**
	Total 569 ng **(28.4%)**
Lane 6: 50% Lysozyme/DNA + DNAase	«10 ng
Lane 7: 50% Lysozyme/DNA RSVE + DNAase	396 ng (7.9%)
Lane 8: 10 ng HE6 Plasmid	
Lane 9: 400 ng HE6 Plasmid	
Lane 10: 20 ng HE 6 Plasmid	
Lane 11: HindIII Ladder	

SuCoil = Supercoiled

A large band of supercoiled plasmid is seen in the protamine RSVE lane which may indicate some enhancement of encapsulation as the protamine appears to give little protection to supercoiled DNA. However, the protamine protects nicked circle and linear DNA from digestion, preventing any quantitative analysis of DNA encapsulation by this DNAase digestion method. ^{32}P labeled DNA was again used in this experiment and showed association of 50%, 28% and 16% (Protamine, Lysozyme, Plain) of the DNA with the RSVE.

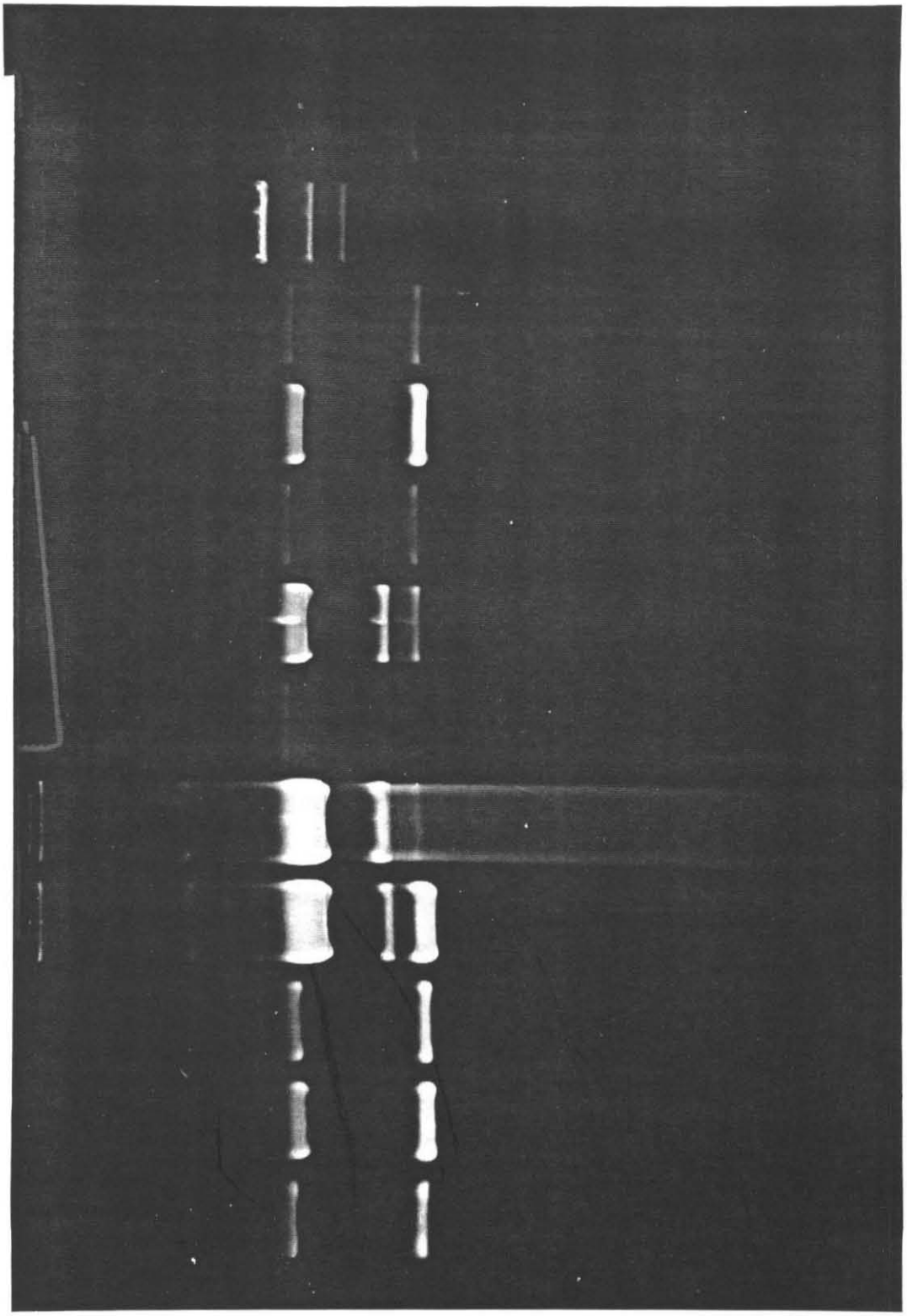
1
2
3
4
5
6
7
8
9
10
11

Figure 5- Size Distribution of RSVE

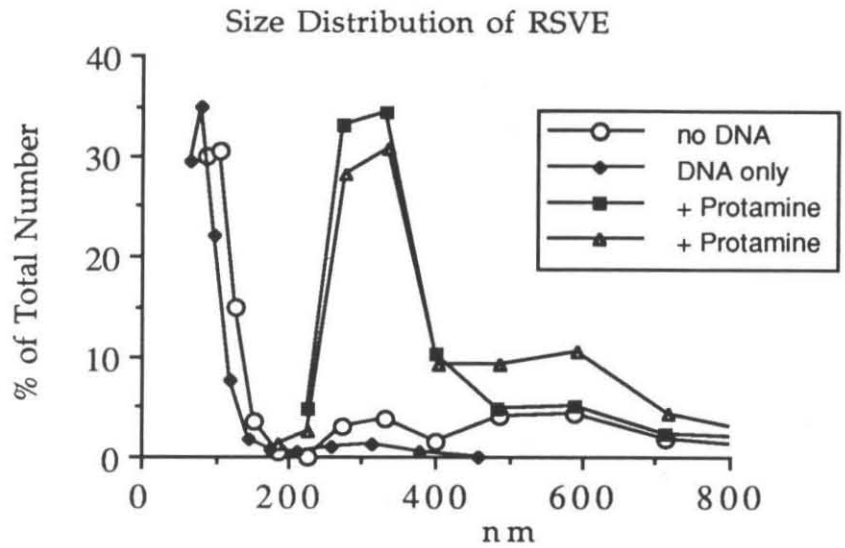

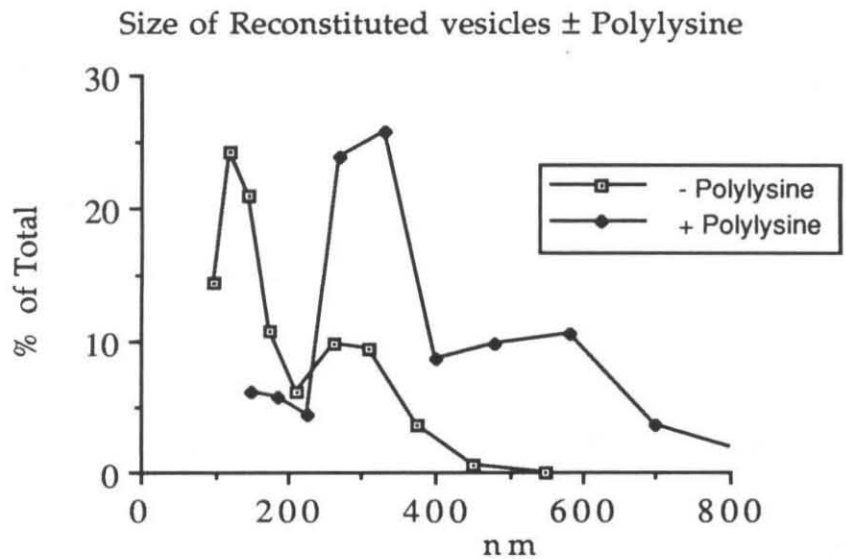

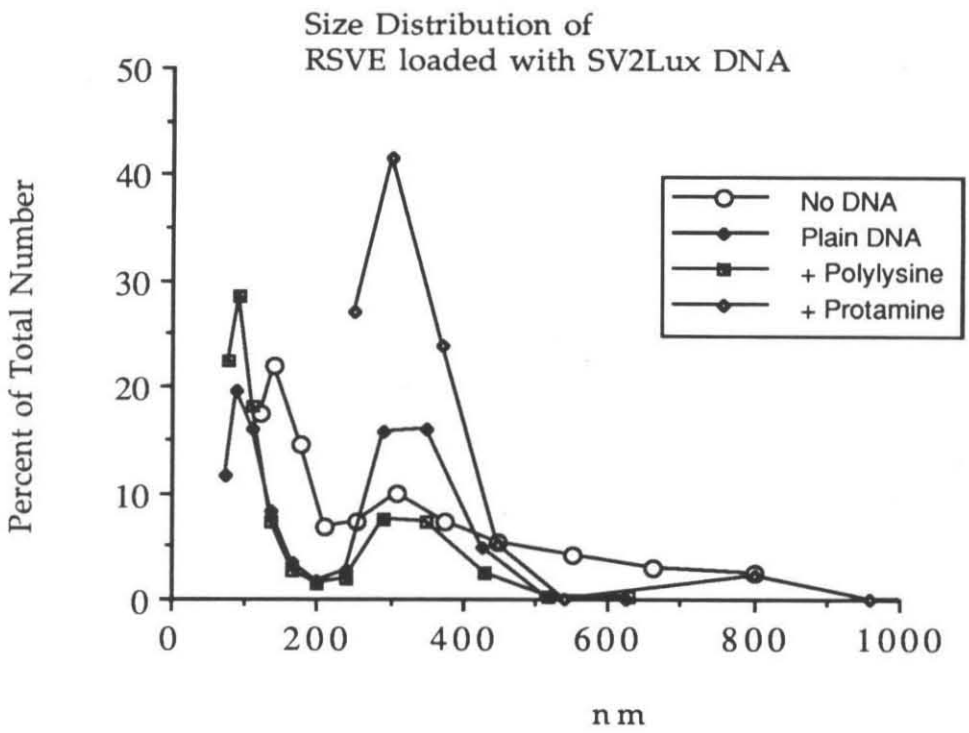
Size Distribution of
RSVE loaded with SV2Lux DNA
Percent of Total Number
50
40
30
20
10
0
0
200
400
600
800
1000
nm
No DNA
Plain DNA
+ Polylysine
+ Protamine

Figure 6- Summary of some fluorescent fusion experiments

Probe	RSVE/Ghost (µg)	t (sec)	%Dequenching	RSVE Contents*
NBD/Rd	5/ 1.5x10^{6}†	2000	4	pDNA
NBD/Rd	5/ 80	1000	4.8	pDNA
NBD/Rd	5/ 80	1000	5.5	pDNA
6% Rd	6/ 80	1000	2.6	
6% Rd	3/ 80	1000	4.0	
6% Rd	6/ 160	1000	3.8	
NBD/Rd	6/ 200	1000	2.7	pDNA
NBD/Rd	3.6/ 200	1000	2.9	pDNA
		30,000	16.3	
NBD/Rd	6/ 50	25,000	8.6	pDNA
NBD/Rd	7.2/ 40	3600	22.4	pDNA+protamine
NBD/Rd	7.2/ 80	3600	16.3	pDNA+protamine

* pDNA = plasmid DNA

† CV-1 cells rather than ghosts

Hemagglutination

RSVE without DNA/Protamine	>25,600 HAU/ml	>172 HAU/ µg protein
RSVE with DNA/Protamine	>25,600 HAU/ml	>70 HAU/ µg protein

Figure 7- Survival and Transfection Results

(a) Experiment 1-

Toxicity and Survival-

Identical loading and transfection experiments were conducted with two plasmids, one containing the luciferase gene under the Rous sarcoma virus (pRSVL) early promotor and the other with the gene under the SV40 early promotor (pSV_2lux). 100 μg of plasmid DNA was loaded into vesicles formed from 5 mg of starting Sendai virus protein with the reconstitution procedure described in methods. An approximate yield of 500 μg protein RSVE was obtained for each reconstitution.

A toxicity experiment was conducted where RSVE were mixed with HL60 cells and counted after one day to determine cell survival.

RSVE (μg)	HL60 Cells	Volume (ml)	Survival (%)
50	10^7	10	90
5	10^6	1	82
10	$5x10^5$	.5	47
10	$5x10^5$	.1	21

Transfection-

Six different preparations of transfected cells were prepared,

	RSVE(μg)	Cells	
Ex. 1-	100	2.0×10^7 HL60 cells	"Low ratio"
Ex. 2-	75	7.5×10^6 HL60 cells	"High ratio"
Ex. 3-	10	7.5×10^5 Cos cells	"Low ratio"
Ex. 4-	20	7.5×10^5 Cos cells	"High ratio"
Ex. 5-	40	7.5×10^5 Cos cells	"High ratio"
Ex. 6-	25	1.3×10^6 Cos cells	"Low ratio"

The "Low ratio" Cos cells were combined together during the processing for the luciferase assay. Top values in the table below are "High ratio" expression and lower values are "Low ratio" values. 25 μl out of 1 ml cell extracts were measured for luciferase activity:

30 second integration	Cos cells	HL60 cells
RSV Promotor	337	107
	664	114
SV40 Promotor	1753	119
	1361	118

A negative control gave a value of 63.

A positive control with a small sample of Cos cells transfected by electroporation gave a value of 2126.

(b) Experiment 2- 10.4 μg of pSV_2Lux DNA were loaded into .5 mg of Sendai virus with the optional addition of 10 μg polylysine or 1 mg protamine. 50 μg of reconstituted protein was added to 10^7 HL60 cells and 20 μg RSVE was added to 2.6 $x10^6$ Cos cells. 25 μl out of 1 ml of the cytoplasm extract was measured for luciferase activity:

30 second integration	Cos Cells	HL60 Cells
Naked DNA	36527	54
+ Polylysine	141	57
+ Protamine	1037	53

A negative control with untransfected Cos cells gave a reading of 53.

A positive control on a small quantity of Cos cells transfected by electroporation gave a reading of 1186.

(c) Experiment 3-

Four experiments were prepared in which 10 μg SV_2Lux DNA was loaded into RSVE,

	Sendai (mg)	Protamine (1 mg)
ex 1.	.35*	√
ex 2.	1	X
ex 3.	1	√
ex 4.	2	√

* Sucrose purified

Cos cells were transfected with these samples. After measuring the luciferase activity in the various samples the activities were normalized for the amount of protein in each sample (the average 25 μl aliquot of cellular extract contained 4-6 μg of protein). The measured activity for 30 μg of protein for 30 seconds,

	Activity
Negative control	85
Electroporated cells	2.3×10^5
ex 1.	726
ex 2.	4812
ex 3.	2663
ex 4.	5100

(d) Experiment 4-

30 μg of SV_2Lux plasmid was loaded into 3.6 mg of Sendai protein with or without 3 mg protamine. 50 μg of the RSVE protein was added to 10^7 HL60 cells or U937 cells. 20 μg of RSVE protein was added to $7x10^5$ Cos cells. 25 μl out of 1 ml cellular extract was measured for luciferase activity with a 10 second integration of released photons. Each of the experiments was performed in duplicate with the following averages being found for expression,

	Cos cells	HL60 cells	U937 cells
Naked DNA	200	14	18
+ Protamine	1600	18	16

A negative control of untransfected Cos cells gave a reading of 16.

A positive control of a small sample of electroporation transfected Cos cells gave an average value of 23,000.

(e) Experiment 5-

Three different plasmids containing different promotors were loaded into RSVE. 21 μg of a plasmid containing the CMV early promotor was loaded into 2.1 μg of Sendai with 200 μg protamine. The same conditions were used for a plasmid containing the Lux gene under the CDM promotor (another CMV promotor). 10 μg of a third plasmid containing the Lux gene under the SV40 early promotor was loaded into .7 mg of Sendai with 66 μg of protamine. 10^7 HL60 cells, 10^7 U937 cells and 6×10^5 Cos cells were transfected with these RSVE. In an additional experiment RNA transcripts coding for the Lux gene were transfected into the cells using Dotma (lipofection). After extracting the cytoplasm from the cells and measuring the amount of luciferase activity (30 sec. integration) in each sample, protein measurements of the samples were made and the samples were normalized for 30 μg of protein. The following values were determined,

	Cos Cells	U937 cells	HL60 cells
Blank	0		
Electroporation	1×10^6		
CMV Pro.	80	0	0
CDM Pro.	11,500	0	0
SV40 Pro.	2400		
RNA, Dotma	600	100	60

Table 1.

Inducers of Differentiation of HL-60 Cells

	Induced Cell Type			
	Granulocyte	Monocyte	Macrophagelike	Eosinophil
Inducing agents	Polar-planer compounds[17]	Vitamin D_3[47-60]	Phorbol esters (TPA)[61,62]	Alkaline media[97]
	Retinoic acid[18]	Na Butyrate[158]	Teleocidin[161,162]	Butyric acid[98]
	Actinomycin D[20]	Lymphocyte-conditioned media[51]		GM-CSF[5]
	Hypoxanthine[20]	DIF[63]		
	Antithymocyte globulin[156]	IFN-γ[48,54-56]		
	Tunicamycin[157]	Tumor necrosis factor[58]		
	6-thioguanine[20]	Ara C[159]		
	L-ethionine[158]	Ara A[160]		

Chapter 7: Conclusions

As separate conclusions were included with each chapter they will not all be repeated here. I will present some of the answers I found to the questions asked in the introduction.

Chapter 2-

How reliable are the available assays for membrane fusion? How can we describe the kinetics of fusion between virus and target cells?

None of the fluorescent assays for membrane fusion are optimal. The definition of membrane fusion determines in part whether the data given by the assays are relevant. Transfer of lipids between adjacent bilayers can occur with or without actual connectivity being established between the internal compartments of the bilayers. The same viral glycoproteins which destabilize a target bilayer allowing a virus to fuse with that bilayer should also catalyze the transfer of lipids between bilayers, due to the hydrophobic domains in these glycoproteins. The exchange of lipids between bilayers is most likely a preliminary step to complete membrane fusion. Therefore fluorescent membrane probe assays are likely to report dequenching (usually interpreted as fusion) even when only exchange is occuring. Contents mixing assays will report fusion long after the membrane continuity between compartments is complete (in addition these content assays are problematic in altering membrane behavior).

Of the two primary probe assays used in this thesis, the R18 fluorescent assay is susceptible to spontaneous transfer of the probe between proximal membranes, but is the only available probe for labeling intact membranes. The NBD/Rd membrane fusion assay system has the advantage of using double chained lipid membrane anchors which are less susceptible to transfer processes. This assay system was used to study fusion when allowed.

Second order bireactant and mass action type kinetic models were both suitable for fitting the dequenching curves given by the interaction of virus with cells. The activity of the virus and the maximum number of sites of interaction of the virus with the cell surface were determined experimentally by studying high virus to cell ratios (to determine saturation of sites) and high cell to virus ratios (to determine viral activity). In general, the assay method used had some effect on the character of the dequenching curve as the curves given by the NBD/Rd assay were of a sigmoidal character and were fit better with the mass action model, while those obtained with the R18 assay were more exponential in character and were fit better with a second order bireactant model. The general rate of reaction for Sendai or mumps virus with a target fusion site was approximately 3×10^9 $M^{-1}sec^{-1}$.

Chapter 3-

What is the optimal detergent for reconstitution? Can one reconstitute functionally active mumps? What happens to reconstituted virus when it is introduced into animal systems?

The products given by octyl glucoside detergent dialysis reconstitution were undesirable as any behavior exhibited by the reconstitute may be attributed to any of the three different reconstituted products, including protein aggregates. Triton X-100 and $C_{12}E_8$ reconstitution products were better defined in size and character and exhibited all the glycoprotein properties of the native mumps and Sendai virus. A maximum fusion activity of ≈30% was found for the reconstituted mumps vesicles, similar to that of the whole mumps virus.

Animal studies with reconstituted Sendai and mumps virus showed that these vesicles acted very similar to liposomes in circulation behavior. Uptake of the "virosomes" occurred primarily in the reticuloendothelial system, i.e., liver and spleen. The uptake of the mumps by the brain of the hamsters was near background blood levels and too near the "noise" level of the assay to draw any conclusive positive results. As an experimental system it was unclear whether the animal model for mumps (newborn Syrian hamsters) had a complete blood brain barrier. The reconstituted vesicles had reasonable stability in serum and good circulation time in the blood.

Chapter 4-

What are the fusion activities and kinetics of the mumps virus? What do these activities tell us about the neurotropism of the virus?

The mumps virus was able to fuse with both erythrocyte ghosts and CV-1 cells, with a temperature optimum of 37° C. The binding site for the virus apparently was sialic acid residues on cellular gangliosides. Greater

than 80% of the virus were active in binding activity. A larger number of virus were able to bind to an erythrocyte than were able to fuse with it, giving some indication that an additional fusion site may be necessary for membrane fusion. As the cell surface became crowded with virus some inhibition of the fusion process occurred. Overall the activities of mumps were very similar to Sendai virus. The virus interacted with the cellular site with a rate constant of $\approx 4 \times 10^9\ M^{-1}sec^{-1}$.

Neurotropic and nonneurotropic strains of mumps are both able to penetrate as far as the ependymal cells of the CNS by crossing into the cerebrospinal fluid at the choroid plexus. The common cellular receptor of mumps, and ability of the virus to fuse with most cells, likely allows the virus to cross into the CNS by infection of the choroid plexus and subsequent budding into the cerebral spinal fluid. Propagation of virus into the neurons by virus-cell fusion may be difficult due to restricted diffusion of the virus into the neuronal interstitial spaces, while cell-cell fusion would allow infection of nearest neighbors and continued penetration of the neuronal matter. This hypothesis would explain why strains of mumps that are non-neurotropic lack syncytial capacity while neurotropic strains are highly syncytial.

Chapter 5-

Can reconstituted Sendai virus be used as a delivery vehicle to H9 and PBL cells, model cell lines for HIV infection?

Reconstituted Sendai virus was able to fuse with both H9 and PBL cells. The process could be blocked by competing for the binding site sialic acids with fetuin or by preventing fusion by cleaving the F protein of the RSVE with trypsin. A large number of fusion events were observed with each cell, for PBL approximately 2 μg of viral protein were observed to fuse with 1 $x10^6$ cells, equal to about 7,800 reconstituted virus per cell.

Reconstituted virus may provide a method for drug delivery to cells. The ability of the reconstituted virus to maintain contents is critical to delivery. Radiolabeled ribozyme was effectively loaded into these vesicles without any degradation. There are a number of research opportunities available in continuing this project.

Chapter 6-

How can one optimize the loading of nucleic acids into the reconstituted Sendai viral envelopes? Can reconstituted Sendai virus be used to transfect HL60 and Cos cells?

Under normal Triton X-100 reconstitution conditions the encapsulation of plasmid size DNA into RSVE was very low, <1%. Polylysine, lysozyme and protamine greatly increased the amount of encapsulated material in the RSVE to between 3 and 10 %. This amount of encapsulated material is approximately equivalent to the amount one would expect to find for the encapsulation of a small, neutral molecule.

Transfection was feasible using the reconstituted virus with luciferase protein being expressed in Cos cells. The efficiency of transfection was no better than already available techniques. No expression was observed in HL60 cells, experimental evidence supporting a hypothesis that material can be delivered to these cells but is not expressed due to an unknown resistance mechanism.

The End.

Appendix 1: Computer program used to perform mass action kinetic fitting on fluorescent data

This program was originally written in the C language by David Baselt to fit STM data curves and modified by David to allow fitting to my fluorescence curves.

The Simulation loop subroutine listed at the end of the program can be varied to describe any number of kinetic schemes or equations.

```
/* SIMULATE.C:  FEEDBACK SIMULATION PROGRAM */

#include <stdio.h>
#include <graph.h>
#include <string.h>
#include <stdlib.h>
#define XMIN 22
#define XMAX 618
#define YMIN 62
#define YMAX 458
#define MIN_POSITION 1
#define MAX_POSITION 20
#define VAR_POSITION 40
#define PRERUN 0

extern void simulate(void);
void plot(void);
void save(void);
void recall(void);
float take_number(int yposition, int xposition, char choice);
void scale(int interval);
void optimize(void);
void skip_line (FILE *fin);
void smooth(void);


float sim_data[1000], exp_data[1000], *data, mult=41.0f;
extern float k1, k2, k3;
long far colors[]={ _BLACK, _BLUE, _GREEN, _CYAN, _RED, _MAGENTA,
  _BROWN, _LIGHTMAGENTA, _GRAY, _LIGHTBLUE, _LIGHTGREEN,
_LIGHTCYAN, _WHITE,
  _LIGHTRED, _LIGHTYELLOW, _BRIGHTWHITE };
int current_color = 1, reps;

int i, x, xmin, xmax, input = 0, something_changed, points=1000;
```

```
float ymin, ymax, yoffset, yfactor, xoffset, xfactor, new_value;
float V0=1e-12, G0=1e-12;

void main()
{
  simulate();
  plot();
   _setvideomode(2);

   printf("Final values:\n");
  printf("k1 = %f\n", k1);
  printf("k2 = %f\n", k2);
  printf("k3 = %f\n", k3);
  printf("M  = %f\n", mult);
  printf("V0 = %f x e-12\n", V0*1e12);
  printf("G0 = %f x e-12\n", G0*1e12);
}

void plot()
{
  char ch;
   float sim_ymin, sim_ymax, exp_ymin, exp_ymax;

   _setvideomode(_VRES16COLOR);
   if (!_remapallpalette(colors)) printf("\a");
   _settextcolor(7);

   _setcolor(11);
   _rectangle(_GBORDER, XMIN-2, YMIN-2, XMAX+2, YMAX+2);
   _setcolor(9);
   _settextposition(1, 0); printf("STEP RESPONSE SIMULATION");
   _settextposition(2, MIN_POSITION); printf("XMIN:      0_");
   _settextposition(2, MAX_POSITION); printf("XMAX:   1000");
   _settextposition(2, VAR_POSITION); printf("1:  %6.3f ", k1);
   _settextposition(3, VAR_POSITION); printf("2:  %6.3f ", k2);
   _settextposition(2, VAR_POSITION+20); printf("3:  %6.3f ", k3);
   _settextposition(3, VAR_POSITION+20); printf("M:  %6.3f ", mult*.01);

  xmin = 0; xmax = 999;
  something_changed = 1;

  for (i=0; i<1000; i++) exp_data[i] = 0;
 exp_data[999] = 100;

  while (1) {
```

```
if (something_changed) {
 exp_ymin = exp_ymax = exp_data[xmin];
  sim_ymin = sim_ymax = sim_data[xmin];

 for (i = xmin+1; i < xmax+1; i++) {
    if (exp_data[i] < exp_ymin) exp_ymin = exp_data[i];
    else if (exp_data[i] > exp_ymax) exp_ymax = exp_data[i];
    if (sim_data[i] < sim_ymin) sim_ymin = sim_data[i];
    else if (sim_data[i] > sim_ymax) sim_ymax = sim_data[i];
    }
  if (sim_ymin < exp_ymin) ymin = sim_ymin;
else                 ymin = exp_ymin;
 if (sim_ymax > exp_ymax) ymax = sim_ymax;
else                 ymax = exp_ymax;

if (ymax == ymin) yfactor = 1;
 else yfactor = (float)(YMAX-YMIN)/(ymax-ymin);
 yoffset = YMAX+ymin*yfactor;
 xfactor = (float)(XMAX-XMIN)/(float)(xmax-xmin);
 xoffset = -xmin*xfactor+XMIN;
  _settextposition(3, MIN_POSITION); printf("YMIN:  %8.2f    ", ymin);
  _settextposition(3, MAX_POSITION); printf("YMAX:  %8.2f    ", ymax);

_setcolor(0);                              /* clear old plot */
  _rectangle(_GFILLINTERIOR, XMIN-1, YMIN-1, XMAX+1, YMAX+1);

if (ymax > 0) {
    _setcolor(11);
    _moveto(XMIN-1, yoffset); _lineto(XMAX+1, yoffset);    /* zero line */
    }
 if ((xmax-xmin) < 51) scale(1);
 else if ((xmax-xmin) < 501) scale(10);
else scale(20);
 _setcolor(9);
  _moveto(XMIN, yoffset-exp_data[xmin]*yfactor);
 for (x = xmin+1; x < xmax+1; x++) {              /* draw new one */
    _lineto(x*xfactor+xoffset, yoffset-exp_data[x]*yfactor);
    }
 _setcolor(10);
  _moveto(XMIN, yoffset-sim_data[xmin]*yfactor);
 for (x = xmin+1; x < xmax+1; x++) {              /* draw new one */
    _lineto(x*xfactor+xoffset, yoffset-sim_data[x]*yfactor);
    }
}
```

```
 if (ch != 'o' || (ch=='o' && kbhit())) {
  ch = getch();
  if (ch == 0) ch = getch();
  reps = 0;
  }
 something_changed = 0;
if (ch == 0x4b || ch == 0x48) {                    /* left arrow */
  if (input == 1 || input == 0) {
      input = 0;
      _settextposition(2, MIN_POSITION+12); printf("_");
      _settextposition(2, MAX_POSITION+12); printf(" ");
      }
  else if (input == 2) {
      input = 1;
      _settextposition(2, MAX_POSITION+12); printf("_");
      _settextposition(2, VAR_POSITION+10); printf(" ");
      }
  else if (input == 3) {
      input = 2;
      _settextposition(2, VAR_POSITION+10); printf("_");
      _settextposition(3, VAR_POSITION+10); printf(" ");
      }
  else if (input == 4) {
      input = 3;
      _settextposition(3, VAR_POSITION+10); printf("_");
      _settextposition(2, VAR_POSITION+30); printf(" ");
      }
  else if (input == 5) {
      input = 4;
      _settextposition(2, VAR_POSITION+30); printf("_");
      _settextposition(3, VAR_POSITION+30); printf(" ");
      }
 }
else if (ch == 0x4d || ch == 0x50) {                /* right arrow */
  if (input == 0) {
      input = 1;
      _settextposition(2, MIN_POSITION+12); printf(" ");
      _settextposition(2, MAX_POSITION+12); printf("_");
      }
  else if (input == 1) {
      input = 2;
      _settextposition(2, MAX_POSITION+12); printf(" ");
      _settextposition(2, VAR_POSITION+10); printf("_");
      }
```

```
 else if (input == 2) {
     input = 3;
     _settextposition(2, VAR_POSITION+10); printf(" ");
     _settextposition(3, VAR_POSITION+10); printf("_");
     }
 else if (input == 3) {
     input = 4;
     _settextposition(3, VAR_POSITION+10); printf(" ");
     _settextposition(2, VAR_POSITION+30); printf("_");
     }
 else if (input == 4 || input == 5) {
     input = 5;
     _settextposition(2, VAR_POSITION+30); printf(" ");
     _settextposition(3, VAR_POSITION+30); printf("_");
     }
}
else if (ch == 's') save();
else if (ch == 'p') {
  smooth(); something_changed = 1;
  _settextposition(2, MAX_POSITION); printf("XMAX:   %4i", xmax);
}
else if (ch == 'r') {
 recall();
 simulate();
 something_changed = 1;
}
else if (ch == 'q') break;
else if (ch == 0x1b);
else if (ch == 'o') {
 optimize();
 reps++;
 something_changed = 1;
}
else if (ch == 'e') {
 _setcolor(0);                          /* clear old plot */
  _rectangle(_GFILLINTERIOR, XMIN-1, YMIN-1, XMAX+1, YMAX+1);
 if (ymax > 0) {
     _setcolor(11);
     _moveto(XMIN-1, yoffset); _lineto(XMAX+1, yoffset);    /* zero line */
     }
     if ((xmax-xmin) < 51) scale(1);
     else if ((xmax-xmin) < 501) scale(10);
     else scale(20);
}
else if (ch == 0x0d);
```

```
   else if (input == 0) {
      if ((new_value=take_number(2, MIN_POSITION+7, ch)) != -1)
xmin=new_value;
     something_changed = 1;
    }
   else if (input == 1) {
      if ((new_value=take_number(2, MAX_POSITION+7, ch)) != -1)
xmax=new_value;
     something_changed = 1;
    }
   else if (input == 2) {
      if ((new_value=take_number(2, VAR_POSITION+5, ch)) >= 0)
k1=new_value*1e+9;
     else if (new_value == -2) k1 *= 1.1;
     else if (new_value == -3) k1 /= 1.1;
      _settextposition(2, VAR_POSITION);   printf("1:  %6.3f", k1/1e+9);
     something_changed = 1;
     simulate();
    }
   else if (input == 3) {
      if ((new_value=take_number(3, VAR_POSITION+5, ch)) >= 0)
k2=new_value/100;
     else if (new_value == -2) k2 *= 1.1;
     else if (new_value == -3) k2 /= 1.1;
      _settextposition(3, VAR_POSITION);   printf("2:  %6.3f", k2*100);
     something_changed = 1;
     simulate();
    }
   else if (input == 4) {
      if ((new_value=take_number(2, VAR_POSITION+25, ch)) >= 0)
k3=new_value/100;
     else if (new_value == -2) k3 *= 1.1;
     else if (new_value == -3) k3 /= 1.1;
      _settextposition(2, VAR_POSITION+20);   printf("3: %7.3f", k3*100);
     something_changed = 1;
     simulate();
    }
   else if (input == 5) {
      if ((new_value=take_number(3, VAR_POSITION+25, ch)) >= 0)
mult=new_value*100;
     else if (new_value == -2) mult *= 1.1;
     else if (new_value == -3) mult /= 1.1;
      _settextposition(3, VAR_POSITION+20);   printf("M:  %6.3f", mult*.01f);
     something_changed = 1;
     simulate();
```

```
    }
   }
}

void save(void)
{
  char filename[35];
  int i;
  FILE *fout;

   _settextposition(1, VAR_POSITION);
  printf("                                ");
   _settextposition(1, VAR_POSITION); printf("Filename:  ");
   scanf("%s", filename);
   if (!strstr(filename, ".")) strcat(filename, ".gra");

   fout = fopen(filename, "w");
   for (i = 0; i < points; i++) fprintf(fout, "%f\n", sim_data[i]);
   _settextposition(1, VAR_POSITION); printf("Last file saved:  %s", filename);
   fclose(fout);
}

void recall(void)
{
  char filename[35], c_dummy[80];
  int i=0, j;
  float f_dummy;
  FILE *fin;

   _settextposition(1, VAR_POSITION);
  printf("                                ");
   _settextposition(1, VAR_POSITION); printf("Filename:  ");
   scanf("%s", filename);
   if (!strstr(filename, ".")) strcat(filename, ".awa");

   if ((fin = fopen(filename, "r")) == 0) {
     _settextposition(1, VAR_POSITION);
    printf("                                ");
     _settextposition(1, VAR_POSITION);
     printf("Cannot open:  %s", filename);
     return;
    }

   for (i=0; i<3; i++) skip_line(fin);
```

```
 for (j=0; j<PRERUN; j++) fscanf(fin, "%f", &f_dummy);
 for (i=0; i<1000; i++) {
   if (fscanf(fin, "%s", c_dummy)==EOF) break;
   if (strncmp(c_dummy, "END", 3)==0) break;
    sscanf(c_dummy, "%f", exp_data+i);
  }
 fclose(fin);
 points = i;
 xmax = i-1;
 xmin = 0;

  _settextposition(2, MIN_POSITION); printf("XMIN:      0");
  _settextposition(2, MAX_POSITION); printf("XMAX:    %4i", xmax);

  _settextposition(1, VAR_POSITION);
 printf("                              ");
  _settextposition(1, VAR_POSITION); printf("V0 x e-12:  ");
 scanf("%f", &V0); V0 *= 1e-12;
  _settextposition(1, VAR_POSITION);
 printf("                              ");
  _settextposition(1, VAR_POSITION); printf("G0 x e-12:  ");
 scanf("%f", &G0); G0 *= 1e-12;
  _settextposition(1, VAR_POSITION);
 printf("                              ");
  _settextposition(1, VAR_POSITION); printf("Loaded file:  %s", filename);
}

float take_number(int yposition, int xposition, char choice)
{
 int i, j;
 char number[10];
 float result;

 i = 0;
 while (choice != 0x0d && choice != 0x1b && choice != '*' && choice != '/') {
  if (choice == 0x08) {                          /* backspace */
    i -= 1;
    if (i < 0) i = 0;
     _settextposition(yposition, xposition-2); printf("       ");
     _settextposition(yposition, xposition-i+5);
     for (j=0; j < i; j++) printf("%c", number[j]);
    }
   else if ( ((choice>47) && (choice<58)) || choice=='.' || choice=='-') {
     number[i] = choice;
     _settextposition(yposition, xposition-2); printf("       ");
```

```
      _settextposition(yposition, xposition-i+4);
      for (j=0; j < i+1; j++) printf("%c", number[j]);
     i++;
     }
    choice = getch();
   }
  number[i] = '\0';
 if     (choice == 0x1b) result = -1;              /* escape = cancel */
 else if (choice ==  '*') result = -2;
 else if (choice ==  '/') result = -3;
 else if (!sscanf(number, "%f", &result)) { result = -1; printf("\a"); }
 return result;
}

void scale(int interval)
{
 int position;

 _setcolor(11);
 for (position = xmin; position < xmax+1; position+=interval) {
   _moveto(position*xfactor+xoffset, YMAX+1);
   _lineto(position*xfactor+xoffset, YMAX-4);
  if ((interval<10 && position%10==0) || position%100==0)
    _lineto(position*xfactor+xoffset, YMAX-9);
   _moveto(position*xfactor+xoffset, YMIN-1);
   _lineto(position*xfactor+xoffset, YMIN+4);
  if ((interval<10 && position%10==0) || position%100==0)
    _lineto(position*xfactor+xoffset, YMIN+9);
  }
}

void optimize(void)
{
 float offspring_array[4], best_array[4], original_array[4], mutation_value;
 float avg, std_dev, best_std_dev, sd_dif, *data, rand_max, r;
 int i, j, x, dummy_direction, dummy_data_type, dummy_mode;

 rand_max = (float)RAND_MAX;

 original_array[0] = offspring_array[0] = k1;
 original_array[1] = offspring_array[1] = k2;
 original_array[2] = offspring_array[2] = k3;
 original_array[3] = offspring_array[3] = mult;

 for (i=0; i<10; i++) {
```

```
   if (i>0) {
     for (j=0; j<4; j++)                    /* generate mutations */
         offspring_array[j] = (((float)rand()/rand_max)*0.191f +
0.909f)*original_array[j];
     k1 = offspring_array[0];
     k2 = offspring_array[1]; if (k2 > 1.0f) k2 = 1.0f;
     k3 = offspring_array[2]; if (k3 > 1.0f) k3 = 1.0f;
     /* mult = offspring_array[3]; */
     }
    simulate();
    data = sim_data;

    std_dev = 0.0f;
    for (x=xmin; x<xmax; x++) {
     sd_dif = sim_data[x] - exp_data[x];
     if (sd_dif < 0) sd_dif *= -1;
     std_dev += sd_dif;
     }

    if (std_dev<best_std_dev || i==0) {      /* see if it's the best so far */
      best_std_dev = std_dev;
      for (j=0; j<4; j++) best_array[j] = offspring_array[j];
     }
   }

  k1 = best_array[0];
  k2 = best_array[1]; if (k2 > 1.0f) k2 = 1.0f;
  k3 = best_array[2]; if (k3 > 1.0f) k3 = 1.0f;
  /* mult = best_array[3]; */

   _settextposition(2, VAR_POSITION); printf("1:  %6.3f ", k1/1e+9);
   _settextposition(3, VAR_POSITION); printf("2:  %6.3f ", k2*100.0f);
   _settextposition(2, VAR_POSITION+20); printf("3: %7.3f ", k3*100.0f);
   _settextposition(3, VAR_POSITION+20); printf("M:  %6.3f ", mult*.010f);
   _settextposition(1, VAR_POSITION);
  printf("Pass: %3i  Std dev: %6.3f   ", reps, best_std_dev/(xmax-xmin));
}

void skip_line (FILE *fin)
{
  int ch;

  while ((ch=fgetc(fin))!='\n' && ch!=0x0d && ch!=0x0a && !feof(fin));
}
```

```
void smooth(void)
{
  int i, j;

  for (j=0; j<2; j++) {
    for (i=0; i<points; i++)
      exp_data[i] = (exp_data[i] + 2*exp_data[i+1] + exp_data[i+2])*0.25;
    points--; xmax--;
    }
}


/* SIMULATION PROGRAM */

extern float sim_data[1000], V0, G0, mult;
extern int points;
float k1 = 0, k2 = 0, k3 = 0;

void simulate()
{
  int i;
  float vg=0, f=0, dvg, df, v, g;

  for (i=0; i<1000; i++) sim_data[i] = 0;
  v = V0; g = G0;

  for (i=0; i<points; i++) {
    dvg = k1*v*g - k2*vg - k3*vg;
    df = k3*vg;
    vg += dvg;
    f += df;
    v = V0 - vg - f;
    g = G0 - vg - f;
     sim_data[i] = mult*f/V0;
    }
}
```